NOTE: Lacks page 72 (missing from deposited hardcopy)
(following "In discussing possible T-odd effects there are three
major lines of enquiry:" the outline of the 3rd line of enquiry is lost.)

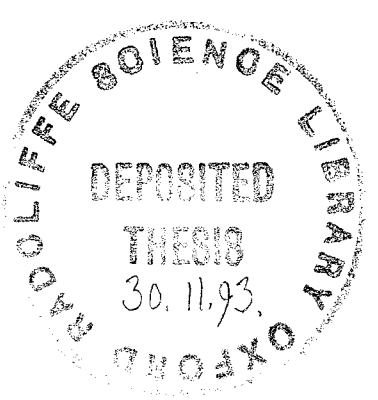
Time Reversal Violation in Atoms

Thesis submitted for the degree of Doctor of Philosophy
in the University of Oxford

Edmund Stephens

St John's College, University of Oxford

Trinity Term 1993



To Neil and Judith

Abstract

Time reversal violation in atoms

E. C. Stephens, St John's College.

Submitted for the degree of Doctor of Philosophy
in the University of Oxford, Trinity Term 1993.

This thesis is about the *direct* study of time reversal invariance in atomic systems. To date, studies of time reversal violation in atoms have mostly been sensitive to time reversal *and* parity violating phenomena such as a static electric dipole moment (edm). While parity symmetry violation is well understood in the standard model as a consequence of electroweak theory, little is known of the corresponding T violating parity invariant physics.

Although there is no direct evidence, the observed CP asymmetry of neutral kaon decays, implies (assuming CPT) the existence of T violation in fundamental physics. There is therefore reason to suspect T violating phenomena may occur in atoms at some level.

We first investigate what is known about the T purity of atomic states, either directly or indirectly, from existing experiments. We then discuss the symmetry properties of static toroidal moments, of which the *tetrapole* is the lowest order T-odd P-even moment. The T impurities also affect the dynamics of the atom in a characterisctic way, and these effects are exploited differently in three classes of experiment which can be sensitive to T violation:

- T-odd correlations: Experiments have been proposed to measure time reversal asymmetry in refractive index or transition rate correlations.

- Plane polarised pumping (PPP): This novel scheme which we have developed produces a characteristic angular momentum alignment in the initial or final state which is a consequence of time reversal violation. We note that such alignments can also occur through virtual decay processes of multiple intermediate levels. This latter effect has features making it distinguishable from the time asymmetry signature, and is in its own right an interesting phenomenon.

- T clocks: When three or more atomic transitions are driven coherently, the evolutions of the population in the atomic states depends on a suitably defined net phase. If this phase is set to zero in the absence of time reversal violation, then the 'return' frequency of the population is a measure of the time asymmetry.

The concern of this thesis is primarily to throw light on the observable atomic consequences of a T violation. We discuss sensitivity to potential T-odd admixtures with the aim of stimulating more detailed experimental study of this subject.

Acknowledgements

More than an acknowledgement is required for Neil and Judith. This thesis is the tangible product of my education and is dedicated to you for your unstinting support and encouragement. I wish also to give my most wholehearted thanks to Pat Sandars, whose time and energy supervising my work has been well appreciated. His pervasive knowledge and phenomenal intuition are a continuing inspiration to me. My thanks also to Keith Burnett and Ed Hinds who have contributed with valuable insight on many occasions.

A special mention for Anders Ynnerman, a great friend and insightful colleague. Ever a source of activity and life, his company is always pleasant and worthwhile, and I hope we can keep in close association as a long and productive friendship. Also Aimee Clinton, Cath "TC" Wilkins and Kimberly Bazar, who have all given me a spiritual equilibrium that goes beyond mere friendship.

Ken Zetie was a ubiquitous consultant on many necessary experimental details. He comprehensively proof read a major part of the thesis, and spurred me onto numerous improvements. My work has often drawn on his eclectic knowledge of nitty-gritty practicalities, for which I am very grateful.

Thanks also to Andy "Flagman" Rowe, Jon Newham, Paul Titcomb, Jerry Hoad and Jim Penman, who have been my enduring social foundation for these great years. Also George "Tart" Woodman and his diverse silly noises, Adam "Bagatelle" Hartley who has taught me to keep an eye on the future(s), Jessica James who deserves a special award for putting up with me, Graham "Cue Ball" Quelch who can produce a miracle before he's finished the impossible, Sue Witney for much needed intelligence about Pat's movements, Bruce "Walrus" Warrington for his judicious pruning, and notably Malcolm "Jock of the Loch" Macpherson whose complete geniality is an entire philosophy of itself.

For my time at INT in Seattle, I am indebted to Eugen Merzbacher for inviting me to participate in such an enjoyable and productive programme. Also to Yulik Khriplovich for many stimulating discussions, Julia Malloy for organising my visit so efficiently, Pippin Sardo for being so wonderful, and to everyone else who made my stay in that beautiful city such a unique experience.

Thank you Quentin for your computer wizardry, Stuart Rae and the others in Keith's group for sharing computer resources, Carol Thomson for great 'pot luck' dinners and Cath Cooper for the barbeques. Also Dan Talmage, Jason Breed, Dave Willis and many others for all the excellent breakfasts we have shared.

This work was supported in part for the first three years by an SERC studentship, and also by the INT in Seattle, WA during my visit there. My thanks also to the staff of St John's college for making my time there so pleasant.

Contents

1 Introduction **1**

1.1 Time reversal 2

1.2 Outline of the thesis 4

2 Time reversal and parity inversion **6**

2.1 Parity Inversion 7

2.1.1 Parity in quantum mechanics 8

2.1.2 The role of parity invariance in atoms and molecules 10

2.2 Time Reversal 12

2.2.1 T reversal in quantum mechanics 13

2.2.2 T reversal of angular momentum states and tensor operators . 15

2.2.3 The role of T invariance in atoms 17

2.3 P,T Phase convention 19

2.4 P and T symmetries of external fields 21

2.5 Violation of P and T symmetry 22

2.6 Atomic parity non-conservation 23

2.7 Atomic T violation 23

2.7.1 Electric dipole moments 24

2.7.2 Radiative interference 24

3 T-odd P-even purity in atoms **27**

3.1 The neutral kaon system 28

3.1.1 CP properties of the kaons 28

3.1.2 CP violation in kaon decay 29

3.2 T violating atomic admixtures 29

3.3 Model independent atomic T impurity limits 30

3.4 Model dependent atomic T impurities 33

3.4.1 Short range interactions 34

3.4.2 Long range interactions 36

3.5 Summary 37

4 Anapole and Tetrapole **38**
4.1 Classical fields . . . 38
4.1.1 Scalar fields . . . 38
4.1.2 Vector fields . . . 39
4.2 Electrostatic fields . . . 39
4.2.1 Electrostatic potential multipole expansion . . . 40
4.2.2 Electric moments of a quantum system . . . 40
4.2.3 P and T properties of the electric moments . . . 41
4.3 Magnetostatic fields . . . 41
4.3.1 Magnetic field multipole expansion . . . 41
4.3.2 The regular magnetic moments . . . 42
4.3.3 Magnetic moments of a quantum system . . . 43
4.3.4 The toroidal magnetic moments . . . 44
4.3.5 Toroidal moments of a quantum system . . . 46
4.3.6 P and T properties of magnetic moments . . . 46
4.4 The electron-nuclear toroidal moment interaction . . . 49
4.5 Toroidal moments in atomic physics . . . 50
4.5.1 The nuclear anapole interaction . . . 50
4.5.2 The nuclear tetrapole interaction . . . 51
4.6 Alternative derivation of toroidal moments . . . 52
4.7 Classical anapoles . . . 53

5 T Violation in atomic transitions **56**
5.1 Review of transition theory . . . 57
5.2 EM multipole expansion . . . 58
5.3 Multipole transition rates . . . 59
5.4 Near resonant two photon transitions . . . 60
5.4.1 Raman processes . . . 60
5.4.2 Solution in the weak field limit . . . 63
5.4.3 Two or more intermediate levels . . . 65
5.5 T impurities and the channel phase . . . 67
5.6 T violation in a two state system . . . 68
5.7 The two channel TV theorem . . . 69
5.8 The T ratio . . . 70
5.9 Overview of TO,PE experiments . . . 71

6 TO,PE absorption correlations **73**
6.1 Single photon correlations . . . 74
6.2 Caesium excitation rate correlations . . . 74
6.2.1 Sensitivity . . . 76
6.3 Thallium refractive index correlations . . . 77
6.3.1 Background absorption . . . 78
6.3.2 TO,PE interference term . . . 80

6.3.3 Sensitivity 81
6.4 Caesium refractive index correlations 82
6.5 Two photon correlations 83
6.6 Summary 84

7 Plane polarised pumping **86**
7.1 PPP in Raman processes 87
7.1.1 The PPP geometry 88
7.1.2 The scalar/tensor and vector amplitudes 89
7.1.3 Scalar/tensor × vector dependence 90
7.1.4 Selection rules 91
7.1.5 Misalignment dependences 91
7.1.6 Circular polarisation impurities 92
7.2 Decay PPP effect 94
7.3 T violation PPP effect 97
7.4 Background transitions 98
7.5 Reversed processes: T reversal character 100
7.6 Doppler broadened populations 102
7.7 Sensitivity 104
7.8 Forbidden transition PPP schemes 105
7.9 Summary 108

8 The PPP effect in caesium **109**
8.1 Dipole matrix elements 110
8.2 The weak field régime 111
8.3 Ordinary transition strength 112
8.4 Decay PPP transition strength 115
8.5 T violating PPP transition strength 116
8.6 Channel phases for 6p TO,PE mixing 116
8.7 Summary 118

9 T clocks **120**
9.1 A simple 3 state system 120
9.1.1 Formal solution of the evolution 121
9.1.2 Analytical solutions 122
9.2 Population beats as a measure of T violation 123
9.2.1 The T ratio for T clocks 124
9.2.2 Sensitivity 127
9.3 Dependence on intensity 128
9.4 Off resonant T clocks 130
9.5 Radio frequency T clocks 132
9.6 Summary 134

10 Conclusion **135**

A Angular momentum and tensor coupling **138**
A.1 Angular momentum eigenstates 138
A.2 Spherical tensors and tensor coupling 140
A.3 Properties of matrix elements 143

B Spherical harmonics **145**
B.1 Scalar field expansions 145
B.2 Vector field expansions 146

C Spherical delta functions **148**

D Dirac matrices and wavefunctions **149**

E Parity violating weak interactions **151**
E.1 Electroweak theory 151
E.2 Atomic parity non-conservation 154

As I returned, I passed again across that minute when she traversed the laboratory. But now her every motion appeared to be the exact inversion of her previous ones. The door at the lower end opened, and she glided quietly up the laboratory, back foremost, and dissappeared behind the door by which she had previously entered.

The Time Machine, H. G. Wells.

Chapter 1

Introduction

Duration in time is the only thing we can measure by thought alone. We are dynamic beings and like all other dynamic systems, time is both a witness and measure to our lives. From the earliest recorded history, time has been reckoned from the periodic features present in the natural world, the day, the lunar month and the seasonal changes in the year. Plato's wrote of time as "an everlasting image moving according to number" - Greek thinkers appreciated the fundamental connection between time and *counting*. These early time keepers measured the periodicities both in the natural world and man made devices and recognised that counting these cycles measures time in a uniform and consistent way.

Time divides happenings *before* and *after* any particular event; it is therefore the meter of change. According to Aristotle, "to be in time and measured by time are the same thing". Some time counting devices, ie clocks, were available to Aristotle and his ilk. For short times, sundials or water clocks could be used (even including an early alarm clock device called a clepsydra used by zealots to cut sleep to a minimum). Longer times were reckoned by counting days and seasons with a calendar, and historical events could be recounted in terms of genealogies, kingships and so on.

In most early cultures, *all* time was cyclic with events of history itself repeating in cycles forever. By contrast, in the Judaeo-Christian tradition there are unique and unrepeatable events such as the life and times of Christ. This establishment of 'linear' time in western culture has been a profound influence on western thought: the past may be fixed, but the future is *free*. The intellectual revolution that this idea entails has arguably underpinned modern science and the promise of improvement of life [27].

These ideas about clocks and counting have been retained to the present day; in the Oxford English dictionary time is defined as

> *Time*, n. *Duration, a limited stretch or space of continued existence, an interval between two successive events.*

Thus a duration of time corresponds to the progress, or evolution, of a system under observation as measured by the successive events which happen. If the state of the

system is recorded at each count of a clock, then a chronology is formed which is a record of what happened in that interval. A convenient visualisation of this is a movie film. Each frame records the state of the system being filmed at regular time intervals, forming an ordered record of what has happened. That different cameras record the same time interval between any two events is a real (ie testable) assumption, that 'physics' - the actual behaviour of things in the real world - does not depend on the choice of time origin. It follows that cyclic processes of all periods keep time in the same way, their time 'counts' being always the same constant ratio of their periods, and that clocks with the same period set up at different times maintain a constant phase lag[1]. An alternative view of this choice is to ask whether it is possible for the sequence of events recorded in a film to happen again at a later time, that is to say a 'remake' which would be identical to the original.

1.1 Time reversal

This thesis is about the *time reversal* symmetry of atomic systems. Of course, unlike the Time Traveller in H. G. Wells' story, our actual course in time is not to be changed, but we can consider the undoing of events (at least algebraically) as a reversal of time which "turns the clock back". Time reversal inverts the succession of events, so statements about the sequencing or movements of the original system are transformed accordingly

$$\begin{aligned} \text{"}A \textit{ before } B\text{"} &\rightarrow \text{"}A \textit{ after } B\text{"} \\ \text{"}\textit{going}\text{"} &\rightarrow \text{"}\textit{coming}\text{"} \end{aligned}$$

This reversal is well illustrated in terms of the movie film analogy. If the frames of a film are shown in reverse order, the process depicted is then the time reversal of the original. Of course, the Time Traveller was *really* travelling backwards in time, and could have used a video camera to record his time reversed viewpoint directly.

Time reversal 'invariance' means that all aspects of this film taken while the Traveller was moving backwards in time, could in principle be reproduced in the real world. We can contrast this with the same situation for transformations such as rotations and translations. Rotational invariance implies, for example, that if a scene is recorded by a tilted camera, then an identical film can be recorded by an untilted camera by suitably rotating the scene being filmed.

Time reversal, an improper transformation, differs from these since there is no reason to suppose that the backwards process is a legitimate process in the real world. If the backwards process does correspond to a real process, then the dynamics

[1]The apparent periods of similar clocks are in fact *not* necessarily the same when in relative motion, or if gravitational fields are present, due to the requirements of relativity. Another quantity, the 'proper time', which is common to both clocks, then must take the place of the apparent time (according to either clock) as a mutually agreeable measurement.

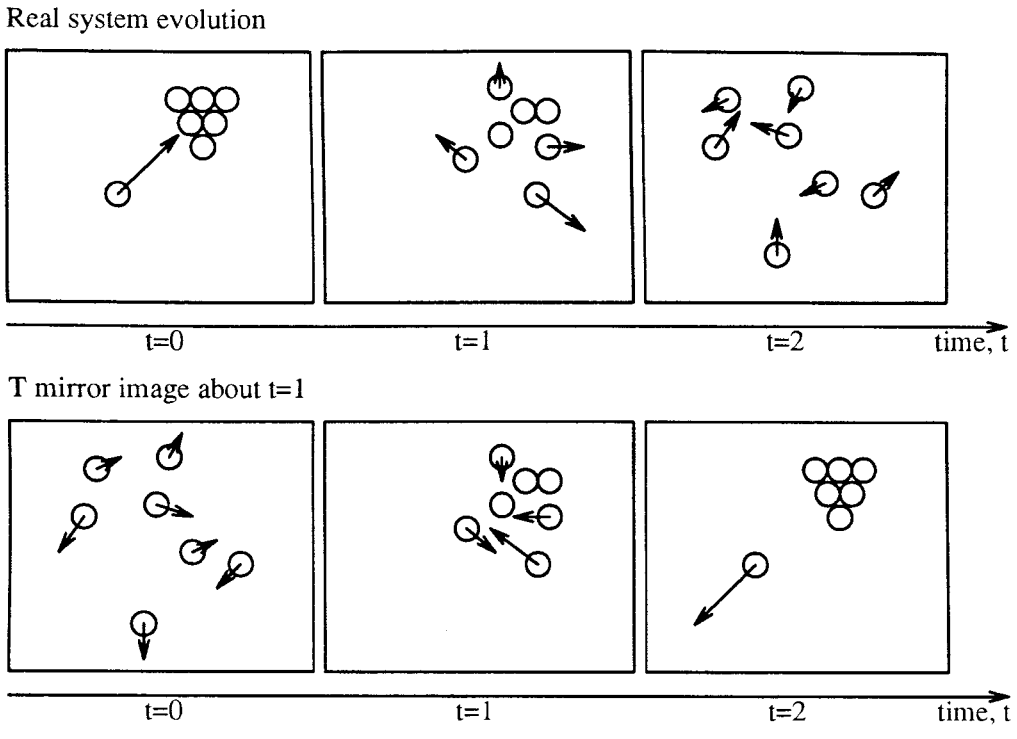


Figure 1.1: Two movies are related by a time reversal about $t = 1$

of the system are said to be time reversal 'invariant'. In fact common sense suggests that such reversed processes are *not* generally legitimate: in the macroscopic world there appears to be a definite 'arrow of time', which governs the direction of all but the simplest processes. This is illustrated by figure 1.1 which shows two movies (with frames taken at times $t = 0, 1, 2$) which are related by a time reversal about $t = 1$. It seems impossible for the lower movie to be a genuine film, since many balls coalescing to eject a single cue ball would be an extraordinary sight. However, first appearances are misleading, since thermodynamic irreversibility is present even when the basic processes are time reversal invariant. The source of the arrow of time is not in the fundamental dynamics, but in the initial conditions. In irreversible processes there are more (usually vastly more) equivalent final states than equivalent initial states, therefore the evolution of the system to the final state is purely a consequence of statistics. This resolves the apparent paradox of time asymmetrical evolution in systems determined by time reversal invariant dynamics.

The assumption of time reversal invariance relates the evolutions of different processes, thereby providing a constraint on their properties. Stationary and periodic systems are special cases in which the evolution forwards and backwards are directly related, and these cases are said to have time reversal symmetry. An early use of time reversal symmetry was by Painlevé in 1904, who showed that a mechanical system initially at rest, cannot at a later time come to rest in an identical configuration but

different net orientation [61]. This seemed at variance with the ability of a cat to twist while falling so as to land on its feet. In fact the cat's manœuvre requires no more than flexibility and was photographed as early as 1894 [56]. Of course so-called 'zero angular momentum' turns do not violate time reversal invariance, which are the basis of many acrobatic and dancing manœuvres [29].

The time reversal transformation is related to the *mirror* transformation in a fundamental way, since the mirror image of the movie, ie its reflection viewed in a mirror, is not really happening. It is convenient to avoid having to specify the plane of the mirror by using *parity inversion* symmetry, which inverts space through the coordinate origin[2]. In parity inverted and mirror reflected movies, the images of handed objects appear oppositely handed.

The same question can be put for both the parity inverted and time reversed films: do the images of real processes represented in the transformed movies correspond to physics? The emphasis here is on physics since statements about parity and time reversal invariance are about *equations* of motion, not about the actual motions of systems [65].

Until recently these symmetries were thought to be a quite natural requirement for physical theories, but like the uniformity of clocks, these are real and *testable* assumptions.

1.2 Outline of the thesis

The aim of this thesis is to throw light on the observable consequences of violation of time reversal invariance in atomic systems. Three classes of experiment are discussed which exploit the T violation in different ways. Because of their well defined internal degrees of freedom, atomic systems have many advantageous features for such experiments. In view of the established body of evidence for parity violation in many systems, including atoms, and the similarities between the parity and time reversal transformations, it seems natural in chapter 2 to discuss and develop time reversal theory to contrast with parity theory. The different combinations of parity and time reversal symmetry 'violation' have distinct consequences for atoms.

Ordinary physics is both parity and time reversal invariant, and there are important differences between time reversal effects which also violate parity symmetry, and those which are parity invariant. The usual shorthand for these are T-odd P-odd (TO,PO) and T-odd P-even (TO,PE) respectively. T-odd P-odd interactions have been the subject of much theoretical and experimental effort, but the current work is concerned with the latter case, ie *direct* tests of time reversal invariance. In chapter 3 we discuss the current knowledge of the T purity of atomic states.

The parity and time reversal symmetries of electrostatic and magnetostatic field distributions are discussed in chapter 4. The magnetic field distributions of the so-called *toroidal* moments are found to have novel parity and time reversal symmetries,

[2]Parity inversion is equivalent to a mirror reflection followed by a 180° rotation.

which imply violations of parity or time reversal. The simplest of these is the *anapole* which is time reversal invariant but parity violating [77]. The second rank analogue of the anapole, which we have called the *tetrapole*, is time reversal violating and parity invariant, so we extend the theory of anapoles to the higher orders.

In atomic systems T-odd P-even interactions lead to impurities in the atomic states, which involve even parity admixtures. These are imaginary relative to the normal (T-even) admixtures. In chapter 5 we discuss the consequences of T impurities in the atomic states for radiative transition processes. The T impurities lead to anomalous interference effects between competing transition amplitudes; these are a measure of T violation and are exploited in different ways by currently proposed schemes.

Finally in the chapters 6-9, three classes of experiments are discussed. These schemes for measuring time reversal violation are distinct from an experimental point of view, and also in the way the symmetry violation is manifested

- T-odd correlations: Kozlov and Porsev [51] have proposed to measure time reversal asymmetry in refractive index of thallium. Preliminary studies of this proposal are currently underway at Oxford [9], and we look at possible enhancements in other schemes.

- Plane polarised pumping (PPP): This novel scheme which we have developed produces a characteristic angular momentum alignment in the initial or final state which is a consequence of time reversal violation. We note that such alignments can also occur through virtual decay processes of multiple intermediate levels. This latter effect has features making it distinguishable from the time asymmetry signature, and is in its own right an interesting phenomenon.

- T clocks: When three or more atomic transitions are driven coherently, the evolutions of the population in the atomic states depends on a suitably defined net phase. If this phase is set to zero in the absence of time reversal violation, then the 'return' frequency of the population is a measure of the time asymmetry.

These schemes exploit the effects of time reversal violation in different ways, and we estimate in each case the sensitivity to TO,PE admixtures.

Chapter 2

Time reversal and parity inversion

The time reversal and parity inversion 'mirror' transformations relate real systems to an appropriate mirror image with the reversed properties of the original. A system is called invariant if it and its mirror image both evolve according to the same equation of motion. Invariance to mirror transformations such as time reversal and parity inversion, was assumed until recently to be a natural requirement for physical theories, but ever since it has been shown that some systems are *not* invariant to parity inversion, there has been great interest in the physical basis for other mirror invariance assumptions.

The emphasis of the present work is towards the *direct* investigation of T invariance in atomic systems. In this chapter, the theory of time reversal is developed, and we examine the consequences of T invariance for atomic systems. Time reversal has much in common with parity inversion, and since there is an established theory of P invariance violation, it is natural to review parity theory and develop time reversal theory in an analogous way.

It is, of course, well known that the simplest versions of the standard model are invariant under a combined parity and charge conjugation (CP) transformation, where charge conjugation is another discrete transformation whose action is to transform particles into antiparticles and vice-versa. The observed neutrino states are the left handed neutrino ν_L and right handed antineutrino $\bar{\nu}_R$, which are CP mirror images. The model is not invariant to either C or P alone since the other neutrino states ν_R and $\bar{\nu}_L$ do not exist in the real world. The C, P and T mirror transformations are connected through the CPT theorem, which is a consequence of the general assumptions of causality and local gauge invariance in field theories [4]. These fundamental assumptions imply invariance to the combined CPT transformation, thus observation of CP violation would be equivalent to T violation in such theories. This situation is known to occur in the decay of the K^0 system [21], so that either CPT or T symmetry is violated. Although the observation of CP violation indicates that T violation is likely at some level, it is neither a direct test of T invariance nor a particularly useful symmetry for atomic systems since their antimatter versions are not generally

available for experiment[1].

2.1 Parity Inversion

In this section the quantum mechanical description of the parity inversion transformation is reviewed. In quantum mechanics the transformation is to be represented as an operator P which acts on wavefunctions and observables. The fundamental action of parity inversion is to invert the spatial coordinates $\boldsymbol{r} = (x, y, z)$

$$\left.\begin{array}{rcl} P : \boldsymbol{r} & \rightarrow & -\boldsymbol{r} \\ P : t & \rightarrow & t \end{array}\right\} \tag{2.1}$$

so $\boldsymbol{r}$ is called P-odd and t is P-even, and similarly the differential operator ∇ is P-odd, and $\frac{\partial}{\partial t}$ is P-even.

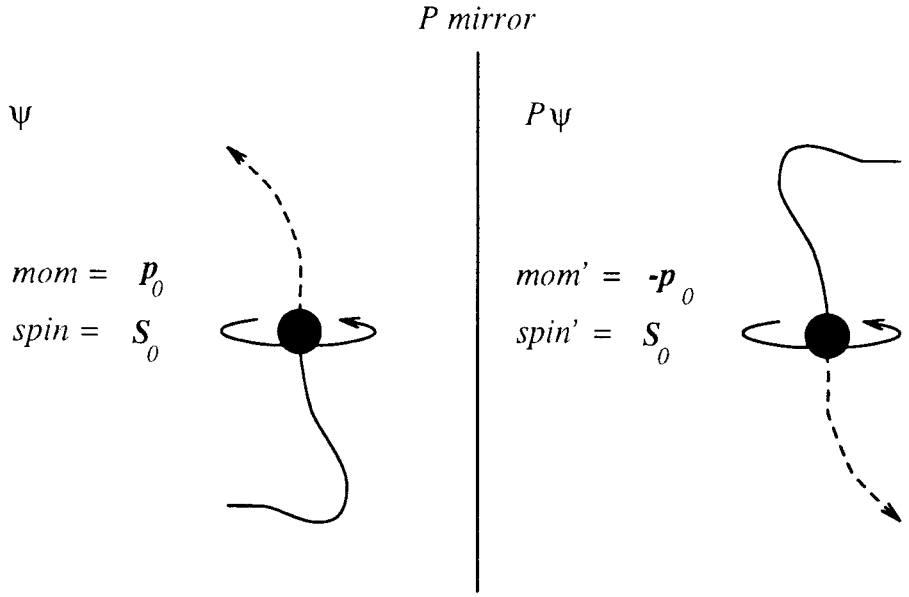


Figure 2.1: Parity mirror image of a classical particle

According to the usual rules of quantum mechanics, a state ψ is transformed by parity to a state $P\psi$ which may or may not be equivalent to the original state. The viewpoint adopted here is to investigate the properties of this new state $P\psi$ in the original coordinate system, and determine whether or not this state represents a physical state[2]. Figure 2.1 illustrates the state ψ of a classical particle, and the state $P\psi$ which is its P mirror image. The initial momentum of $P\psi$ is opposite

[1] Possible exceptions are hydrogen and muonium which have sufficiently simple antimatter images, and C eigenstate atoms such as positronium, antiprotonic hydrogen and heavy quark-antiquark systems.

[2] This viewpoint is therefore that of an *active* transformation.

to ψ, and in a parity invariant evolution, the future trajectory (shown dotted) is the inversion of the original.

The physical requirement on the transformed state $P\psi$ is that its observable quantities must be related to those of the untransformed state ψ by the coordinate transformation in eqn 2.1. For example the momentum $\boldsymbol{p} = m\frac{\partial \boldsymbol{r}}{\partial t}$ is P-odd according to the coordinate transformation. If ψ has momentum expectation value $\boldsymbol{p}_0 = \langle \psi \,|\, \boldsymbol{p} \,|\, \psi \rangle$, then $P\psi$ must have an opposite momentum, ie $\langle P\psi \,|\, \boldsymbol{p} \,|\, P\psi \rangle = -\boldsymbol{p}_0$. The angular momentum operator $\boldsymbol{L} = \boldsymbol{r} \times \boldsymbol{p}$ is P-even, so $P\psi$ has the same angular momentum expectation value as ψ. Similarly, a measurable displacement $\boldsymbol{r}_2 - \boldsymbol{r}_1$ is P-odd, lengths $|\boldsymbol{r}_2 - \boldsymbol{r}_1|$ and time intervals $t_2 - t_1$ are P-even and so on. This situation applies equally to non-stationary states which evolve so that at all times t, the observables of ψ and $P\psi$ are parity inverted. Given these physical requirements of the parity inverted state, the question of parity invariance is: *if a state ψ is inverted by the parity transformation, is the parity inverted state $P\psi$ a physical state?*

Ordinary physics is parity invariant, in that the parity inverted state does represent a physical state. If however, an interaction is present which leads to an evolution different to that of the parity inverted state, then that interaction is said to be a parity violating interaction. An example of such an interaction is in nuclear β^- decay, in which the momentum of the ejected electron with respect to the initial angular momentum of the nucleus is opposite in the inverted system. The nucleus is of definite parity symmetry, so that parity invariance requires that angular distribution of β decays $I(\theta)$ would be symmetrical about the $\theta = \pi/2$ plane, so that $I(\pi - \theta) = I(\theta)$. This is not the case in experiment. In 1957, Wu [76] cooled a ^{60}Co sample to around 0.01K inside a solenoid, so that a high proportion of the nuclear spins $\boldsymbol{\sigma}$ were aligned with the magnetic field. The angular distribution of the β particle emission was consistent with a distribution of the form

$$I(\theta) = 1 - \frac{\boldsymbol{\sigma}.\boldsymbol{p}}{E} = 1 - \frac{v}{c}\cos\theta \tag{2.2}$$

This asymmetry in $I(\theta)$ shows that the evolution of the system (namely the decay) is not parity invariant.

2.1.1 Parity in quantum mechanics

A starting point for deriving the form of the parity operator P is the assumption that the kinematic Hamiltonian - that of a free particle not subject to any interactions - is parity invariant. The form of P can be derived using only the symmetry properties of the Hamiltonian, since a parity invariant evolution is required if the states ψ and $P\psi$ are to remain parity images of each other satisfying the physical requirements specified in section §2.1. This approach also facilitates the analogous treatment of the time reversal operator.

In quantum mechanics, the equation of motion for the particle wavefunction $\psi(\boldsymbol{r}, t)$

is the Schrödinger wave equation

$$H_0\psi = i\frac{\partial\psi}{\partial t} \tag{2.3}$$

where H_0 is the kinematic Hamiltonian. According to the usual rules of quantum mechanics, the parity operator P acts on wavefunctions and operators to produce transformed quantities

$$P : \psi \rightarrow P\psi \tag{2.4}$$

$$P : Q \rightarrow PQP^{-1} \tag{2.5}$$

The equation of motion of the transformed wavefunction $P\psi$ comes from applying the parity operator to both sides of eqn 2.3

$$PH_0P^{-1}\,P\psi = Pi\frac{\partial}{\partial t}P^{-1}\,P\psi \tag{2.6}$$

Parity invariance requires the transformed state $P\psi$ to evolve according to the same equation of motion as the original state ψ. The coordinate transformations implies that $\frac{\partial}{\partial t}$ is P-even, and the kinematic Hamiltonian H_0 is by assumption P-even, so that $PiP^{-1} = i$. The latter implies that P is unitary ($P^{-1} = P^\dagger$) and hence the following matrix identity

$$\langle\psi' \,|\, Q \,|\, \psi\rangle = \left\langle P\psi' \,\middle|\, PQP^{-1} \,\middle|\, P\psi \right\rangle \tag{2.7}$$

Conventionally the parity operator is written $P = UP_0$, where P_0 inverts only explicit $\boldsymbol{r}$ and $\boldsymbol{\nabla}$, and U is a unitary operator operating on other parts (eg the spin). The form of the operator U depends on the representation to be used, which for spin $\frac{1}{2}$ particles such as an electron is the Dirac representation. The kinematic Hamiltonian in this case is given by

$$H_0 = c\boldsymbol{\alpha}.\boldsymbol{p} + (\beta - 1)mc^2 \tag{2.8}$$

where $\boldsymbol{\alpha}$ and β are Dirac matrices (see appendix D). For the H_0 to be P-even, both $\boldsymbol{\alpha}.\boldsymbol{p}$ and β must be P-even. From the coordinate transformation the momentum operator $\boldsymbol{p} = -i\hbar\boldsymbol{\nabla}$ is P-odd, so U is constrained by the required symmetries of $\boldsymbol{\alpha}$ and β

$$P\boldsymbol{\alpha}P^{-1} = U\boldsymbol{\alpha}U^\dagger = -\boldsymbol{\alpha} \tag{2.9}$$

$$P\beta P^{-1} = U\beta U^\dagger = \beta \tag{2.10}$$

An operator satisfying these conditions is $U = \beta$ so that

$$P = \beta P_0 \tag{2.11}$$

and the parity transformation of a spin $\frac{1}{2}$ Dirac wavefunction is given by

$$P : \psi(\boldsymbol{r}, t) \rightarrow P\psi(\boldsymbol{r}, t) = \beta\psi(-\boldsymbol{r}, t) \tag{2.12}$$

The phase of P is chosen so as to be Hermitian. The form of the parity operator in different representations is obtained similarly to the Dirac case. In both the Pauli (2-spinor) representation and the Klein-Gordon representations, the parity operator is just the coordinate transformation $P = P_0$.

2.1.2 The role of parity invariance in atoms and molecules

The connection in classical and quantum mechanics, between invariance of a system to a unitary transformation and an associated conservation law, is well established in standard texts [36, 57]. The conservation law implies the existence of a constant of the motion in classical mechanics, or a conserved quantum number in quantum mechanics. The electromagnetic interaction between the constituent particles in an atomic or molecular system is parity invariant[3] so the atomic Hamiltonian $H = H_0 + H_{EM}$ is P-even, and commutes with parity $[H, P] = 0$. This invariance under parity implies that there exists a parity quantum number which is part of a diagonal representation of the stationary states. If the eigenstates are not degenerate then the states are also parity eigenstates, while for non-eigenstates it follows that the states ψ and $P\psi$ are degenerate.

This has the immediate consequence that stationary states, solutions of the time independent Schrödinger equation $H\psi = E\psi$, can be chosen to be simultaneously parity and energy eigenstates. Also, from eqn 2.11 applying parity operator twice $P^2 = \beta P_0 \beta P_0 = 1$, ie the operator P is self inverse, so the overlap of a state ψ and the transformed state $P\psi$ satisfies

$$\langle \psi | P\psi \rangle = \left\langle P\psi | P^2\psi \right\rangle = \langle \psi | P\psi \rangle^* \tag{2.14}$$

The scalar product $\langle \psi | P\psi \rangle$ is real, so that if ψ is a parity eigenstate, then its parity eigenvalue is ± 1.

In complex systems such as chiral molecules there are, to a very good approximation, two essentially degenerate states ψ_L and ψ_R connected (upto an arbitrary phase) by the parity transformation. These states are *not* parity or energy eigenstates since the true eigenstates of the Hamiltonian are the superposition states $\psi_\pm \propto \psi_L \pm \psi_R$. Left isolated for long enough (assuming some damping is present) the system will evolve to the lower of $\psi_\pm$ but the characteristic time of this process can be very long. An example system is the ammonia (NH_3) molecule which has two effectively degenerate states with the nitrogen above $\psi_\uparrow$ and below $\psi_\downarrow$ the hydrogens, relative to the total angular momentum. The states $\psi_\uparrow$ and $\psi_\downarrow$ are mirror reflections since the axial vector angular momentum is P-even. The true eigenstates are the parity eigenstates $\psi_\pm \propto \psi_\uparrow \pm \psi_\downarrow$, which are not degenerate because the tunnelling between $\psi_\uparrow$

[3]The electromagnetic interaction between two particle 4-vector current densities $j^\mu(1)$ and $j^\mu(2)$ is obtained from $U(1)$ gauge invariance: $H_{EM} = j_\mu(1)A^\mu(2)$, where the field $A^\mu(2)$ is the vector potential associated with the current $j^\mu(2)$. The field and current are related by the linear wave equation $\partial_\nu \partial^\nu A^\mu = \mu_0 j^\mu$ so A^μ can be expanded in a basis of plane waves (ie photons) of the form $A^\mu(x) = A_0^\mu \exp(ix_\nu q^\nu)$ where q^μ is the 4-momentum transfer. The plane waves are solutions of the wave equation, and have current density (in mks units) $\mu_0 j^\mu = -q_\nu q^\nu A^\mu(x) = -q^2 A^\mu(x)$

$$H_{EM} = -\mu_0 j_\mu(1) \frac{1}{q^2} j^\mu(2) \tag{2.13}$$

which is manifestly P-even since the coordinates of both particles are inverted and the currents j^μ and momentum transfer q^μ are of definite P symmetry.

and ψ_1 couples the states. Their energy splitting is given by the tunnelling matrix element, $\Delta E = 2\langle\psi_L \mid H \mid \psi_R\rangle$, which is small (the tunnelling barrier for a small molecule such as ammonia is about 1Åwide). The energy splitting of the parity eigenstates can be in the MHz range for small molecules (eg 2.4MHz for ammonia), but larger molecules have essentially zero tunnelling probability, and therefore negligible splitting and an effectively infinite relaxation time.

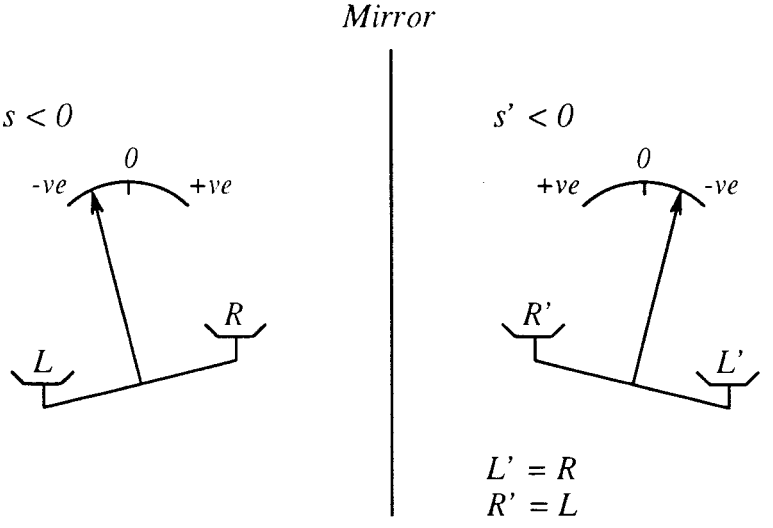


Figure 2.2: Parity balance

A thought experiment to measure parity invariance violation would be to weigh left and right handed isomers on a balance, as illustrated in figure 2.2. These could be samples of left handed and right handed sugar, which can be identified by an optical activity experiment. In the real world, on the left, the left handed isomer may be heavier than the right handed isomer, ie there is some interaction V which is different for the L and R states, so that the scale reading

$$s = \langle R \mid V \mid R\rangle - \langle L \mid V \mid L\rangle < 0 \tag{2.15}$$

The scale reading is a scalar quantity, so that in the parity image $s' = s < 0$ in the parity image, where s' is similarly defined in terms of the parity images L' and R'. In the parity mirror image, the transformed optical activity experiment shows 'left' for L' and 'right' for R'; parity violation follows from their identification with the real states as they would be measured by the untransformed optical activity experiment. These are $L' = R$ and $R' = L$, so that in the parity image balance

$$s' = s = \langle L \mid V' \mid L\rangle - \langle R \mid V' \mid R\rangle < 0 \tag{2.16}$$

and hence $V' = -V$, ie V must contain a pseudoscalar (P-odd) component.

In atoms there are, in principle, no degeneracies so the atomic states are well defined parity eigenstates, with parity eigenvalue ± 1. Eqn 2.7 yields an important

selection rule for matrix elements between parity eigenstates of operators which have *definite* parity symmetry. If an operator Q has parity symmetry $(-1)^{\pi}$, and the states are parity eigenstates with parity eigenvalues $(-1)^{\pi(\psi)}$ and $(-1)^{\pi(\psi')}$ then

$$\langle \psi' \,|\, Q \,|\, \psi \rangle = (-1)^{\pi+\pi(\psi)+\pi(\psi')} \langle \psi' \,|\, Q \,|\, \psi \rangle \tag{2.17}$$

so that the matrix element is non-zero only if $\pi(\psi) + \pi(\psi') = \pi + even$, which is an extension of Laporte's rule. For spherical tensor operators, the parity symmetry can be defined from any of the components Q^k_q since angular momentum which interrelates them is P-even. The parity symmetry of Q is given by

$$P : Q^k_q = P Q^k_q P^{-1} = (-1)^{\pi} Q^k_q \tag{2.18}$$

Examples are the spin operator $\sigma^1_0 = \sigma_z$ which has $\pi = 0$, and the spherical harmonic components C^k_q which have $\pi = k$. If Q is P-odd then π is odd and if Q is P-even then π is even. When Q is P-odd, then from eqn 2.17 it has zero diagonal matrix elements between parity eigenstates, and non-zero off-diagonal matrix elements only between opposite parity states.

2.2 Time Reversal

We now develop the quantum mechanical description of the time reversal transformation analogously to parity inversion, as an operator T acting on wavefunctions and observables. The fundamental action of time reversal is the coordinate transformation which reverses the time coordinate t but leaves $\boldsymbol{r}$ unchanged

$$\left.\begin{array}{lcl} T : t & \rightarrow & -t \\ T : \boldsymbol{r} & \rightarrow & \boldsymbol{r} \end{array}\right\} \tag{2.19}$$

The spatial coordinates $\boldsymbol{r}$ and differentials $\boldsymbol{\nabla}$ are T-even, while t and its differential $\frac{\partial}{\partial t}$ are T-odd.

The time reversal operator T transforms a state $\psi(t)$ into the state $T\psi(t)$. Here we have written the time dependence explicitly, with the original state $\psi(t)$ and the transformed state $T\psi(t)$ both evolving forwards in time. Like the previous analysis for parity, the active transformation viewpoint is used, in which the properties of the time reversed state $T\psi$ are investigated in the original coordinates to determine whether or not $T\psi$ represents a physical state. Figure 2.3 illustrates the same state ψ of the classical particle in figure 2.1, and the state $T\psi$ which is its T mirror image. The momentum and spin are both reversed, and the future (dotted) evolution of the T mirror image lies exactly along the past (solid) trajectory of the original.

The physical requirement on the transformed state $T\psi$ is that, at time t, its observable quantities are related by the coordinate transformation of eqn 2.19, to the those which the untransformed state ψ possessed at time $-t$. Taking the same example

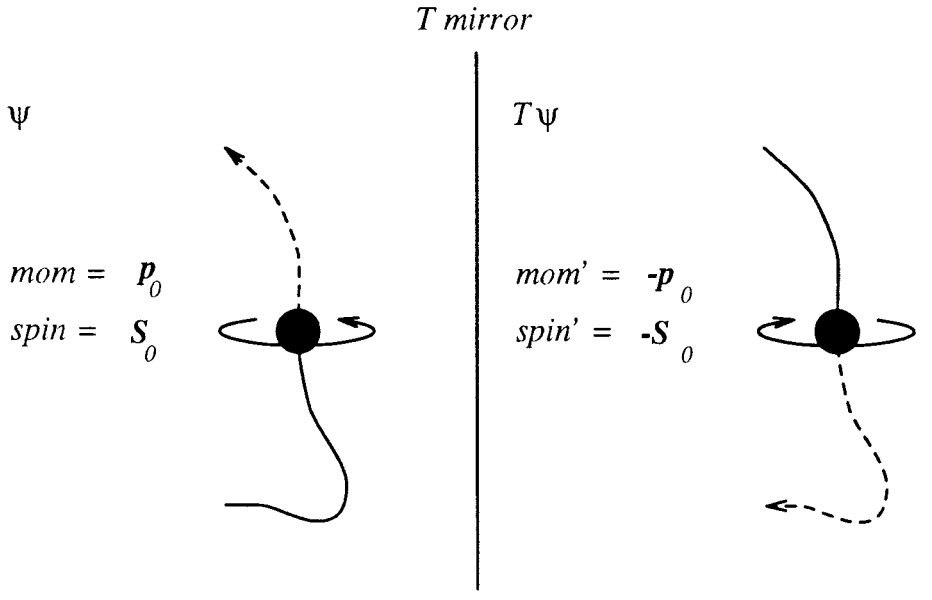


Figure 2.3: T reversal mirror image of a classical particle

as before, the momentum $\boldsymbol{p} = m\frac{\partial \boldsymbol{r}}{\partial t}$ is T-odd according to the coordinate transformation. If ψ has the momentum expectation value given by the function $\boldsymbol{p}_0(t) = \langle \psi(t) \,|\, \boldsymbol{p} \,|\, \psi(t) \rangle$, then the transformed state at time t must have the opposite momentum to that which the original state possessed at time $-t$, ie $\langle T\psi(t) \,|\, \boldsymbol{p} \,|\, T\psi(t) \rangle = -\boldsymbol{p}_0(-t)$. Other T-odd quantities such as the angular momentum operator $\boldsymbol{L} = \boldsymbol{r} \times \boldsymbol{p}$ also have the opposite expectation value at time t to that which the untransformed state had at time $-t$, and a time interval between two events $t_2 - t_1$ is T-odd because the events 1 and 2 in the evolution of ψ, occur in the reverse order in the evolution of the T reversed state $T\psi$. On the other hand, T-even quantities such as a measurable length $|\boldsymbol{r}_2 - \boldsymbol{r}_1|$, are equal to that of the original state at time $-t$ and so on. Given these physical requirements of the time reversed state, the question of time reversal invariance is: *if a state $\psi(t)$ is T reversed, does the evolution of the time reversed state $T\psi(t)$ correspond to that of a physical state?*

2.2.1 T reversal in quantum mechanics

The starting point for deriving the form of the time reversal operator T is the same assumption called upon for the parity derivation in §2.1, that the kinematic Hamiltonian is time reversal invariant. If the initial conditions are T reversed in the proper way at a defined time $t = 0$, then a T invariant evolution is sufficient to ensure the physical requirements specified in §2.2 are satisfied.

The equation of motion determining the evolution of the transformed wavefunction $T\psi$ in time, is obtained by applying the T operator to the Schrödinger wave

equation

$$TH_0T^{-1}T\psi = Ti\frac{\partial}{\partial t}T^{-1}\,T\psi \tag{2.20}$$

where H_0 is the kinematic Hamiltonian. Time reversal invariance requires the transformed state $T\psi$ to evolve according to the same equation of motion as the original state ψ. The coordinate transformations implies that $\frac{\partial}{\partial t}$ is T-odd, and the kinematic Hamiltonian H_0 is by assumption T-even, so that $TiT^{-1} = -i$. The complex phase i is T-odd and hence T must contain the complex conjugation operator K, which has the following action on wavefunctions and operators

$$K : \psi = K\psi = \psi^* \tag{2.21}$$

$$K : Q = KQK^{-1} = Q^* \tag{2.22}$$

The K operator used in this way to complex conjugate the states and operators in a matrix element, leads to the relation

$$\langle\psi' \,|\, Q \,|\, \psi\rangle = \langle\psi'^* \,|\, Q^* \,|\, \psi^*\rangle^* = \left\langle K\psi' \,\middle|\, KQK^{-1} \,\middle|\, K\psi\right\rangle^* \tag{2.23}$$

The time reversal operator is therefore *anti-unitary*, and is conventionally written $T = UKT_0$ where T_0 inverts only explicit t and $\frac{\partial}{\partial t}$, and U is a unitary operator operating on the spin parts. The unitary part UT_0 can be inserted in eqn 2.23 to give the counterpart of eqn 2.7 for the time reversal operator

$$\langle\psi' \,|\, Q \,|\, \psi\rangle = \left\langle T\psi' \,\middle|\, TQT^{-1} \,\middle|\, T\psi\right\rangle^* \tag{2.24}$$

As before, the Dirac form of the Hamiltonian H_0 determines the form of the operator U. T invariance means that H_0 is T-even, so that both $\boldsymbol{\alpha}.\boldsymbol{p}$ and β must be T-even. The momentum $\boldsymbol{p}$ is T-odd, so U is constrained by the following symmetries of $\boldsymbol{\alpha}$ and β

$$T\boldsymbol{\alpha}T^{-1} = U\boldsymbol{\alpha}^*U^\dagger = -\boldsymbol{\alpha} \tag{2.25}$$

$$T\beta T^{-1} = U\beta^*U^\dagger = \beta \tag{2.26}$$

An operator satisfying these conditions is $U = i\sigma_y$ so that

$$T = i\sigma_y KT_0 \tag{2.27}$$

and the time reversal transformation of a Dirac wavefunction is given by

$$T : \psi(\boldsymbol{r}, t) \rightarrow T\psi(\boldsymbol{r}, t) = i\sigma_y\psi(\boldsymbol{r}, -t)^* \tag{2.28}$$

The form of the T reversal operator in different representations is obtained similarly to the Dirac case. In the Pauli (2-spinor) representation $T = i\sigma_y KT_0$, and in the Klein-Gordon representation $T = KT_0$.

2.2.2 T reversal of angular momentum states and tensor operators

The properties of angular momentum eigenstates and spherical tensor operator components under time reversal are essential to T symmetry arguments in atomic physics. The angular momentum operator $\boldsymbol{j}$ is derived from rotational arguments (see appendix A.1) and its components are T-odd, therefore

$$T: j_z \rightarrow T j_z T^{-1} = -j_z \tag{2.29}$$
$$T: \boldsymbol{j}^2 \rightarrow T \boldsymbol{j}^2 T^{-1} = \boldsymbol{j}^2 \tag{2.30}$$

If an angular momentum eigenstate $|\gamma jm\rangle$ is T reversed, what are the angular momentum properties of transformed state $T|\gamma jm\rangle$? For simplicity we assume no degeneracy, in which case eqns 2.29 and 2.30 imply the transformed state is in the same γj manifold

$$j_z T|\gamma jm\rangle = -T j_z |\gamma jm\rangle = -mT|\gamma jm\rangle \tag{2.31}$$
$$\boldsymbol{j}^2 T|\gamma jm\rangle = T\boldsymbol{j}^2|\gamma jm\rangle = j(j+1)T|\gamma jm\rangle \tag{2.32}$$

so the transformed state $T|\gamma jm\rangle$ is proportional to the state $|\gamma j -m\rangle$

$$T: |\gamma jm\rangle \rightarrow T|\gamma jm\rangle = (-1)^{\phi(\gamma jm)}|\gamma j -m\rangle \tag{2.33}$$

The phase $\phi(\gamma jm)$ is not completely arbitrary. Its dependence on m is constrained by the phase relation between m states in the $|\gamma jm\rangle$ manifold. This can be seen from the operation of the ladder operators $j_\pm$ on the transformed state

$$\begin{aligned} j_\pm T|\gamma jm\rangle &= (-1)^{\phi(\gamma jm)} j_\pm |\gamma j -m\rangle \\ &= (-1)^{\phi(\gamma jm)}((j \mp m + 1)(j \pm m))^{\frac{1}{2}}|\gamma j -m \pm 1\rangle \end{aligned} \tag{2.34}$$

The ladder operators transform under T as $T j_\pm T^{-1} = -j_\mp$, so that

$$\begin{aligned} j_\pm T|\gamma jm\rangle &= -T j_\mp |\gamma jm\rangle \\ &= (-1)^{1+\phi(\gamma jm\mp 1)}((j \mp m + 1)(j \pm m))^{\frac{1}{2}}|\gamma j -m \pm 1\rangle \end{aligned} \tag{2.35}$$

To reconcile eqns 2.34 and 2.35 for all $|jm\rangle$ states, the phase $\phi(\gamma jm)$ must be of the form $p(\gamma j) - m$, where $p(\gamma j)$ is a phase chosen according to some convention. The T transformed state is therefore

$$T: |\gamma jm\rangle \rightarrow T|\gamma jm\rangle = (-1)^{p(\gamma j)-m}|\gamma j -m\rangle \tag{2.36}$$

The T reversal properties of spherical tensor components follow in an analogous way from their angular momentum properties (appendix A.2). The T reversal of

a spherical tensor component Q_q^k of definite T symmetry is proportional to the $-q$ component since

$$\left[j_z, TQ_q^kT^{-1}\right] = -T\left[j_z, Q_q^k\right]T^{-1} = -qTQ_q^kT^{-1} \quad (2.37)$$

$$\left[\boldsymbol{j}^2, TQ_q^kT^{-1}\right] = T\left[\boldsymbol{j}^2, Q_q^k\right] = j(j+1)TQ_q^kT^{-1} \quad (2.38)$$

so that the transformed component $TQ_q^kT^{-1}$ is proportional to Q_{-q}^k. As in the case of state vectors, the operation of the ladder operators constrains the phase of the transformed component so that

$$T:\ Q_q^k \rightarrow TQ_q^kT^{-1} = (-1)^{\tau-q}Q_{-q}^k \quad (2.39)$$

The phase τ is analogous to the $p(\gamma j)$ of eqn 2.36, except that it is *not* arbitrary. The $q = 0$ component is of definite Hermiticity and can have diagonal matrix elements, whose phase is determined by Hermiticity. The phase τ is in fact the T signature defined by

$$T: Q_0^k \rightarrow TQ_0^kT^{-1} = (-1)^{\tau}Q_0^k \quad (2.40)$$

Examples are the spin operator $\sigma_0^1 = \sigma_z$ and the complex phase i, which are T-odd and so have $\tau = 1$, while the spherical harmonic components C_0^k are T-even so have $\tau = 0$.

The T reversal transformation of angular momentum eigenstates (eqn 2.36) and spherical tensors (eqn 2.39), yield an explicit form of eqn 2.24 for angular momentum quantised systems

$$\left\langle \gamma' j' m' \middle| Q_q^k \middle| \gamma j m \right\rangle = (-1)^{p(\gamma' j')-p(\gamma j)+\tau} \left\langle \gamma' j' -m' \middle| Q_{-q}^k \middle| \gamma j -m \right\rangle^* \quad (2.41)$$

The implications of this result are not immediately clear, since eqn 2.41 relates different matrix elements. However, the states $|\gamma j m\rangle$ and $|\gamma j -m\rangle$ are also related to each other by 180° rotational symmetry. We define a rotation R to be a 180° rotation about the y axis. The operator R which performs this transformation is the unitary operator [18]

$$R = e^{-i\pi j_y} \quad (2.42)$$

which has the following transformation properties

$$R:\ |\gamma j m\rangle \rightarrow R|\gamma j m\rangle = (-1)^{j-m}|\gamma j -m\rangle \quad (2.43)$$

$$R:\ Q_q^k \rightarrow RQ_q^kR^{-1} = (-1)^{k-q}Q_{-q}^k \quad (2.44)$$

and the following matrix element identity for angular momentum states

$$\left\langle \gamma' j' m' \middle| Q_q^k \middle| \gamma j m \right\rangle = (-1)^{j'-j+k} \left\langle \gamma' j' -m' \middle| Q_{-q}^k \middle| \gamma j -m \right\rangle \quad (2.45)$$

The combined transformation TR is the 180° rotation R *and* T reversal T (in either order, since R and T commute) can have angular momentum eigenstates. Combining eqns 2.41 and 2.45 it can be seen that T reversal invariance implies a *phase* constraint on matrix elements

$$\left\langle \gamma' j' m' \middle| Q_q^k \middle| \gamma j m \right\rangle = (-1)^{p(\gamma' j')-p(\gamma j)+j'-j+k+\tau} \left\langle \gamma' j' m' \middle| Q_q^k \middle| \gamma j m \right\rangle^* \quad (2.46)$$

determined by the adopted convention on the wavefunction symmetry $p(\gamma j)$.

2.2.3 The role of T invariance in atoms

The electromagnetic Hamiltonian, eqn 2.13, is manifestly T-even as well as P-even, so that the basic atomic Hamiltonian is T invariant. Being anti-unitary, T reversal invariance has no associated constant of the motion or 'conservation' law, as is the case for parity. Instead we show in this section that there is an implication of twofold degeneracies in systems of half integral spin, and also consequences for physical observables.

If a stationary state ψ has T reversal $T\psi$, which may or may not be the same state, then applying eqn 2.24 to the scalar product gives

$$\langle\psi|T\psi\rangle = \left\langle T\psi|T^2\psi\right\rangle^* = \left\langle T^2\psi|T\psi\right\rangle \tag{2.47}$$

What is the value of $T^2\psi$? If ψ is a single particle Dirac state, the form of T derived in §2.2.1 gives $T^2 = (i\sigma_y K T_0)^2 = -1$, so $T^2\psi = -\psi$. If a system contains two particles, then the coordinates of both particles are inverted, ie $T = T_1 T_2$ (T_1 and T_2 commute), and in this case $T^2 = T_1^2 T_2^2 = (-1)^2 = 1$. For many particle systems, if there are an even number of particles then $T^2 = 1$, while an odd number of particles have $T^2 = -1$. This suggests a connection between T^2 and the angular momentum of the system. In general it is possible to write $T^2 = \eta$, where $\eta = 1$ for systems with *integer* spin, and $\eta = -1$ for systems with *half integer* spin. The scalar product therefore becomes

$$\langle\psi|T\psi\rangle = \eta\,\langle\psi|T\psi\rangle \tag{2.48}$$

Of interest here are systems with half integer spin ($\eta = -1$), for which the above implies $\langle\psi|T\psi\rangle = 0$, ie ψ and $T\psi$ are orthogonal states. If ψ is an energy eigenstate, then $T\psi$ is degenerate with ψ in a T invariant system, since if $H\psi = E\psi$ then $HT\psi = ET\psi$. On the other hand, if ψ and $T\psi$ are *not* energy eigenstates, they still have the same expectation energy since (H being Hermitian) $\langle\psi\,|\,H\,|\,\psi\rangle = \langle T\psi\,|\,H\,|\,T\psi\rangle$. This is the basis of Kramers' degeneracy, and being a T invariance argument, applies even when all rotational symmetry has been removed such as in an inhomogeneous crystal.

Analogously to the parity balance, a thought experiment can be constructed to measure the Kramers degeneracy between $\pm m$ angular momentum eigenstates. This is illustrated in figure 2.4 in which the $+m$ state outweighs the $-m$ state, ie the $\pm m$ states are not degenerate, with $+m$ having the higher energy. The scale reading can be written

$$s = \langle -m\,|\,V\,|\,-m\rangle - \langle +m\,|\,V\,|\,+m\rangle < 0 \tag{2.49}$$

and is a scalar quantity (in equilibrium), so the T mirror image reads $s' = s < 0$. Just as the real handedness of the parity images had to be identified, so also the identification $m' = -m$ must be made in order to identify the T violation. The scale reading in the T mirror image balance is therefore

$$s' = s = \langle +m\,|\,V'\,|\,+m\rangle - \langle -m\,|\,V'\,|\,-m\rangle < 0 \tag{2.50}$$

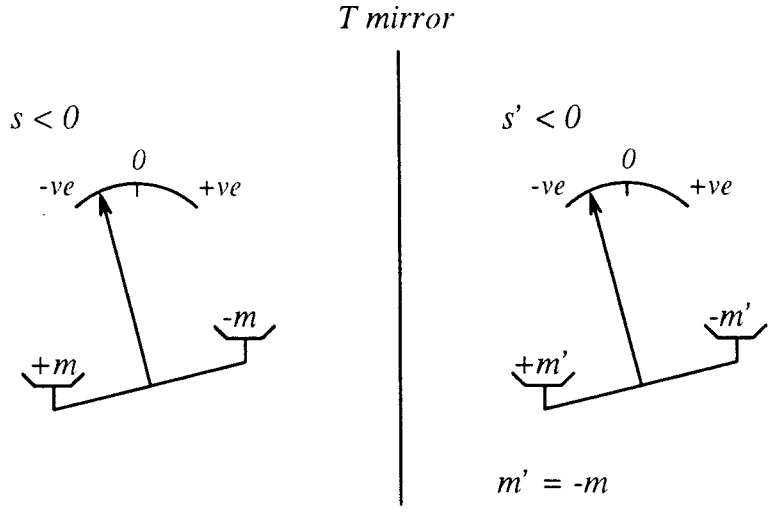


Figure 2.4: T reversal balance

and hence $V' = -V$, ie V contains a T-odd component. Although strictly a T invariance argument, a violation of Kramers' degeneracy requires parity mixed states. For isolated atoms, T-odd P-odd interactions are needed to lift the Kramers' degeneracy, while T-odd P-even interactions cannot (because these give imaginary admixtures).

T invariance, by fixing the absolute phase of diagonal and the relative phases of off diagonal matrix elements, also has consequences for physical observables. These fall into two distinct classes: expectation values, generally static observables which are diagonal matrix elements, and others which are the modulus squared of an amplitude from (one or more) off diagonal matrix elements.

The phase of diagonal matrix elements is a special case of eqn 2.46, in which the arbitrary phases $p(\gamma j)$ cancel, so that

$$\left\langle \gamma jm \left| Q_0^k \right| \gamma jm \right\rangle = (-1)^{k+\tau} \left\langle \gamma jm \left| Q_0^k \right| \gamma jm \right\rangle^* \tag{2.51}$$

Physical observables are represented in quantum mechanics as Hermitian operators, so have *real* expectations. Those operators which, through eqn 2.51, are also imaginary by T invariance must therefore be zero. Non-zero expectation values in a T invariant system have $k + \tau = \ even$, ie T-even if k is even, and T-odd if k is odd. For example, the electric charge operator q, is T-even and rank 0 so can be non-zero, while the electric dipole moment $\boldsymbol{d} = q\boldsymbol{r}$, is T-even and rank 1 so is forbidden by T invariance.

Physical quantities such as transition or decay rates depend on the modulus squared of one or more amplitudes, which are off diagonal matrix elements. If the amplitude of only one channel contributes then clearly the modulus squared is altogether independent of the phases. When more than one channel amplitude contributes, the amplitude of each process has no absolute phase constraint, but the *relative* phases are specified from T invariance by eqn 2.46. Matrix elements of two operators Q_1

and Q_2 have the same end states, so their relative phase is

$$\eta_{12} = k_2 - k_1 + \tau_2 - \tau_1 \tag{2.52}$$

independent of the phase convention. If two processes have effective operators of definite rotational and T reversal symmetry, then there can only be interference effects if the relative phase $\eta_{12} = even$, so that there can be a term linear in the components of both processes; while if $\eta_{12} = odd$, then only terms quadratic in each process can occur.

The relationships between the phases of radiative transition matrix elements is determined by this latter argument. Two processes with the same phase can give interference terms, ie linear in the dependence of both processes. If they are relatively imaginary then only quadratic terms can occur. In a T invariant system, only certain combinations of components, which are T-even under T reversal of the external fields, may occur in radiative interference.

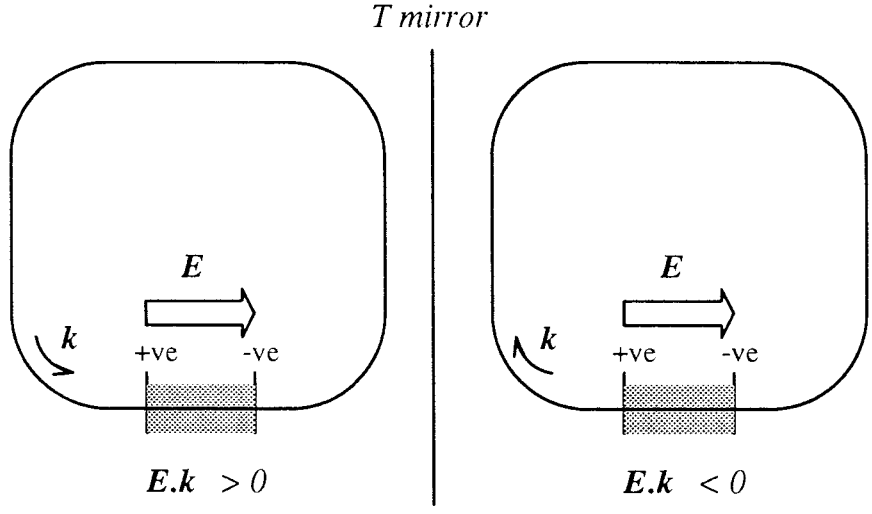


Figure 2.5: T violation in a ring interferometer

An illustration of a T-odd correlation effect is in the ring laser shown in figure 2.5. If some medium (shaded) is an optically active medium, with a refractive index proportional to $\boldsymbol{E}.\boldsymbol{k}$, then the T mirror image has the opposite contribution to the refractive index. The optical depths of the two systems are therefore different, so that their evolutions (eg of circulating wave packets) are no longer T reversals, and the system therefore violates T invariance.

2.3 P,T Phase convention

Although a variety of phase conventions are to be found in the literature, we have chosen to develop a more systematic phase convention which is particularly suited to atomic physics.

It is worth noting that the choice of phase convention does not affect any of the observable implications in the previous section. The choice of a particular wavefunction T symmetry is therefore purely a matter of convenience. Sachs [65] uses a convention equivalent to $p(\gamma j) = 1$ so that angular momentum eigenstates $|jm\rangle$ and the spherical harmonics Y_m^l have the same T reversal character, while Edmonds [28] chooses $p(\gamma j) = j$ in keeping with the spherical harmonics $\mathcal{Y}_m^l$ of Bethe [11] which differ from the usual Condon and Shortley harmonics Y_m^l by a phase $(-1)^l$.

These conventions for the T symmetry of wavefunctions involving only the angular momenta of the states lead to more complicated conventions for coupled wavefunctions, which are not equivalent to the single particle convention. In the context of atomic physics, the 'usual' phase convention is defined in terms of matrix elements, and the following phase convention makes all the ordinary atomic structure matrix elements real:

All reduced matrix elements of the spherical harmonics C^k are real.

The phase of a matrix element $M(Q)$ is given by eqn 2.46 in terms of the wavefunction phases $p(\gamma j)$ and $p(\gamma' j')$

$$M(Q)^* = (-1)^{p(\gamma' j') - p(\gamma j) + j' - j + k + \tau} M(Q) \tag{2.53}$$

where $M(Q)$ is a shorthand for some matrix element of the operator Q

$$M(Q) = \left\langle \gamma' j' m' \middle| Q_q^k \middle| \gamma j m \right\rangle \tag{2.54}$$

The matrix elements of tensors are proportional to the reduced matrix elements, with a real coefficient given by the Wigner-Eckart theorem (eqn A.52). The non-zero matrix elements of C_q^k are those satisfying the parity selection rule $\pi(\gamma) + \pi(\gamma') = k$ where $\pi(\gamma)$ and $\pi(\gamma')$ are the parity signatures of the wavefunctions $|\gamma j m\rangle$ and $|\gamma' j' m'\rangle$. A choice of phase $p(\gamma j)$ such that matrix elements, and hence the reduced matrix elements, of the C tensor are real is therefore $p(\gamma j) \equiv \pi(\gamma) - j$. In this convention, the T symmetry of the wavefunctions is

$$T\,|\gamma j m\rangle = (-1)^{\pi(\gamma) - j - m}\,|\gamma j\, -m\rangle \tag{2.55}$$

and when Q is of definite rotational, parity and T reversal symmetry then the phase of its matrix elements depend only on these signatures

$$M(Q)^* = (-1)^{k + \pi + \tau} M(Q) \tag{2.56}$$

where the operator Q has tensor rank k, P signature π and T signature τ. The matrix elements $M(C)$ are real since the harmonics C_q^k have parity signature $\pi = k$ and T signature $\tau = 0$. That the phase of the matrix elements depends only on the operator's symmetry also implies that coupled angular momentum wavefunctions have the same T reversal character as that of uncoupled wavefunctions. This is possible because the

angular momentum coupling coefficients are chosen to be real. The T symmetry of a coupled two particle wavefunction is given by applying eqn 2.55 to the expansion of product wavefunctions

$$T\,|(\gamma_1 j_1 \gamma_2 j_2) J M\rangle = (-1)^{\pi(1)+\pi(2)-J-M}\,|(\gamma_1 j_1 \gamma_2 j_2) J\,-M\rangle \tag{2.57}$$

which has the same form as eqn 2.55 since the total parity of the coupled wavefunction is $\pi(\Gamma) = \pi(1) + \pi(2)$.

2.4 P and T symmetries of external fields

In any experiment, interactions among the internal degrees of freedom are coupled to components of external fields which can form quantisation axes. So for example in a collision experiment, a contribution to some reaction cross section may depend on the spin and momentum of the incident particle, or in a decay process an ejected particle may have direction correlated with the angular momentum of the source. In the context of atomic physics experiments, external fields or axes fall into three classes

- Selection of initial (or final) momentum $\boldsymbol{p}$ (particularly in collisions), angular momentum $\boldsymbol{J}$ (atomic polarisation) and position $\boldsymbol{r}$ (atomic interferometry).
- Static fields, either electric $\boldsymbol{E}$ or magnetic $\boldsymbol{B}$, or gradients of these[4] can perturb the atomic states, affecting the energy levels or transition rates.

[4]A distinction must be made between the symmetry properties of a field at a point and of the field distribution as a whole. The intrinsic parity symmetry of a field is the symmetry of the uniform field, while the symmetry of the global field distribution may have the same or opposite symmetry (or no particular symmetry). This distinction is illustrated with following two examples which are particular electrostatic and magnetostatic fields.

An electric field $\boldsymbol{E}(\boldsymbol{r})$ is a vector field, odd under parity in that a *uniform* electric field is reversed by parity inversion P : $\boldsymbol{E} = \boldsymbol{E}' = -\boldsymbol{E}$, but the transformation of a non-uniform field is given by P : $\boldsymbol{E}(\boldsymbol{r}) = \boldsymbol{E}'(\boldsymbol{r}') = -\boldsymbol{E}(-\boldsymbol{r})$. The electric field due to an isolated unit charge (a monopole) is of the form $\boldsymbol{E}(\boldsymbol{r}) = \boldsymbol{r}/\,|\boldsymbol{r}|^3$, upto some constant. The vector $\boldsymbol{r}$ is P-odd, so the parity transformed field distribution is $\boldsymbol{E}'(\boldsymbol{r}') = -(-\boldsymbol{r})/\,|-\boldsymbol{r}|^3 = \boldsymbol{r}/\,|\boldsymbol{r}|^3$, which is the same as the untransformed field $\boldsymbol{E}(\boldsymbol{r})$. The field distribution therefore has *even* parity symmetry, reflecting the spherical symmetry of the monopole.

A further example is a magnetic field $\boldsymbol{B}(\boldsymbol{r})$ which is an axial-vector field, even under parity in that a uniform magnetic field is invariant to parity inversion P : $\boldsymbol{B} = \boldsymbol{B}' = \boldsymbol{B}$. The transformation of a non-uniform field is now P : $\boldsymbol{B}(\boldsymbol{r}) = \boldsymbol{B}'(\boldsymbol{r}') = \boldsymbol{B}(-\boldsymbol{r})$. The magnetic field distribution of a wire carrying a current $\boldsymbol{j}$ is of the form $\boldsymbol{B}(\boldsymbol{r}) = \hat{\boldsymbol{\phi}}/\,|\boldsymbol{r}|$ (in right handed cylindrical polars). The azimuthal vector $\hat{\boldsymbol{\phi}}$ is P-odd, so the parity transformed field distribution is $\boldsymbol{B}'(\boldsymbol{r}') = (-\hat{\boldsymbol{\phi}})/\,|-\boldsymbol{r}| = -\hat{\boldsymbol{\phi}}/\,|\boldsymbol{r}|$, which is the reverse of the untransformed field $\boldsymbol{B}(\boldsymbol{r})$. The field distribution therefore has *odd* parity symmetry, which can be seen also from the symmetry of the current source: the current $\boldsymbol{j}$ which is odd under parity (P : $\boldsymbol{j} = \boldsymbol{j}' = -\boldsymbol{j}$), so that in the parity transformed wire, the current is reversed and the field circulates the wire in a left handed ($-\hat{\boldsymbol{\phi}}$) sense.

- Oscillating fields inducing an atomic transition are described by a polarisation $\boldsymbol{\varepsilon}$ and wave vector $\boldsymbol{k}$, which affect the transition amplitude of atomic states depending on the angular momentum and symmetry of the transition.

In transition rates, the polarisation $\boldsymbol{\varepsilon}$ is not itself an observable quantity, since the transition rate depends on the modulus square of the matrix element. The observable therefore depends on a square of the polarisation such as the scalar product $\boldsymbol{\varepsilon}.\boldsymbol{\varepsilon}^*$ which is P and T-even, or with circular polarisation, the spin of the photon $\boldsymbol{\sigma} = i\boldsymbol{\varepsilon}\times\boldsymbol{\varepsilon}^*$ which is P-even T-odd. A summary of the P and T symmetry of various external fields and coordinates is given in table 2.1.

	P-even	P-odd
T-even	$\boldsymbol{\varepsilon}.\boldsymbol{\varepsilon}^*$	$\boldsymbol{E}, \boldsymbol{r}, \nabla$
T-odd	$\boldsymbol{B}, \boldsymbol{J}, \boldsymbol{\sigma}$	$\boldsymbol{k}, \boldsymbol{p}$

Table 2.1: Symmetries of external fields and axes

Of these, the atomic momentum $\boldsymbol{p}$ is important in collision and scattering experiments, while displacements and field gradient terms are important in atomic interferometry. These are not the subject of this thesis, which is about T violation in the internal dynamics of the atom. In this case, the only two remaining P-odd observables are the photon wave vector $\boldsymbol{k}$ and a possible electric field $\boldsymbol{E}$. Therefore T-odd P-even correlations of interest are either the product of three angular momenta from $\boldsymbol{B}, \boldsymbol{J}, \boldsymbol{\sigma}$ (a magnetic field $\boldsymbol{B}$ lifts the j_z degeneracy of atomic levels, so acts as an angular momentum operator), or else are proportional to products of $\boldsymbol{E}$ and $\boldsymbol{k}$ of which $\boldsymbol{E}.\boldsymbol{k}$ is the simplest example [69].

2.5 Violation of P and T symmetry

So far in this chapter, the form and properties of the parity and time reversal transformation have been discussed, and also the consequences of invariance to these transformations for atomic and molecular systems. The 'ordinary' interactions (namely the strong interactions and electromagnetism) are P and T invariant to current experimental accuracy. When invariance to P or T symmetry is *violated*, then the corresponding constraint on the atomic matrix elements is no longer exact. In the case of parity violation, the energy eigenstates are no longer parity eigenstates allowing non-zero matrix elements of P-odd operators. The situation is more subtle for T violation which only alters the relative phases of matrix elements. The remainder of this chapter is a discussion of the signatures of P and T violation in the context of atomic physics.

2.6 Atomic parity non-conservation

Until the 1950's it was thought that parity invariance was a natural property of physical laws but the discovery of parity violation in β decay experiments [52] showed that the weak force violates parity. The parity violating interactions are included in the standard model picture of the weak interaction. A brief overview of the parity violating weak interactions is given in appendix E and covered in more detail in standard texts [8, 62, 66].

The signatures of atomic PNC are P-odd combinations of external field components from table 2.1, for example the asymmetry in the beta decay intensity of eqn 2.2, contained a part proportional to the P-odd signature $\boldsymbol{\sigma}.\boldsymbol{p}$. As discussed in section §2.1, parity invariance in this case requires $I(\pi - \theta) = I(\theta)$ where θ is the angle between the electron spin $\boldsymbol{\sigma}$ (defined by orientation in a magnetic field) and the momentum vector $\boldsymbol{p}$ of the electron. Any part of $I(\theta) \propto \boldsymbol{\sigma}.\boldsymbol{p} \propto cos(\theta)$ is therefore evidence for violation of parity symmetry in the decay process.

Another effect of PNC on an atomic scale is exploited in 'optical rotation' experiments, which measure the contributions to the refractive index proportional to P-odd T-even combinations of fields such as $\boldsymbol{\sigma}.\boldsymbol{k}$. The polarisation vector of linearly polarised light in the medium is then rotated because the σ_+ and σ_- components propagate at different speeds. Optical rotation measurements have been made in lead [30], thallium [74] and bismuth [55]. Other correlations such as $\boldsymbol{\sigma}.\boldsymbol{E} \times \boldsymbol{B}$ in caesium [60] have been measured, all of which are consistent with the usual PNC interaction due to the Z^0 electron-nuclear interaction.

2.7 Atomic T violation

Studies of T violation in atoms have mostly concentrated on searches for a permanent electric dipole moment (edm). In particular, experimental measurements have set upper limits on the edms of the electron, neutron and also of some atoms and molecules. These upper limits can also be used to set upper limits on T-odd P-even interactions of interest in this thesis.

Interactions giving rise to edms must have T-odd P-odd symmetry, but one can also obtain limits on T-odd P-even interactions, which are the subject of this thesis, from edm measurements. Therefore a summary of the symmetry arguments is given here. A full discussion of the types and signatures of edm interactions is given by Sandars [67, 68].

For investigation of T-odd but P-even effects, we must look at the dynamics of the atom. The current work does not include scattering or collision processes, so that 'dynamics' effectively means *radiative transitions*. T invariance has definite consequences for the relative phases between the multipole transition matrix elements, through applying the results of section §2.2.3. These phase relations are equivalent to Lloyd's theorem [53], in determining which multipole transition processes can have

interference effects. It is these interference effects, which contain the T-odd P-even correlations which are the signatures of T violating but P conserving impurities in the atomic states.

2.7.1 Electric dipole moments

The permanent electric dipole moment (edm) of a quantum state is defined in terms of the *linear* shift of the energy eigenvalue as a uniform electric field $\boldsymbol{E}$ is applied. If the energy shift due to the electric field is W, then the components of the dipole moment $\boldsymbol{d}$ are defined [67] as the following

$$d_\alpha = \lim_{E \to 0} -\frac{\partial W}{\partial E_\alpha} \tag{2.58}$$

where the use of the limit $E \to 0$ removes the effect of induced dipole moments. The interaction of the dipole and electric field is $H = -\boldsymbol{E}.\boldsymbol{d}$, where the dipole moment operator for a system of charged particles i is given by $\boldsymbol{d} = \sum_i q_i \boldsymbol{r}_i$. If the states ψ are non-degenerate, then the linear energy shift of is given by $W = -\boldsymbol{E}.\langle \psi \,|\, \boldsymbol{d} \,|\, \psi \rangle$ in the $E \to 0$ limit.

The the operator $\boldsymbol{d}$ is odd under parity and even under time reversal. For a non-degenerate atomic state ψ, the edm vector defined above is just the expectation $\langle \boldsymbol{d} \rangle \equiv \langle \psi \,|\, \boldsymbol{d} \,|\, \psi \rangle$. If the state ψ is of definite parity symmetry, then the parity relation eqn 2.17 gives $\langle \boldsymbol{d} \rangle = \langle P\psi \,|\, P\boldsymbol{d}P^{-1} \,|\, P\psi \rangle = -\langle \psi \,|\, \boldsymbol{d} \,|\, \psi \rangle = -\langle \boldsymbol{d} \rangle$, which implies $\langle \boldsymbol{d} \rangle = 0$ for parity eigenstates so an atomic edm is therefore forbidden by parity invariance. Similarly, if the state ψ is a state of definite angular momentum $|jm\rangle$, then the TR reversal relation eqn 2.46 gives $\langle \boldsymbol{d} \rangle^* = -\langle \boldsymbol{d} \rangle$, which also implies $\langle \boldsymbol{d} \rangle = 0$ since Hermiticity requires $\langle \boldsymbol{d} \rangle$ to be real. Since atomic states are of definite angular momentum an edm is forbidden by T invariance as well as P invariance. This treatment is sufficient for considering non-degenerate angular momentum eigenstates even in magnetic fields, since they remain TR eigenstates. More rigorous proofs can be found in the literature which deal with the invariance requirements for edms of non-eigenstates [37, 67].

A simple picture of why an angular momentum eigenstate should not have an edm is as follows. The dipole orientation is measured relative to a quantisation axis, which can be the angular momentum vector $\boldsymbol{J}$. The energy shift W of the state in an electric field is proportional to the scalar product $\boldsymbol{J}.\boldsymbol{d}$ (ie a linear Stark effect), which has P-odd T-odd symmetry, so if the system is simultaneously a P and TR eigenstate then the energy shift W must be zero. Therefore the dipole moment is zero in the absence of P and T violation.

2.7.2 Radiative interference

In the presence of an electromagnetic field an atom may absorb or return energy to the electromagnetic field, making an atomic transition, through coupling of the atom

to the radiation field. In general terms, we show here how some radiative interference effects are a manifestation of T-odd P-even effects in the atoms [65].

The quantum mechanical description of transition theory is dealt with in many standard texts [54, 75], and summarised in chapter 5. The transition amplitudes between atomic states are matrix elements of an effective operator V^{EM}, which can be expanded

$$V^{EM} \propto i\boldsymbol{\varepsilon}.\boldsymbol{\alpha}e^{i\boldsymbol{k}.\boldsymbol{r}} = i\boldsymbol{\varepsilon}.\boldsymbol{\alpha}\left(1 + i\boldsymbol{k}.\boldsymbol{r} - \frac{1}{2!}(\boldsymbol{k}.\boldsymbol{r})^2 + \ldots\right) \tag{2.59}$$

where $\boldsymbol{k}$ is the radiation wave vector and $\boldsymbol{\varepsilon}$ is the polarisation vector. The terms in this expansion contain the multipole interactions since each factor $\boldsymbol{k}.\boldsymbol{r}$ allows atomic transitions of higher rank. The higher order terms are suppressed since the expansion coefficient $\boldsymbol{k}.\boldsymbol{r} \sim a_0/\lambda$ is small for atomic systems. The n^{th} term in the expansion contains parts of rank n and $n-1$ rotational symmetry, which are the electric $E(n)$ and magnetic $M(n-1)$ transition operators. The transition amplitude between the atomic states i and f is the matrix element $A_{fi} \equiv \left\langle f \left| V^{EM} \right| i \right\rangle$. The amplitude contribution of the n^{th} term in eqn 2.59 can be written [65]

$$A_{fi}^{(n)} \propto |\boldsymbol{k}|\,\boldsymbol{\varepsilon}.\boldsymbol{D}_{fi}^{(n)} + i\boldsymbol{\varepsilon}\times\hat{\boldsymbol{k}}.\boldsymbol{M}_{fi}^{(n-1)} \tag{2.60}$$

The two parts are the $E(n)$ and $M(n-1)$ multipole transition amplitudes

$$A_{fi}^{E(n)} \propto |\boldsymbol{k}|\,\boldsymbol{\varepsilon}.\boldsymbol{D}_{fi}^{(n)} \tag{2.61}$$

$$A_{fi}^{M(n-1)} \propto i\boldsymbol{\varepsilon}\times\hat{\boldsymbol{k}}.\boldsymbol{M}_{fi}^{(n-1)} \tag{2.62}$$

where $\boldsymbol{D}^{(n)}$ is the electric 2^n-pole moment, and $\boldsymbol{M}^{(n-1)}$ is the magnetic 2^{n-1}-pole moment, which are of the form

$$\boldsymbol{D}^{(n)} = -\frac{e}{n!}\sum_i \boldsymbol{r}_i(\hat{\boldsymbol{k}}.\boldsymbol{r}_i)^{n-1} \tag{2.63}$$

$$\boldsymbol{M}^{(n)} = -\frac{\mu_B}{(n-1)!}\sum_i \left\{\frac{1}{n+1}\left[\boldsymbol{l}_i\,,\,(\hat{\boldsymbol{k}}.\boldsymbol{r}_i)^{n-1}\right]_+ + \boldsymbol{\sigma}_i(\hat{\boldsymbol{k}}.\boldsymbol{r}_i)^{n-1}\right\} \tag{2.64}$$

for a system of electrons i.

Physical observables depend on the modulus square of the net amplitude. If the k^{th} term $A_{fi}^{(k)}$ is the leading contribution to the total transition amplitude then

$$|A_{fi}|^2 = \left|A_{fi}^{E(k)} + A_{fi}^{M(k-1)}\right|^2 \tag{2.65}$$

neglecting higher order terms, which are smaller by a factor $(\boldsymbol{k}.\boldsymbol{r})^2 \sim (a_0/\lambda)^2 \ll 1$. The interference of these two amplitudes, $A_{fi}^{E(k)}$ and $A_{fi}^{M(k-1)}$, depends on the relative phases of their matrix element parts, which are determined by the T invariance arguments of section §2.2.3. Although this argument is independent of the choice

	Rank, k	Parity, π	T reversal, τ	$k+\pi+\tau$	phase
$\boldsymbol{D}_{fi}^{(k)}$	k	k	*even*	*even*	*real*
$\boldsymbol{M}_{fi}^{(k-1)}$	$k-1$	k	*odd*	*even*	*real*

Table 2.2: Symmetries of multipole transition matrix elements

of a phase convention, it is simplest to use the phase convention of section §2.3 for convenience, in which case the phase of the $\boldsymbol{D}_{fi}^{(k)}$ and $\boldsymbol{M}_{fi}^{(k-1)}$ matrix elements follows from eqn 2.56. Table 2.2 gives the parity and T reversal signatures required, obtained from their explicit expressions, eqns 2.63 and 2.64. In this phase convention we find that all the electric and magnetic multipole moments are real.

This is effectively a proof of Lloyd's theorem that the relative phases of competing electromagnetic amplitudes equal to 0 or π [53]. Since the $\boldsymbol{D}^{(k)}$ and $\boldsymbol{M}^{(k-1)}$ matrix elements are real, it follows that the $A_{fi}^{E(k)}$ and $A_{fi}^{M(k-1)}$ amplitudes have relative phase $\pm\pi/2$. Therefore the square of the amplitude can be written

$$|A_{fi}|^2 = \left|A_{fi}^{E(k)}\right|^2 + \left|A_{fi}^{M(k-1)}\right|^2 \tag{2.66}$$

with the interference cross terms exactly cancelling

$$2\,Re\left[A_{fi}^{E(k)^*} A_{fi}^{M(k-1)}\right] = 0 \tag{2.67}$$

When T violating interactions are present, this phase relationship is broken down and the interference terms can be non-zero. In chapter 5, we shall discuss how in the presence of T violation, interference terms like eqn 2.67 can then be a measure of the atomic T impurities.

Chapter 3

T-odd P-even purity in atoms

In the previous chapter, the theory of T violation was reviewed in a slightly unusual way, by stressing the close analogies to the parity transformation. Most studies of T violation in atoms have been of T *and* P violating effects, such as edms, which can lead to shifts in the frequency of atomic transitions. The emphasis of the current work is on T but *not* P violating effects, about which relatively little is known.

We first discuss the neutral kaon system, whose decay is to date the only experimentally observed instance of CP violation. Assuming CPT, the CP asymmetry of the decay can arise from T violation in the kaons, so there is reason to suspect T violating phenomena may occur in atoms at some level.

The question to be addressed in this chapter is: *what do we know about the T purity of atomic states?* At present, there is little direct experimental information. For example, in a recent experiment the Michigan group has investigated the magnetic field induced E1 transition between the 2^3S_1 and 2^1P_1 levels in positronium [25]. They set an upper limit on the C-odd P-even matrix element $\langle 2^3P_1 \mid H_C \mid 2^1P_1 \rangle < 65\,\mathrm{MHz}$, which can be interpreted as a limit on T-odd P-even coupling via the CPT theorem. However, written as an admixture this limit corresponds to a rather weak constraint $\delta_T < 4 \times 10^{-2}$.

Indirect limits on T purity can also be obtained. We show that some T impurities can combine with atomic PNC admixtures to produce an edm. The parity mixing of atomic states due to electroweak interactions is well established and has been measured in several atomic systems (see for example a recent review by Stacey [72]), so the very precise measurements of atomic edm therefore lead to indirect limits on T-odd P-even admixtures.

Finally we discuss the expected contributions from some proposed model interactions. Khriplovich and Conti [24] have argued that the combination of T-even P-odd (PNC) electroweak and T-odd P-even processes can give T-odd P-odd effective interactions, in higher order, leading to non-zero edms. The combination of these interactions in this case is at particle physics energies, but is model dependent. Limits on the relevant coupling constants, obtained directly from the measurements of the electron and nucleon edms, can then be used to find the maximum atomic admixtures

expected from each of these model interactions.

3.1 The neutral kaon system

The neutral kaon system is so far the only experimental instance for violation of CP invariance, which is equivalent to T (assuming CPT). Since T violation has not been observed elsewhere, it is natural to include a discussion of the kaon system even though there is no immediate extension to atomic physics interactions. On the other hand, the fact that CP violation has been observed in one system indicates that one can expect to find T violation in atomic systems at some level.

3.1.1 CP properties of the kaons

The existence in the standard model of only left handed neutrinos ν_L and right handed anti-neutrinos $\bar{\nu}_R$ means the theory is not invariant under individual P and C transformations. In both cases, the neutrino and anti-neutrino states are transformed to wrong-handed states which are experimentally absent. The theory can however be invariant under the combined CP transformation which connects only the observed neutrino states.

The neutral kaons K^0 and $\bar{K}^0$ are produced in strong interactions as flavour eigenstates ($K^0 = \bar{s}d$ and $\bar{K}^0 = s\bar{d}$) which are distinguishable by their mode of production, for example $\pi^- p \rightarrow K^0 \lambda$ and $\pi^+ p \rightarrow \bar{K}^0 K^+ p$. These flavour eigenstates are connected by the CP transformation upto an arbitrary phase; conventionally the states are related by $CP\,|K^0\rangle = \left|\bar{K}^0\right\rangle$. The K mesons have mass $m_K \approx 500 MeV$ and can therefore decay to pions and leptons through the weak decay of the strange quark. The pions have mass $m_\pi \approx 140 MeV$, so 2π and 3π decays are energetically allowed. Experimentally though, it is found that the K mesons seem to be superpositions of two different particles K_L and K_S which have different decay lifetimes and decay modes

$$\tau(K_S \rightarrow 2\pi) = 0.9 \times 10^{-10} sec \tag{3.1}$$

$$\tau(K_L \rightarrow 3\pi) = 0.5 \times 10^{-7} sec \tag{3.2}$$

These different lifetimes and decay modes are a consequence of CP invariance. The low q of the pion decays indicates that the pions are produced with no net orbital angular momentum, so the 2π and 3π states are eigenstates of CP with eigenvalue $+1$ and -1 respectively. The K_L and K_S states are therefore CP eigenstates given by

$$K_S \propto K^0 + \bar{K}^0 \quad \ldots \quad CP = +1 \tag{3.3}$$

$$K_L \propto K^0 - \bar{K}^0 \quad \ldots \quad CP = -1 \tag{3.4}$$

These states are the mass eigenstates and are degenerate to first order, but have different higher order energy terms determined by CP symmetry. Their experimental

mass splitting is $m(K_L) - m(K_S) = 3.52 \times 10^{-6}\, eV$. A summary of these and other properties of the kaon system are given in many standard texts [38, 62].

3.1.2 CP violation in kaon decay

In 1964 Christenson *et al* [21] found that the K_L particle does have a small 2π decay branching ratio consistent with violation of CP symmetry. The measure of *direct* CP violation in the kaon system is usually quoted as the amplitude ratio

$$\left|\frac{A(K_L \to \pi^+\pi^-)}{A(K_S \to \pi^+\pi^-)}\right| = (2.27 \pm 0.02) \times 10^{-3} \tag{3.5}$$

Similarly, the CP violation implies a charge asymmetry in the angular distribution of leptonic decay modes of the CP eigenstate K_L to $\pi^+ e^- \bar{\nu}_e$ and $\pi^- e^+ \nu_e$. Although there is no established theory of CP violation, CP and T violation can occur in the standard model either in the Higgs sector, or as phases in the Kobayashi-Maskawa quark flavour mixing matrix, which is unitary in CP or T invariant models [38].

As well as CP violation, the leptonic and pion decay mode amplitudes can be also be used to test invariance under T and CPT symmetry independently. If the relative amplitude (and phase) of the K_L and K_S decays to some state f is $\eta_f = A(K_L \to f)/A(K_S \to f)$, then the above CP violating ratio is just $|\eta_{\pi^+\pi^-}|$. By combining the amplitude ratios of different processes, it is possible to construct quantities sensitive to T and CPT violation. One such quantity, a combination of the 2π decay ratios $\eta_{\pi^0\pi^0}$ and $\eta_{\pi^+\pi^-}$, was proposed in 1970 by Ashkin and Kabir [7]. A very detailed analysis of the invariance requirements of this and other combinations is given by Sachs [65]. Both the magnitude and phase of $\eta_{\pi^0\pi^0}$ and $\eta_{\pi^+\pi^-}$ have been measured, and these constitute a measurement of T violation, of the same magnitude as CP violation, and a limit on CPT violation consistent with zero.

3.2 T violating atomic admixtures

The K^0 meson system is to date the only experimentally observed instance of CP or T violation. Many nuclear physics experiments have investigated the T-odd P-even and T-odd P-odd contributions to scattering and decay processes with no significant difference from zero. For example, experiments have measured the contributions to the intensity of gamma decays proportional to $\Delta I \propto \boldsymbol{j}.\boldsymbol{k} \times \boldsymbol{\varepsilon}\, \boldsymbol{j}.\boldsymbol{k}\, \boldsymbol{j}.\boldsymbol{\varepsilon} \sin\eta$, where $\boldsymbol{j}$ is the nuclear spin, which are sensitive to T-odd P-even interactions. The angle η in such experiments is a direct measure of T violation, which may occur in the electromagnetic strong or weak interactions. The results of these and other such experiments essentially place an upper limit to such T violation of $\eta < 10^{-3} radians$, consistent with zero [41]. The upper limits on the imaginary parts of the β decay weak coupling constants have been obtained on the level 10^{-4} [46]. However, the measurements of

nuclear and particle physics phenomena are not simply related to atomic T violation, except by model dependent arguments.

The T-odd P-even mixing of atomic states can be expressed as the result of an effective atomic TO,PE Hamiltonian H_T. The net atomic Hamiltonian then consists of three parts

$$H_{atom} = H_0 + H_{hfs} + H_T \tag{3.6}$$

where H_0 is the full T invariant Hamiltonian for the atom apart from the hyperfine interactions in H_{hfs}, plus the additional T violating part of interest H_T. We assume that the atomic states are angular momentum eigenstates satisfying

$$H_0 \left|\gamma J M\right\rangle = E_{\gamma J} \left|\gamma J M\right\rangle \tag{3.7}$$

where γ represents all the other quantum numbers necessary to specify the state. We also assume that H_{hfs} couples in the nuclear spin so that the hyperfine states $\left|\gamma J\, F\right\rangle$ have energies

$$E_{\gamma J\, F} = E_{\gamma J} + \left\langle \gamma J\, F \right| H_{hfs} \left| \gamma J\, F \right\rangle \tag{3.8}$$

It is convenient to write the effective T-odd P-even Hamiltonian in a tensor form which distinguishes the different ranks k of the nuclear spin dependences

$$H_T = \sum_k T_N^k . U_e^k \tag{3.9}$$

where T_N^k is a nuclear moment and U_e^k acts on the electrons. The terms of each rank have very different effects on the observability of the admixtures.

The $k = 0$ part of eqn 3.9 is the result of interactions between electrons or of scalar electron-nuclear interactions. The $k \geq 1$ terms are nuclear spin dependent interactions, for which some hyperfine structure of the atomic levels must be resolved. As is standard in hyperfine structure work, we define the admixture coefficient in the stretched state $F = I + J$

$$i\delta_{T,k}^{(\gamma' J', \gamma J)} = \frac{\left\langle \gamma' J'\, F = I+J \left| T_N^k . U_e^k \right| \gamma J\, F = I+J \right\rangle}{E_{\gamma J F} - E_{\gamma' J' F}} \tag{3.10}$$

which is the imaginary admixture of $\left|\gamma' J'\, F = I+J\right\rangle$ into $\left|\gamma J\, F = I+J\right\rangle$. Admixtures for other F levels can be obtained from eqn 3.10 using standard angular momentum theory.

3.3 Model independent atomic T impurity limits

Although there have been no direct measurements of atomic T impurities in atoms, we now show that some T-odd P-even admixtures can combine with PNC admixtures to produce an atomic edm. Experimental upper limits exist for the edms of

atoms including caesium, thallium and mercury, as well as some molecules (see eg reviews [33, 70]).

It is now well known that the atomic states are parity mixed, that is they contain small admixtures of opposite parity states induced by PNC electroweak interactions

$$\left|\tilde{i}\right\rangle = |i\rangle + \sum_j \frac{|j\rangle \langle j \,|\, H_{PNC} \,|\, i\rangle}{E_i - E_j} \tag{3.11}$$

where the states $|j\rangle$ are of opposite parity to $|i\rangle$. The mixing of the states leads to non-zero electric dipole matrix elements between states i, f of the same parity

$$d_{PNC}^{(f,i)} = \left\langle \tilde{f} \,|\, \boldsymbol{d} \,|\, \tilde{i} \right\rangle \tag{3.12}$$

which is imaginary in our phase convention.

If the states i, f are also mixed by a rank k TO,PE interaction with mixing coefficient defined as eqn 3.10, then there is a real atomic edm given by

$$d_i = -i \left[\delta_{T,k}^{(i,f)} d_{PNC}^{(f,i)} - \delta_{T,k}^{(f,i)} d_{PNC}^{(i,f)} \right] = -2i \delta_{T,k}^{(i,f)} d_{PNC}^{(f,i)} \tag{3.13}$$

Thus if the PNC dipole matrix element $d_{PNC}^{(f,i)}$ is known then the TO,PE admixture is directly related to the edm measurement.

Element Transition	Tl $6p_{1/2} \rightarrow 6p_{3/2}$	Tl $6p_{1/2} \rightarrow 7p_{1/2}$	Cs $6s_{1/2} \rightarrow 7s_{1/2}$
$d_{PNC}^{(f,i)}$	-23.1 ± 3.5 $\times 10^{-11}\, iea_0$	-7.6 ± 1.4 $\times 10^{-11}\, iea_0$	-0.8252 ± 0.0184 $\times 10^{-11}\, iea_0$
EDM	1.6 ± 5 $\times 10^{-24}$ ecm	1.6 ± 5 $\times 10^{-24}$ ecm	-1.8 ± 8 $\times 10^{-24}$ ecm
$\delta_{T,k}^{(f,i)}$ limit	$\delta_{T,k=1}^{(6p_{3/2},6p_{1/2})} < 2 \times 10^{-6}$	$\delta_{T,k=0,1}^{(7p,6p)} < 6 \times 10^{-6}$	$\delta_{T,k=0,1}^{(7s,6s)} < 100 \times 10^{-6}$

Table 3.1: Experimental limits on T-odd P-even admixtures

Two elements, caesium and thallium, have had both the PNC dipole and their edms measured. The current experimental limit on the atomic edm of caesium is less than $d_{Cs} < (-1.8 \pm 8) \times 10^{-24}$ ecm [59], and thallium has a comparable limit $d_{Tl} < (-1.6 \pm 5) \times 10^{-24}$ ecm [1]. The caesium and thallium PNC dipole matrix elements have been measured directly as E1 transition amplitudes in recent PNC experiments [60, 74]. In thallium, the PNC dipoles are known for two transitions $6p_{1/2} \rightarrow 6p_{3/2}$ and $6p_{1/2} \rightarrow 7p_{1/2}$, while in caesium only the $6s_{1/2} \rightarrow 7s_{1/2}$ is known. These experimental results are shown in table 3.1 along with the resulting

limit on the TO,PE mixings for those levels obtained from eqn 3.13. In the $\frac{1}{2} \rightarrow \frac{1}{2}$ transitions, TO,PE admixtures of ranks $k = 0, 1$ can occur. The limit obtained is in fact on a sum of these terms, but if there are no 'conspiratorial' cancellations, then we can assume the limits apply to each seperately. In addition, because thallium has nuclear spin of $I = \frac{1}{2}$ only rank $k < 2$ TO,PE interactions can be present. The $6p_{1/2} \rightarrow 6p_{3/2}$ limit is therefore only on $k = 1$ interactions.

Element Transition	Hg $6s^2 \rightarrow 6s7s\,^3S_1$	Hg $6s^2 \rightarrow 6s6d\,^3D_1$	Cs $6s_{1/2} \rightarrow 5d_{3/2}$
$d_{PNC}^{(f,i)}$	$8\times10^{-11}\,iea_0$	$3\times10^{-11}\,iea_0$	$0.6\times10^{-11}\,iea_0$
EDM	0 ± 3 $\times10^{-27}$ ecm	0 ± 3 $\times10^{-27}$ ecm	-1.8 ± 8 $\times10^{-24}$ ecm
$\delta_{T,k}^{(f,i)}$ limit	$\delta_{T,k=1}^{(6s7s,6s^2)} < 3\times10^{-9}$	$\delta_{T,k=1}^{(6s5d,6s^2)} < 9\times10^{-9}$	$\delta_{T,k=1,2}^{(5d,6s)} < 120\times10^{-6}$

Table 3.2: Experimental limits on T-odd P-even admixtures

There are two disadvantages in relying entirely on present experimental data. The first is that there is no limit on rank 2 or higher terms. The second is that no use has been made of the much more precise measurement of the edm of mercury, whose ground state has measured edm less than $d_{Hg} < 3\times10^{-27}$ ecm [43]. Information about rank $k = 2$ admixtures can be obtained for caesium $6s_{1/2} \rightleftharpoons 5d_{3/2}$ mixing. Mercury has nuclear spin $I = \frac{1}{2}$ and ground state $J = 0$, so only rank $k = 1$ admixtures, such as $6s7s\,^3S_1$ or $6s5d\,^3D_1$, can give a dipole moment. Since the PNC dipoles in these cases have not been measured, we must obtain them by summing over opposite parity admixtures

$$d_{PNC}^{(f,i)} = \sum_j \left[\frac{\langle f \,|\, \boldsymbol{d} \,|\, j \rangle \langle j \,|\, H_{PNC} \,|\, i \rangle}{E_i - E_j} + \frac{\langle f \,|\, H_{PNC} \,|\, j \rangle \langle j \,|\, \boldsymbol{d} \,|\, i \rangle}{E_f - E_j} \right] \tag{3.14}$$

We estimated the caesium $6s, 5d$ PNC dipole matrix element numerically using standard methods for the single particle case, giving $d_{PNC}^{5d,6s} \sim 0.6\times10^{-11}\,iea_0$ [13, 39]. The situation is more complex in mercury: the PNC matrix elements are expected to be larger because of their marked Z dependence, but we have not attempted a serious two electron calculation. Instead we estimate the mercury d_{PNC} amplitudes from scaling the corresponding caesium PNC matrix elements, using the Bouchiat formula [17] (see appendix E), and the relevant dipole matrix elements as $\Delta E^{-\frac{1}{2}}$, where ΔE is the energy denominator, giving $d_{PNC}^{7s,6s} \sim 8\times10^{-11}\,iea_0$ and $d_{PNC}^{6d,6s} \sim 3\times10^{-11}\,iea_0$. These crude estimates are presented in table 3.2 with the implied limit on the TO,PE admixture from the edm measurement.

3.4 Model dependent atomic T impurities

T violating terms can exist in extensions of the standard model, for instance if the Kobayashi-Maskawa mass matrix is non-unitary. These forms of T-odd and CP-odd interactions between the light quarks give rise directly to the kaon decay, and indirectly to T-odd P-odd effects such as the neutron dipole moment [44]. These extensions to the standard model have been comprehensively discussed in a recent review by Peskin [63].

In section §3.2 the atomic T-odd P-even Hamiltonian was written as a sum of terms, according to the tensor rank k of the interactions with the nuclear spin. The terms of each rank are also distinct from a model interaction point of view. Model interactions are not only interesting as possible sources of T violation, but the form of the interactions also determine the 'selection' rules for T-odd P-even level mixing. The lowest rank contributions are of particular interest:

- k=0: Very little is known about scalar (ie nuclear spin independent) interactions. In the usual Dirac formalism there are no one particle scalar TO,PE operators, but two particle rank $k = 1$ interactions such as a long range electron-electron interaction[1] are possible, eg as eqn 3.15 (below), and come into this category. Likely states which would be mixed by these interactions are $6s_{1/2}$ and $ns_{1/2}$ in caesium, and $6p_{1/2}$ and $np_{1/2}$ in thallium.

- k=1: These include the fermion-fermion interactions discussed by Khriplovich and Conti [24], which arise from the exchange of an axial vector boson. In a relativistic formulation, this two particle interaction can be as (units $\hbar = c = 1$)

$$H_T = \frac{4\pi\beta_{12}}{\mu^2 - q^2}\,\frac{1}{2m}\, i\bar{\psi}_1\gamma_5\sigma^{\mu\nu}q_\nu\psi_1\;\bar{\psi}_2\gamma_\mu\gamma_5\psi_2 \tag{3.15}$$

  where q_ν is the momentum transfer and the mass m makes β_{12} a dimensionless coupling constant analogous to the electromagnetic coupling $\alpha \approx 1/137$. The mass m is conventionally taken to be the proton mass m_p. There are two important versions of this interaction: a massless boson ($\mu = 0$) would lead to a long range interaction, while a heavy boson leads to a short range interaction which becomes a contact interaction in the $q^2 \to 0$ limit. These interactions are discussed in the following sections.

- k=2: An interesting possibility is interaction of the rank 2 extension of the anapole, the *tetrapole* [15]. A nuclear tetrapole moment would interact with a gradient of the electron current near the nucleus. Existence of a non-zero nuclear tetrapole moment would be evidence for a T-odd nucleon-nucleon interaction; the properties of the tetrapole are discussed in detail in chapter 4.

[1] Khriplovich has shown that the short range interaction between identical fermions vanishes exactly in the $q^2 \to 0$ limit [48].

As well as interaction within the atom, there may also be T-odd P-even interactions between the atom as a whole and external fields. For instance, there may be an atomic tetrapole moment which would orient the atom by interacting with external currents.

Khriplovich and Conti [24] have shown that interactions such as eqn 3.15 can combine with PNC electroweak processes in higher orders, to produce T-odd P-odd effective interactions. The relevant coupling constants can then be directly related to the experimental edm measurements of the electron and nucleon. In this way, they have deduced upper limits on the coupling constants β_{12} for electron-electron, electron-quark, quark-electron (with the derivative in the electron vertex) and quark-quark interactions.

We now look at two distinct forms of eqn 3.15 taking either a heavy boson exchange, $\mu = M_X$, which we take to have mass of order $M_X \sim 100\,\mathrm{GeV}$ leading to a short range interaction, or a massless boson, $\mu = 0$ leading to a long range force. The limits deduced from particle physics considerations lead in each case, to a maximum possible contribution to the atomic TO,PE impurities expected from that interaction.

3.4.1 Short range interactions

If the exchange boson mass in eqn 3.15 is heavy compared to the nucleon mass, ie $\mu = M_X \gg m_n$, then the T-odd interaction is a short range contact interaction on the atomic scale. The coupling constant limits for these are for electron-quark $\beta_{eq} < 10^{-6}$, quark-electron $\beta_{q\epsilon} < 3\times10^{-8}$ and quark-quark interactions $\beta_{qq} < 3\times10^{-7}$ [24].

An important class of these interactions is between the atomic electrons and nucleons. There is no immediate suppression factor of the electron-quark interaction when averaging over the nucleon. From dimensional arguments, the quark vertex averaged over the nucleon wavefunction is of the same order of magnitude as a nucleon vertex [45], ie we can write

$$\bar{q}\gamma_5\sigma_{\mu\nu}q_\nu q \rightarrow \langle\psi_N \,|\, \beta\gamma_5\sigma_{\mu\nu}k_\nu \,|\, \psi_N\rangle \tag{3.16}$$

and the coupling constants for the nucleon are of the same order as for the quarks, ie $\beta_{eN} \approx \beta_{eq}$ etc.

The non-relativistic reduction of eqn 3.15 expressed in terms of electron-nucleon coupling constants β_{eN} and $\beta_{N\epsilon}$ is a rank $k = 1$ contact interaction

$$H_T = \frac{2\pi}{\mu^2 m_p}\,[\boldsymbol{\nabla}, \delta(\boldsymbol{r})]\,.\,[i\beta_{eN}\,\langle\boldsymbol{\sigma}\rangle_n \times\boldsymbol{\gamma} + \beta_{N\epsilon}\,\langle\boldsymbol{\sigma}\rangle_n\,\gamma_5] \tag{3.17}$$

Non-relativistically, the operators $[\boldsymbol{\nabla}, \delta(\boldsymbol{r})]\,\gamma_5$ and $[\boldsymbol{\nabla}, \delta(\boldsymbol{r})]\times\boldsymbol{\gamma}$ have matrix elements proportional to Z^3, and as with PNC matrix elements, relativistic effects introduce a correction factor which further favours heavy atoms.

An example admixture is of the $6p_{3/2}$ level into the $6p_{1/2}$ ground state of neutral thallium. The matrix element between these states is of order

$$\left\langle 6p_{3/2} \,\|\, H_T \,\|\, 6p_{1/2} \right\rangle \approx \frac{i\beta}{\mu^2 m_p} \frac{\hbar^4}{c^2} R(6p_{3/2}, 6p_{1/2}) \tag{3.18}$$

where the dimensional factor $\hbar^4/c^2$ gives the matrix elements units of energy, and to order of magnitude accuracy β is either of the electron-nucleon β_{eN} or nucleon-electron β_{Ne} coupling constants. R is the radial matrix element

$$R(i,j) = \left. \frac{P_i Q_j - Q_i P_j}{r^3} \right|_{r=0} \tag{3.19}$$

where $P(r)$ and $Q(r)$ are the Dirac radial wavefunctions (see appendix D), which is a well defined quantity for $p_{1/2}, p_{3/2}$ and $s_{1/2}, d_{3/2}$ matrix elements, and zero otherwise.

Element	Z	orbitals	R
^{11}B	5	$2p_{1/2}$,$2p_{3/2}$	-0.22
^{27}Al	13	$3p_{1/2}$,$3p_{3/2}$	-3.4
^{69}Ga	31	$4p_{1/2}$,$4p_{3/2}$	-83
^{115}In	49	$5p_{1/2}$,$5p_{3/2}$	-500
^{205}Tl	81	$6p_{1/2}$,$6p_{3/2}$	-7300

Table 3.3: Radial integral $R(np_{3/2}, np_{1/2})$ for ns^2np series

Table 3.3 shows values of $R(np_{3/2}, np_{1/2})$, units a_0^{-4}, calculated numerically for the $ns^2np_{1/2}$ configuration series (boron through thallium) using single particle RSCF wavefunctions in a so-called V_{n-1} potential. The thallium matrix element eqn 3.18 therefore has value of order

$$\left\langle 6p_{3/2} \,\|\, H_T \,\|\, 6p_{1/2} \right\rangle \sim i\beta \, 1.5 \times 10^{-13} \,\mathrm{eV} \tag{3.20}$$

The admixture of $6p_{3/2}$ into $6p_{1/2}$ is this matrix element over the energy denominator $E(6p_{3/2}) - E(6p_{1/2}) \approx 1\,\mathrm{eV}$ so that finally

$$\delta_T^{(6p_{3/2}, 6p_{1/2})} < 1.5 \times 10^{-13} \beta \tag{3.21}$$

This contribution is very small indeed: with coupling constant $\beta \sim 10^{-6}$, the impurity is $\delta_T \sim 10^{-19}$. The order of magnitude of these interactions is much smaller than the short range PNC interactions (namely the Z^0 exchange). This is because the short range T-odd electronic interactions are of the form $[\boldsymbol{\nabla}, \delta(\boldsymbol{r})]\,\gamma_5$, while the PNC interaction is proportional to $\delta(\boldsymbol{r})\gamma_5$. The gradient term (ie the velocity of the

electron) becomes an extra factor $Z\alpha$ in the atomic matrix element, so that the net Z dependence is the same as the spin independent PNC interaction (which is coherently enhanced in a heavy nucleus so that $Q_W \propto Z$). The ratio of the typical TO,PE matrix element to the typical spin independent PNC matrix element is therefore

$$\frac{\langle H_T \rangle}{\langle H_{PNC} \rangle} \sim \beta \frac{m_e}{m_p} \sim 10^{-9} \tag{3.22}$$

taking $\beta \sim 10^{-6}$. The factor m_e/m_p relates the mass scale of the electron to the conventional mass dimension which is was chosen in eqn 3.15 to be that of the proton[2]. The smallness of short range TO,PE interaction is related to the physics of the T violation of the heavy particle. The T violation is essentially a kinematic effect at the energy scale of the heavy particle, so that the atomic admixtures from such interactions are negligible.

3.4.2 Long range interactions

It is interesting to estimate the same corresponding matrix element for a long range interaction, although Khriplovich and Conti have argued that light atoms are preferable to heavy atoms in this case. The non-relativistic reduction of the long range interaction can be written in terms of the corresponding long range electron-nucleon and nucleon-electron coupling constants to a massless axial vector boson (units $\hbar = c = 1$)

$$H_T = \frac{1}{4m_e m_p}\left[\beta_+ \, i(\boldsymbol{\sigma}.\boldsymbol{p}\,\boldsymbol{\sigma}_N.\boldsymbol{p}\,\frac{1}{r} - \frac{1}{r}\boldsymbol{\sigma}_N.\boldsymbol{p}\,\boldsymbol{\sigma}.\boldsymbol{p}) - \beta_- \frac{\boldsymbol{\sigma}\times\boldsymbol{\sigma}_N.\boldsymbol{l}}{r^3}\right] \tag{3.23}$$

where $\beta_\pm = \beta_{eN} \pm \beta_{Ne}$. The two parts of this interaction are of about the same size; their matrix elements between atomic states are of order

$$\langle H_T \rangle \approx \frac{\beta_\pm}{4m_e m_p}\left\langle \frac{1}{r^3} \right\rangle \tag{3.24}$$

For heavy atoms the dependence of $\langle 1/r^3 \rangle$ on the atomic number is like $Z_i Z_o^2/a_0^3$ [75] where to order of magnitude accuracy $Z_i \approx Z$ and $Z_o \approx 1$. Putting $Z = 81$ (thallium) this matrix element has the value

$$\langle H_T \rangle \approx \frac{\beta_\pm}{4m_e m_p}\frac{\hbar^3 Z}{c a_0^3} \approx 2\times 10^{-3}\beta_\pm \,\mathrm{eV} \tag{3.25}$$

where the dimensional factor $\hbar^3/c$ gives the matrix element units of energy. This matrix element over the energy denominator, of order 1 eV, gives the upper bound on the T impurity from this cause

$$\delta_T^{(6p_{3/2},6p_{1/2})} < 2\times 10^{-3}\beta_\pm \tag{3.26}$$

[2]In nuclear and particle physics, the natural mass scale is of the proton, so that the T-odd coupling β is at the $m_p \sim$ 1GeV energy scale. In atomic physics, one could have chosen the electron mass m_e scale, but that would only transfer the factor m_e/m_p into the limit on the effective coupling β' (at the electron mass scale).

Assuming the long range electron-nucleon couplings are of the same order as the corresponding short range couplings $\beta_{\pm} < 10^{-6}$ then the T impurity from this interaction is of order $\delta_T \sim 2 \times 10^{-9}$. The long range T-odd interaction admixtures are not suppressed as were the short range interactions. However, although T-odd photon-fermion interactions have been investigated theoretically [47], recent work does not leave much hope for observation of TO,PE photon-fermion interactions in low energy experiments. Measurements of the two photon annihilation cross-section at 91 GeV [3, 5], indicate for example, that the T-odd (ie imaginary) part of the nuclear magnetic transition moment does not exceed about $10^{-16}\mu_N$ [49].

3.5 Summary

T violation is directly connected with the unsolved problem of CP violation through the CPT theorem. The observation of CP violation in the neutral kaons leads us to expect either T violation or (possibly) CPT violation in atomic systems at some level.

Apart from the K^0 meson observations of CP violation, very little is known either experimentally or theoretically about T-odd interactions. The lack of information about the T purity of atomic states is our motivation for studying TO,PE phenomena in this thesis. Such limits as we have come indirectly from the very precise edm measurements, which imply limits on certain T impurities. These model independent limits on T purity from scalar and nuclear spin dependent interactions, are summarised in tables 3.1 and 3.2.

The limits obtained from model interactions are more pessimistic. In particular, short range electron-nucleon interactions, eg due to exchange of an unknown heavy particle, are strongly suppressed on dimensional grounds. The T violation is essentially a kinematic effect at the energy scale of the heavy particle, so that the atomic admixtures from these are negligible. On the other hand, although TO,PE interactions between electrons and other light or massless particles are usually small in most models, there is no dimensional argument which suppresses these interactions.

While the outlook from 'standard' particle physics is pessimistic, it does not by any means exclude atomic T violation. The remainder of this thesis explores the implications of T reversal symmetry violation both for static electromagnetic moments and radiative transitions.

Chapter 4

Anapole and Tetrapole

The static electromagnetic multipole moments that non-degenerate quantum systems such as atoms may have are restricted by the requirements of P and T invariance. The charge, magnetic dipole, electric quadrupole and so on are P and T even and therefore permitted. If P and T are both violated by some interaction then electric dipole and magnetic quadrupole moments become possible.

An important feature of the above electromagnetic moments is that there are no multipole moments which are P-odd T-even or P-even T-odd. There has been much interest paid to a P-odd T-even *anapole* [77] current distribution which is a novel effect of PNC electroweak forces. In this chapter the development of anapole theory is reviewed and extended to the higher rank versions of the anapole, which are called the *toroidal* moments. In particular the quadrupole toroidal moment, the so-called *tetrapole* moment [6, 15], which is the lowest order term with T-odd P-even symmetry. The interest in this chapter is to extend the analysis of the anapole, considering the general toroidal moment field expansion and the tetrapole in particular.

4.1 Classical fields

In this section the expansion of classical scalar and vector fields by multipole rank is reviewed. The form and properties of the toroidal moments arise naturally as an extension of the theory. The formalism of the multipole expansion can be found in many standard texts [18, 26, 42].

4.1.1 Scalar fields

An arbitrary scalar field $U(\boldsymbol{r}) = U(r, \theta, \phi)$ may be expanded as a series of spherical harmonics C^l_m (Appendix B) which are spherical tensors

$$U(\boldsymbol{r}) = \sum_{l,m} U_{lm}(r) C^l_m(\theta, \phi) \tag{4.1}$$

where the coefficients of this expansion are functions $U_{lm}(r)$ of the radial coordinate

$$U_{lm}(r) = \frac{4\pi}{2l+1} \int C^l_m(\theta', \phi')^* U(r, \theta', \phi')\, d\Omega' \tag{4.2}$$

The coefficient functions $U_{lm}(r)$ transform as components of a tensor of rank l and constitute the expansion of the field $U(\boldsymbol{r})$.

4.1.2 Vector fields

An arbitrary vector field $\boldsymbol{A}(\boldsymbol{r}) = \boldsymbol{A}(r, \theta, \phi)$ may be expanded into components of suitable spherical basis

$$\boldsymbol{A}(\boldsymbol{r}) = \sum_i A_i(\boldsymbol{r})\, \boldsymbol{e}_i \tag{4.3}$$

In particular, vector fields may be expanded by tensor rank in terms of the vector spherical harmonics $\boldsymbol{C}^{(l,1)L}_{M}(\theta, \phi)$ (see Appendix B). It can be shown that the three vector fields

$$\boldsymbol{\nabla} U_{lm}(r) C^l_m \ , \ \boldsymbol{L} U_{lm}(r) C^l_m \text{ and } \boldsymbol{\nabla} \times \boldsymbol{L}\, U_{lm}(r) C^l_m \tag{4.4}$$

transform as spherical tensors of rank l [18] and are a more convenient set than the vector spherical harmonics themselves for making a multipole expansion of a vector field. Using the multipole expansion of a scalar field given by eqn 4.1, the vector field $\boldsymbol{A}(\boldsymbol{r})$ may be written in terms of three arbitrary scalar fields $f(\boldsymbol{r})$, $g(\boldsymbol{r})$ and $h(\boldsymbol{r})$

$$\boldsymbol{A}(\boldsymbol{r}) = \boldsymbol{\nabla} \times \boldsymbol{L}\, f(\boldsymbol{r}) + \boldsymbol{L}\, g(\boldsymbol{r}) + \boldsymbol{\nabla}\, h(\boldsymbol{r}) \tag{4.5}$$

where the expansion functions of the scalar fields f, g and h are $f_{lm}(r)$, $g_{lm}(r)$ and $h_{lm}(r)$. In terms of the vector field $\boldsymbol{A}(\boldsymbol{r})$ the scalars f, g and h are given by

$$\boldsymbol{\nabla}^2 \boldsymbol{L}^2 f(\boldsymbol{r}) = -\boldsymbol{L} \times \boldsymbol{\nabla} \,.\, \boldsymbol{A}(\boldsymbol{r}) \tag{4.6}$$

$$\boldsymbol{L}^2 g(\boldsymbol{r}) = \boldsymbol{L} \,.\, \boldsymbol{A}(\boldsymbol{r}) \tag{4.7}$$

$$\boldsymbol{\nabla}^2 h(\boldsymbol{r}) = \boldsymbol{\nabla} \,.\, \boldsymbol{A}(\boldsymbol{r}) \tag{4.8}$$

which follow directly from eqn 4.5 by use of vector identities.

4.2 Electrostatic fields

The electrostatic field $\boldsymbol{E}(\boldsymbol{r})$ produced by a source charge density $\rho(\boldsymbol{r})$ satisfies the Maxwell equation $\boldsymbol{\nabla} \times \boldsymbol{E} = 0$. Therefore the electric field is the gradient of the electrostatic scalar potential $\boldsymbol{E}(\boldsymbol{r}) = -\boldsymbol{\nabla}\phi(\boldsymbol{r})$, where $\phi(\boldsymbol{r})$ is the usual solution to Poisson's equation with source charge density $\rho(\boldsymbol{r})$

$$\phi(\boldsymbol{r}) = \frac{1}{4\pi\epsilon_0} \int \frac{\rho(\boldsymbol{r}')}{|\boldsymbol{r} - \boldsymbol{r}'|}\, d\tau' \tag{4.9}$$

4.2.1 Electrostatic potential multipole expansion

The classical electric multipole moments Q_{kq} of a system of point charges q_i are conventionally defined by

$$Q_{kq} = \sum_i q_i \, r_i^k \, C_q^k(\theta_i, \phi_i) \tag{4.10}$$

The potential $\phi(\boldsymbol{r})$ can be expanded using the identity

$$\frac{1}{|\boldsymbol{r} - \boldsymbol{r}'|} = \sum_{k,q} \frac{r_<^k}{r_>^{k+1}} C_q^k(\theta', \phi')^* C_q^k(\theta, \phi) \tag{4.11}$$

in eqn 4.9, to give a series of multipole components whose coefficients Q_{kq} are the generalisation of eqn 4.10 for the continuous charge density $\rho(\boldsymbol{r}')$. Outside the charge distribution, $r > r'$, the radial parts in eqn 4.11 are distinct with $r_> = r$ and $r_< = r'$. If the scalar field $\phi(\boldsymbol{r})$ is expanded into multipole components, then the coefficient functions $\phi_{kq}(r)$ defined by eqn 4.2 are

$$\phi_{kq}(r) = \frac{1}{4\pi\epsilon_0} \frac{Q_{kq}}{r^{k+1}} \tag{4.12}$$

where

$$Q_{kq} = \int \rho(\boldsymbol{r}') r'^k C_q^k(\theta', \phi') \, d\tau' \tag{4.13}$$

The external electrostatic potential is therefore

$$\phi(\boldsymbol{r}) = \frac{1}{4\pi\epsilon_0} \sum_{k,q} \frac{Q_{kq}^*}{r^{k+1}} \, C_q^k(\theta, \phi) \tag{4.14}$$

4.2.2 Electric moments of a quantum system

In a quantum system of point-like charged particles, the charge density is defined in terms of the wavefunction $\Psi(\{\boldsymbol{r}_i\})$ of the particles

$$\rho(\boldsymbol{r}) = \Psi^* \textstyle\sum_i q_i \delta(\boldsymbol{r}_i - \boldsymbol{r}) \, \Psi \tag{4.15}$$

where q_i is the charge of the i^{th} particle at position $\boldsymbol{r}_i$. The classical expression in eqn 4.10 becomes a spherical tensor operator Q_q^k

$$Q_q^k = \sum_i q_i r_i^k \, C_q^k(\theta_i, \phi_i) \tag{4.16}$$

If the wavefunction of the particles is a stationary state of definite angular momentum $\Psi_{J,M}$, then the k^{th} electric multipole moment (EK) of the distribution is defined as the expectation matrix element

$$Q_k = \left\langle \Psi_{J,J} \middle| Q_0^k \middle| \Psi_{J,J} \right\rangle \tag{4.17}$$

which is the expectation of Q_0^k in the stretched state.

4.2.3 P and T properties of the electric moments

The parity and time reversal properties of the EK multipole moments are obtained from the operator Q_0^k. The spherical harmonics C_q^k have parity $(-1)^k$ and are T even, and the scalar r ($= |\boldsymbol{r}|$) is both P and T even. Therefore Q_0^k has parity $(-1)^k$ and is T even.

The above P and T symmetry of the EK moments can be used to determine which moments are *allowed* and which *forbidden* in a static P and T invariant system. It follows from eqn 4.17 using eqn 2.7 that the odd rank moments are zero if the state Ψ is a parity eigenstate

$$Q_k = (-1)^k Q_k \tag{4.18}$$

The odd rank moments are also forbidden in a T invariant system. The Q_0^k operator is Hermitian, so the expectations Q_k are real. The reality of the expectation matrix element is defined (independent of phase convention) by eqn 2.46

$$Q_k = (-1)^k Q_k^* \tag{4.19}$$

The odd rank moments are imaginary by T invariance but also real, since the electric multipole operator Q_0^k is Hermitian, so are therefore zero.

To summarise, the electric multipole moments allowed in a P and T invariant system are EO (charge), E2, E4 ..., and the moments E1 (dipole), E3 ... are forbidden by both P and T invariance.

4.3 Magnetostatic fields

The magnetostatic field produced by a source current density $\boldsymbol{j}(\boldsymbol{r})$ satisfies Maxwell equations $\boldsymbol{\nabla}.\boldsymbol{B} = 0$ and $\boldsymbol{\nabla} \times \boldsymbol{B} = \mu_0 \boldsymbol{j}$. Using eqn 4.5 such a magnetic field may be written in terms of two scalar fields

$$\boldsymbol{B}(\boldsymbol{r}) = i\boldsymbol{\nabla} \times \boldsymbol{L} f(\boldsymbol{r}) + i\boldsymbol{L} g(\boldsymbol{r}) \tag{4.20}$$

An extra phase factor i is included in the definition so that $\boldsymbol{B}(\boldsymbol{r})$ is real, and the gradient term has been set to zero since it is not related to the current distribution $\boldsymbol{j}(\boldsymbol{r})$.

4.3.1 Magnetic field multipole expansion

The multipole expansion of the magnetic field follows from eqn 4.20 by solving for $f(\boldsymbol{r})$ and $g(\boldsymbol{r})$. These are related to the source current $\boldsymbol{j}(\boldsymbol{r})$ through eqn 4.6 by taking the curl of eqn 4.20

$$\boldsymbol{\nabla}^2 \boldsymbol{L}^2 f(\boldsymbol{r}) = i\mu_0 \boldsymbol{L}.\boldsymbol{j}(\boldsymbol{r}) \tag{4.21}$$

$$\boldsymbol{L}^2 g(\boldsymbol{r}) = -\mu_0 \boldsymbol{r}.\boldsymbol{j}(\boldsymbol{r}) \tag{4.22}$$

Equation 4.21 is Poisson's equation for $\boldsymbol{L}^2 f$ with solution

$$\boldsymbol{L}^2 f(\boldsymbol{r}) = -\frac{i\mu_0}{4\pi}\int \frac{\boldsymbol{L}'.\boldsymbol{j}(\boldsymbol{r}')}{|\boldsymbol{r}-\boldsymbol{r}'|}\,d\tau' \tag{4.23}$$

From eqns 4.22 and 4.23, the different nature of the f and g parts of the magnetic field is apparent. Mathematically, the $\boldsymbol{\nabla}^2$ in eqn 4.21 propagates $f(\boldsymbol{r})$ outside the region of the source, while $\boldsymbol{L}^2$ does not have this effect. The f fields are therefore non-zero outside the region of the source current and are the 'regular' magnetic multipole fields; the g fields only exist where the source current exists and are the 'local' or *toroidal* multipole fields. Eqns 4.23 and 4.22 are linear, so $f(\boldsymbol{r})$ and $g(\boldsymbol{r})$ may be obtained by expansion in spherical harmonics, which are eigenvalues of $\boldsymbol{L}^2$, using eqn 4.1. The series expansion coefficients $f_{kq}(r)$ and $g_{kq}(r)$ are then obtained using the orthogonality relation (eqn B.6) [15]

$$f_{kq}(r) = -\frac{i\mu_0}{4\pi}\frac{1}{k(k+1)}\int \frac{r_<^k}{r_>^{k+1}}\,(-1)^q C^k_{-q}(\theta',\phi')\,\boldsymbol{L}'.\boldsymbol{j}(\boldsymbol{r}')\,d\tau' \tag{4.24}$$

$$g_{kq}(r) = -\frac{\mu_0}{4\pi}\frac{2k+1}{k(k+1)}\int \frac{\delta_{r',r}}{r'^2}\,(-1)^q C^k_{-q}(\theta',\phi')\,\boldsymbol{r}'.\boldsymbol{j}(\boldsymbol{r}')\,d\tau' \tag{4.25}$$

The expressions 4.24 and 4.25 can now be used to expand the'regular' and 'local' parts of the magnetic field

$$\boldsymbol{B}(\boldsymbol{r}) = \boldsymbol{B}_{reg}(\boldsymbol{r}) + \boldsymbol{B}_{local}(\boldsymbol{r}) \tag{4.26}$$

where

$$\boldsymbol{B}_{reg}(\boldsymbol{r}) = \sum_{k,q} i\boldsymbol{\nabla}\times\boldsymbol{L}\,C^k_q(\theta,\phi)\,f_{kq}(r) \tag{4.27}$$

$$\boldsymbol{B}_{local}(\boldsymbol{r}) = \sum_{k,q} i\boldsymbol{L}\,C^k_q(\theta,\phi)\,g_{kq}(r) \tag{4.28}$$

The 'regular' fields are those of the usual magnetostatic multipole moments, while the 'local' fields are those of the toroidal multipole moments.

4.3.2 The regular magnetic moments

The magnetic multipole moments M_{kq} of a classical current source $\boldsymbol{j}(\boldsymbol{r})$ in a static distribution of magnetisation $\boldsymbol{M}(\boldsymbol{r})$, is conventionally defined by [18]

$$M_{kq} = \frac{i}{k+1}\int r^k C^k_q(\theta,\phi)\,\boldsymbol{L}.\boldsymbol{J}(\boldsymbol{r})\,d\tau \tag{4.29}$$

where $\boldsymbol{J} = \boldsymbol{j} + \boldsymbol{M}$. In a quantum system the current $\boldsymbol{j}$ is associated with the orbital motion of charged particles, and the magnetisation $\boldsymbol{M}$ with their spin.

Outside the region of the source current $r > r'$ the magnetic field contains only the $f_{kq}(r)$ parts. From eqns 4.27, 4.24 and 4.29 the magnetic field is

$$\boldsymbol{B}(\boldsymbol{r}) = \frac{i\mu_0}{4\pi} \sum_{k,q} \frac{1}{k} M^*_{kq} \boldsymbol{\nabla} \times \boldsymbol{L} \frac{C^k_q(\theta,\phi)}{r^{k+1}} \tag{4.30}$$

The following identity splits the magnetic field into two parts

$$\boldsymbol{\nabla} \times \boldsymbol{L} \frac{C^k_q}{r^{k+1}} = -ik\boldsymbol{\nabla} \frac{C^k_q}{r^{k+1}} - i\boldsymbol{r}\boldsymbol{\nabla}^2 \frac{C^k_q}{r^{k+1}} \tag{4.31}$$

The latter part may be dropped outside the source current, since it is only non-zero at $r = 0$. This leaves a field which is the gradient of a scalar potential $V_M(\boldsymbol{r})$ analogous in form to the electrostatic potential

$$\boldsymbol{B}(\boldsymbol{r}) = -\boldsymbol{\nabla} V_M(\boldsymbol{r}) \tag{4.32}$$

$$V_M(\boldsymbol{r}) = -\frac{\mu_0}{4\pi} \sum_{k,q} \frac{M^*_{kq}}{r^{k+1}} C^k_q(\theta,\phi) \tag{4.33}$$

4.3.3 Magnetic moments of a quantum system

In a quantum system of moving particles, the current density and magnetisation are defined in terms the wavefunction $\Psi(\{\boldsymbol{r}_i\})$ of the particles. The charge density and magnetisation are separate only in the non-relativistic limit [34]. For a single particle of mass m and charge q, the net current $\boldsymbol{J}(\boldsymbol{r})$ in a state $\psi(\boldsymbol{r})$ is given by

$$\begin{aligned} \boldsymbol{J}(\boldsymbol{r}) &= \boldsymbol{j}(\boldsymbol{r}) + \boldsymbol{M}(\boldsymbol{r}) \\ &= -i\frac{q\hbar}{2m} g_l \left(\psi^* \boldsymbol{\nabla} \psi - \psi \boldsymbol{\nabla} \psi^*\right) + \frac{q\hbar}{2m} g_s \psi^* \boldsymbol{\nabla} \times \boldsymbol{S}\, \psi \end{aligned} \tag{4.34}$$

where g_l, g_s are the particle orbital and spin Landé factors.

It can be shown that the contributions from the two gradient terms are equivalent, and the classical expression given by eqn 4.29 then becomes a spherical tensor operator M^k_q

$$M^k_q = \frac{q\hbar}{2m} \boldsymbol{\nabla} \left(r^k C^k_q(\theta,\phi)\right) \left[\frac{2}{k+1} g_l \boldsymbol{L} + g_s \boldsymbol{S}\right] \tag{4.35}$$

If the wavefunction of the particles is a stationary state of definite angular momentum $\Psi_{J,M}$, then the k^{th} magnetic multipole moment (MK) of the distribution is defined as the expectation matrix element

$$M_k = \left\langle \Psi_{J,J} \middle| M^k_0 \middle| \Psi_{J,J} \right\rangle \tag{4.36}$$

which is the expectation of M^k_0 in the stretched state.

4.3.4 The toroidal magnetic moments

The magnetic fields associated with the g solutions of eqn 4.22 do not propagate out from the source currents; these fields have been called the 'local' fields [14]. The multipole moments which characterise a multipole expansion of these fields are the toroidal moments. It is convenient to derive the multipole expansion of the whole interaction between the local fields and external currents, rather than a direct expansion of the fields. The interaction energy for a classical system can be written in terms of the magnetic vector potential of the local fields, due to an internal current distribution $\boldsymbol{j}_i(\boldsymbol{r})$, and an external current distribution $\boldsymbol{j}_e(\boldsymbol{r})$ in the following form

$$W = -\int \boldsymbol{j}_e(\boldsymbol{r}).\boldsymbol{A}_{local}(\boldsymbol{r})d\tau \tag{4.37}$$

where $\boldsymbol{A}_{local}(\boldsymbol{r})$ is the vector potential due to the internal currents. The vector potential, defined by $\boldsymbol{B} = \boldsymbol{\nabla} \times \boldsymbol{A}$ follows from eqn 4.28 since $\boldsymbol{L} = -i\,\boldsymbol{r} \times \boldsymbol{\nabla} = i\,\boldsymbol{\nabla} \times \boldsymbol{r}$

$$\boldsymbol{A}_{local}(\boldsymbol{r}) = \sum_{k,q} -\boldsymbol{r}\, C_q^k(\theta,\phi)\, g_{kq}(r) \tag{4.38}$$

where the radial functions $g_{kq}(r)$ are given by eqn 4.25. The toroidal moments are obtained from eqn 4.37 recast as a sum of multipole interactions. The toroidal moment of rank k interacts with a k^{th} gradient of the external current density. The Taylor expansion of the external current density near $r = 0$ is given by

$$\boldsymbol{j}_e(\boldsymbol{r}) = \sum_l \int \delta(\boldsymbol{r}')\, \frac{1}{l!}\, (\boldsymbol{r}.\boldsymbol{\nabla}')^l\, \boldsymbol{j}_e(\boldsymbol{r}')\, d\tau' \tag{4.39}$$

where the three dimensional delta function is related to the one dimensional delta function of the radial coordinate by

$$\delta(\boldsymbol{r}) = \frac{\delta(r)}{4\pi r^2} \tag{4.40}$$

The classical energy (eqn 4.37) becomes

$$W = \sum_{k,q,l} \frac{1}{l!} \iint C_q^k(\theta,\phi)\, g_{kq}(r)\, \delta(\boldsymbol{r}')\, (\boldsymbol{r}.\boldsymbol{\nabla}')^l\, \boldsymbol{r}.\boldsymbol{j}_e(\boldsymbol{r}')\, d\tau\, d\tau' \tag{4.41}$$

To separate the $\boldsymbol{r}$ and $\boldsymbol{r}'$ integrals, the vectors can be recoupled to a tensor form. The l^{th} term in the above expansion is the leading term of the rank $l+1$ interaction, other ranks present in the recoupling are much smaller than corresponding contributions from lower order Taylor expansion terms. Therefore only the rank $l+1$ coupled part need be retained and we may put

$$(\boldsymbol{r}.\boldsymbol{\nabla}')^l\, \boldsymbol{r}.\boldsymbol{j}_e(\boldsymbol{r}') = \sum_m (-1)^m\, (\boldsymbol{r}\ldots\boldsymbol{r})^{l+1}_{-m} \cdot \left((\boldsymbol{\nabla}'\ldots\boldsymbol{\nabla}')^l j_e(\boldsymbol{r}')\right)^{l+1}_m \tag{4.42}$$

where the notation $(\boldsymbol{A}\ldots\boldsymbol{A})^l$ represents the stretched recoupling of l vectors $\boldsymbol{A}$ to rank l. Since $(\boldsymbol{r}\ldots\boldsymbol{r})^{l+1}_{-m} \propto r^{l+1}\,C^{l+1}_{-m}$, the angular part of the integral in eqn 4.41 is only non-zero for $l = k-1, m = q$. The $\boldsymbol{r}$ and $\boldsymbol{r}'$ parts then separate

$$W = \sum_{k,q} \frac{(-1)^q}{(k-1)!} \int (\boldsymbol{r}\ldots\boldsymbol{r})^k_{-q}\; C^k_q(\theta,\phi)\, g_{kq}(r)\, d\tau \int \delta(\boldsymbol{r}') \left((\boldsymbol{\nabla}'\ldots\boldsymbol{\nabla}')^{k-1} j_e(\boldsymbol{r}')\right)^k_q d\tau' \tag{4.43}$$

The first integral depends on the $g_{kq}(r)$ functions which contain the internal currents. Substituting for $g_{kq}(r)$ from eqn 4.25 the above becomes

$$-\frac{\mu_0}{4\pi}\frac{2k+1}{k(k+1)} \iint (\boldsymbol{r}\ldots\boldsymbol{r})^k_{-q}\; C^k_q(\theta,\phi)\frac{\delta_{r',r}}{r'^2}\,(-1)^q C^k_{-q}(\theta',\phi')\,\boldsymbol{r}'.\boldsymbol{j}_i(\boldsymbol{r}')\, d\tau\, d\tau' \tag{4.44}$$

which reduces to

$$-\mu_0 \frac{1}{k(k+1)} \int (\boldsymbol{r}\ldots\boldsymbol{r})^k_{-q}\; \boldsymbol{r}.\boldsymbol{j}_i(\boldsymbol{r})\, d\tau \tag{4.45}$$

The second integral is a $(k-1)^{th}$ derivative of the current density at the origin, which is assumed to be regular over the region of the internal currents $\boldsymbol{j}_i(\boldsymbol{r})$, and so is just the value of that derivative at the origin

$$\left((\boldsymbol{\nabla}\ldots\boldsymbol{\nabla})^{k-1} j_e\right)^k_q (0) \tag{4.46}$$

The classical energy is now in the form of a sum of multipole interactions between the internal current density $\boldsymbol{j}_i(\boldsymbol{r})$ and coupled gradients of the external current density $\boldsymbol{j}_e(\boldsymbol{r})$

$$W = -\sum_{k,q} \frac{\mu_0(-1)^q}{(k+1)!} \int_i (\boldsymbol{r}\ldots\boldsymbol{r})^k_{-q}\; \boldsymbol{r}.\boldsymbol{j}_i(\boldsymbol{r})\, d\tau\; \left((\boldsymbol{\nabla}\ldots\boldsymbol{\nabla})^{k-1} j_e\right)^k_q (0) \tag{4.47}$$

To simplify the form of eqn 4.47, the stretched recouplings can be reduced to single tensors. The $(\boldsymbol{r}\ldots\boldsymbol{r})^k_q$ is proportional to $r^k C^k_q$ and $\left(\boldsymbol{\nabla}\ldots\boldsymbol{\nabla}^{k-1}\boldsymbol{j}_i\right)^k_q(0)$ can be rewritten in terms of a spherical delta function $\delta^k_q(\boldsymbol{r})$ (Appendix C)

$$(\boldsymbol{r}\ldots\boldsymbol{r})^k_q = \left(\frac{k!}{(2k-1)!!}\right)^{\frac{1}{2}} r^k C^k_q(\theta,\phi) \tag{4.48}$$

$$\left((\boldsymbol{\nabla}\ldots\boldsymbol{\nabla})^{k-1} j_e\right)^k_q (0) = ((k-1)!(2k-3)!!)^{\frac{1}{2}} \int_e \left(\delta^{k-1}(\boldsymbol{r})\boldsymbol{j}_e(\boldsymbol{r})\right)^k_q d\tau \tag{4.49}$$

Also from current conservation $\boldsymbol{\nabla}.\boldsymbol{j} = 0$

$$\boldsymbol{\nabla}.r^{k+2}C^k_q\boldsymbol{j} = r^k C^k_q\,\boldsymbol{r}.\boldsymbol{j} + \frac{1}{2}(k(2k-1))^{\frac{1}{2}} r^{k+1}\left(C^{k-1}\boldsymbol{j}\right)^k_q \tag{4.50}$$

Putting these into eqn 4.47 the interaction energy can be written in terms of the toroidal moments T_{kq}

$$W = -\frac{\mu_0}{4\pi} \sum_{k,q} T^*_{kq} \int_e \left(\delta^{k-1}(\boldsymbol{r}) \boldsymbol{j}_e(\boldsymbol{r})\right)^k_q \, d\tau \tag{4.51}$$

where

$$T_{kq} = -\frac{2}{k+1} \int_i \pi r^{k+1} \left(C^{k-1} \boldsymbol{j}_i(\boldsymbol{r})\right)^k_q \, d\tau \tag{4.52}$$

defines the toroidal moment components of the internal current distribution.

4.3.5 Toroidal moments of a quantum system

As with the regular magnetic moments, in a quantum system the classical energy becomes a matrix element. In the case of the toroidal moments it is simple to use the relativistic form of the internal current density in eqn 4.52

$$\boldsymbol{j}_i(\boldsymbol{r}) = qc \, \psi^\dagger \boldsymbol{\alpha} \, \psi \tag{4.53}$$

where ψ is a Dirac single particle state and q the particles' charge. If the wavefunction is in a stationary state of definite angular momentum $\psi_{j,m}$ then only the $q = 0$ toroidal moment is non-zero. The classical definition, eqn 4.52, becomes a spherical tensor operator T^k_q

$$T^k_q = -\frac{2qc}{k+1} \pi r^{k+1} \left(C^{k-1} \boldsymbol{\alpha}\right)^k_q \tag{4.54}$$

As for the regular magnetic moments, the k^{th} toroidal multipole moment (TK) of a wavefunction of definite angular momentum $\Psi_{J,M}$, is defined as the expectation matrix element

$$T_k = \left\langle \Psi_{J,J} \middle| T^k_0 \middle| \Psi_{J,J} \right\rangle \tag{4.55}$$

which is the expectation of T^k_0 in the stretched state.

4.3.6 P and T properties of magnetic moments

	Parity	T reversal
M^k_0	$(-1)^{k+1}$	Odd
T^k_0	$(-1)^k$	Odd

Table 4.1: P and T symmetries of magnetic multipole operators

The parity and time reversal properties of the regular MK magnetic multipole moments given by eqn 4.35, and the local TK toroidal multipole moments given by eqn 4.54, are obtained from the P and T symmetry of the operators M_0^k and T_0^k. The current operator $\boldsymbol{\alpha}$ is P-odd T-odd, the gradient operator $\boldsymbol{\nabla}$ is P-odd T-even and the angular momentum operators $\boldsymbol{L}$ and $\boldsymbol{S}$ are P-even T-odd. Therefore the operators M_0^k and T_0^k have the symmetries under P and T shown in table 4.1. As with the electric multipoles the P and T symmetry determine which multipole field distributions may exist in a P and T invariant system.

Parity symmetry, from eqn 2.7, requires the even MK moments and the odd TK moments to be zero since

$$M_k = (-1)^{k+1} M_k \tag{4.56}$$

$$T_k = (-1)^k T_k \tag{4.57}$$

while time reversal symmetry, from eqn 2.46 requires the even MK moments and the even TK moments to be imaginary and therefore zero, since Hermiticity requires these to be real

$$M_k^* = (-1)^{k+1} M_k \tag{4.58}$$

$$T_k^* = (-1)^{k+1} T_k \tag{4.59}$$

	P Invariant	P Violating
T Invariant	E0 (charge), M1, E2...	T1 (anapole), T3...
T Violating	T2 (tetrapole), T4...	E1 (electric dipole), M2...

Table 4.2: Invariance requirements of electromagnetic multipoles

The MK magnetic multipole moments allowed in a P and T invariant system are therefore M1 (magnetic dipole), M3 ..., and the moments M2, M4 ...are forbidden by both P and T invariance. None of the TK multipole moments are allowed in a P and T invariant system; the even TK moments conserve P and violate T invariance, while the odd TK moments violate P and conserve T invariance. The lowest order current distributions, which are the MK and TK sources of each symmetry, are shown in figure 4.1.

The symmetries of all the multipole moments, including the EK moments from section §4.2.3, are summarised in table 4.2 which places the EK, MK and TK static electromagnetic moments by their P and T invariance requirements. In a P and T invariant system, only the E0 (charge), M1 (magnetic dipole), E2 and so on can have non zero values. The existence of any of the other moments is therefore evidence for corresponding P and/or T violating internal interactions.

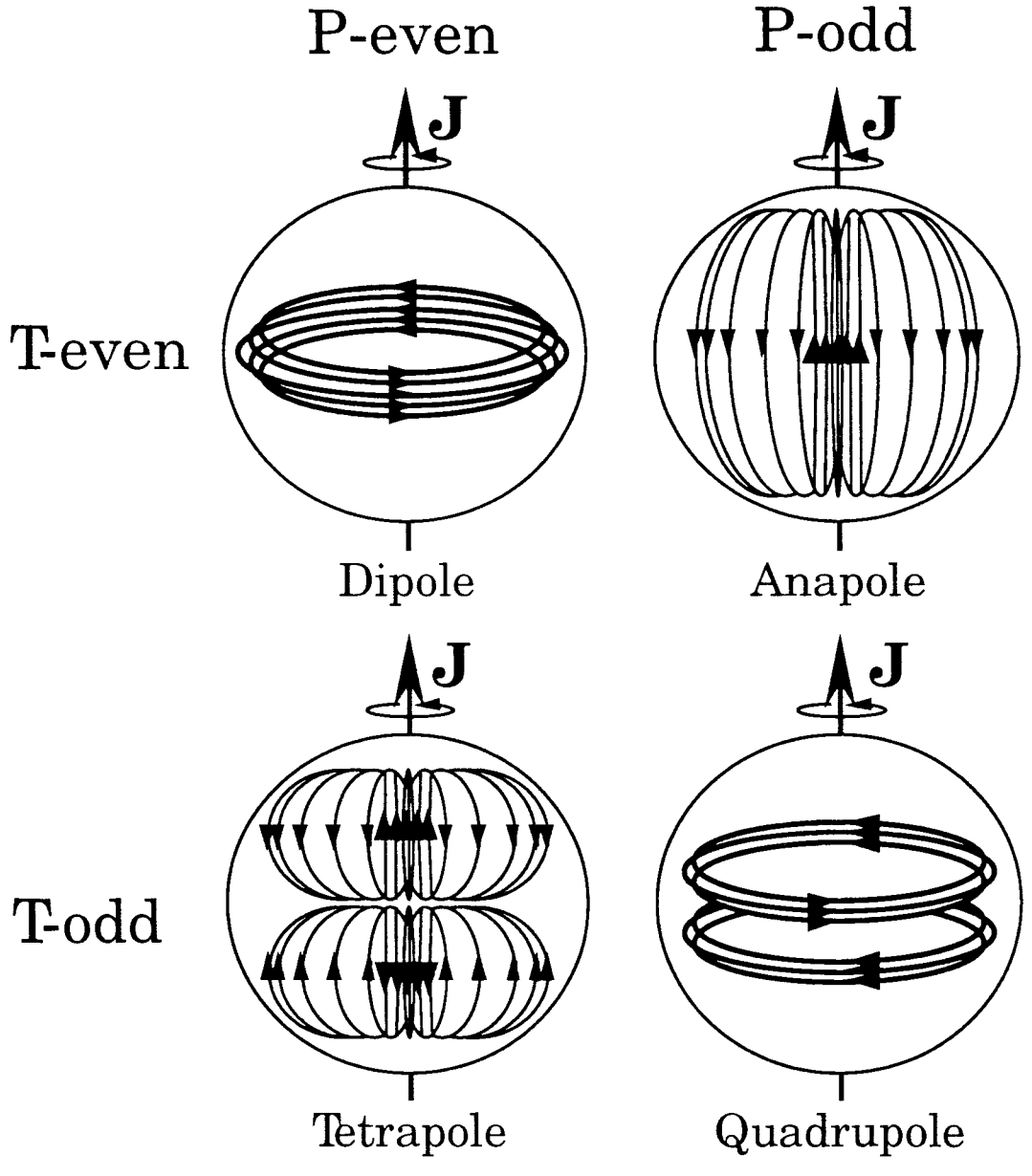


Figure 4.1: Current distribution symmetries

4.4 The electron-nuclear toroidal moment interaction

The classical interaction of an atomic electron with the nuclear toroidal moments given by eqn 4.51, becomes a matrix element M_{fi} between two electronic states i and f with the external current density defined by

$$\boldsymbol{j}_e(\boldsymbol{r}) = -ec\,\psi_f^\dagger(\boldsymbol{r})\boldsymbol{\alpha}\psi_i(\boldsymbol{r}) \tag{4.60}$$

If the electronic states are electronic angular momentum states $\psi_{j,m}$ and $\psi_{j',m'}$ and the nucleus is in a state of definite nuclear spin $\Psi_{I,M}$ then the interaction matrix element of the toroidal moments with the electron is diagonal in j so $m' = m$

$$M = \frac{ec\mu_0}{4\pi}\sum_k \left\langle \Psi_{I,M} \left| T_0^k \right| \Psi_{I,M} \right\rangle \left\langle \psi_{j',m} \left| \left(\delta^{k-1}(\boldsymbol{r})\boldsymbol{\alpha}\right)_0^k \right| \psi_{j,m} \right\rangle \tag{4.61}$$

where from the Wigner Eckart theorem, the nuclear part of the matrix element is proportional to the toroidal moment T_k.

When the electron and nucleus are not in separate spin eigenstates but in a coupled state of the electronic and nuclear spins, the effective operator is nuclear spin dependent. The toroidal moments are aligned with the nuclear spin $\boldsymbol{I}$ so the nuclear moment operator T_q^k can be replaced by an effective operator

$$T_q^k = \frac{\left\langle II \left| T_0^k \right| II \right\rangle}{\left\langle II \left| \mathcal{I}_0^k \right| II \right\rangle} \mathcal{I}_q^k \tag{4.62}$$

where $\left\langle II \left| T_0^k \right| II \right\rangle = T_k$ is the k^{th} toroidal moment, and $\mathcal{I}^k$ is some k^{th} rank tensor of the nuclear spin, such as $(\boldsymbol{I}\ldots\boldsymbol{I})^k$, but is chosen here for convenience to be normalised so that $\left\langle II \left| \mathcal{I}_0^k \right| II \right\rangle = 1$. Since the coupled wavefunctions are superpositions of decoupled wavefunctions, each having a matrix element of the form of eqn 4.61, the matrix element between coupled states $\psi_{(jI)f,m}$ and $\psi_{(j'I)f,m}$ is

$$M = \frac{ec\mu_0}{4\pi}\sum_k T_k \left\langle \psi_{(j'I)f,m} \left| \mathcal{I}^k . \left(\delta^{k-1}(\boldsymbol{r})\boldsymbol{\alpha}\right)^k \right| \psi_{(jI)f,m} \right\rangle \tag{4.63}$$

The k^{th} toroidal moment interaction on the electron is the perturbation term

$$V^{TK} = \frac{ec\mu_0}{4\pi} T_k\, \mathcal{I}^k . \left(\delta^{k-1}(\boldsymbol{r})\boldsymbol{\alpha}\right)^k \tag{4.64}$$

The form of eqn 4.64 determines the selection rules for perturbation admixtures of the electronic states by a nuclear toroidal moment. These come from the electronic part of the matrix element

$$\left\langle \psi_{n',\kappa',m'} \left| \left(\delta^{k-1}(\boldsymbol{r})\boldsymbol{\alpha}\right)_q^k \right| \psi_{n,\kappa,m} \right\rangle \tag{4.65}$$

where $\psi_{n,\kappa,m}$ and $\psi_{n',\kappa',m'}$ are Dirac single particle wavefunctions (appendix D) which are of the form

$$\psi_{n,\kappa,m}(\boldsymbol{r},\boldsymbol{\sigma}) = \frac{1}{r}\begin{bmatrix} P_{n,\kappa}(r)\chi_{\kappa,m}(\Omega,\boldsymbol{\sigma}) \\ iQ_{n,\kappa}(r)\chi_{-\kappa,m}(\Omega,\boldsymbol{\sigma}) \end{bmatrix} \tag{4.66}$$

In an atomic potential *with a finite nucleus* the wavefunctions are continuous and regular at the origin. The radial dependence near the nucleus is like $r^{|\kappa|-1} = r^{j-\frac{1}{2}}$, so the two states in the matrix element in eqn 4.65 have a combined radial dependence of $r^{j'+j-1}$. The matrix element is therefore non-zero only for $j + j' = k$ since the spherical delta function $\delta^{k-1}(\boldsymbol{r})$ in V^{TK} selects only $r^{k-1}C^{k-1}$ terms.

In addition to the selection rule $j + j' = k$, another selection rule follows directly from parity invariance of the (unperturbed) states. The single particle states $\psi_{n,\kappa,m}$ have parity $(-1)^l$, while the parity of the V^{TK} interaction is $(-1)^k$, therefore only states such that $l + l' = k$ are mixed.

4.5 Toroidal moments in atomic physics

The lowest order toroidal moments are the anapole and tetrapole moments. The anapole (T1) moment has P-odd T-even symmetry, so a nuclear anapole would contribute to the spin dependent PNC interaction. The tetrapole (T2) has P-even T-odd symmetry, so the nuclear tetrapole would be the leading second rank PE,TO electromagnetic interaction.

4.5.1 The nuclear anapole interaction

The theory of anapoles remained a curiosity of parity violation until the 1970's when the first atomic PNC experiments started to produce positive results. The form of the atomic anapole interaction given by the $k = 1$ term in eqn 4.64 was first derived by Flambaum and Khriplovich [31]. Subsequently detailed calculations of anapole moments in various systems including nuclei [31, 32], atoms [6, 15, 60] and also molecules [50], have been made based on the predictions of electroweak theory. Measurements of the spin dependent atomic PNC (eg in caesium [60]) are consistent with that predicted to arise from a nuclear anapole moment.

The nuclear anapole moment causes $s_{1/2}$ and $p_{1/2}$ states to be mixed and contributes to the spin dependent PNC interaction. In atomic units the anapole interaction is given by

$$V^{anapole} = \frac{a}{I}\,\boldsymbol{I}.\boldsymbol{\alpha}\,\delta(\boldsymbol{r}) \tag{4.67}$$

where the anapole moment $a = \langle II \,|\, a_0 \,|\, II \rangle$ interacts with the electron current density at the origin. The nuclear anapole moment is defined classically as an integral over the nuclear current distribution

$$\boldsymbol{a} = -\int \pi\, r^2\, \boldsymbol{j}_n(\boldsymbol{r})\, d\tau_n \tag{4.68}$$

This formula can be used to derive an approximate analytical expression for the anapole moment due to the parity violating electroweak force [32]. Using a simple shell model of a spherical nucleus the anapole moment of a heavy nucleus is

$$\boldsymbol{a} = \frac{G_F}{\sqrt{2}} \frac{9ge\mu}{10mr_N} \frac{K\,A^{2/3}}{I(I+1)} \boldsymbol{I} \tag{4.69}$$

where $K = (I+\frac{1}{2})(-1)^{I+\frac{1}{2}-L}$, μ and L are the magnetic moment and orbital quantum number of the unpaired valence nucleon, r_N is the nuclear radius and A the atomic mass. The constant g characterises the meson-nucleon interaction and differs for protons and neutrons ($g_p \approx 4$ and $g_n \approx 1$). The dependence on A is that of $\langle r_N \rangle^2$. The dimensionless constant κ_a used to characterise the anapole interaction is defined by

$$\kappa_a = \frac{9}{10}\, g\, (\alpha\mu/mr_N^2)\, A^{2/3} \tag{4.70}$$

so that the anapole interaction is given by

$$V^{anapole} = \frac{G_F}{\sqrt{2}} \frac{K\,\boldsymbol{I}.\boldsymbol{\alpha}}{I(I+1)} \kappa_a\, \delta(\boldsymbol{r}) \tag{4.71}$$

Values of κ_a for some nuclei derived from eqn 4.69 are given in table 4.3 with the nucleon couplings as $g_p = 4$ and $g_n = 1$.

Nucleus	κ_a
^{133}Cs	0.33
$^{203,205}Tl$	0.44
^{207}Pb	0.45
^{209}Bi	−0.08

Table 4.3: Some κ_a values in a simple shell model [32]

4.5.2 The nuclear tetrapole interaction

The nuclear tetrapole interaction is the $k = 2$ term in eqn 4.64. There has been some theoretical interest in the static and radiative properties of classical toroidal field distributions in nuclear systems [10, 58]. Following Boston and Sandars [15], we now give the quantum mechanical interaction of an atom with a nuclear tetrapole moment. The selection rules are now $j + j' = 2$ and $l + l' = 2$ so the states mixed

are $s_{1/2}$ with $d_{3/2}$ and $p_{1/2}$ with $p_{3/2}$. In atomic units the tetrapole interaction is given by

$$V^{tetrapole} = -\frac{\sqrt{6}\,T}{I(2I-1)}\,(\boldsymbol{I}\boldsymbol{I})^2\,.\,([\boldsymbol{\nabla},\delta(\boldsymbol{r})]\,\boldsymbol{\alpha})^2 \tag{4.72}$$

where the tetrapole moment $T = \langle II\,|\,T_0^2\,|\,II\rangle$ interacts with the gradient of the electron current density at the origin since

$$-\,ec\int \psi^\dagger\,([\boldsymbol{\nabla},\delta(\boldsymbol{r})]\,\boldsymbol{\alpha})_q^2\,\psi\,d\tau = (\boldsymbol{\nabla}\boldsymbol{j})_q^2\,(0) \tag{4.73}$$

The tetrapole moment is defined classically as an integral over the nuclear current distribution from eqn 4.52, putting $k = 2$

$$T_q^2 = -\frac{2}{3}\int \pi\,r^3\,\left(C^1\boldsymbol{j}_n(\boldsymbol{r})\right)_q^2\,d\tau_n \tag{4.74}$$

If there are T-odd forces within the nucleus, the tetrapole can arise naturally within a nucleus of sufficient angular momentum. An order of magnitude upper limit is obtained if unit T-odd impurities are present; the tetrapole is then of order

$$T_{max} \sim \frac{r_n^2}{a_0^2}\,\mu_N \tag{4.75}$$

where $\mu_N \sim \int \boldsymbol{r}\times\boldsymbol{j}(\boldsymbol{r})\,d\tau$ is the nuclear magnetic moment, and r_n is the nuclear radius.

4.6 Alternative derivation of toroidal moments

In section §4.3.5 the toroidal moments TK of a current distribution were derived from the interaction of the local magnetic field with an arbitrary external current density. The local field was expanded into components of different tensor rank corresponding to the toroidal moments of the internal currents. The k^{th} toroidal moment interacts with a $(k-1)^{th}$ gradient of the external current density $\left((\boldsymbol{\nabla}\ldots\boldsymbol{\nabla})^{k-1}\boldsymbol{j}_\epsilon\right)_q^k$.

An alternative is to consider an external current with just this property, whose interaction with unknown internal currents is therefore a pure toroidal interaction. The working is analogous to that used by Boston [14] but extended to the higher rank moments. A suitable external current is

$$j_{e\mu}^{\,1}(\boldsymbol{r}) = \frac{(-1)^{k+1}}{(k-1)!}\left(\frac{2k+1}{3}\right)^{\frac{1}{2}}\left((\boldsymbol{r}\ldots\boldsymbol{r})^{k-1}K^k\right)_\mu^1 \tag{4.76}$$

which satisfies the condition

$$\left((\boldsymbol{\nabla}\ldots\boldsymbol{\nabla})^{k-1}\boldsymbol{j}_\epsilon(\boldsymbol{r})\right)_q^k = K_q^k \tag{4.77}$$

where the components K_q^k are constants. This external current has the following properties

$$\begin{array}{ll} \boldsymbol{\nabla} \times \boldsymbol{j}_e = 0 & \boldsymbol{\nabla}^2 \boldsymbol{j}_e = 0 \\ \boldsymbol{r}.\boldsymbol{\nabla}\, \boldsymbol{j}_e = (k-1)\boldsymbol{j}_e & \boldsymbol{\nabla}\, \boldsymbol{r}.\boldsymbol{j}_e = k\, \boldsymbol{j}_e \end{array} \tag{4.78}$$

The field associated with the current density $\boldsymbol{j}_e(\boldsymbol{r})$ can be obtained from solving Maxwell's equations. In the Coulomb gauge $\boldsymbol{\nabla}.\boldsymbol{A}_e = 0$ the vector potential satisfies $\boldsymbol{\nabla}^2\, \boldsymbol{A}_e = -\mu_0\, \boldsymbol{j}_e$, which has solution

$$\boldsymbol{A}_e = \mu_0 \left(\alpha\, r^2 \boldsymbol{j}_e + \beta\, \boldsymbol{r}\, \boldsymbol{r}.\boldsymbol{j}_e \right) \tag{4.79}$$

where the constants α and β are

$$\alpha = -\frac{(k+3)/2}{(2k+3)(k+1)} \qquad \beta = \frac{1}{(2k+3)(k+1)} \tag{4.80}$$

The identity $\boldsymbol{\nabla} r^2 \boldsymbol{r}.\boldsymbol{j}_e = 2\boldsymbol{r}\, \boldsymbol{r}.\boldsymbol{j}_e + k r^2 \boldsymbol{j}_e$ simplifies eqn 4.79, from which the term which is a gradient of a scalar can be dropped

$$\boldsymbol{A}_e = -\frac{\mu_0}{4\pi} \frac{2}{k+1} \pi r^2 \boldsymbol{j}_e \tag{4.81}$$

The interaction energy between the internal currents $\boldsymbol{j}_i$ and the external field can be written in the following form

$$W = -\int \boldsymbol{j}_i.\boldsymbol{A}_e\, d\tau = \frac{\mu_0}{4\pi} \int \frac{2k}{(k+1)!} \pi r^2 \left(\boldsymbol{r} \ldots \boldsymbol{r}\, \boldsymbol{j}_i \right)^k .K^k\, d\tau \tag{4.82}$$

Substituting the definition of the current gradient K^k gives an equivalent form of the interaction to the previous result obtained in section §4.3.4. The stretched recouplings are given by eqns 4.48 and 4.49 and give

$$W = \frac{\mu_0}{4\pi} \int \frac{2\pi}{k+1} r^{k+1} \left(C^{k-1} \boldsymbol{j}_i \right)^k d\tau_i . \int \left(\delta^{k-1} \boldsymbol{j}_e(\boldsymbol{r}) \right)^k d\tau_e \tag{4.83}$$

which yields the same expression for T_q^k as eqn 4.52.

4.7 Classical anapoles

In this section the torque due to a penetrating external current on a classical macroscopic current distribution with anapole symmetry is derived. The system in figure 4.2 is a torus wound like a solenoid, with a surface current density $\boldsymbol{j}_i$, so that the magnetic field $\boldsymbol{B}$ is confined to the interior of the torus. The torus is oriented with the symmetry axis along the $\hat{\boldsymbol{z}}$ axis. The external current density $\boldsymbol{J}$ which penetrates through the interior is at an angle θ to the $\hat{\boldsymbol{z}}$ axis. The magnetic field $\boldsymbol{B}(\boldsymbol{r})$ inside the torus is uniform and oriented in the azimuthal ($\hat{\boldsymbol{\phi}}$) direction [26].

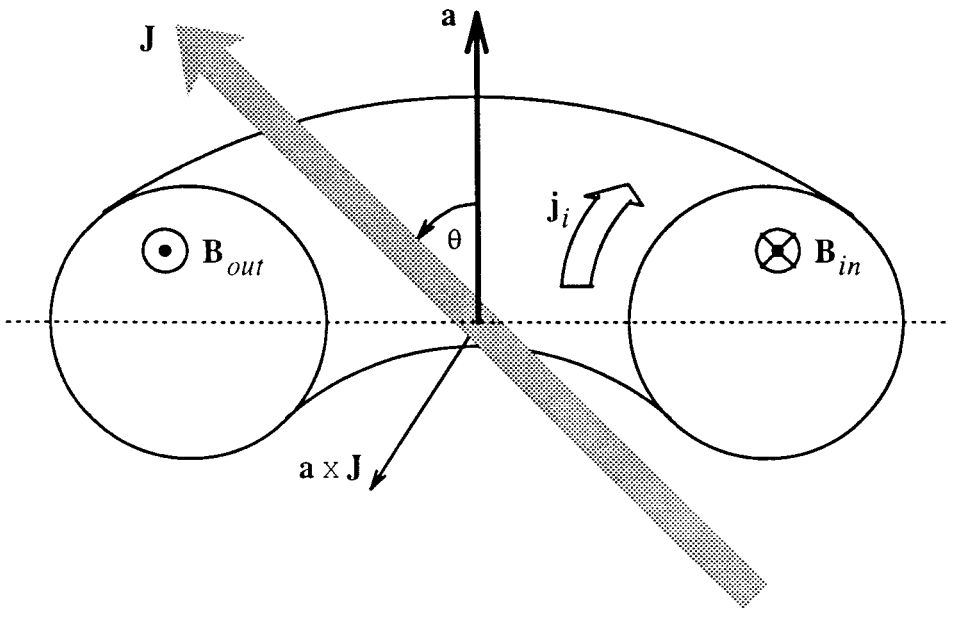


Figure 4.2: A classical anapole

The anapole moment is given by eqn 4.68 can be recast as an integral over the internal field $\boldsymbol{B}(\boldsymbol{r})$ using vector identities

$$\boldsymbol{a} = -\int \pi r^2 \boldsymbol{j}_i(\boldsymbol{r})\, d\tau = \frac{2\pi}{\mu_0} \int \boldsymbol{B}(\boldsymbol{r}) \times \boldsymbol{r}\, d\tau \tag{4.84}$$

The anapole vector is oriented along the symmetry axis, and in the same direction as the currents on the inner surface of the torus. The total couple $\boldsymbol{\Gamma}$ on the torus is given by the net torque on the torus due to the Lorentz force $\boldsymbol{F} = \boldsymbol{J} \times \boldsymbol{B}$

$$\boldsymbol{\Gamma} = \int \boldsymbol{r} \times \boldsymbol{F}\, d\tau = -\int \boldsymbol{r}.\boldsymbol{J}\boldsymbol{B}(\boldsymbol{r})\, d\tau \tag{4.85}$$

where the condition $\boldsymbol{r}.\boldsymbol{B}(\boldsymbol{r}) = 0$ holds inside the torus. Both the anapole moment and the couple are proportional to the same integral over the magnetic field $\boldsymbol{B}(\boldsymbol{r})$, which can therefore be eliminated

$$\boldsymbol{\Gamma} = \frac{\mu_0}{4\pi}\, \boldsymbol{a} \times \boldsymbol{J} \tag{4.86}$$

The element of work on rotating the torus through a small angle $d\boldsymbol{\theta}$ is $dU = \boldsymbol{\Gamma}.d\boldsymbol{\theta}$, therefore the potential at angle θ is given by

$$U = -\frac{\mu_0}{4\pi}\, \boldsymbol{a}.\boldsymbol{J} \tag{4.87}$$

The anapole therefore seeks to be *aligned* with the penetrating current density.

The higher order toroidal moments are obtained by arranging anapoles in appropriate configurations. For instance two adjacent anapoles with opposing anapole

moments on the same axis, constitute a tetrapole. The interaction with current gradients arises naturally in this way. For example the tetrapole seeks to be aligned with the gradient of the penetrating current density, so as to minimise the total alignment energy of the two opposing but separated anapoles, while higher order toroidal moments seek correspondingly higher order gradients

Chapter 5

T Violation in atomic transitions

We now turn to the question of how T-odd P-even impurities in atomic states, can lead to T violating phenomena in atomic dynamics. The dynamics considered in this chapter are radiative transitions due to applied electromagnetic fields, possibly in the presence of static electric and magnetic fields. Collisions and atomic interferometry phenomena, involving motion of the atomic centre of mass, are not considered here.

First the simple theory of radiative transitions is reviewed. The Rabi amplitudes, matrix element in units s^{-1}, are convenient for expressing the transition rates, since the Rabi rate is the natural frequency of the process, and therefore compares directly to frequency offsets, decay widths and so on. We also use a suitably defined 'unitless' transition matrix element, which is of order unity for an allowed electric dipole transition. The Rabi amplitudes can be written as the unitless matrix element times the square root of the intensity and a dimensional constant.

We then obtain the transition operators for 'forbidden' processes, such as the magnetic dipole (M1) and electric quadrupole (E2) transitions. These are derived in the usual way from a multipole expansion of the electromagnetic interaction. For single photon schemes, higher order multipole transition processes are essential since T impurities have no effect on the transition rate of a single allowed transition.

As well as single photon transitions, the theory of near resonant two photon transitions is developed. In these processes, the transitions have *different* frequencies, and one or more atomic levels are close to the intermediate resonance. The appearance of final state interactions, due to the spontaneous decay of the intermediate levels, in these processes places limitations on sensitivity to T violation effects. We derive the form of the transition strength in detail for the case of Raman transitions, as this is the essential basis for the novel plane polarised pumping (PPP) effect, which is the subject of chapters 7-8.

The net effect of the T impurities in the atomic states on any particular transition amplitude can be expressed as a single phase $\phi_T^{(M)}$ for each competing channel M. We show that TO,PE effects can only depend on the differences between two such *channel phases*, and we find that for this difference to be non-zero, there must be at least two interfering channels which are distinct processes.

5.1 Review of transition theory

In the simplest of treatments, atoms in an electromagnetic field are perturbed according to the time dependent Schrödinger equation. Since the Schrödinger equation is linear, complicated waveforms can be built up by superposition of plane waves, which have vector potential of the form $A^\mu = (\phi/c, \boldsymbol{A})$ given by

$$\boldsymbol{A}(\boldsymbol{r},t) = A\boldsymbol{\varepsilon}\sin(\boldsymbol{k}.\boldsymbol{r}-\omega t) \tag{5.1}$$
$$\phi(\boldsymbol{r},t) = 0 \tag{5.2}$$

where the frequency ω and wave vector $\boldsymbol{k}$ have dispersion relation $\omega = c\,|\boldsymbol{k}|$, and $\boldsymbol{\varepsilon}$ is the polarisation vector. The corresponding electric and magnetic fields of the same wave are given by

$$\boldsymbol{E}(\boldsymbol{r},t) = -\frac{\partial \boldsymbol{A}}{\partial t} - \boldsymbol{\nabla}\phi = A\omega\boldsymbol{\varepsilon}\cos(\boldsymbol{k}.\boldsymbol{r}-\omega t) \tag{5.3}$$
$$\boldsymbol{B}(\boldsymbol{r},t) = \boldsymbol{\nabla}\times\boldsymbol{A} = A\boldsymbol{k}\times\boldsymbol{\varepsilon}\cos(\boldsymbol{k}.\boldsymbol{r}-\omega t) \tag{5.4}$$

Each plane wave interacts independently with the atomic electrons (charge $-e$), which can be written in Hamiltonian form

$$H_{EM} = j_\mu A^\mu = ecA\boldsymbol{\alpha}.\boldsymbol{\varepsilon}\sin(\boldsymbol{k}.\boldsymbol{r}-\omega t) \tag{5.5}$$

In the rotating wave approximation, the perturbation can be written as a sum of a positive frequency part proportional to $\exp(-i\omega t)$, and a negative frequency part proportional to $\exp(i\omega t)$

$$H_{EM} = V^{EM}e^{-i\omega t} + V^{EM\dagger}e^{i\omega t} \tag{5.6}$$

where

$$V^{EM} = -\frac{i}{2}ecA\boldsymbol{\alpha}.\boldsymbol{\varepsilon}e^{i\boldsymbol{k}.\boldsymbol{r}} \tag{5.7}$$

The positive frequency part is the dominant contribution to absorption transitions, and the negative frequency part for stimulated emission (e.g. Raman transitions). It can be shown [54] that when there is no damping, such as radiative decay or loss of coherence through collisions, a two state atom oscillates between its initial state i and the other state f. The probability of the atom being in state f at time t is oscillatory [54]

$$P_f(t) = |b_{fi}|^2\,\frac{\sin^2(\frac{1}{2}\Omega t)}{\frac{1}{4}\Omega^2} \tag{5.8}$$

where $\Omega^2 = (\omega_0-\omega)^2 + 4\,|b_{fi}|^2$, and the oscillatory rate b_{fi} is called the Rabi amplitude

$$b_{fi} = \left\langle f \left| V^{EM} \right| i \right\rangle/\hbar \tag{5.9}$$

The Rabi rate $|b_{fi}|$ is the natural time scale of the $i \rightarrow f$ transition, and has units s^{-1}. The Rabi oscillations are damped by the spontaneous decay of the upper state, and also by other processed such as collisions which cause loss of coherence. If the decay halfwidth (at half maximum) is γ, then the weak field régime corresponds to the limit $|b| \ll \gamma$ in which the atom and radiation are uncoupled. The limit of the transition probability given by eqn 5.8 for small times much less than the oscillation time $bt \ll 1$ increases quadratically

$$P_f(t) = |b_{fi}|^2 t^2 \tag{5.10}$$

If the atom interacts for much longer than the damping period $\gamma t \gg 1$, then the atoms do not oscillate, and the rate of change of population in states i and f becomes linear. In this case a transition rate can be defined [54]

$$T_{i \rightarrow f} = |b_{fi}|^2 \frac{2\gamma}{(\omega_{if} - \omega)^2 + \gamma^2} \tag{5.11}$$

In both these limits, the transition probability depends on the modulus square of the Rabi amplitudes, which is called 'strength' $S_{i \rightarrow f}$ of the transition

$$S_{i \rightarrow f} = |b_{fi}|^2 \tag{5.12}$$

which is the matrix element part of the transition rate (with units s^{-2}). The weak field condition $|b| \ll \gamma$ will always hold for sufficiently low intensity light, and is used throughout this section since saturation effects are not essential to T violation arguments.

5.2 EM multipole expansion

Radiative interference in violation of Lloyd's theorem is one possible probe of the T invariance of the internal dynamics of the atom. In single photon transitions this requires interference of higher multipole processes which have the same parity symmetry, but different rank. The terms in the multipole expansion are the transition operators each of definite rotational, parity and T reversal symmetry.

The matrix element $\langle f \,|\, V \,|\, i \rangle$ determines the types and strengths of transitions that are possible, depending on the angular momentum and other properties of the states i and f. At typical atomic transition energies, the transition wavelength is much greater than the atomic size. The perturbation V^{EM} is usually expanded in powers of $\boldsymbol{k}.\boldsymbol{r}$, each term being higher order and weaker transitions.

$$V^{EM} = -\frac{i}{2} ecA\boldsymbol{\alpha}.\boldsymbol{\varepsilon} \left(1 + i\boldsymbol{k}.\boldsymbol{r} - \frac{1}{2!}(\boldsymbol{k}.\boldsymbol{r})^2 + \ldots\right) \tag{5.13}$$

The first term is the odd parity electric dipole (E1) interaction, the second term is of even parity and can be recoupled to give the magnetic dipole (M1) and electric

quadrupole (E2) interactions and so on. The multipole interactions (E1, M1, E2, ...) have definite parity and time reversal symmetry, and the lowest order of these are as follows

$$V^{E1} = -\frac{i}{2}ecA\boldsymbol{\varepsilon}.\boldsymbol{\alpha} \tag{5.14}$$

$$V^{M1} = \frac{1}{2}ecA\,(\boldsymbol{\varepsilon}\,\boldsymbol{k})^1\,.\,(\boldsymbol{r}\,\boldsymbol{\alpha})^1 \tag{5.15}$$

$$V^{E2} = \frac{1}{2}ecA\,(\boldsymbol{\varepsilon}\,\boldsymbol{k})^2\,.\,(\boldsymbol{r}\,\boldsymbol{\alpha})^2 \tag{5.16}$$

It is convenient to express these transition operators in atomic units. The vector potential A is related to the intensity by $I = \frac{1}{2}\epsilon_0 c\omega^2 A^2$. The atomic units interactions U^{EM} are defined so that the U^{E1} matrix element is unity if the dipole matrix element $\langle f \,|\, \boldsymbol{\varepsilon}.\boldsymbol{r} \,|\, i\rangle = a_0$

$$V^{EM} = \frac{1}{2}A\omega e a_0 U^{EM} \tag{5.17}$$

In this way the lowest order transition operators are

$$U^{E1} = -\boldsymbol{\varepsilon}.\boldsymbol{d} \tag{5.18}$$

$$U^{M1} = \frac{\alpha}{2}\,\boldsymbol{\varepsilon}\times\hat{\boldsymbol{k}}.\boldsymbol{\mu} \tag{5.19}$$

$$U^{E2} = -\frac{i\alpha\,\omega}{\sqrt{6}}\,(\boldsymbol{\varepsilon}\hat{\boldsymbol{k}})^2.Q^2 \tag{5.20}$$

where all the quantities are in atomic units: the dipole $\boldsymbol{d}$ is in units ea_0, $\boldsymbol{\mu}$ in units μ_B, Q in units ea_0^2, and the frequency atomic unit has mks value $\omega_{au} \equiv \alpha c/a_0 = 4.13\times 10^{16}\,\mathrm{s}^{-1}$. The vector $\hat{\boldsymbol{k}}$ is the unit vector along the photon wave vector $\hat{\boldsymbol{k}} = \frac{c}{\omega}\boldsymbol{k}$ and α is the fine structure constant. The Rabi amplitude can be written in terms of the U matrix element as

$$b_{fi} = \frac{A\omega e a_0}{2\hbar}\,\langle f \,|\, U \,|\, i\rangle = 1.1\times 10^8 I^{\frac{1}{2}} U_{fi} \tag{5.21}$$

with the intensity I in units W/cm^2.

5.3 Multipole transition rates

The order of magnitude strengths of the multipole transitions follow from the above. The relative strength of transitions can be estimated by assuming the matrix element is unity in atomic units for an appropriate pair of states. For the E2 matrix element, a typical atomic energy level spacing is taken to be 2eV or approximately $1/10^{th}$ atomic unit. Thus the matrix elements are

$$\left|U_{fi}^{E1}\right|^2 \sim 1 \tag{5.22}$$

$$\left|U_{fi}^{M1}\right|^2 \sim \frac{\alpha^2}{4} \tag{5.23}$$

$$\left|U_{fi}^{E2}\right|^2 \sim \frac{\alpha^2}{600} \tag{5.24}$$

The transition rate of an allowed electric dipole at line centre is proportional to the square of the Rabi rate $T = \frac{2}{\gamma}|b|^2$. With light intensity $I = 1\,\mathrm{W/cm^2}$ and a decay halfwidth of $\gamma = 2\pi \times 10\,\mathrm{MHz}$ the transition rate is $T \approx 4\times10^8 s^{-1}$. The higher order transition rates are scaled by the square of the Rabi rates, and in comparing the order of magnitude transition rate to allowed transitions, it is assumed that the upper state is not metastable and has the same decay width 10 MHz. Taking $\alpha \approx 1/137$, typical transition rates are

$$\begin{aligned} T^{E1} &\sim 4\times10^8\, s^{-1} \\ T^{M1} &\sim 5\times10^3\, s^{-1} \\ T^{E2} &\sim 40\, s^{-1} \end{aligned} \tag{5.25}$$

The M1 and E2 processes are fundamentally of the same order, but at frequencies much less than the atomic unit $\omega \ll \omega_{au}$ the E2 rate is suppressed relative to the M1 by a factor of order $(\omega/\omega_{au})^2 \ll 1$. Higher multipole transitions are increasingly weak - the transition rates reduce by a factor of order α^2 for each order.

5.4 Near resonant two photon transitions

Two or more photon transitions are higher order processes in a different sense to the multipole transitions. The theory of transitions involving more than one absorption or stimulated emission is more complex due to the effects of atomic resonances. In particular we find that damping of the atomic states through spontaneous decay processes can mimic T violation to some extent in these processes.

There are two kinds of two photon processes: a transition can be driven by second order interactions with the same field, or by coherent interaction of two different fields. In this section, we discuss the latter class when near resonance with a third 'intermediate' level. The possible T violation mimicking of decay processes requires a careful review of these processes, and we discuss specifically a near resonant Raman process. These are fundamental to the novel decay and T violation phenomena discussed in chapter 7.

5.4.1 Raman processes

The simplest process to discuss is a near resonant Raman process with *one* intermediate level, where both transitions are electric dipole transitions as illustrated in figure 5.1. When not within a decay width of resonance with the excited state e, the population of e is small; the two photon transition depends on the coherences of the level e with the initial and final states (i and f), ie the *off diagonal* components of the density matrix for the transition. The level e can decay by spontaneous emission, and the coherences of e with the states i and f are damped by the total decay width γ_e.

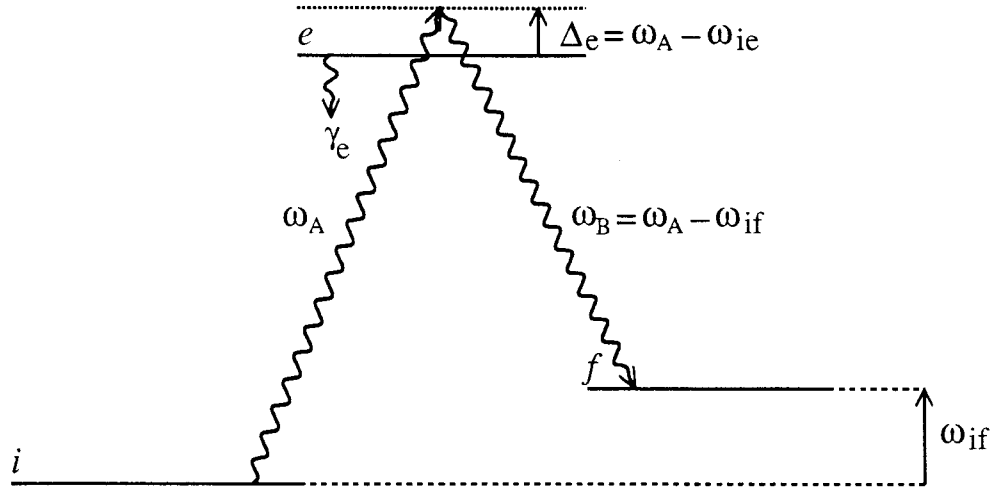


Figure 5.1: Raman transition with a near resonant intermediate level

In the dipole approximation, the electromagnetic Hamiltonian for two waves 1 and 2 of different frequencies, can be written

$$V^{EM} = -\frac{1}{2}\left[E_A \boldsymbol{\epsilon}_A . \boldsymbol{d}\, e^{-i\omega_A t} + E_B \boldsymbol{\epsilon}_B . \boldsymbol{d}\, e^{-i\omega_B t} + \textit{complex conjugate}\right] \tag{5.26}$$

where ω_A and ω_B are the frequencies, E_A and E_B are the electric field strength, and $\boldsymbol{\epsilon}_A$ and $\boldsymbol{\epsilon}_B$ are the polarisation vectors of the waves. If the intermediate level is close to resonance (compared to ω_{if}), then the rotating wave approximation can be applied, in which only one term in V^{EM} contributes significantly to each transition. In the Raman configuration of figure 5.1, the $e^{-i\omega_A t}$ term is dominant for the $i \rightarrow e$ absorption, and the $e^{+i\omega_B t}$ term for the $e \rightarrow f$ stimulated emission.

In a density matrix treatment, the equation of motion which gives the evolution of atom in the absence of damping terms is

$$\dot{\boldsymbol{\rho}} = \frac{i}{\hbar}\left[\boldsymbol{\rho}, H_0 + V^{EM}\right] \tag{5.27}$$

where H_0 is the atomic Hamiltonian of which i, f, and e are eigenstates, and $\boldsymbol{\rho}$ is the density matrix with a time independent basis

$$\boldsymbol{\rho} = \sum_{ij} \rho_{ij} \left|i\right\rangle \left\langle j\right| \tag{5.28}$$

In the rotating wave approximation, only one of the terms in V^{EM} contributes significantly to each transition matrix element, so that the non-zero matrix elements of V^{EM} are

$$V_{ie} = \hbar b_{ie}^{(A)} e^{-i\omega_A t} \tag{5.29}$$

$$V_{ef} = \hbar b_{ef}^{(B)} e^{i\omega_B t} \tag{5.30}$$

and their complex conjugates (V is Hermitian, so $V_{ji} = V_{ij}^*$). The Rabi rates $b_{ie}^{(A)}$ and $b_{ef}^{(B)}$ are proportional to the field strengths and atomic matrix elements of the corresponding transitions, which have selection rules depending on their respective polarisation vectors[1]

$$b_{ie}^{(A)} = -\frac{1}{2} E_A \langle i \,|\, \boldsymbol{\epsilon}_A . \boldsymbol{d} \,|\, e \rangle \tag{5.31}$$

$$b_{ef}^{(B)} = -\frac{1}{2} E_B \langle e \,|\, \boldsymbol{\epsilon}_B^* . \boldsymbol{d} \,|\, f \rangle \tag{5.32}$$

Finally, damping terms are required which are entered in the conventional manner. For simplicity, we assume here that only damping from radiative decay is important for the intermediate level e, which gives a decay half width γ_e. The real decay of population from e to i and f are the *partial* widths $\gamma_{e\to i}$ and $\gamma_{e\to f}$. If collisional and other damping effects are negligible, then the off diagonal decay width is

$$\gamma_e = \sum_{m_i} \gamma_{e\to i} + \sum_{m_f} \gamma_{e\to f} \tag{5.33}$$

Unlike the upper level e, in a Raman process the state f is long lived with negligible damping, so that for ordinary interaction times equilibrium is *not* reached. The population in the f level and associated off diagonal components must therefore be obtained as time dependent solutions of the density matrix equations.

The decay terms are included in the equations of motion for the density matrix components in the usual way,

$$\dot{\rho}_{ii} = \frac{i}{\hbar} [\boldsymbol{\rho}, V]_{ii} + 2\gamma_{e\to i} \rho_{ee} \tag{5.34}$$

$$\dot{\rho}_{ie} = i\rho_{ie}\omega_{ie} + \frac{i}{\hbar} [\boldsymbol{\rho}, V]_{ie} - \gamma_e \rho_{ie} \tag{5.35}$$

$$\dot{\rho}_{ee} = \frac{i}{\hbar} [\boldsymbol{\rho}, V]_{ee} - 2\gamma_e \rho_{ee} \tag{5.36}$$

$$\dot{\rho}_{if} = i\rho_{if}\omega_{if} + \frac{i}{\hbar} [\boldsymbol{\rho}, V]_{if} \tag{5.37}$$

$$\dot{\rho}_{ef} = -i\rho_{ef}\omega_{fe} + \frac{i}{\hbar} [\boldsymbol{\rho}, V]_{ef} - \gamma_e \rho_{ef} \tag{5.38}$$

$$\dot{\rho}_{ff} = \frac{i}{\hbar} [\boldsymbol{\rho}, V]_{ff} + 2\gamma_{e\to f} \rho_{ee} \tag{5.39}$$

and their complex conjugates $\rho_{ji} = \rho_{ij}^*$. In the absence of damping for the ρ_{if} and ρ_{ff} components, the above is valid close to the $\omega_A - \omega_B = \omega_{if}$ two photon resonance, for time t such that $(\omega_A - \omega_B - \omega_{if})t \ll 1$.

[1] The dependence of the polarisation vectors is retained explicitly as a superscript, which facilitates discussions about the dependence of terms on the polarisation vectors, and of T reversed processes for which the role of the transitions is reversed.

In beam experiments, the atoms in the beam are perturbed during the transit time, typically of order $t \sim 10^{-6}$ *sec.* The decay width for levels which are not metastable is typically of order $\gamma \sim 2\pi \times 10\,\mathrm{MHz}$, large enough so that $\gamma t \gg 1$, so that the state e is in equilibrium with the driving radiation. The components ρ_{if} and ρ_{ff} have no damping terms and are not in equilibrium, so that in this approximation $\rho_{if} \propto t$ and $\rho_{ff} \propto t^2$ while $\rho_{ff} \ll 1$. The population in f also comes from the real (ie incoherent) population in e given by ρ_{ee}, either via a spontaneous decay or stimulated emission. The real population ρ_{ee} is in equilibrium for times $\gamma t \gg 1$, so that the contribution to ρ_{ff} due to spontaneous emission increases *linearly* with t. From dimensional arguments the stimulated emission from incoherent population in e is suppressed relative to coherent two photon transitions by $\gamma_e t$ when close to resonance or $\Delta_e t$ when off resonance with the intermediate level by offset Δ_e.

5.4.2 Solution in the weak field limit

The density matrix equations of motion can be solved in the weak field limit with initial condition $\rho_{ii} = 1$ and $\rho_{ee} = \rho_{ff} = 0$. The density matrix components decrease in magnitude from ρ_{ii} to ρ_{ff} in the following way

$$1 \approx \rho_{ii} \gg \rho_{ie} \gg \rho_{if} \gg \rho_{ef} \gg \rho_{ff} \tag{5.40}$$

In this approximation the component $\rho_{ii}(t) = 1$ and the remaining equations of motion, eqns 5.35-5.39, are simplified by keeping only the largest contributions in each equation according to the above hierarchy

$$\dot{\rho}_{ie} = i\rho_{ie}\omega_{ie} + \frac{i}{\hbar}V_{ie} - \gamma_e\rho_{ie} \tag{5.41}$$

$$\dot{\rho}_{ee} = \frac{i}{\hbar}(\rho_{ei}V_{ie} - V_{ei}\rho_{ie}) - 2\gamma_e\rho_{ee} \tag{5.42}$$

$$\dot{\rho}_{if} = i\rho_{if}\omega_{if} + \frac{i}{\hbar}\rho_{ie}V_{ef} \tag{5.43}$$

$$\dot{\rho}_{ef} = -i\rho_{ef}\omega_{fe} + \frac{i}{\hbar}(\rho_{ee}V_{ef} - V_{ei}\rho_{if}) - \gamma_e\rho_{ef} \tag{5.44}$$

$$\dot{\rho}_{ff} = \frac{i}{\hbar}(\rho_{ef}V_{fe} - V_{ef}\rho_{fe}) + 2\gamma_{e\to f}\rho_{ee} \tag{5.45}$$

The component ρ_{ie} is driven by $V_{ie} \propto e^{i\omega_A t}$ and is in equilibrium with the radiation for $\gamma_e t \gg 1$. The steady state solution for ρ_{ie} has the same oscillatory phase $e^{i\omega_A t}$ as the driving radiation, which is removed by defining $\rho_{ie} = \tilde{\rho}_{ie}e^{i\omega_A t}$. The equation of motion for $\tilde{\rho}_{ie}$ is

$$\dot{\tilde{\rho}}_{ie} + i\omega_A\tilde{\rho}_{ie} = i\tilde{\rho}_{ie}\omega_{ie} + ib_{ie}^{(A)} - \gamma_e\tilde{\rho}_{ie} \tag{5.46}$$

and in the steady state solution, $\tilde{\rho}_{ie}$ becomes constant, so that $\dot{\tilde{\rho}}_{ie} = 0$, which gives

$$\tilde{\rho}_{ie} = \frac{b_{ie}^{(A)}}{\omega_A - \omega_{ie} - i\gamma_e} \tag{5.47}$$

The ρ_{ee} component is similarly in equilibrium with the radiation. The population is real and has no oscillatory time dependence

$$\dot{\rho}_{ee} = i(\tilde{\rho}_{ei} b_{ie}^{(A)} - \tilde{\rho}_{ie} b_{ei}^{(A)}) - 2\gamma_e \rho_{ee} \tag{5.48}$$

Putting $\dot{\rho}_{ee} = 0$ gives the population of e in the steady state

$$\rho_{ee} = \frac{1}{\gamma_e} Im\left[\tilde{\rho}_{ie} b_{ei}^{(A)}\right] = \frac{\left|b_{ei}^{(A)}\right|^2}{(\omega_A - \omega_{ie})^2 + \gamma_e^2} \tag{5.49}$$

The ρ_{ee} component is the incoherent population of e. The coherent two photon process depends on ρ_{if} driven from ρ_{ie} by $V_{ef} \propto e^{-i\omega_B t}$. The oscillatory time dependence of ρ_{if} is therefore $e^{i(\omega_A - \omega_B)t}$, which is removed by defining $\rho_{if} = \tilde{\rho}_{if} e^{i(\omega_A - \omega_B)t}$. Since there is no damping term, there is no equilibrium condition and the equation of motion for $\tilde{\rho}_{if}$ is a differential equation

$$\dot{\tilde{\rho}}_{if} + i(\omega_A - \omega_B - \omega_{if})\tilde{\rho}_{if} = i\tilde{\rho}_{ie} b_{ef}^{(B)} \tag{5.50}$$

and satisfying the initial condition $\tilde{\rho}_{if}(0) = 0$. The solution for $\tilde{\rho}_{if}(t)$ is

$$\tilde{\rho}_{if}(t) = \frac{\tilde{\rho}_{ie} b_{ef}^{(B)}}{\omega_A - \omega_B - \omega_{if}} \left[1 - e^{-i(\omega_A - \omega_B - \omega_{if})t}\right] \tag{5.51}$$

which for $(\omega_A - \omega_B - \omega_{if})t \ll 1$ is linear in t

$$\tilde{\rho}_{if}(t) = i\tilde{\rho}_{ie} b_{ef}^{(B)} t = \frac{i b_{ie}^{(A)} b_{ef}^{(B)} t}{\omega_A - \omega_{ie} - i\gamma_e} \tag{5.52}$$

The component ρ_{ef} is driven from ρ_{ee} by $V_{ef} \propto e^{-i\omega_B t}$ and from ρ_{if} by $V_{ei} \propto e^{-i\omega_A t}$. Both terms give an oscillatory time dependence $e^{-i\omega_B t}$, which is removed by defining $\rho_{ef} = \tilde{\rho}_{ef} e^{-i\omega_B t}$. The equation of motion for $\tilde{\rho}_{ef}$ is

$$\dot{\tilde{\rho}}_{ef} - i(\omega_B - \omega_{fe} + i\gamma_e)\tilde{\rho}_{ef} = i b_{ef}^{(B)} \rho_{ee} - i b_{ei}^{(A)} \tilde{\rho}_{if} \tag{5.53}$$

with initial condition $\tilde{\rho}_{ef}(0) = 0$. On the right hand side of eqn 5.53, the ρ_{ee} term is constant and the $\tilde{\rho}_{if}$ term proportional to t. The ρ_{ee} term gives rise to the stimulated emission from the incoherent population in e, while the ρ_{if} term contains the coherent transition amplitudes. The ratio of these terms is of order

$$\frac{b_{ef}^{(B)} \rho_{ee}}{b_{ei}^{(A)} \tilde{\rho}_{if}} = \frac{b_{ef}^{(B)}\, Im[\tilde{\rho}_{ie} b_{ei}^{(A)}]/\gamma_e}{b_{ei}^{(A)} b_{ef}^{(B)} \tilde{\rho}_{ie} t} \approx \frac{1}{\gamma_e t} \ll 1 \tag{5.54}$$

Putting $\tilde{\rho}_{if}(t) = i\tilde{\rho}_{ie} b_{ef}^{(B)} t$, the solution for $\tilde{\rho}_{ef}(t)$ and $\gamma_e t \gg 1$ is

$$\tilde{\rho}_{ef}(t) = \frac{i b_{ei}^{(A)} \tilde{\rho}_{ie} b_{ef}^{(B)} t}{\omega_B - \omega_{fe} + i\gamma_e} \tag{5.55}$$

Finally the population in f, according to eqn 5.45, comes from $\tilde{\rho}_{ef}$ and also by spontaneous decay from ρ_{ee}

$$\dot{\rho}_{ff} = 2\ Im\left[b_{fe}^{(B)}\tilde{\rho}_{ef}\right] + 2\gamma_{e\to f}\rho_{ee} \tag{5.56}$$

Substituting for all the density matrix components in terms of the Rabi rates, the ρ_{ff} equation becomes

$$\dot{\rho}_{ff} = 2\ Im\left[\frac{ib_{fe}^{(B)}b_{ei}^{(A)}t}{\omega_B - \omega_{fe} + i\gamma_e} \times \frac{b_{ie}^{(A)}b_{ef}^{(B)}}{\omega_A - \omega_{ie} - i\gamma_e}\right] + \frac{2\gamma_{e\to f}\left|b_{ie}^{(A)}\right|^2}{(\omega_A - \omega_{ie})^2 + \gamma_e^2} \tag{5.57}$$

with initial condition $\rho_{ff}(0) = 0$. Eqn 5.57 can be integrated directly to give $\rho_{ff}(t)$. The first term is greatly simplified in the current situation, since the driving frequencies are close to the two photon resonance condition $\omega_A - \omega_B = \omega_{if}$. On resonance, the frequency offsets are equal so $\omega_B - \omega_{fe} = \omega_A - \omega_{ie}$. The population in state f at time t is therefore

$$\rho_{ff}(t) = \left|\frac{b_{ie}^{(A)}b_{ef}^{(B)}}{\omega_A - \omega_{ie} - i\gamma_e}\right|^2 t^2 + \frac{2\left|b_{ie}^{(A)}\right|^2\gamma_{e\to f}t}{(\omega_A - \omega_{ie})^2 + \gamma_e^2} \tag{5.58}$$

The two terms in eqn 5.58 are the dominant processes in the weak field limit. The population in f increases quadratically from the coherent two photon process, and linearly from background transition rate once the intermediate level e has reached equilibrium.

The component of the population in f increasing quadratically with t is then due to the coherent two photon transition. An effective $i \to f$ transition strength $S_{i\to f}$ can be defined as the matrix element part

$$S_{i\to f} = \left|\frac{b_{fe}^{(B)}b_{ei}^{(A)}}{\omega_{ie} - \omega_A - i\gamma_e}\right|^2 = \frac{\left|b_{fe}^{(B)}\right|^2\left|b_{ei}^{(A)}\right|^2}{\left(\omega_{ie} - \omega_A\right)^2 + \gamma_e^2} \tag{5.59}$$

which (like the background term) depends only on the square of the transition amplitudes and a Lorentzian resonance profile. Hence T impurities in the atomic states cannot affect the transition strength, since the effect of T impurities is at most to change the phase of the transition Rabi rates. This is an illustration of the factorisation theorem of section §5.7; there is only one channel for the two photon process, therefore the transition strength is insensitive to T violation.

5.4.3 Two or more intermediate levels

This suggests that with two or more channels, T violation effects can be present in the transition strength. In real atoms, there is often a hyperfine structure consisting of many closely spaced levels. Repetition of the above treatment for multiple intermediate levels, as shown in figure 5.2, gives a generalised form for the transition

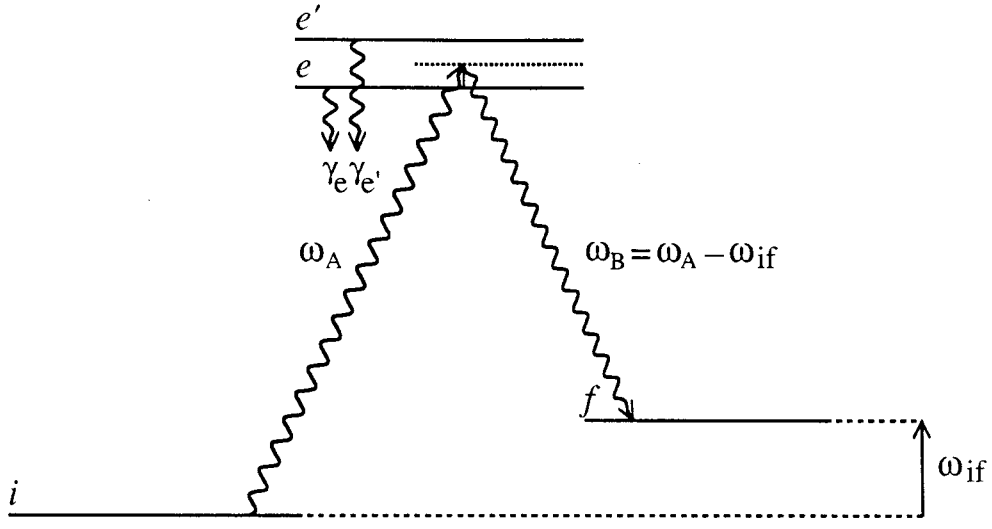


Figure 5.2: Raman transition with two near resonant intermediate levels

strength. The intermediate levels are not coupled with each other by the radiation, so the equations of motion for components ρ_{ie}, ρ_{ee} and ρ_{ef} of each intermediate level e are unchanged. However, the equations for ρ_{if} and ρ_{ff} now involve a summation over the couplings with all the intermediate levels

$$\dot{\rho}_{if} = i\rho_{if}\omega_{if} + \frac{i}{\hbar}\sum_e \rho_{ie}V_{ef} \tag{5.60}$$

$$\dot{\rho}_{ff} = \frac{i}{\hbar}\sum_e(\rho_{ef}V_{fe} - V_{ef}\rho_{fe}) + \sum_e 2\gamma_{e\to f}\rho_{ee} \tag{5.61}$$

where the V_{ie} and V_{ef} driving fields can have different Rabi matrix elements $b_{ie}^{(A)}$ and $b_{fe}^{(B)}$ for each e. The analysis leading to eqn 5.58 can be repeated with the summations over intermediate levels in the equations for ρ_{if} and ρ_{ff}. The same radiation drives all the $i \to e$ and $e \to f$ transitions, so the oscillatory time dependences of all the components is the same as for the single intermediate level. The solution for the component $\tilde{\rho}_{if}$ is now

$$\tilde{\rho}_{if}(t) = i\sum_e \tilde{\rho}_{ie}b_{ef}^{(B)}t = \sum_e \frac{ib_{ie}^{(A)}b_{ef}^{(B)}t}{\omega_A - \omega_{ie} - i\gamma_e} \tag{5.62}$$

where the $\tilde{\rho}_{ie}$ are of the same form as eqn 5.47. The summation in the ρ_{ff} equation is an *independent* summation over the off diagonal components $\rho_{e'f}$. The expression for

the quadratically growing population and background[2] is finally

$$\rho_{ff}(t) = \left| \sum_e \frac{b_{ie}^{(A)} b_{ef}^{(B)}}{\omega_A - \omega_{ie} - i\gamma_e} \right|^2 t^2 + \sum_e \frac{2\left|b_{ie}^{(A)}\right|^2 \gamma_{e\to f} t}{(\omega_A - \omega_{ie})^2 + \gamma_e^2} \tag{5.64}$$

when on the two photon resonance. The strength of the $i \to f$ two photon process is therefore given by

$$S_{i\to f} = \left| \sum_e \frac{b_{fe}^{(A)} b_{ei}^{(B)}}{\omega_{ie} - \omega_A - i\gamma_e} \right|^2 \tag{5.65}$$

This is equivalent to the form for the transition rate of a two photon excitation process given by Bjorkholm and Liao [12]. The presence of the summation *inside* the modulus squared means that the amplitudes of different channels can have interference terms. The decay gives the effective two photon amplitude an extra phase proportional to the decay width, which can potentially mimic T violation.

5.5 T impurities and the channel phase

The T impurities in the atomic states have imaginary phase relative to ordinary admixtures, which are real in the usual phase convention. Their effect is therefore to change the phase of transition process amplitudes. It is convenient to define the net phase added to each process amplitude due to the T violation, as the *channel phase*. The channel phase can be different for each transition channel amplitude, and takes account both the atomic selection rules of the transition, and the T impurities in the relevant atomic states. Therefore in the presence of an unspecified T violating interaction, a transition matrix element M can then be written

$$M = \exp\left(i\phi_T^{(M)}\right) M_0 \approx \left(1 + i\phi_T^{(M)}\right) M_0 \tag{5.66}$$

where M_0 is in the absence of T violation. The channel phase $\phi_T^{(M)}$ is the ratio of the transition amplitudes via atomic T impurities to the ordinary amplitude M_0.

[2]The term neglected in eqn 5.55 which is the stimulated emission from the incoherent population of e depends on both $b_{ie}^{(A)}$ and $b_{ef}^{(B)}$. The extra population due to this process contributes $\Delta\rho_{ff}$ to the background transition rate where

$$\Delta\rho_{ff} = \sum_e \frac{2\gamma_e t \left|b_{ie}^{(A)}\right|^2 \left|b_{ef}^{(B)}\right|^2}{\left((\omega_A - \omega_{ie})^2 + \gamma_e^2\right)^2} \tag{5.63}$$

which shares the $|b|^4$ dependence on the driving fields, but cannot have any interference terms leading to PPP signatures. Its ratio to the coherent process is at most $1/\gamma_e t \ll 1$ when on resonance with an intermediate level. $\Delta\rho_{ff}$ is also smaller than the ordinary background transition rate by a factor $|b_{ef}|^2/(\Delta_e^2 + \gamma_e^2) \ll 1$ in the weak field limit.

The channel phase can be written in terms of the first order perturbation of the atomic states by the TO,PE Hamiltonian H_T. If the effective operator for a transition process is Q, with matrix element $M_0 = Q_{fi}$ in the absence of T violation, then the channels via the admixtures of the perturbation H_T have effective operator

$$Q^{(T)} = H_T \frac{1}{\overleftarrow{E}_0 - H_0} Q + Q \frac{1}{\overrightarrow{E}_0 - H_0} H_T \tag{5.67}$$

where the operators $\overleftarrow{E}_0$ and $\overrightarrow{E}_0$ extract the energy eigenvalue of the bra and ket states respectively in the transition matrix element. They are Hermitian conjugates, so that $Q^{(T)}$ is Hermitian when Q and H_T are Hermitian. The operator $Q^{(T)}$ is the effective transition operator for the T impurity channels, and has imaginary matrix elements with respect to the unperturbed operator Q. The net transition matrix element therefore becomes

$$M = Q_{fi} + Q_{fi}^{(T)} = \left(1 + \frac{Q_{fi}^{(T)}}{Q_{fi}}\right) M_0 \tag{5.68}$$

so the channel phase is given by

$$i\phi_T^{(M)} = \frac{Q_{fi}^{(T)}}{Q_{fi}} \tag{5.69}$$

which is proportional to the TO,PE perturbation. If both the ordinary and T impurity channels are of the same multipole order, then the channel phase is a factor of order unity times the T impurities. It is also possible for the TO,PE interaction admixtures to permit a more allowed transition to occur, in which case the channel phase then contains an enhancement factor.

5.6 T violation in a two state system

The situation is particularly simple for magnetic dipole transitions in a two state system, in which the states ψ and ψ' have the same angular momentum and parity. In the usual phase convention, the magnetic dipole operator μ_z is chosen to have real matrix elements. The contribution of the interaction H_T is given by the effective operator $\mu_z^{(T)}$ which contains the first order perturbation terms

$$\mu_z^{(T)} = H_T \frac{1}{\overleftarrow{E}_0 - H_0} \mu_z + \mu_z \frac{1}{\overrightarrow{E}_0 - H_0} H_T \tag{5.70}$$

In the usual phase convention, the magnetic dipole transition μ_z matrix elements are real, so the matrix elements of $\mu_z^{(T)}$ are imaginary. The magnetic dipole matrix element therefore acquires an imaginary part

$$\left\langle \psi' \left| \mu_z^{(T)} \right| \psi \right\rangle = i\delta_T \left[\langle \psi' \,|\, \mu_z \,|\, \psi' \rangle - \langle \psi \,|\, \mu_z \,|\, \psi \rangle \right] \tag{5.71}$$

with $\delta_T = \delta_T(\psi', \psi)$ the admixture of ψ' into ψ

$$i\delta_T^{(\psi',\psi)} = \frac{\langle \psi' \,|\, H_T \,|\, \psi \rangle}{E - E'} \tag{5.72}$$

The remaining dipole matrix elements are diagonal matrix elements, and are just the magnetic moments μ, μ' of the states. For angular momentum states γjm and $\gamma' jm$, eqn 5.71 therefore becomes

$$\left\langle \psi' \left| \mu_z^{(T)} \right| \psi \right\rangle = i\delta_T \,(\mu' - \mu) = -i\delta_T \, m \,(g' - g)\, \mu_B \tag{5.73}$$

where g and g' are the Landé g-factors of the levels. The ordinary dipole matrix element is given by

$$\langle \psi' \,|\, \mu_z \,|\, \psi \rangle = \langle \gamma' jm \,|\, \mu_z \,|\, \gamma jm \rangle = m \, \frac{\langle \gamma' j \,\|\, \boldsymbol{\mu} \,\|\, \gamma j \rangle}{\langle j \,\|\, \boldsymbol{j} \,\|\, j \rangle} \tag{5.74}$$

so the channel phase of the $\psi \rightarrow \psi'$ M1 transition is therefore

$$\phi_T = -(g' - g)\, \delta_T \, \frac{\langle j \,\|\, \mu_B \boldsymbol{j} \,\|\, j \rangle}{\langle \gamma' j \,\|\, \boldsymbol{\mu} \,\|\, \gamma j \rangle} \tag{5.75}$$

which is proportional to the T impurity δ_T and the difference of the Landé g-factors. The channel phase in this example is independent of m, ie does not depend on the atomic orientation. This is the case in general when the T violation is internal to the atom.

5.7 The two channel TV theorem

In the previous section, it was shown that TO,PE perturbations result in a net phase change of transition matrix elements, which we have called the channel phase. The *magnitude* of the matrix element is not affected by these T violations to first order. If there is only one channel, then the transition strength is proportional to the square of the Rabi amplitude, b, given by eqn 5.11, which is proportional to the matrix element. Only the phase of the amplitude is changed, so $|b|^2$ is unchanged

$$|b|^2 \rightarrow |(1 + i\phi_T)b|^2 = |b|^2 \tag{5.76}$$

where ϕ_T is the channel phase for that amplitude. In a situation where there are two or more channels, then the transition strength is proportional to the sum of the Rabi amplitudes squared. If the two channels 1 and 2 are *distinct*, ie their matrix elements are not proportional to one another, then the channel phases of the amplitudes b_1 and b_2 are not necessarily equal so that

$$\begin{aligned} |b_1 + b_2|^2 &\rightarrow \left|(1 + i\phi_T^{(1)})b_1 + (1 + i\phi_T^{(2)})b_2\right|^2 \\ &= |b_1 + b_2|^2 + 2(\phi_T^{(1)} - \phi_T^{(2)}) Im[b_1^* b_2] \end{aligned} \tag{5.77}$$

where $\phi_T^{(1)}$ and $\phi_T^{(2)}$ are the two channel phases. The interference term in eqn 5.77 is proportional to the difference of the channel phases, and can contain T-odd P-even combinations of the external axes and field components involved in the two processes.

5.8 The T ratio

The transition strength is the modulus squared of the amplitudes of contributing channels. The two channels of interest, which interfere to give the TO,PE signature in the presence of T violation are denoted A and B. In terms of the Rabi amplitudes of the channels, the transition strength S is of the form

$$S = |b_{bak} + b_A + b_B|^2 \tag{5.78}$$

where b_A and b_B are the Rabi amplitudes for the A and B channels and b_{bak} contains the amplitudes of all other background processes. It is sufficient to consider only processes which are of definite rotational and parity symmetry, since other process can be expanded as a sum of definite symmetry parts by taking suitable linear combinations of external field projections. The relative phase of their amplitudes (or their given phases in any particular phase convention) are then defined from the T invariance requirements of section §2.2.3. It is also possible that one or other of the amplitudes is zero in the absence of T violation, in which case there can be no interference at all. In an experiment to measure T violation related interference of the amplitudes b_A and b_B, their product should be proportional to some T-odd P-even combination of external field components. In the absence of T violation, Lloyd's theorem (section §2.7.2) requires that such products are purely imaginary, so that

$$\Delta S = b_A^* b_B + b_A b_B^* = 2Re[b_A^* b_B] = 0 \tag{5.79}$$

In the presence of T violation the phase relationship of the two channels is broken, and there can be TO,PE correlations if the two channels have different channel phases resulting from the T impurities in the atomic states

$$b_A \rightarrow (1 + i\phi_T^{(A)})b_A \tag{5.80}$$

$$b_B \rightarrow (1 + i\phi_T^{(B)})b_B \tag{5.81}$$

In this case, the interference terms in eqn 5.79 can be non-zero and is proportional to the difference of $\phi_T^{(A)}$ and $\phi_T^{(B)}$

$$\Delta S = 2\,Re\left[(1 - i\phi_T^{(A)})b_A^*\,(1 + i\phi_T^{(B)})b_B\right] = 2\,(\phi_T^{(A)} - \phi_T^{(B)})\,Im\,[b_A^* b_B] \tag{5.82}$$

which is zero unless $\phi_T^{(A)} \neq \phi_T^{(B)}$ for which the channels must be distinct.

The TO,PE interference terms are analogous to those in atomic TE,PO (PNC) experiments, which are also zero in the absence an imaginary admixture. In PNC

experiments, the measured quantity for a given atomic transition, is conventionally quoted as a dimensionless ratio R of the parity violating to ordinary amplitudes. In the current work, we have defined an analogous ratio T which is equal to the ratio of the T violating to ordinary amplitudes.

The T ratio is defined as the *visibility* of the TO,PE interference signal, which can be written a linear combination of transition strength measurements proportional to the TO,PE part of the interference terms ΔS

$$T \equiv \frac{S_+ - S_-}{S_+ + S_-} \tag{5.83}$$

where $S_\pm$ are the transition strengths with external fields set so that the *sign* of the TO,PE signature is ± 1. In terms of the Rabi amplitudes for the channels, the T ratio can be written simply as a ratio of the different amplitudes

$$T = \frac{2\,\phi_T\, Im[b_A^* b_B]}{|b_{bak} + b_A + b_B|^2} \tag{5.84}$$

where $\phi_T = \phi_T^{(A)} - \phi_T^{(B)}$, which is zero in the absence of T violation.

The net sensitivity to TO,PE admixtures depends both on the T ratio for the atomic transition, and also on the signal to noise ratio in the relevant measurement. In a beam experiment where the signal is the number of atoms N in some atomic state, then the statistical signal to noise ratio is $\sqrt{N}$. For a positive measurement the visibility of the interference must exceed the fractional signal to noise ratio so that

$$T > \frac{1}{\sqrt{N}} \tag{5.85}$$

This quantity is therefore a convenient route for finding the potential sensitivity of experiments.

5.9 Overview of TO,PE experiments

The remainder of this thesis is to be a discussion of three major classes of experiment which are promising candidates for investigation of T-odd P-even effects. In discussing possible T-odd effects there are three major lines of enquiry:

1. What experimental schemes are possible probes of the T purity of the atomic states? What are the expected signatures of T violating effects to be measured, and how do these differ from the dominant systematic effects?

2. Closely related is the choice of atomic (or molecular) transitions to use. What kinds of TO,PE interactions are the different schemes sensitive to? What atomic structure is prerequisite for the chosen scheme, and are there any transitions with particular atomic enhancements?

Chapter 6

TO,PE absorption correlations

The simplest class of T violation experiments are measurements of T-odd P-even radiative interferences in an atomic transition strength, which are forbidden by T invariance through Lloyd's theorem. The T violation is identified by the associated T-odd P-even correlation in the external field components on which the amplitudes depend.

There has been discussion for some time of studying TO,PE correlations as a measure of T violation. The transition strength can be measured either as the excitation probability of the atoms, or from the absorption of the light. Sandars [69] has noted that $\boldsymbol{E}.\boldsymbol{k}$ is the only TO,PE one photon signature for transitions between angular momentum eigenstates. This signature implies a different transition strength for laser beams with wavevector parallel and antiparallel to an applied electric field $\boldsymbol{E}$ (see figure 2.5 on page 19).

Enhancement of the T violation is possible in certain cases such as the caesium $6s \rightarrow 7s$ or thallium $6p_{1/2} \rightarrow 7p_{1/2}$ transitions, which have highly forbidden background transitions. The caesium example is closely related to existing PNC experiments, so that the sensitivity of a T violation scheme can be estimated without detailed analysis.

Kozlov and Porsev [51] have proposed a scheme to measure the TO,PE correlation in the refractive index of atomic thallium vapour, near the $1.28\,\mu$m transition. Preliminary tests are currently underway for this transition in Oxford [9]. Our analysis is consistent with that of Kozlov and Porsev, but also extendible to the other hyperfine transitions. We then contrast the thallium transition with a similar scheme using the caesium $6s \rightarrow 7s$ transition, in which the T violation is enhanced.

Finally, we have also looked at two photon transition correlations, which have large potential enhancements. Limitations on possible signatures are also removed and, in particular, the transition wavevectors can both be perpendicular to the electric field, which is experimentally favourable.

6.1 Single photon correlations

The signature $\boldsymbol{E}.\boldsymbol{k}$ is the only TO,PE correlation for single photon transitions between eigenstates. Combinations of the atomic and photon angular momenta with a static magnetic field $\boldsymbol{B}$, such as $\boldsymbol{J}.\boldsymbol{\sigma} \times \boldsymbol{B}$, vanish if the states are quantised along $\boldsymbol{B}$ because $\langle \boldsymbol{J} \times \boldsymbol{B} \rangle = 0$. One might also hope to see the TO,PE correlation $\boldsymbol{I}.\boldsymbol{b} \times \boldsymbol{B}$ in a nuclear magnetic resonance (NMR) experiment, which gives different rates for spin transitions from $I_x = \pm m_x$ states in a static B_z field and rf radiation $b_y \cos \omega t$. For a spin $\frac{1}{2}$ nucleus the detailed balance of the $\uparrow_x \rightleftharpoons \downarrow_x$ transitions would then be broken. However in this case T violation cannot give rise to this effect, since in such two state systems detailed balance is also a consequence of Hermiticity.

In a single photon experiment, the active channels in the TO,PE interference term must, between them, contain dependence on both $\boldsymbol{E}$ and $\boldsymbol{k}$. The dependence on the electric field comes from the Stark effect, which mixes atomic states of opposite parity through the perturbation $V = -\boldsymbol{E}.\boldsymbol{d}$. The dependence on the photon wavevector $\boldsymbol{k}$ must come from one of the channels being a higher multipole 'forbidden' transition. The situation is very different for odd and even parity transitions

- Odd parity: If one amplitude is a Stark induced M1 or E2 transition, then the background amplitude can be an allowed E1 transition. An $\boldsymbol{E}.\boldsymbol{k}$ interference can in principle occur but is limited by saturation of the strong E1 transition. At first sight an odd parity $\Delta J = 2$ transition avoids this problem, but one can show that the interference terms then vanish exactly[1].

- Even parity: In this case, the Stark induced amplitude is an E1 transition, which competes with a weaker M1 or E2 background. The maximum interference signal is now much greater, as it is determined by saturation of a weaker transition.

Only even parity transitions are of importance for TO,PE experiments since the saturation effect for odd parity transitions limits the intensity and therefore the contribution of the interference term.

6.2 Caesium excitation rate correlations

Absorption, ie excitation rate, experiments of an atomic transition are conceptually the simplest atomic phenomenon in which to observe TO,PE correlations. We consider the case when the measured quantity is the number of atoms, initially in the

[1]It can be shown from angular momentum considerations that there are no $\boldsymbol{E}.\boldsymbol{k}$ type interference terms for an E1(T) amplitude involving a $\Delta J = 2$ single photon process. This is because components of the external fields in the admixed matrix element must couple to rank 1 since the only external field in E1(T) is the polarisation vector, ie of rank 1. It follows that such interference terms vanish exactly for a $\Delta J = 2$ transition.

ground state i, detected after an interaction time t in an excited state f. The $i \to f$ excitation probability for a small interaction time t is given by

$$P_f = S_{i \to f}\, t^2 \tag{6.1}$$

where the detection efficiency is taken as unity, and the transition strength is the square of the Rabi amplitude $S_{i \to f} = |b_{fi}|^2$.

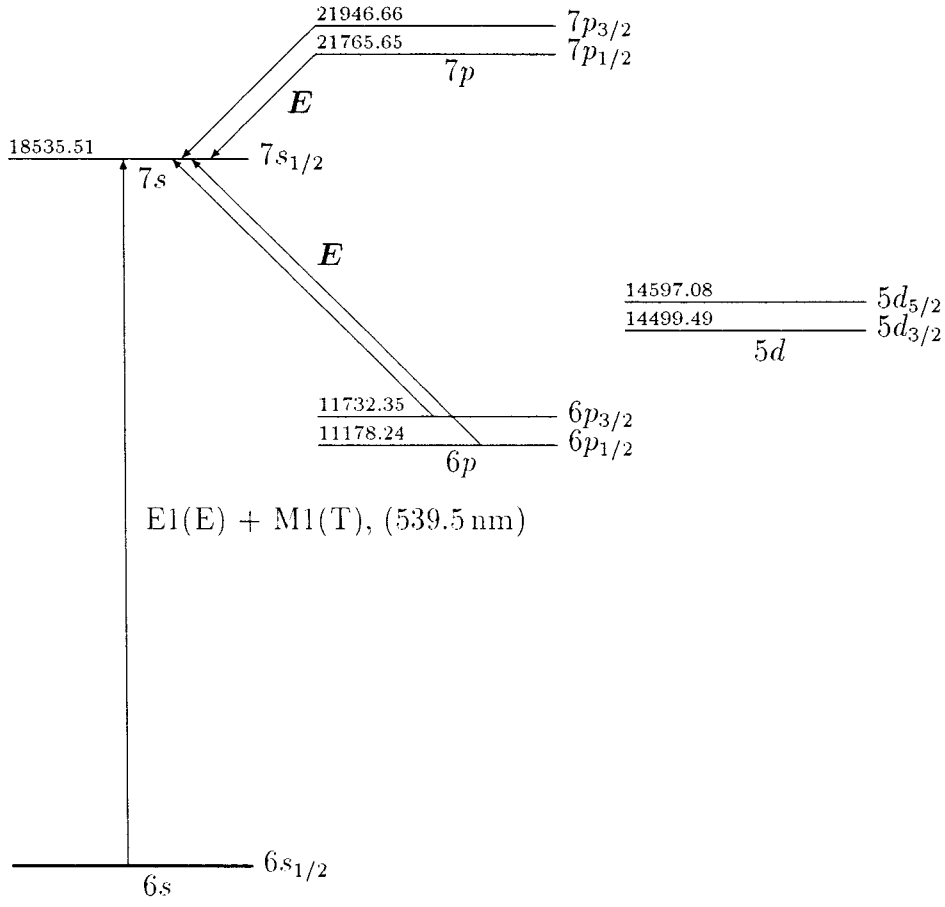


Figure 6.1: Low lying terms of caesium

A simple but useful example of a one photon process is the electric field induced $6s \to 7s$ transition in caesium, of wavelength $\lambda = 539.5\,\mathrm{nm}$ shown in figure 6.1. This is the strongest process, since the M1 is very weak - its effective dipole is of order $-0.4 \times 10^{-4} \mu_B$ [35]. This transition has been studied intensively in connection with parity non-conservation and is well understood. The ns and $n'p$ levels are mixed by the electric field $\boldsymbol{E}$, which then give a dipole matrix element, for example via $6p$ admixtures as shown in the figure.

Neutral caesium atoms are experimentally available in neutral atom traps and as an atomic beam. In a neutral atom trap there can be of order $N_0 \sim 10^{10}$ interacting

atoms at a very low temperature with a long interaction time $t \sim 0.1$s. In a high flux atomic beam, there can be of order $N_0 \sim 10^{15}$ atoms but these interact for a much shorter time of order $t \sim 3\mu$s. For simplicity, we consider here a beam experiment so that the measured signal is the number of excited atoms $N = N_0 P_f$ downstream of the interaction region, with statistical signal to noise ratio of order $\sqrt{N}$.

It is straightforward to show that the vector part of the Stark induced dipole transition, which we write as E1(E), has amplitude proportional to $\boldsymbol{E} \times \boldsymbol{\varepsilon}$, where $\boldsymbol{E}$ is the electric field and $\boldsymbol{\varepsilon}$ the polarisation vector. The TO,PE M1 amplitude is proportional to $\boldsymbol{k} \times \boldsymbol{\varepsilon}$ with the correct relative phase to give a TO,PE interference proportional to $\boldsymbol{E}.\boldsymbol{k}$ in the transition strength.

Because of the selection rules of the magnetic dipole operator, the M1 amplitude will depend only on the mixing of the $6s$ and $7s$ levels into each other. For scalar ($k = 0$) TO,PE interactions, the situation is that of the two state system discussed in section §5.6. The imaginary part of the dipole matrix element is proportional to the difference of the Landé g-factors, which gives amplitude

$$\mu_{T,k=0} = \left\langle 7s \left| \mu_z^{(T)} \right| 6s \right\rangle = i\delta_T m(g_{7s} - g_{6s})\mu_B \tag{6.2}$$

where δ_T is the admixture of $7s$ into the $6s$ level. The $6s$ and $7s$ levels have the same g-factor $g = g_s$ upto relativistic corrections; their difference is $g_{7s} - g_{6s} = 5.6 \times 10^{-5}$.

For nuclear spin dependent ($k \neq 0$) TO,PE interactions one can readily show that the TO,PE M1 for the $F \to F'$ transition is

$$\mu_{T,k\neq 0} = \left\langle 7s\, F' \left| \mu_z^{(T)} \right| 6s\, F \right\rangle = -i\left[\delta_T(F') - \delta_T(F)\right] \langle F' \,|\, \mu_z \,|\, F \rangle \tag{6.3}$$

which is zero for $F = F'$. The $k \neq 0$ admixtures $\delta_T(F)$ of hyperfine levels are related by a trace condition $\sum_F (2F+1)\delta_T(F) = 0$, so that $\delta_{T,k\neq 0} \equiv \delta_T(4) = -\frac{7}{9}\delta_T(3)$ where $\delta_{T,k\neq 0}$ is the TO,PE mixing of the $F = 4$ 'stretched' levels.

6.2.1 Sensitivity

The process is very similar to the corresponding T invariant hyperfine induced M1 discussed by the Bouchiat group [16]. Because of the extensive work that has been done on this transition, it is possible to make an estimate of the TO,PE sensitivity without detailed analysis. We simply make the plausible assumption that the TO,PE M1 amplitude can be measured to the same precision as the PNC dipole amplitude, which has experimental value $d_{PNC} = -0.8252(184) \times 10^{-11}\, iea_0$ [13, 60], ie precision $\Delta d_{PNC} = 1.8 \times 10^{-13}\, iea_0$. The equivalent TO,PE M1 transition amplitude is smaller by a factor $\alpha/2 \sim 4 \times 10^{-3}$, so we obtain a likely precision of $\Delta\mu_T \approx 5 \times 10^{-11}\, i\mu_B$. Using this precision, we obtain from eqn 6.2 the sensitivity to the scalar TO,PE admixture of $7s$ into the ground state

$$\delta_{T,k=0}^{(7s,6s)} > 1 \times 10^{-6} \tag{6.4}$$

and from eqn 6.3 for nuclear spin dependent admixtures

$$\delta_{T,k\neq 0}^{(7s,6s)} > 5\times 10^{-11} \tag{6.5}$$

taking $\langle F' \,|\, \mu_z \,|\, F \rangle \approx \mu_B$.

6.3 Thallium refractive index correlations

An alternative to excitation rate experiments is to measure the refractive index of an atomic gas. Here the measured quantity is the optical depth of a gas cell rather than the number of atoms excited. Close to an atomic resonance, the refractive index is proportional to the transition strength and can therefore be a measure of TO,PE correlations. By circulating the light through the cell many times, the optical depth of order one absorption length can be obtained. Essentially all the photons are then used whereas in excitation experiments only a small fraction of atoms are excited.

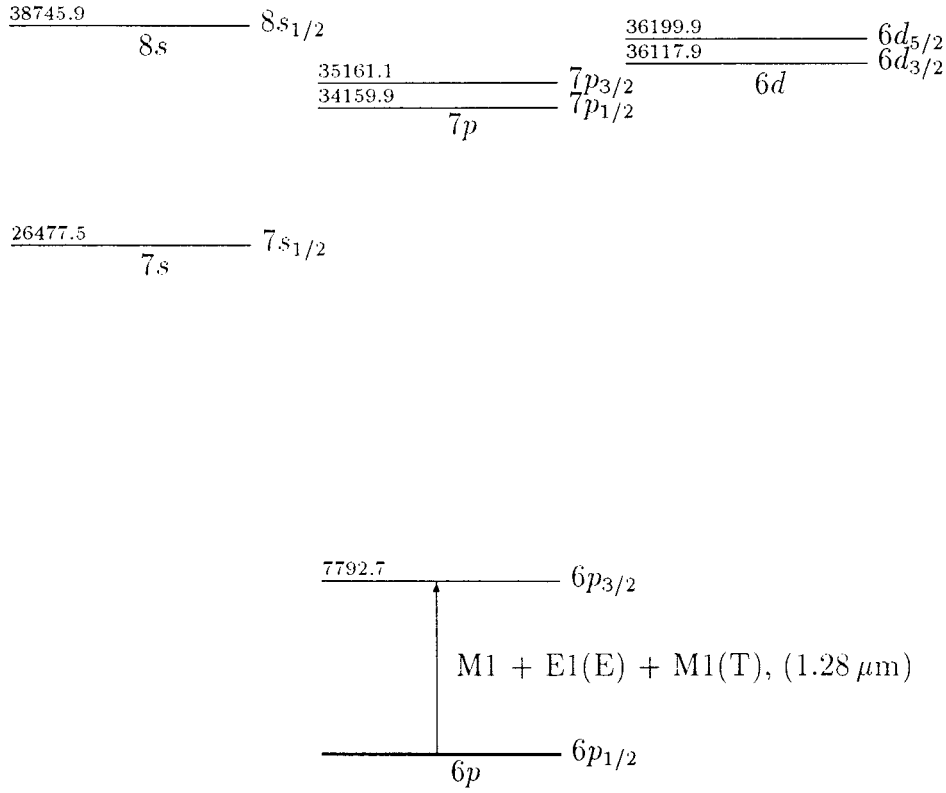


Figure 6.2: Low lying terms of thallium

The low lying terms of neutral thallium are shown in figure 6.2, with the $6p_{1/2} \rightarrow 6p_{3/2}$ resonance at 1.28 μm shown. The transition amplitude close to resonance is

dominated by the direct M1 amplitude, but in an electric field there is also an E1(E) amplitude through Stark admixtures of ns and nd levels. The T purity of the thallium $6p$ levels is directly measured by the interference of the M1 and E1(E) amplitudes, in our notation only $k = 1$ nuclear spin dependent T violating interactions are measured in the stable isotopes $^{203,205}Tl$ which have spin $I = \frac{1}{2}$.

Using angular momentum theory, it can be shown that only the vector part of the E1(E) amplitude can contribute to the TO,PE interference with the M1(T) amplitude. In thallium the opposite parity levels are distant compared to the $6p$ splitting, so the vector amplitude is suppressed. The larger term in the E1(E) amplitude is the rank 2 part, which can only interfere with the much weaker E2 transition; either way the interference in the transition strength is weak compared to the background.

In the paper by Kozlov and Porsev [51], which we shall refer to as 'K&P', the authors discuss the $F = 0 \rightarrow F' = 1$ transition. We treat the cancellation of terms in the vector E1(E) amplitude explicitly, allowing extension of the analysis to other transitions[2]. Following K&P, we take a gas cell of temperature $1200°C$, density $N_0 = 0.66 \times 10^{18}\ \mathrm{cm}^{-3}$ with a moderate field $E \sim 10^3\ \mathrm{V/cm}$ and frequency offset 5 Doppler widths.

6.3.1 Background absorption

The refractive index of an atomic gas close to an atomic resonance is proportional to the transition strength. In terms of the unitless matrix elements the complex susceptibility is of the following form [54]

$$\chi(\omega) = \frac{N_0 e^2 a_0^2}{\varepsilon_0 \hbar} \, |U_{fi}|^2 \, \frac{\omega_{if} - \omega + i\gamma}{(\omega_{if} - \omega)^2 + \gamma^2} \tag{6.6}$$

where N_0 is the number of interacting atoms in the state i, ω is the frequency of the light close to an atomic resonance between states i and f of half width γ.

In a Doppler broadened population, the susceptibility should be averaged by the Maxwell-Boltzmann distribution of velocity classes. The probability distribution for the atoms having incident frequency ω' to $\omega' + d\omega'$ in their rest frame is given by

$$p(\omega' - \omega)\, d\omega' = \frac{1}{\Delta\sqrt{\pi}} \, \exp\left[-\frac{(\omega - \omega')^2}{\Delta^2}\right] d\omega' \tag{6.7}$$

where ω is the unshifted frequency, and the Doppler half width is given by

$$\Gamma_D \equiv \sqrt{\ln 2}\, \Delta = \left(\frac{2 \ln 2\, k_B T}{M c^2}\right)^{\frac{1}{2}} \omega_{if} \tag{6.8}$$

[2]The hyperfine splitting of the $6p_{1/2}$ $F = 0, 1$ levels is 21 GHz which is well resolved with Doppler broadening $\Gamma_D \sim 2\pi \times 0.2\,\mathrm{GHz}$. The splitting of the $6p_{3/2}$ $F = 1, 2$ levels is smaller, of order 0.5 GHz, so is only just resolved.

in which M is the atomic mass and T is the temperature. The Doppler width is $\Gamma_D = 2\pi \times 0.224\,\mathrm{GHz}$, which is much larger than other broadenings of order $\gamma \sim 2\pi \times 30\,\mathrm{MHz}$. The effective susceptibility is the average over the velocity distribution of the atoms

$$\bar{\chi}(\omega) = \int \chi(\omega')\, p(\omega' - \omega) d\omega' = \frac{N_0 e^2 a_0^2}{\varepsilon_0 \hbar}\, |U_{fi}|^2\, \frac{1}{\Delta} [g(z) - if(z)] \tag{6.9}$$

The real functions f and g describe the lineshape as a function of the complex detuning parameter $z = (\omega_{if} - \omega - i\gamma)/\Delta$ and are given by

$$f(z) + ig(z) = \sqrt{\pi}\, e^{-z^2} [1 - \mathrm{erf}(-iz)] \tag{6.10}$$

and $\mathrm{erf}(z)$ is the Gaussian error function [2]. At offset $(\omega - \omega_{if})/\Gamma_D = 5$ the detuning parameter is $z = 4.16 - 0.107i$, which gives

$$f(z) = -6.78 \times 10^{-3} \tag{6.11}$$

$$g(z) = 0.248 \tag{6.12}$$

and their ratio is $|g/f| = 36.6$. We note that in the Doppler broadened limit $\Gamma_D \gg \gamma$, the real refractive index is independent of our rather arbitrary choice of γ.

The complex refractive index $n(\omega)$ contains real (dispersive) and imaginary (absorptive) parts, and is related to the susceptibility by

$$n^2(\omega) = (\eta + i\kappa)^2 = 1 + \bar{\chi}(\omega) \tag{6.13}$$

where η is the real refractive index, and κ is called the extinction coefficient as functions of the frequency ω. Therefore if $\bar{\chi}(\omega)$ is known, then the real and imaginary parts of the refractive index are determined. At low gas density the susceptibility is small $|\bar{\chi}(\omega)| \ll 1$ so that

$$\eta + i\kappa \approx 1 + \frac{1}{2}\bar{\chi}(\omega) \tag{6.14}$$

where the real refractive index η determines the optical depth of the gas, while the imaginary part is associated with absorption in the medium.

The susceptibility $\bar{\chi}(\omega)$ is related to the transition strength by eqn 6.9. The $F = 0 \rightarrow F' = 1$ M1 matrix element is $\left\langle 6p_{3/2}\, 1 \,|\, \mu_z \,|\, 6p_{1/2}\, 0 \right\rangle = \mu_B/\sqrt{6}$, so the M1 transition amplitude is

$$U_{1,0}^{M1} = \frac{\alpha}{\sqrt{24}} = 1.5 \times 10^{-3} \tag{6.15}$$

which from eqn 6.9 gives susceptibility $\bar{\chi}(\omega) = 1.4 \times 10^{-5}(1 - 0.022i)$.

The atomic absorption depth L_0 is defined as the depth at which transmitted light falls to $1/e$ of the initial intensity, eg $I(z) = I_0 e^{-z/L_0}$ along the z axis, where

$$L_0^{-1} \equiv \frac{2\omega\kappa}{c} = \frac{\omega}{c}\, Im\, \bar{\chi}(\omega) \tag{6.16}$$

Here the transition wavenumber is $k = \omega/c = 2\pi \times 7792.7\,\mathrm{cm}^{-1}$, giving absorption length $L_0 \sim 1\,\mathrm{m}$ in agreement with K&P.

6.3.2 TO,PE interference term

In the presence of T violation, the M1 can interfere with the Stark induced dipole E1(E) amplitude, due to admixtures of opposite parity levels $ns_{1/2}$ and $n'd_{3/2}$. Only the vector part of the E1(E) amplitude contributes to the TO,PE interference, which has amplitude proportional to $\boldsymbol{E}\times\boldsymbol{\varepsilon}$. The M1 amplitude is proportional to $\boldsymbol{k}\times\boldsymbol{\varepsilon}$ so that, as for caesium, the TO,PE interference is proportional to $\boldsymbol{E}.\boldsymbol{k}$.

The parity mixing of the states by an electric field $\boldsymbol{E}$ is given by perturbation $V_E = -\boldsymbol{E}.\boldsymbol{d}$. The effective operator for the Stark induced dipole amplitude can then be written in the following form

$$U^{E1(E)} = \boldsymbol{E}.\boldsymbol{d}\,\frac{1}{\overleftarrow{E}_0 - H_0}\,\boldsymbol{\varepsilon}.\boldsymbol{d} + \boldsymbol{\varepsilon}.\boldsymbol{d}\,\frac{1}{\overrightarrow{E}_0 - H_0}\,\boldsymbol{E}.\boldsymbol{d} \tag{6.17}$$

where the operators $\overleftarrow{E}_0$ and $\overrightarrow{E}_0$ extract the energy eigenvalue of the bra and ket states respectively. Inserting complete sets of states gives the ordinary perturbation expansion. This effective operator can be recoupled as a sum of scalar products of tensors $(\hat{\boldsymbol{E}}\boldsymbol{\varepsilon})^k.\boldsymbol{t}^k$, and the matrix element of the rank k part of the E1(E) amplitude can be conveniently be written in terms of this effective operator

$$U^{E1(E)k}_{F',F} = \left\langle 6p_{3/2}\,F' \middle| (\hat{\boldsymbol{E}}\boldsymbol{\varepsilon})^k.\boldsymbol{t}^k \middle| 6p_{1/2}\,F \right\rangle \tag{6.18}$$

where $\boldsymbol{t}^k$ has components

$$t^k_q = E\left(\boldsymbol{d}\left[\frac{1}{\overleftarrow{E}_0 - H_0} + (-1)^k\frac{1}{\overrightarrow{E}_0 - H_0}\right]\boldsymbol{d}\right)^k_q \tag{6.19}$$

In thallium the closest opposite parity levels, $7s_{1/2}$ and $6d_{3/2}$ are at energy several times the $6p_{1/2}, 6p_{3/2}$ splitting. In the vector E1(E) amplitude, the phase $(-1)^k$ in eqn 6.19 can lead to cancellation between the admixtures in the two levels. Indeed, these cancellations must occur because the Stark admixtures and dipole transition both have the same dipole matrix elements. Inserting a summation over the opposite parity levels nlj, the reduced matrix element of $\boldsymbol{t}^1$ can be written explicitly for this thallium transition

$$\begin{aligned}\left\langle 6p_{3/2}\left\|\,\boldsymbol{t}^1\,\right\|6p_{1/2}\right\rangle &= \frac{E}{E_s}\sum_{nlj}\left\langle 6p_{3/2}\,\|\,\boldsymbol{d}\,\|\,nlj\right\rangle\left\langle nlj\,\|\,\boldsymbol{d}\,\|\,6p_{1/2}\right\rangle \\ &\quad\times\left[\frac{E_{6p_{3/2}}-E_{6p_{1/2}}}{E_{6p_{3/2}}-E_{nlj}} - \frac{E_{6p_{3/2}}-E_{6p_{1/2}}}{E_{6p_{1/2}}-E_{nlj}}\right]\end{aligned} \tag{6.20}$$

where the electric field scale $E_s \equiv \hbar\Delta\omega/ea_0$ is a 'saturation' field, defined that two opposite parity levels with unit dipole matrix element ea_0 be fully mixed. In this way, the $6p$ energy splitting $\Delta\tilde{\nu} = 7792.7\,\mathrm{cm}^{-1}$ provides a natural scale for the electric field $E_s = 1.8\times10^8\,\mathrm{V/cm}$, giving $E/E_s = 5.6\times10^{-6}$. The factor in square

brackets is a dimensionless suppression factor 0.122 for the $7s_{1/2}$ level, 0.059 for $6d_{3/2}$ and smaller for more distant levels. Taking only these two levels, we have estimated $\left\langle 6p_{3/2} \| \boldsymbol{t}^1 \| 6p_{1/2} \right\rangle \approx -0.60\, E/E_s = -3.4{\times}10^{-6}$, so the $F = 0 \rightarrow F' = 1$ E1(E) transition amplitude is

$$U_{1,0}^{E1(E)1} = \frac{i}{\sqrt{12}} \left\langle 6p_{3/2} \left\| \boldsymbol{t}^1 \right\| 6p_{1/2} \right\rangle = -1.0 \times 10^{-6}\, i \tag{6.21}$$

which is much weaker than the direct $M1$ amplitude, so gives negligible contribution to the background absorption.

The T ratio is the ratio of the TO,PE interference term strength to the background transitions. We define the T impurity as the TO,PE mixing of the $F = 1$ levels $\delta_T \equiv \delta_T(1)$, since the $F = 0, 2$ levels are not mixed. The channel phase for the $0 \rightarrow 1$ M1 amplitude can then be written

$$\phi_T^{(0,1)} = -\delta_T \frac{\left\langle 6p_{1/2}\, 1 \| \boldsymbol{\mu} \| 6p_{1/2}\, 0 \right\rangle}{\left\langle 6p_{3/2}\, 1 \| \boldsymbol{\mu} \| 6p_{1/2}\, 0 \right\rangle} = \frac{1}{\sqrt{2}}\, \delta_T \tag{6.22}$$

The vector E1(E) amplitude is not affected by the TO,PE $6p$ mixing because the operator $\boldsymbol{t}^1$ has the property of vanishing for diagonal matrix elements. The T ratio of this transition is therefore

$$T = \frac{2\, M1(T)\, E1(E)^1}{|M1|^2} = 2\phi_T^{(0,1)}\, \frac{E1(E)^1}{M1} = 1.0 \times 10^{-3} \delta_T \tag{6.23}$$

which is consistent with the result of K&P. The 'enhancement' factor is 1/1000, ie in fact a suppression of the effect due to the interference requiring the weaker Stark induced dipole process, which must compete against a strong M1 background.

6.3.3 Sensitivity

We have shown that T violation leads to an interference term in the transition strength proportional to $\boldsymbol{E}.\boldsymbol{k}$, which implies through eqn 6.9 a fractional contribution to the refractive index $\Delta\eta$ of different sign for counter propagating beams in an electric field. The optical depths for the two beams are $L_\pm = L(1 \pm \Delta\eta)$, where $\Delta\eta$ is given by

$$\Delta\eta = \frac{1}{2}\, T\, Re\, \bar{\chi}(\omega) \tag{6.24}$$

since the T ratio is the fractional strength of the TO,PE interference term.

The optical depths of two counter propagating beams are different by twice the TO,PE contribution to the refractive index $\Delta\eta$ times the gas depth L. If two beams are recombined so that they interfere, then the phase change in their interference pattern on reversing the cell electric field is

$$\Delta\phi \equiv 4\Delta\eta L\, \frac{\omega}{c} \tag{6.25}$$

We take two absorption lengths $L = 2L_0$ gas depth (as K&P), which maximises the signal to noise ratio. The absorption length L_0 is given by eqn 6.16 and substituting eqns 6.24, and 6.23,

$$\Delta\phi = 4T\,\frac{g}{f} = 0.15\,\delta_T \tag{6.26}$$

which is the shift in the phase of the interference fringes on reversing the electric field.

The sensitivity is determined by the signal to noise ratio, which is limited by the 'shot noise' of the laser. Light power 1 W at the transition wavelength $1.28\,\mu$m has flux of order $\Phi \sim 6\times10^{18}$ photons per second. The statistical noise level in the phase measurement is therefore of order $2\pi/\sqrt{\Phi} = 2.5\times10^{-9}$. K&P take a reasonable statistical noise limit, ie the smallest measurable fringe shift, of order $\Delta\phi_{min} \sim 10^{-10}$. Equation 6.25 gives the phase shift directly in terms of the T ratio, so that this scheme has sensitivity to admixtures

$$\delta_{T,k=1} > 7\times10^{-10} \tag{6.27}$$

This sensitivity is consistent with that of K&P, who express their result in terms the coupling constants on a model interaction. We note here that our treatment can be extended to the other hyperfine transitions, because we have explicitly treated the cancellation of the vector E1(E) amplitude.

6.4 Caesium refractive index correlations

It is interesting to contrast the corresponding sensitivity of a caesium $6s \rightarrow 7s$ refractive index scheme. The vector E1(E) amplitude is proportional to the vector polarisibility, known experimentally $\beta = 26.8(8)\,a_0^3$, so that

$$U_{7s,6s}^{E1(E)} \approx \beta\,\frac{E}{E_{au}} \approx 5\times10^{-6} \tag{6.28}$$

where $E_{au} = 2\,Ry/ea_0$ and taking electric field $E = 10^3$ V/cm.

Transition	T-even	T-odd	Background
Tl $6p_{1/2} \rightarrow 6p_{3/2}$	$E1(E) = 1.0\times10^{-6}$	$M1(T) = 1.0\times10^{-3}\,\delta_T$	$M1 = 1.5\times10^{-3}$
Cs $6s_{1/2} \rightarrow 7s_{1/2}$	$E1(E) = 5\times10^{-6}$	$M1(T) = 7\times10^{-3}\,\delta_T$	

Table 6.1: Comparison of Cs and Tl T-even and T-odd amplitudes

As before, this amplitude interferes with the TO,PE M1 amplitude. We consider first hyperfine dependent ($k \neq 0$) mixings which give M1(T) amplitude of order $U_{7s,6s}^{M1(T)} \sim 7\times10^{-3}\,\delta_T$. The T-even and T-odd unitless amplitudes are shown in

table 6.1 for this caesium transition and the previous thallium case. Importantly, the background for caesium is the vector E1(E) transition, since the M1 is so forbidden (the scalar E1(E) amplitude vanishes for $\boldsymbol{E} \parallel \boldsymbol{k}$). The T violation is therefore enhanced because the T-odd channel is a much stronger M1 process

$$T = \frac{2\,M1(T)\,E1(E)^1}{|E1(E)^1|^2} \sim 3\times10^3\delta_T \tag{6.29}$$

a factor 3×10^6 larger than the thallium T ratio.

However, this enhancement is largely fictitious because the weakness of the background transition strength means that the signal is no longer limited by the absorption length. We take a lower temperature 200°C and frequency detuning of only one Doppler half width, which is now $\Gamma_D = 2\pi \times 0.42\,\mathrm{GHz}$ for this transition. With the same number of atoms in the initial state as for the thallium $N_0 = 0.66\times10^{18}\,\mathrm{cm}^{-3}$ we obtain, after some calculation, a rather large absorption length $L_0 \sim 200\,\mathrm{m}$.

In a reasonable gas depth $L = 2\,\mathrm{m}$, only 1% of the photon flux therefore contribute to the signal, and in addition, closer to resonance the lineshape factor is reduced to $g/f = 1.3$. These factors remove some of the initial enhancement, giving finally a T-odd interference fringe shift

$$\Delta\phi \sim 13\,\delta_{T,k\neq0} \tag{6.30}$$

which is a factor 500 enhanced compared to the thallium fringe shift (eqn 6.26) in terms of its corresponding admixture. The TO,PE M1 amplitude from scalar ($k = 0$) admixtures are suppressed by the cancellation of the g-factors giving

$$\Delta\phi \sim 7\times10^{-4}\,\delta_{T,k=0} \tag{6.31}$$

which is less enhanced, but still offers some sensitivity.

Taking the same precision $\Delta\phi_{min} \sim 10^{-10}$, the sensitivity of the caesium scheme corresponding to eqns 6.4 and 6.5, for $k = 0$ and $k \neq 0$, can be readily deduced

$$\delta^{7s,6s}_{T,k=0} > 2.5\times10^{-8} \tag{6.32}$$

$$\delta^{7s,6s}_{T,k\neq0} > 1.4\times10^{-12} \tag{6.33}$$

both of which significantly better than the previous results.

The caesium scheme differs from thallium in not being absorption length limited, so that the sensitivity increases with the gas depth or density. We note here that similar potential enhancement exists for the thallium $6p_{1/2} \rightarrow 7p_{1/2}$ transition, in which the vector E1(E) amplitude between p states is not suppressed as it is for s states.

6.5 Two photon correlations

The theory of near resonant two photon Raman transitions was developed in section §5.4, and is trivially modified for excitation to a metastable excited state $i \rightarrow f$

close to resonance with one or more intermediate levels e. In these schemes there may be two channels A and B for the $i \rightarrow e$ transition and a common $e \rightarrow f$ process. The coherent two photon transition strength in then given by

$$S_{i \rightarrow f} = \left| \sum_e \frac{b'_{fe}(b^{(A)}_{ei} + b^{(B)}_{ei})}{\omega_{ie} - \omega - i\gamma_e} \right|^2 \tag{6.34}$$

where the transition frequencies are ω and ω', and the two photon resonance condition is $\omega + \omega' = \omega_{if}$.

A feature of such schemes is that an enhancement of the TO,PE interference term can be achieved, where one of the transitions is odd parity and $\Delta J = 2$. The T violating channel can then be an electric dipole through T impurities E1(T). The TO,PE interaction must be nuclear spin dependent, so that levels of different J can be mixed, allowing a $\Delta J = 1$ dipole transition. Also, the signature must involve the polarisation of the second transition in a coherent two photon process, which complicates the reversal signature of the measurement. The extra complexity of the signature does however remove the requirement that the electric field and laser wavevectors be parallel. In particular, there are signatures in which the E2(E) transition wavevector and the electric field can be perpendicular, which is experimentally favourable.

The background E1 transitions through hyperfine admixtures are of order $\delta_{hfs} \sim 10^{-6}$. Interference with a Stark induced quadrupole amplitude can then give correlations linear in $\boldsymbol{E}$ and $\boldsymbol{k}$. We therefore anticipate a maximum enhancement of the T violation by a factor

$$T_{max} = \frac{\langle E1(T) \rangle}{\langle E1(hfs) \rangle} = \frac{\delta_T}{\delta_{hfs}} \sim 10^6 \delta_T \tag{6.35}$$

where this maximum is achieved if the E2(E) and E1(hfs) amplitudes are equal. However, the E2(E) amplitude is usually much weaker for practical electric fields, unless there is a nearly degenerate opposite parity level.

We note that the damping by spontaneous decay of the intermediate levels, mimics T violation to some extent. Its similarity with T violation comes from the $i\gamma$ associated with the lifetime of the intermediate levels in eqn 6.34. The effect is an additional phase of order $\gamma/\Delta\omega$ to the effective two photon amplitudes, where $\Delta\omega$ is the splitting of the intermediate levels. This decay effect is discussed in detail in the next chapter, and can be distinguished from genuine T violation by resolving the lineshapes of the intermediate level resonances.

6.6 Summary

We have shown that experiments measuring TO,PE correlations in radiative interference, can be a sensitive test of T violation. One such scheme, proposed by Kozlov and Porsev [51], to measure the $\boldsymbol{E}.\boldsymbol{k}$ component of the refractive index of thallium close to the $6p_{1/2} \rightarrow 6p_{3/2}$ transition, and preliminary tests for an experiment are

currently underway at Oxford. Our results are consistent with that of Kozlov and Porsev, and extendible to the other hyperfine components. The sensitivity, expressed as an admixture, is of order 7×10^{-10} for rank $k=1$ TO,PE interactions.

In some cases, such as the caesium $6s \rightarrow 7s$ and thallium $6p_{1/2} \rightarrow 7p_{1/2}$ transitions, the T violation is enhanced because the direct M1 is highly suppressed. For caesium, all the necessary quantities are known experimentally, leading to sensitivities of order 10^{-8} for $k=0$, and 10^{-12} for $k \neq 0$ interactions.

Two photon TO,PE correlation schemes can have large enhancement by using an odd parity $\Delta J = 2$ transition as background, allowed through hyperfine mixing. A TO,PE interference can then occur between a Stark induced quadrupole E2(E), and a T violating dipole E1(T). However, we have not found an example significantly more sensitive than the single photon schemes. In addition, there is a systematic due to the damping by spontaneous decay of the intermediate levels. The decays give the effective two photon amplitudes an additional phase, which mimics T violation to some extent.

Chapter 7

Plane polarised pumping

In two photon processes new possibilities emerge, since the wave vector and polarisation of the additional photon allow a class of T-odd P-even signatures so far not exploited - the scalar product of three angular momenta, and not involving any external electric or magnetic fields. A simple example is the product $\boldsymbol{\sigma}' . \boldsymbol{\sigma}_A \times \boldsymbol{\sigma}_B$, where $\boldsymbol{\sigma}_A$ and $\boldsymbol{\sigma}_B$ are the spins of two circularly polarised photons[1], and $\boldsymbol{\sigma}'$ probes the angular momentum of the atom. This signature differentiates atoms which are in $+m$ and $-m$ states quantised along the $\boldsymbol{\sigma}'$ direction, and thus leads to anomalous optical pumping of the initial or final state. The correlation with both polarisation vectors enables the two photon transitions to be distinguished from the background transition rate due to spontaneous emissions.

We point out here that there also exist signatures giving a similar pumping effect using only plane polarised light. We have called these *plane polarised pumping* (PPP), of which the simplest example is $\boldsymbol{\sigma}' . \boldsymbol{\varepsilon}_A \times \boldsymbol{\varepsilon}_B \boldsymbol{\varepsilon}_A . \boldsymbol{\varepsilon}_B$. In this and similar PPP signatures, the driving fields are independent, with different frequencies ω_A and ω_B and their polarisation vectors $\boldsymbol{\varepsilon}_A$ and $\boldsymbol{\varepsilon}_B$ are real.

This class of experiments is unusual in not requiring forbidden transitions or external fields. To exploit the PPP effect one can either cycle the population via a spontaneous decay to the ground state, building up its alignment, or else study the forwards and reversed dependence on angular momentum state populations. In this chapter the PPP effect is derived for Raman processes, with the latter approach in mind.

We note that although PPP effects can be a probe of T-odd P-even atomic impurities, a similar effect can occur through the decay of the intermediate levels in multiphoton processes, which mimics to some extent the effects of T violation. We show that the decay effect can be distinguished from T violation both by their relationship to the reversed transitions (ie their T reversal character) and by resolving the intermediate levels. The order of magnitude of the decay effect is $\gamma/\Delta\omega$ times

[1] The spin $\boldsymbol{\sigma}$ is the direction of circular polarisation of the photon, or equivalently $\lambda \hat{\boldsymbol{k}}$ where $\hat{\boldsymbol{k}}$ is the momentum direction and λ the helicity.

the non-PPP transition rate, where γ is the decay width of the intermediate levels, and $\Delta\omega$ is their energy splitting. Although the PPP effect is primarily of interest in this thesis as a signature of T violation, the decay effect itself is expected to be an observable and interesting phenomenon.

In two (or more) photon transitions, the frequencies and geometries can be arranged in a Doppler free configuration. This is done by having counter propagating waves for two step excitation processes so that the sum of the frequencies is constant, or by having two collinear waves for Raman processes so that the difference of their frequencies is constant. Unfortunately, the intermediate level or levels in both cases is then *not* Doppler free; since the spectrum of intermediate levels is central to our analysis, we consider first atoms (eg in a collimated beam) with a sufficiently small Doppler width, so that the intermediate levels can be resolved. However, we note that the PPP effects do not vanish in a Doppler broadened population of atoms. Even when the Doppler width is much larger than the intermediate level splitting, the decay and T violation PPP effects do *not* average to zero.

7.1 PPP in Raman processes

In the following sections, the PPP effect is derived for a Raman process between states i and f near resonant with at least two intermediate levels e, e', as discussed in section §5.4 and illustrated in figure 5.2 on page 66. A simple geometry is used, with the atoms in a collimated beam and in a specified angular momentum state quantised along a suitably defined z axis[2]. The driving field polarisation vectors $\boldsymbol{\epsilon}_{A,B}$ are real (plane polarisation) and in the x, y plane. Before deriving the form of the PPP transition strength, symmetry arguments can be used to identify its selection rules, T reversal character and dependence on the polarisation vectors.

The relevant expression for the two photon transition probability was derived in chapter 5. In the weak field limit the probability P_f of the atoms being in state f after an interaction time t is given by eqn 5.64, which can be written as

$$P_f(t) = S_{i\to f}\, t^2 + \sum_e P'_e \gamma_{e\to f}\, t \tag{7.1}$$

where $S_{i\to f}$ is the coherent two photon transition strength, P'_e is the equilibrium population of the intermediate level and $\gamma_{e\to f}$ is the partial decay width to f. The form of the two photon strength is the essential element of this chapter. It is given by eqn 5.65, which we repeat here for clarity

$$S_{i\to f} = \left| \sum_\epsilon \frac{b_{fe}^{(A)} b_{ei}^{(B)}}{\omega_{i\epsilon} - \omega_A - i\gamma_\epsilon} \right|^2 \tag{7.2}$$

[2] An implicit assumption here is that the initial state is quantised along the axis described by $\boldsymbol{\epsilon}_A \times \boldsymbol{\epsilon}_B$. In fact the states are measured along some axis $\boldsymbol{\sigma}'$ which may not be exactly aligned. The effect of misalignment is discussed in section §7.1.5 and vanishes to first order.

where on the two photon resonance $\omega_A - \omega_B = \omega_{if}$ the symmetry between states i and f and the two frequencies comes from the writing the resonance condition as

$$\omega_{ie} - \omega_A = \omega_{fe} - \omega_B \tag{7.3}$$

The final state interactions which in this case produce the decay PPP effect, arise from the $i\gamma$, which adds an effective phase to the two photon transition matrix elements.

7.1.1 The PPP geometry

The PPP transition strength is defined to be that part of the total strength $S_{i\to f}$ which is not equal for the $+m$ and $-m$ angular momentum states. The $\pm m$ states are related by the transformation operator R_x defined as $e^{-i\pi j_x}$, which rotates the coordinates through 180° about the x axis, and transforms $R_x |jm\rangle = (-1)^{2j} |j\ -m\rangle$. The total strength contains an ordinary term S_0 which is the same for the $\pm m$ states, ie *even* in m, and the PPP term ΔS which is *odd* in m, so that

$$S_{im\to fm'} = S_{0im\to fm'} + \Delta S_{im\to fm'} \tag{7.4}$$

$$S_{i-m\to f-m'} = S_{0im\to fm'} - \Delta S_{im\to fm'} \tag{7.5}$$

The symmetry of $S_{i\to f}$ under rotations of the states can be related to symmetries of the external coordinates defined by the driving field polarisation vectors. The polarisation vectors of the light waves driving the Raman transition are in the x, y plane at an angle θ to each other as shown in figure 7.1. One of the polarisation vectors $\boldsymbol{\varepsilon}_A$ can be chosen arbitrarily to be along the x axis, so that $\boldsymbol{\varepsilon}_A.\boldsymbol{r} = x$ and $\boldsymbol{\varepsilon}_B.\boldsymbol{r} = x\cos\theta + y\sin\theta$. The transition strength can be written symbolically as a function of

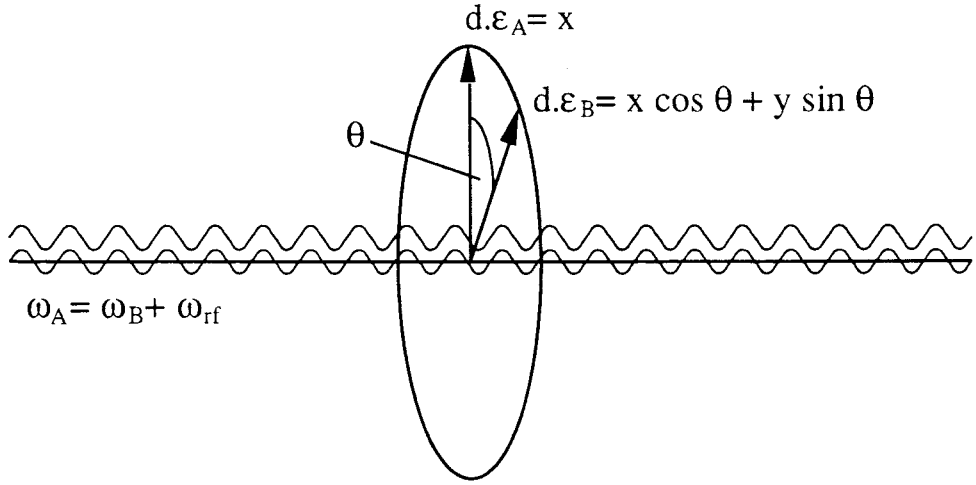


Figure 7.1: Geometry of plane polarised pumping transition

the light wavevectors $\boldsymbol{k}_{A,B}$ and polarisation vectors $\boldsymbol{\varepsilon}_{A,B}$. Transformations can then

be applied to the light fields, written in terms of the unit vector basis $(\vec{\imath},\vec{\jmath},\vec{k})$ *of the original coordinates.* Under R_x the unit vectors transform as follows

$$R_x : (\vec{\imath},\vec{\jmath},\vec{k}) \rightarrow R_x(\vec{\imath},\vec{\jmath},\vec{k})R_x^{-1} = (\vec{\imath},-\vec{\jmath},-\vec{k}) \tag{7.6}$$

The total strength must be invariant to rotations of the whole system of atom and light fields. Applying R_x to both the atomic states and the light fields gives a different system of states and fields which must have the same transition strength, so that

$$\begin{aligned} S_{im\rightarrow fm'}(\boldsymbol{k}_{A,B} \parallel \vec{k}, \boldsymbol{\varepsilon}_A = \vec{\imath}, \boldsymbol{\varepsilon}_B = \vec{\imath}\cos\theta + \vec{\jmath}\sin\theta) = \\ S_{i-m\rightarrow f-m'}(\boldsymbol{k}_{A,B} \parallel -\vec{k}, \boldsymbol{\varepsilon}_A = \vec{\imath}, \boldsymbol{\varepsilon}_B = \vec{\imath}\cos\theta - \vec{\jmath}\sin\theta) \end{aligned} \tag{7.7}$$

Equation 7.7 relates transition strengths between $+m$ and $-m$ states of the atom, but the light fields of the original and rotated system are not equivalent. Because the transitions are electric dipole transitions, reversing just the wavevectors $\boldsymbol{k}_{A,B} \rightarrow -\boldsymbol{k}_{A,B}$ does not alter the strength which depends only on the polarisation vectors, therefore

$$S_{im\rightarrow fm'}(\boldsymbol{\varepsilon}_B = \vec{\imath}\cos\theta + \vec{\jmath}\sin\theta) = S_{i-m\rightarrow f-m'}(\boldsymbol{\varepsilon}_B = \vec{\imath}\cos\theta - \vec{\jmath}\sin\theta) \tag{7.8}$$

where the $\boldsymbol{k}_{A,B}$ vectors and $\boldsymbol{\varepsilon}_A = \vec{\imath}$, being the same on both sides, have been omitted. The only difference in eqn 7.8 between the light fields is in the relative sign of the x and y components. The $+m$ and $-m$ transitions were also defined by eqns 7.4-7.5 in terms of S_0 and ΔS. Substituting from eqn 7.8, the number of y components in the even term S_0 must be *even*, and in the odd term ΔS must be *odd*. Similarly the number of x components in S_0 is *even*, and in ΔS is *odd*.

7.1.2 The scalar/tensor and vector amplitudes

The field strengths can be set to $eE_A = eE_B = 2\hbar$ without loss of generality, so the transition Rabi rates which occur in the transition strength are

$$b_{ei}^{(A)} = x_{ei} \tag{7.9}$$

$$b_{fe}^{(B)} = x_{fe}\cos\theta + y_{fe}\sin\theta \tag{7.10}$$

where the matrix elements of x, y are $x_{ij} = \langle i \,|\, x \,|\, j\rangle$ and $y_{ij} = \langle i \,|\, y \,|\, j\rangle$. The matrix element part of the amplitude $M_{fi} = b_{fe}^{(B)} b_{ei}^{(A)}$ contains the products $x_{fe}x_{ei}$ and $y_{fe}x_{ei}$ parts which have *even* and *odd* symmetry respectively under R_x rotations of the polarisations, reflecting their scalar/tensor and vector characters. It is convenient to separate these terms explicitly by their angular dependence. The $x_{fe}x_{ei}$ part is proportional to $\cos\theta$, which is a combination of scalar $\boldsymbol{\varepsilon}_A.\boldsymbol{\varepsilon}_B$ and rank 2 tensor product $(\boldsymbol{\varepsilon}_A\boldsymbol{\varepsilon}_B)_0^2$ of the polarisation vectors. The $y_{fe}x_{ei}$ part is proportional to $\sin\theta$, which is part of the vector product $(\boldsymbol{\varepsilon}_A \times \boldsymbol{\varepsilon}_B)_0$.

Angular momentum states have the property that x and y matrix elements between them are related. Since $x \pm iy \propto rC^1_{\pm 1}$ satisfies $\langle j'm' \mp 1 \,|\, x \pm iy \,|\, jm \rangle = 0$, the x and y matrix elements are therefore related by

$$\langle j'm' \,|\, y \,|\, jm \rangle = (-1)^{\frac{m'-m+1}{2}} i \langle j'm' \,|\, x \,|\, jm \rangle \tag{7.11}$$

so that the y matrix elements are imaginary relative to the same matrix element of x (both are zero when $m' = m$).

The Rabi rates in eqn 7.2 can therefore be written as a sum of two amplitudes A^e_{ST} and A^e_V for each intermediate level e, which are the *scalar/tensor* and *vector* contributions for each channel [40]

$$M_{fi} \equiv b^{(B)}_{fe} b^{(A)}_{ei} = x_{fe} x_{ei} \cos\theta + y_{fe} x_{ei} \sin\theta = A^e_{ST} + iA^e_V \tag{7.12}$$

where in the usual phase convention the x matrix element is real so that according to eqn 7.11 both A_{ST} and A_V as defined are real in a T invariant system. In terms of x and y coordinate matrix elements, they are given by

$$A^e_{ST} = x_{fe} x_{ei} \cos\theta \tag{7.13}$$

$$iA^e_V = y_{fe} x_{ei} \sin\theta \tag{7.14}$$

In terms of these amplitudes, the total strength is given by

$$S_{i \to f} = \left| \sum_e \frac{A^e_{ST} + iA^e_V}{\omega_{ie} - \omega - i\gamma_e} \right|^2 \tag{7.15}$$

where $\omega \equiv \omega_A$ determines the spectrum over the intermediate level resonances.

7.1.3 Scalar/tensor × vector dependence

We here point out that the PPP terms ΔS defined by eqns 7.4 and 7.5 have an odd number of y components and must therefore be of the form *scalar/tensor* × *vector*.

In the absence of the decay term these amplitudes do not interfere since the transition strength contains only $|A_{ST}|^2$ and $|A_V|^2$. If the states i and f are angular momentum states im and fm' then $S_{im \to fm'} = S_{i-m \to f-m'}$. The equality of the transition strength from the im and $i-m$ states, means that the expectation orientation of the atom is unchanged after the transition.

When there are two or more intermediate levels, interference terms may occur in the transition giving *scalar/tensor* × *vector* PPP terms. With just two intermediate levels e, e', these are

$$\Delta S \propto \left(A^e_{ST} A^{e'}_V - A^e_V A^{e'}_{ST} \right) \propto \sin\theta \cos\theta = \boldsymbol{\sigma}'.\boldsymbol{\varepsilon}_A \times \boldsymbol{\varepsilon}_B \, \boldsymbol{\varepsilon}_A.\boldsymbol{\varepsilon}_B \tag{7.16}$$

where $\boldsymbol{\sigma}'$ is the axis of quantisation for preparation or measurement of the states. Thus $S_{jm \to j'm'} \neq S_{j-m \to j'-m'}$, which implies alignment of the i and f levels along

the axis perpendicular to the plane of the two polarisation vectors. The dependence of ΔS on the angle θ in this geometry comes immediately from eqns 7.13 and 7.14. ΔS is zero when the angle θ is 0°, 90°, 180° or 270°, and a maximum when θ is 45°, 135°, 225° or 315° changing sign every 90°.

7.1.4 Selection rules

The selection rules for the Raman $i \rightarrow f$ transition when both polarisation vectors are in the x, y plane are $\Delta m = 0$ or ± 2. The matrix element for the level e should be summed over the degenerate magnetic substates m_e. The amplitudes can therefore be written

$$A^e_{ST} = \sum_{m_e} \langle fm' \,|\, x \,|\, em_e \rangle \langle em_e \,|\, x \,|\, im \rangle \cos\theta \tag{7.17}$$

$$iA^e_V = \sum_{m_e} \langle fm' \,|\, y \,|\, em_e \rangle \langle em_e \,|\, x \,|\, im \rangle \sin\theta \tag{7.18}$$

where the vector term contains a y matrix element which is imaginary. The matrix elements for the $m_e = m' \pm 1$, we write as amplitudes a_e and b_e for each level, which are the matrix element expressions

$$a_e = \langle fm' \,|\, x \,|\, em'+1 \rangle \langle em'+1 \,|\, x \,|\, im \rangle \tag{7.19}$$

$$b_e = \langle fm' \,|\, x \,|\, em'-1 \rangle \langle em'-1 \,|\, x \,|\, im \rangle \tag{7.20}$$

In terms of a_e and b_e, the amplitudes A_{ST} and A_V are given in the simple forms

$$A^e_{ST} = (a_e + b_e)\cos\theta \tag{7.21}$$

$$A^e_V = (a_e - b_e)\sin\theta \tag{7.22}$$

The a and b amplitudes shall be used for arguments in this chapter, but are also a convenient way of calculating the matrix elements, since the linear combinations $a \pm b$ are essentially just the amplitudes A_{ST} and A_V without the angular dependence.

The selection rules of the *scalar/tensor* × *vector* terms in the PPP transition strength, eqn 7.16, can be obtained by substituting the $a \pm b$ forms of the amplitudes

$$A^e_{ST}A^{e'}_V - A^e_V A^{e'}_{ST} = -2\,(a_e b_{e'} - b_e a_{e'})\sin\theta\cos\theta \tag{7.23}$$

Clearly for $\Delta m = -2$ transitions $a_e = a_{e'} = 0$, and for $\Delta m = +2$ transitions $b_e = b_{e'} = 0$. Therefore ΔS vanishes when $\Delta m = \pm 2$, so that only $\Delta m = 0$ transitions (ie $m' = m$) can have a PPP effect.

7.1.5 Misalignment dependences

If the light wavevectors are not aligned, the misalignment could potentially give rise to alignment of the states. The direction of the PPP alignment is the perpendicular

to the polarisation vectors $\boldsymbol{\varepsilon}_A \times \boldsymbol{\varepsilon}_B$, and this direction should be the same as the $\boldsymbol{\sigma}'$ axis which probes the atomic alignment. With a small misalignment, it is still possible to choose arbitrarily an x axis $\boldsymbol{\varepsilon}_A = \vec{\imath}$ but if the z axis is along $\boldsymbol{\sigma}'$, then there is now a small component $\eta\vec{k}$ in ε_B so that

$$\boldsymbol{\varepsilon}_A.\boldsymbol{r} = x \tag{7.24}$$

$$\boldsymbol{\varepsilon}_B.\boldsymbol{r} = x\cos\theta + y\sin\theta + \eta z \tag{7.25}$$

The matrix element part of the two photon transition amplitude M_{fi} given by eqn 7.12, now contains a $z_{fe}x_{ei}$ term

$$M_{fi} \equiv b_{fe}^{(B)} b_{ei}^{(A)} = x_{fe}x_{ei}\cos\theta + y_{fe}x_{ei}\sin\theta + \eta\, z_{fe}x_{ei} \tag{7.26}$$

However, the matrix element of $z = rC_0^1$ is diagonal in m states, so that the $z_{fe}x_{ei}$ term connects $\Delta m = \pm 1$ $i \rightarrow f$ transitions. Therefore the $\Delta m = 0$ transitions are not affected to first order by the misalignment. The $\Delta m = \pm 1$ transitions are even in m so that $S_{im\rightarrow fm\pm 1} = S_{i-m\rightarrow f-m\mp 1}$ and there is no polarisation.

7.1.6 Circular polarisation impurities

Also of great importance is that there should be no pumping if either of the driving fields is not exactly plane polarised. If one of the fields, for example $\boldsymbol{\varepsilon}_A$ has a small component of circularly polarised light, then the equilibrium orientation of the intermediate level population is different from the ground state. The background transition rate will then have a pumping component from normal spontaneous emission. This is ordinary optical pumping, and is independent of the angle θ and therefore easily distinguished from the PPP effect. Therefore the circular polarisation impurities might only produce PPP mimicking terms (ie with the characteristec $\sin\theta\cos\theta$ angular dependence) in the two photon transition strength.

The arbitrary choice of x axis is unaffected by the circular polarisation component, so a circular polarisation impurity can be introduced into the polarisation vector $\boldsymbol{\varepsilon}_A$, in the following form

$$\boldsymbol{\varepsilon}_A = (1-\eta)\,\vec{\imath} + \sqrt{2}\,\eta\,\hat{e}_{-1} \tag{7.27}$$

where $\hat{e}_{-1} = (\vec{\imath} - i\vec{\jmath})/\sqrt{2}$ is a unit vector in the spherical basis, and the factor $(1-\eta)$ scales the plane polarisation component so that the polarisation remain a unit vector $|\boldsymbol{\varepsilon}_A| = 1$. Expressed in terms of only the cartesian basis, the vector has an imaginary component

$$\boldsymbol{\varepsilon}_A = \vec{\imath} + i\eta\,\vec{\jmath} \tag{7.28}$$

which has circular polarisation content

$$\boldsymbol{\sigma}_A \equiv i\boldsymbol{\varepsilon}_A \times \boldsymbol{\varepsilon}_A^* = 2\eta\,\vec{k} \tag{7.29}$$

ie a small right handed component (along the wavevector axis). The imaginary $\vec{\jmath}$ component in eqn 7.28 gives the Rabi amplitude $b_{ei}^{(A)}$ an iy_{ei} contribution, which is

real. Even so, the circular polarisation impurity mixes x and y components of the second transition, and may therefore lead to interference of $\sin\theta$ and $\cos\theta$ terms.

The net matrix element part of the transition strength M_{fi} is modified by the circular polarisation impurity to the following form

$$M_{fi} \equiv b_{fe}^{(B)} b_{ei}^{(A)} = (x_{fe}\cos\theta + y_{fe}\sin\theta)(x_{ei} + i\eta\, y_{ei}) \tag{7.30}$$

$$= (x_{fe}x_{ei} + i\eta\, x_{fe}y_{ei})\cos\theta + (y_{fe}x_{ei} + i\eta\, y_{fe}y_{ei})\sin\theta \tag{7.31}$$

For $\Delta m = \pm 2$ transitions, only one state in each level e contributes, which is the state $m_e = m \pm 1$. In this case, all the coordinate matrix elements are proportional

$$y_{fe}x_{ei} = \mp i x_{fe}x_{ei} \tag{7.32}$$

$$x_{fe}y_{ei} = \mp i x_{fe}x_{ei} \tag{7.33}$$

$$y_{fe}y_{ei} = -x_{fe}x_{ei} \tag{7.34}$$

so that finally

$$M_{fi} = x_{fe}x_{ei}(1 \mp i\eta)\,(\cos\theta \mp i\sin\theta) = x_{fe}x_{ei}\, e^{\mp i\eta}\, e^{\mp i\theta} \tag{7.35}$$

The angular dependence θ is independent of the level e, so factorises out of the transition strength. In fact the dependence on the impurity η also factorises out so that the $\Delta m = \pm 2$ transitions still have no resulting pumping effect.

In the $\Delta m = 0$ transitions, the two states $m_e = m \pm 1$ contribute for each intermediate level e. The x and y matrix element products can be reduced to two terms $x_{fe}x_{ei}$ and $y_{fe}x_{ei}$ since in this case

$$x_{fe}y_{ei} = -y_{fe}x_{ei} \tag{7.36}$$

$$y_{fe}y_{ei} = x_{fe}x_{ei} \tag{7.37}$$

and these remaining products can be written in terms of the a and b amplitudes defined by eqns 7.21 and 7.22

$$x_{fe}x_{ei} = (a + b) \tag{7.38}$$

$$y_{fe}x_{ei} = i(a - b) \tag{7.39}$$

so that the transition strength matrix element M_{fi} becomes

$$M_{fi} = [(a + b) + \eta(a - b)]\cos\theta + i\,[(a - b) + \eta(a + b)]\sin\theta \tag{7.40}$$

The amplitudes A_{ST} and A_V are therefore modified by the circular polarisation impurity η and are now given by

$$A_{ST} = [(a + b) + \eta(a - b)]\cos\theta \tag{7.41}$$

$$A_V = [(a - b) + \eta(a + b)]\sin\theta \tag{7.42}$$

The PPP transition strength is still given by eqn 7.16, determined from symmetry arguments unaffected by the impurity η. Substituting the a and b forms of the amplitudes the required *scalar/tensor* $\times$ *vector* product is given by

$$A^{\epsilon}_{ST}A^{\epsilon'}_{V} - A^{\epsilon}_{V}A^{\epsilon'}_{ST} = -2\left(a_{\epsilon}b_{\epsilon'} - b_{\epsilon}a_{\epsilon'} + O(\eta^2)\right)\sin\theta\cos\theta \tag{7.43}$$

where the dependence on the impurity η cancels to first order. There is therefore *no* PPP mimicking effect due to circular polarisation impurities in the driving fields.

7.2 Decay PPP effect

When a decay term is present, the $i\gamma_{\epsilon}$ in the denominator has the effect of an extra phase in the transition amplitude, which allows the *scalar/tensor* and *vector* parts to interfere in the transition strength to give the PPP strength. This can also arise from an anomalous phase in the matrix elements arising from T impurities in the atomic states.

The transition strength $S_{i\to f}$ is the square of the sum of amplitudes of each intermediate states, which when expanded contains terms which are the square of the individual amplitudes, and also terms which involve both intermediate levels

$$\begin{aligned} S_{i\to f} = &\sum_{\epsilon}\left[|A^{\epsilon}_{ST}|^2 + |A^{\epsilon}_{V}|^2\right] f^{\epsilon}_{0}(\omega) \\ &+ \sum_{\epsilon,\epsilon'\neq\epsilon}(A^{\epsilon}_{ST} + iA^{\epsilon}_{V})(A^{\epsilon'}_{ST} - iA^{\epsilon'}_{V})(f^{\epsilon,\epsilon'}_{1}(\omega) + if^{\epsilon,\epsilon'}_{2}(\omega)) \end{aligned} \tag{7.44}$$

where $f^{\epsilon}_{0}(\omega)$ is a Lorentzian lineshape function centred on $\omega_{i\epsilon}$ with width γ_{ϵ}

$$f^{\epsilon}_{0}(\omega) = \frac{1}{(\omega_{i\epsilon} - \omega)^2 + \gamma^2_{\epsilon}} \tag{7.45}$$

and $f^{\epsilon,\epsilon'}_{1}(\omega)$ and $f^{\epsilon,\epsilon'}_{2}(\omega)$ are two different lineshape functions for each pair e, e' of intermediate levels

$$f^{\epsilon,\epsilon'}_{1}(\omega) = \frac{(\omega_{i\epsilon} - \omega)(\omega_{i\epsilon'} - \omega) + \gamma_{\epsilon}\gamma_{\epsilon'}}{((\omega_{i\epsilon} - \omega)^2 + \gamma^2_{\epsilon})((\omega_{i\epsilon'} - \omega)^2 + \gamma^2_{\epsilon'})} \tag{7.46}$$

$$f^{\epsilon,\epsilon'}_{2}(\omega) = \frac{\gamma_{\epsilon}(\omega_{i\epsilon'} - \omega_{i\epsilon}) - (\omega_{i\epsilon} - \omega)(\gamma_{\epsilon'} - \gamma_{\epsilon})}{((\omega_{i\epsilon} - \omega)^2 + \gamma^2_{\epsilon})((\omega_{i\epsilon'} - \omega)^2 + \gamma^2_{\epsilon'})} \tag{7.47}$$

The functions $f_{1,2}(\omega)$ are plotted out in figure 7.2 to illustrate the qualitative difference for a simple case, taking only two intermediate levels e, e' with equal decay rates $\gamma_{\epsilon} = \gamma_{\epsilon'} = \gamma$, and frequency splitting $\omega_{\epsilon\epsilon'} \equiv \omega_{i\epsilon'} - \omega_{i\epsilon} = 10\gamma$. From inspection of eqns 7.46 and 7.47, f_1 and f_2 are even and odd respectively to swapping $e \rightleftharpoons e'$, ie $f^{\epsilon',\epsilon}_{1} = f^{\epsilon,\epsilon'}_{1}$ and $f^{\epsilon',\epsilon}_{2} = -f^{\epsilon,\epsilon'}_{2}$. It follows that the e, e' and e', e terms in eqn 7.44 are complex conjugate pairs. Also, putting $e' = e$ gives $f^{\epsilon,\epsilon}_{1}(\omega) = f^{\epsilon}_{0}(\omega)$ and $f^{\epsilon,\epsilon}_{2}(\omega) = 0$.

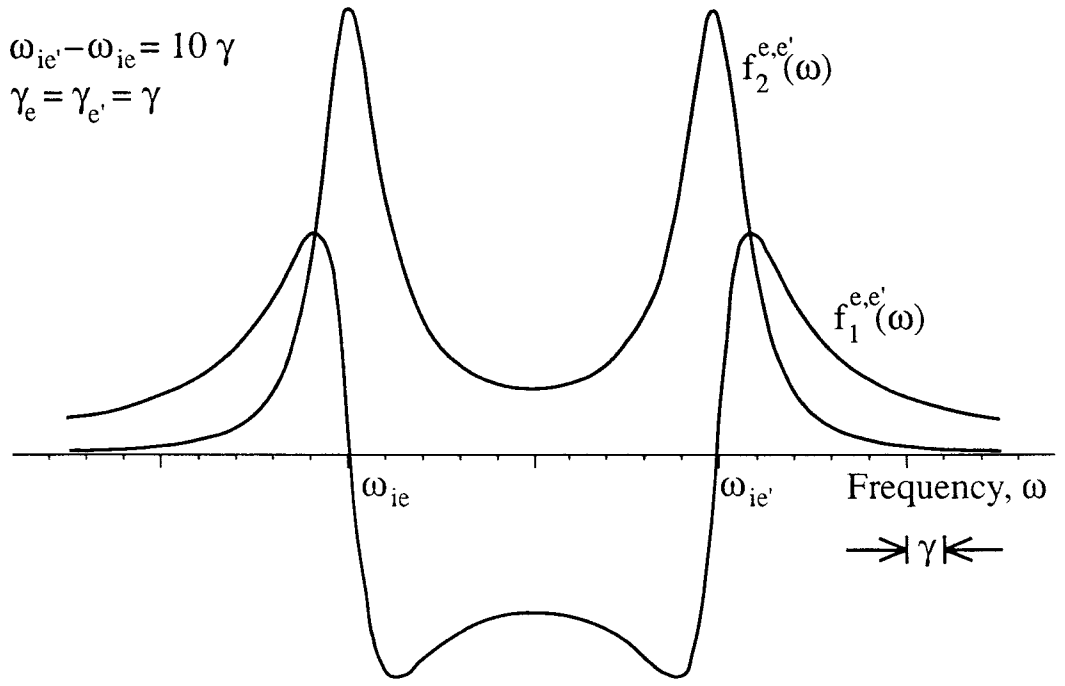


Figure 7.2: Example plot of functions $f_{1,2}(\omega)$

In terms of these lineshape functions, the ordinary part of the transition strength for the $i \rightarrow f$ transition, can be written

$$\begin{aligned} S_0 &= \sum_{\epsilon} \left[|A^{\epsilon}_{ST}|^2 + |A^{\epsilon}_{V}|^2 \right] f^{\epsilon}_0(\omega) \\ &\quad + 2 \sum_{\epsilon,\epsilon'>\epsilon} \left(A^{\epsilon}_{ST} A^{\epsilon'}_{ST} + A^{\epsilon}_{V} A^{\epsilon'}_{V} \right) f_1^{\epsilon,\epsilon'}(\omega) \end{aligned} \tag{7.48}$$

which is of the form *scalar/tensor*^{2} + *vector*^{2}. The PPP part is given by

$$\Delta S_\gamma = 2 \sum_{\epsilon,\epsilon'>\epsilon} \left(A^{\epsilon}_{ST} A^{\epsilon'}_{V} - A^{\epsilon}_{V} A^{\epsilon'}_{ST} \right) f_2^{\epsilon,\epsilon'}(\omega) \tag{7.49}$$

which is of the form *scalar/tensor* $\times$ *vector*.

The Lorentzian function $f_0(\omega)$ and the two photon lineshape functions $f_{1,2}(\omega)$ given by eqns 7.46 and 7.47, have different relative magnitudes over the resonances. Four régimes are distinguished in table 7.1, where the typical frequency detuning $\Delta\omega$ is from the nearest intermediate level resonance, which we assume well resolved $\omega_{\epsilon\epsilon'} \gg \gamma$. The function $f_1(\omega)$ has a zero very close to the line centre, and is largest in the line wings, with a dispersive tail off resonance, while $f_2(\omega)$ is largest at the line centre and falls sharply off resonance.

Assuming that the matrix elements are all of the same order, and that there is no strong cancellation, the relative magnitudes of S_0 and ΔS_γ are just the ratios of their

Lineshape function	Near line centre $\Delta\omega \ll \gamma$	In line wings $\Delta\omega \sim n\gamma$	Off resonance $\Delta\omega \sim \omega_{ee'}$	Far off resonance $\Delta\omega \gg \omega_{ee'}$
$f_0(\omega)$	$\frac{1}{\gamma^2}$	$\frac{1}{n^2\gamma^2}$	$\frac{1}{\omega_{ee'}^2}$	$\frac{1}{\Delta\omega^2}$
$f_1(\omega)$	0	$\frac{1}{n\gamma\omega_{ee'}}$	$\frac{1}{\omega_{ee'}^2}$	$\frac{1}{\Delta\omega^2}$
$f_2(\omega)$	$\frac{1}{\gamma\omega_{ee'}}$	$\frac{1}{n^2\gamma\omega_{ee'}}$	$\frac{\gamma}{\omega_{ee'}^3}$	$\frac{\gamma\omega_{ee'}}{\Delta\omega^4}$

Table 7.1: Lineshape functions $f_{0,1,2}(\omega)$ magnitudes in four régimes of typical detuning $\Delta\omega$ from intermediate level resonance which are resolved $\omega_{ee'} \gg \gamma$.

respective lineshape functions. The ordinary strength S_0 given by eqn 7.48 has two parts: one containing $f_0(\omega)$ Lorentzian terms for each resonance, and the other term with $f_1(\omega)$ lineshape. From table 7.1 the $f_1(\omega)$ is much smaller than $f_0(\omega)$ close to resonance, becoming comparable only far off resonance, so we can neglect the $f_1(\omega)$ term.

$\Delta S_\gamma/S_0$	Near line centre $\Delta\omega \ll \gamma$	In line wings $\Delta\omega \sim n\gamma$	Off resonance $\Delta\omega \sim \omega_{ee'}$	Far off resonance $\Delta\omega \gg \omega_{ee'}$
$\frac{f_2(\omega)}{f_0(\omega)}$	$\frac{\gamma}{\omega_{ee'}}$	$\frac{\gamma}{\omega_{ee'}}$	$\frac{\gamma}{\omega_{ee'}}$	$\frac{\gamma\omega_{ee'}}{\Delta\omega^2}$

Table 7.2: Ratio of decay PPP to total strength $\Delta S_\gamma/S_0$ in four typical detuning régimes as table 7.1.

To order of magnitude accuracy the ratio of the PPP strength to the ordinary strength $\Delta S_\gamma/S_0$ is just the ratio of the f_2 and f_0 lineshape functions. The ratio f_2/f_0 is given in table 7.2 for the four frequency detuning régimes, and is of the same order to this accuracy over the resonances

$$\frac{\Delta S_\gamma}{S_0} \approx \frac{\gamma}{\omega_{ee'}} \tag{7.50}$$

and falls (as $1/\Delta\omega^2$) when far off resonance. The decay PPP strength for the example resonance of figure 7.2 is therefore of order 10% of the background two photon strength.

7.3 T violation PPP effect

If T impurities are present in the atomic states i or f, then the x and y matrix elements acquire an anomalous phase proportional to the T impurity. The admixtures are diagonal in F, so give the *same* extra phase to the scalar/tensor and vector amplitudes

$$A^{\epsilon}_{ST} \rightarrow (1 + i\phi^{\epsilon}_{T})A^{\epsilon}_{ST} \tag{7.51}$$

$$A^{\epsilon}_{V} \rightarrow (1 + i\phi^{\epsilon}_{T})A^{\epsilon}_{V} \tag{7.52}$$

where the channel phases $\phi^{(\epsilon)}_{T}$ are of the order the T impurities. The expansion of the transition strength is now slightly modified from that in the last section

$$\begin{aligned} S_{i\rightarrow f} &= \sum_{\epsilon} \left[|A^{\epsilon}_{ST}|^2 + |A^{\epsilon}_{V}|^2 \right] f^{\epsilon}_{0}(\omega) \\ &+ \sum_{\epsilon,\epsilon' \neq \epsilon} (1 + i\phi^{\epsilon,\epsilon'}_{T})(A^{\epsilon}_{ST} + iA^{\epsilon}_{V})(A^{\epsilon'}_{ST} - iA^{\epsilon'}_{V})(f^{\epsilon,\epsilon'}_{1}(\omega) + if^{\epsilon,\epsilon'}_{2}(\omega)) \end{aligned} \tag{7.53}$$

where $\phi^{\epsilon,\epsilon'}_{T} \equiv \phi^{\epsilon}_{T} - \phi^{\epsilon'}_{T}$ is the anomalous T-odd phase. The real part of the transition strength now contains an additional term with the characteristic *scalar/tensor*$\times$*vector* dependence on the polarisation vectors. This term is the T violation PPP effect, which has a different lineshape $f_1(\omega)$ over the intermediate resonances

$$\Delta S_{TV} = 2 \sum_{\epsilon,\epsilon' > \epsilon} (A^{\epsilon}_{ST}A^{\epsilon'}_{V} - A^{\epsilon}_{V}A^{\epsilon'}_{ST})\phi^{\epsilon,\epsilon'}_{T} f^{\epsilon,\epsilon'}_{1}(\omega) \tag{7.54}$$

The net PPP strength for the $i \rightarrow f$ transition is therefore

$$\Delta S_{i\rightarrow f} = 2 \sum_{\epsilon,\epsilon' > \epsilon} (A^{\epsilon}_{ST}A^{\epsilon'}_{V} - A^{\epsilon}_{V}A^{\epsilon'}_{ST})(f^{\epsilon,\epsilon'}_{2}(\omega) + \phi^{\epsilon,\epsilon'}_{T} f^{\epsilon,\epsilon'}_{1}(\omega)) \tag{7.55}$$

The frequency dependence of the decay and T violation parts are quite different, as illustrated by figure 7.2. The spectrum of ΔS over the resolved intermediate resonances is therefore a possible way of distinguishing the two terms.

As in the previous section the ratio of the T violating PPP strength to the total strength can be estimated assuming that the matrix elements are all of the same order, and that there are no strong cancellations. The ordinary strength S_0 can again be taken as $f_0(\omega)$, while the T violation PPP strength ΔS_{TV} has lineshape $f_1(\omega)$. To order of magnitude accuracy, the ratio of the T violation PPP strength to the ordinary strength is therefore

$$\frac{\Delta S_{TV}}{S_0} \sim \frac{f_1}{f_0}\,\phi_T \tag{7.56}$$

where the anomalous phase $\phi_T = \phi^{\epsilon}_{T} - \phi^{\epsilon'}_{T}$ is due to T violation. The ratio $f_1(\omega)/f_0(\omega)$ is given in table 7.3 for the four frequency detuning régimes, using the values of table 7.1. The T violation PPP strength is suppressed relative to the ordinary strength

$\Delta S_{TV}/S_0$	Near line centre $\Delta\omega \ll \gamma$	In line wings $\Delta\omega \sim n\gamma$	Off resonance $\Delta\omega \sim \omega_{ee'}$	Far off resonance $\Delta\omega \gg \omega_{ee'}$
$\frac{f_1(\omega)}{f_0(\omega)}$	0	$\frac{n\gamma}{\omega_{ee'}}$	1	1

Table 7.3: Ratio of T violating PPP to total strength $\Delta S_{TV}/S_0$ in four typical detuning régimes as table 7.1.

close to resonance, and is largest off resonance where the ratio of the lineshape functions is of order unity

$$\frac{\Delta S_{TV}}{S_0} \sim \phi_T \tag{7.57}$$

There is no enhancement by detuning far off resonance, where the total signal is weaker.

7.4 Background transitions

A background transition rate comes from the spontaneous decay of the intermediate levels. These are in equilibrium for $\gamma t \gg 1$, so the background transition probability grows linearly with the interaction time t. The total probability per atom of being in the final state f after a time t is the sum of the two photon transition probability, which is quadratic in t, and background which is linear in t

$$P_f = S_{i\to f} t^2 + \sum_e P'_e \gamma_{e\to f} t \tag{7.58}$$

where $\gamma_{e\to f}$ is the partial width for decay to the final state of interest. If the field intensities are equal then to order of magnitude accuracy $b^{(B)} = b^{(A)} = b$ and the two photon strength is

$$S \approx \frac{|b|^4}{\Delta\omega^2 + \gamma^2} \tag{7.59}$$

where $\Delta\omega$ is an effective offset from intermediate resonance. After time $t \gg 1/\gamma$, the populations of the intermediate levels P'_e reach equilibrium, which is to order of magnitude accuracy given by

$$P'_e \approx \frac{|b|^2}{\Delta\omega^2 + \gamma^2} \tag{7.60}$$

Hence the ratio of contributions of the two photon to background processes in the final state population is of order

$$\frac{P^{(2)}}{P^{bak}} = \frac{S_{i\to f} t^2}{P'_e \gamma t} \approx \frac{|b|^2 t}{\gamma} \tag{7.61}$$

which, remarkably, is independent of the resonance offset $\Delta\omega$. This ratio should be greater than unity to have a clear two photon signal, which is equivalent to

$$|b|^2 t^2 \gg \gamma t \tag{7.62}$$

ie the one photon transition rate to the intermediate levels should be greater than the dissipation rate from spontaneous decay.

To estimate the relative magnitudes, we can take typical values from the caesium $6s_{1/2} \rightarrow 6p_{3/2}$ system, which is discussed in detail in chapter 8. The decay half width is $\gamma = 2\pi \times 5.27\text{MHz} = 33.1 \times 10^6 \text{s}^{-1}$ so an interaction time $t \approx 3\mu\text{s}$ gives $\gamma t = 100$. The Rabi amplitude is given by eqn 5.21 in terms of the dipole matrix element

$$|b|^2 = (1.1 \times 10^8)^2 I \, |d|^2 \tag{7.63}$$

where d is the dipole component matrix element for the transition. The reduced dipole matrix element is $d = \left\langle 6s_{1/2} \parallel \boldsymbol{d} \parallel 6p_{3/2} \right\rangle \approx 6.4\, ea_0$, but the matrix element d is diluted by an angular factor; these are of order $1/\sqrt{3}$ because d is one component, and also a factor $1/\sqrt{2I+1} = 1/\sqrt{8}$ since the states are hyperfine coupled. The matrix element is therefore of order $d \sim 1.3ea_0$. The requirement for a clear two photon signal, eqn 7.62, for this system determines the minimum intensity

$$I_{min} = \frac{10^{-3}}{d^2} = 0.5\,\text{mW/cm}^2 \tag{7.64}$$

above which the two photon transition probability will exceed the background transitions.

For the weak field assumptions to be valid, a maximum intensity is determined by the requirement that both the intermediate levels and the final state are not saturated, ie $P'_e \ll 1$ and $P_f \ll 1$. The background transitions give $P_f \sim P'_e \gamma t$, so that $P_f \ll 1$ is the more stringent requirement. In the four régimes of frequency detuning $\Delta\omega$ the weak field limits impose the following intensity requirements

- Near line centre $\Delta\omega \ll \gamma$: On resonance the two photon transition probability is the square of the background, so the weak field limit is given by $P'_e \gamma t = 10^3 \, |d|^2 \, I \ll 1$. The maximum intensity is therefore

$$I_{max} = 0.5\,\text{mW/cm}^2 \tag{7.65}$$

  which is the intensity at which the population in the final state is of order unity. This is the same intensity as I_{min} required for the two photon transitions to equal the background.

- In line wings $\Delta\omega \sim n\gamma$: Away from the line centre, the two photon transition probability is larger than the background transitions at saturation, so the weak

field limit is now determined by $St^2 = 10^6 |d|^2 I^2/n^2$ and the maximum intensity is

$$I_{max} = \frac{n}{2} \mathrm{mW/cm^2} \tag{7.66}$$

The ratio of the two photon transition probability to the background is given by $I_{max}/I_{min} = n$.

- Off resonance $\Delta\omega \sim \omega_{ee'}$: The upper levels in question are the $6p_{3/2}$ hyperfine $F = 3, 4$ levels, which have separation $\omega_{ee'} = 2\pi \times 201.2\mathrm{MHz}$. The detuning is therefore of order $n = \frac{1}{2}\omega_{ee'}/\gamma \approx 20$ linewidths between the two resonances, so that for this case the maximum intensity is

$$I_{max} = 10\,\mathrm{mW/cm^2} \tag{7.67}$$

assuming both resonances contribute equally, then the signal to background ratio is $n = 40$.

- Far off resonance $\Delta\omega \gg \omega_{ee'}$: The number of linewidths detuning $n = \Delta\omega/\gamma$ continues to increase the ratio of the signal to background, as long as the driving fields can saturate the transition. However, there is little motivation for a large detuning, since the decay PPP strength falls sharply, and the T violation PPP strength is no longer enhanced.

While the two photon PPP signal can be separated from the background by its distinct angular dependence, it is desirable to maximise the two photon transitions by not being too close to either intermediate level. The intensity requirement of order $\mathrm{mW/cm^2}$ is not large. The decay PPP effect in this system is of order $\gamma/\omega_{ee'} = 2.5\%$. The lack of signal near the resonances is a problem for distinguishing the decay and T violation PPP terms by their lineshapes, but in the next section we discuss achieving this by measuring the reversed transitions.

7.5 Reversed processes: T reversal character

It has been shown that the decay and T violation PPP effects can be distinguished through their different dependence on the spectrum of the intermediate levels. In this section the reversed processes from level $f \to i$ are discussed. The relationships between the $i \pm m \to f \pm m$ and $f \pm m \to i \pm m$ transitions are different for the two effects, and potentially provide a further method to distinguish them.

In the reversed process $fm \to im$ the order of the transitions is reversed; the polarisation vectors are associated with the (different) frequencies of the $i \to e$ and $e \to f$ transitions respectively. If scalar/tensor and vector amplitudes for the reversed process are denoted $\bar{A}_{ST}$ and $\bar{A}_V$ then the matrix element part of the $f \to i$ amplitude is

$$M_{if} = b_{ie}^{(A)} b_{ef}^{(B)} = \bar{A}_{ST}^{e} + i\bar{A}_V^{e} \tag{7.68}$$

where $\bar{A}_{ST}$ and $\bar{A}_V$ are given by

$$\bar{A}^{\epsilon}_{ST} = x_{ie}x_{\epsilon f}\cos\theta = x^*_{fe}x^*_{ei}\cos\theta = A^{\epsilon}_{ST}{}^* \quad (7.69)$$

$$i\bar{A}^{\epsilon}_{V} = x_{ie}y_{\epsilon f}\sin\theta = y^*_{fe}x^*_{ei}\sin\theta = -iA^{\epsilon}_{V}{}^* \quad (7.70)$$

The energy denominator for the reversed $f \rightarrow i$ process is $\omega_{fe} - \omega_B - i\gamma_e$, ie interchanging the roles of the two transitions. The two photon resonance condition can be rewritten as $\omega_{f\epsilon} - \omega_B = \omega_{i\epsilon} - \omega_A$, so that in terms of the amplitudes for the forwards transition A^{ϵ}_{ST} and A^{ϵ}_{V}, the transition strength is

$$S_{f-i} = \left| \sum_{\epsilon} \frac{A^{\epsilon}_{ST}{}^* - iA^{\epsilon}_{V}{}^*}{\omega_{i\epsilon} - \omega - i\gamma_e} \right|^2 \quad (7.71)$$

The difference between this strength and that of the $i \rightarrow f$ transition, eqn 7.15, can be seen in either of two ways. By taking the complex conjugate of the amplitudes, the expressions are identical except for the sign of the decay term $i\gamma$ in S_{i-f} and $-i\gamma$ in S_{f-i}, which changes the sign of f_2 but not f_1 in the PPP term of the reversed process. Alternatively, in the expansion of S_{f-i}, the amplitudes (including contributions from the T impurities) in the numerator are the complex conjugate of the previous case with the functions $f_{1,2}$ unchanged. Both these views are identical and give a PPP term for the reverse process

$$\Delta S_{f-i} = -2 \sum_{\epsilon,\epsilon'>\epsilon} (A^{\epsilon}_{ST}A^{\epsilon'}_{V} - A^{\epsilon}_{V}A^{\epsilon'}_{ST})(f_2^{\epsilon,\epsilon'}(\omega) - \phi_T^{\epsilon,\epsilon'} f_1^{\epsilon,\epsilon'}(\omega)) \quad (7.72)$$

Comparison with the corresponding $i \rightarrow f$ PPP term in eqn 7.55, shows that the decay and T violation effects have different relative signs in the $f \rightarrow i$ transitions. The relationship between the PPP transition strengths of the $im = fm$ transitions, for the decay and T violating effects are

$$\Delta S_{\gamma f-i} = -\Delta S_{\gamma i-f} \quad (7.73)$$

$$\Delta S_{TVf-i} = \Delta S_{TVi-f} \quad (7.74)$$

The transitions between the $-m$ states are related to the $+m$ transitions by the usual rotational arguments, so that the four transitions $i \pm m = f \pm m$ have rates as shown in figure 7.3 where the ordinary part of the transition strength S_0 is the same for all four transitions.

In the above treatment, the transition strengths of reverse processes were calculated by setting up the atom in the state fm, with the geometry and frequencies of the system unchanged. The relationships between the transition strengths of processes reversed in this way are defined by the principle of detailed balance. When the states involved are angular momentum states, the principle of detailed balance states: *The rate of the transition* $im \rightarrow fm$ *is equal to the rate of the T reversed process* $f-m \rightarrow i-m$. This principle should and does hold in the absence of T violation, as illustrated in figure 7.3. These are equal because the matrix element part

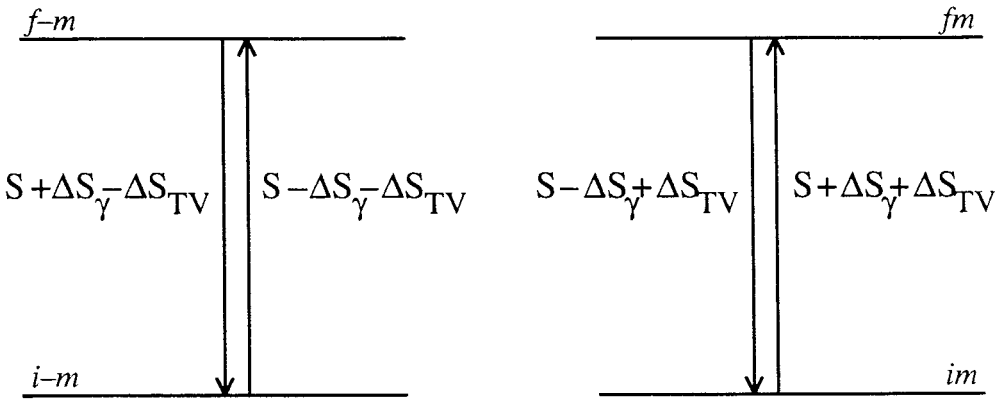


Figure 7.3: PPP terms in transitions between $\pm m$ states

of the amplitudes for each channel are equal, since using Hermiticity and T reversal relations

$$M_{fi} = b_{f\epsilon}^{(B)} b_{\epsilon i}^{(A)} = b_{i'\epsilon'}^{(A)} b_{\epsilon' f'}^{(B)} = M_{i'f'} \tag{7.75}$$

where $i' \equiv Ti$ etc... (the states ϵ and $\epsilon' \equiv T\epsilon$ are degenerate so are equivalent when summed). However, the rates of the transitions $im \rightarrow fm$ and its inverse $fm \rightarrow im$ are *not* related by detailed balance; without decay terms these are equal (from rotational arguments), and when decay terms are present there is a pumping effect which favours one of the two states im or fm.

7.6 Doppler broadened populations

In an ensemble of atoms with a thermal velocity distribution, the frequency of the driving fields in the frame of an atom is shifted according to a Maxwell-Boltzmann distribution. For the Raman process, the two photon transition is made Doppler free by having the light wavevectors $\boldsymbol{k}_{A,B}$ collinear. In this situation, the atoms only differ in the resonance with the intermediate levels relative to the frequency ω_A in the rest frame of the atom (see section §6.3.1, page 78).

The Doppler half width is given by eqn 6.8, and is typically of order $\Gamma_D \sim 10^{-6}\omega_A \sim$ GHz. If the intermediate levels have splittings $\Delta\omega \leq$ GHz, then the ordinary and PPP transition strengths are *averaged* over frequency, weighted by the probability distribution given by eqn 6.7, and the effective number of interacting atoms is given by the ratio of the natural to Doppler linewidths $N/N_0 \sim \gamma/\Gamma_D$. For simplicity, we assume that the Doppler width is much larger than hyperfine structure, so that the effective transition strength per atom is

$$S_{i\rightarrow f}^{eff} = \frac{N}{N_0} \int S_{i\rightarrow f}(\omega)\, d\omega \tag{7.76}$$

where typically $N \sim 10^{-3} N_0$ for natural linewidth $\gamma \sim$ MHz. The frequency dependence of $S_{i\to f}$ is entirely contained in the lineshape functions $f_{0,1,2}(\omega)$. The Lorentzian lineshape function averages to

$$\int f_0^e(\omega)\, d\omega = \frac{\pi}{\gamma_e} \tag{7.77}$$

while f_1 and f_2 average to

$$\int f_1^{e,e'}(\omega)\, d\omega = \frac{2\pi(\gamma_{e'} + \gamma_e)}{(\omega_{ie'} - \omega_{ie})^2 + (\gamma_{e'} + \gamma_e)^2} \tag{7.78}$$

$$\int f_2^{e,e'}(\omega)\, d\omega = \frac{2\pi(\omega_{ie'} - \omega_{ie})}{(\omega_{ie'} - \omega_{ie})^2 + (\gamma_{e'} + \gamma_e)^2} \tag{7.79}$$

The effective ordinary strengths per atom, which is the frequency dependent strength averaged over the velocity distribution of the atoms, is given by

$$\begin{aligned} S_0^{eff} &= \sum_e \frac{\pi}{\gamma_e} \left[|A_{ST}^e|^2 + |A_V^e|^2 \right] \\ &\quad + \sum_{e,e'>e} \frac{4\pi(\gamma_{e'} + \gamma_e)}{(\omega_{ie'} - \omega_{ie})^2 + (\gamma_{e'} + \gamma_e)^2} (A_{ST}^e A_{ST}^{e'} + A_V^e A_V^{e'}) \end{aligned} \tag{7.80}$$

where the first part is the dominant contribution, since the latter term is smaller by a factor of order $(\gamma/\omega_{ee'})^2$. Similarly the effective decay and T violation PPP strengths are

$$\Delta S_\gamma^{eff} = \sum_{e,e'>e} \frac{4\pi(\omega_{ie'} - \omega_{ie})}{(\omega_{ie'} - \omega_{ie})^2 + (\gamma_{e'} + \gamma_e)^2} (A_{ST}^e A_V^{e'} - A_V^e A_{ST}^{e'}) \tag{7.81}$$

$$\Delta S_{TV}^{eff} = \sum_{e,e'>e} \frac{4\pi \phi_T^{e,e'}(\gamma_{e'} + \gamma_e)}{(\omega_{ie'} - \omega_{ie})^2 + (\gamma_{e'} + \gamma_e)^2} (A_{ST}^e A_V^{e'} - A_V^e A_{ST}^{e'}) \tag{7.82}$$

where the γ_e linewidths are the natural linewidths, and *not* the Doppler widths. We therefore expect that the PPP effects from both decays and T violation are not averaged to zero even in the Doppler broadened limit.

In eqn 7.80, the ordinary strength is dominated by the background transition rate due to the spontaneous decay of real population in the intermediate levels. For two levels the ratio of the PPP strength to the ordinary strength is given by

$$\frac{\Delta S_\gamma^{eff}}{S_0^{eff}} \approx \frac{4\gamma_e \gamma_{e'}}{(\omega_{ie'} - \omega_{ie})(\gamma_{e'} + \gamma_e)} \approx \frac{\gamma_e + \gamma_{e'}}{\omega_{ie'} - \omega_{ie}} \tag{7.83}$$

if the level splitting $\omega_{ee'} = \omega_{ie'} - \omega_{ie} \gg \gamma_{e,e'}$, ie the non-Doppler broadened e, e' levels are well resolved. The PPP strength in the Doppler limit is of order $\gamma/\omega_{ee'}$ of the total strength. The T violation PPP ratio to the ordinary strength becomes

$$\frac{\Delta S_{TV}^{eff}}{S_0^{eff}} = \frac{4\gamma_e \gamma_{e'}}{(\omega_{ie'} - \omega_{ie})^2} \phi_T^{e,e'} \tag{7.84}$$

so that the T violation PPP is suppressed by $(\gamma/\omega_{ee'})^2$.

Although it is interesting that the PPP effect can still exist in Doppler broadened gases, the decay PPP strength is not enhanced relative to the ordinary two photon strength. The T violation strength is in fact suppressed relative to the non-Doppler case by a factor $(\gamma/\omega_{ee'})^2$. At the same time the signal, which is proportional to the number of interacting atoms N, is reduced by a factor $\gamma/\Gamma_D \sim 10^{-3}$.

7.7 Sensitivity

When the wavelength is set between the intermediate resonances, the dominant transition process is the coherent two photon transition, with the spontaneous emission background of order $\gamma/\omega_{ee'} \sim 2.5\%$. Only the PPP part of the measured population in the final state displays the characteristic $\sin\theta\cos\theta$ dependence on the angle θ between the polarisation vectors as well as the frequency spectrum over the intermediate levels. Misalignments and circular polarisation impurities do not contribute to first order. We consider first measurement of the decay PPP effect as an interesting phenomenon in its own right, then the possible separation of a T violating effect from comparison of the $i \to f$ and $f \to i$ transitions.

The PPP strength can be extracted from its dependence on the polarisation vectors, ie on the angle θ between $\boldsymbol{\varepsilon}_A$ and $\boldsymbol{\varepsilon}_B$. The ordinary strength S_0 has $\cos^2\theta$ and $\sin^2\theta$ terms; only the PPP strength ΔS depends on $\cos\theta\sin\theta$.The quantity measured is the number of atoms N which have made a transition after the interaction time t. So for the $i \to f$ transition, with all the atoms initially in state i,

$$N = N_0 P_f = N_0 S_{i\to f} t^2 + \textit{background} \tag{7.85}$$

where N_0 is the number of atoms participating. The following linear combination therefore extracts just the PPP transition terms

$$\frac{\Delta S}{S_0} = \frac{N_{\pi/4} - N_{3\pi/4} + N_{5\pi/4} - N_{7\pi/4}}{N_{\pi/4} + N_{3\pi/4} + N_{5\pi/4} + N_{7\pi/4}} \tag{7.86}$$

since the N_0 and t^2 dependence of N cancels. The numerator of eqn 7.86 extracts just the $\sin 2\theta$ component of the transition strength, and is zero for $S = constant$, $\sin\theta$, $\cos\theta$ and $\cos 2\theta$ parts. The ratio $\Delta S/S_0$ should be greater than the statistical noise in N, which is of order $\sqrt{N}$. For the PPP effect to be visible, we therefore require

$$\frac{\Delta S}{S_0} > \frac{1}{\sqrt{N}} \sim 10^{-5} \tag{7.87}$$

taking $N \sim 10^{10}$ atoms. Typical systems, as discussed in section §7.4, can have $\Delta S/S_0$ of order 2.5% which should therefore be observable.

The sum of the PPP strengths $\Delta S = \Delta S_\gamma + \Delta S_{TV}$ for each transition can be extracted from the angular dependence, eg using eqn 7.86. As discussed in section §7.3,

the two effects combine in different ways for the four transitions between the m and $-m$ states of the i and f levels. The T ratio for the PPP systems is given by the following linear combination

$$T = \frac{\Delta S_{TV}}{S_0} = \frac{S_{im\to fm} - S_{f-m\to i-m} + S_{fm\to im} - S_{i-m\to f-m}}{S_{im\to fm} + S_{f-m\to i-m} + S_{fm\to im} + S_{i-m\to f-m}} \tag{7.88}$$

which extracts the T violating part as a ratio to the ordinary strength. Substituting for ΔS_{TV} from eqn 7.54 gives the enhancement ratio. We take a system with only two intermediate levels, and not within a linewidth of the intermediate resonances

$$T \approx \phi_T \tag{7.89}$$

where ϕ_T is the loop phase, which is the difference of the channel phases. There is no enhancement factor, and a positive measurement should be more than the fractional statistical noise $1/\sqrt{N}$, which gives sensitivity to

$$\varphi_T > \frac{1}{\sqrt{N}} \sim 10^{-5} \tag{7.90}$$

taking $N \sim 10^{10}$.

7.8 Forbidden transition PPP schemes

The Raman systems so far considered have been involving two allowed (E1) transitions. We now generalise these results to include forbidden transitions, eg magnetic dipole (M1) and electric quadrupole (E2) systems. The motivation for using forbidden transitions is clear from section §7.4, which showed that the decay effect is of order $\gamma/\Delta\omega$ of the ordinary two photon rate. Forbidden (ie even parity transitions) involve long lived (metastable) levels for which γ can be very small. In practice, a lower limit on the effective linewidth of the upper level is either the interaction time (eg transit time of an atomic beam) or the radiation bandwidth.

The two photon transition strength given by eqn 7.2 in terms of the Rabi rates $b_{ie}^{(A)}$ and $b_{ef}^{(B)}$ of the two transitions is the same for forbidden transitions with the appropriate interaction matrix element. The Rabi amplitudes can be written in terms of the 'unitless' transition matrix elements defined in section §5.2, which are of order unity for an allowed transition. Off resonance by $\Delta\omega \gg \gamma$, the transition probability $P_f = S_{i\to f}t^2$ is of order

$$P_f \sim \frac{10^{32} I_A I_B}{\Delta\omega^2} \left| U^{(A)} U^{(B)} \right|^2 t^2 \tag{7.91}$$

which is of order unity for an allowed transition with $I_{A,B} \sim 1\mathrm{W/cm}^2$, $t \sim 1\mu s$ and $\Delta\omega \sim 10^{10}\mathrm{s}^{-1}$. For forbidden transitions, either larger driving field amplitudes

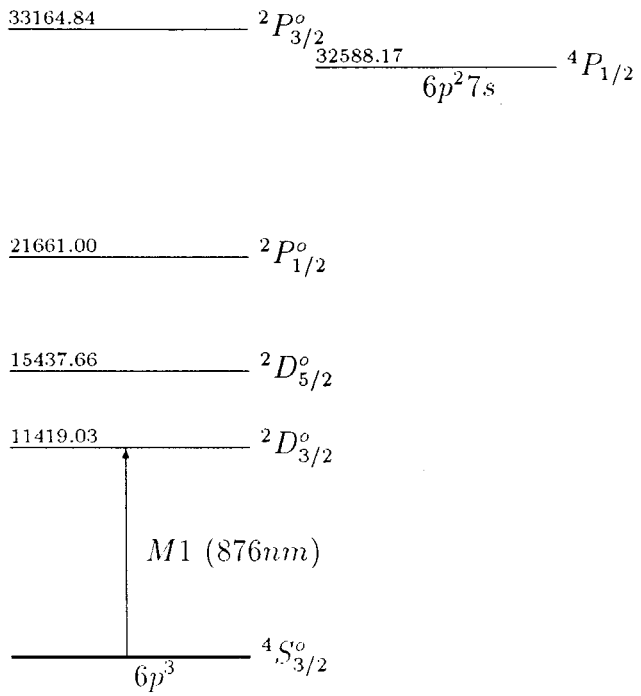


Figure 7.4: Low lying terms of Bi

or longer interaction times are required, eg the M1 matrix element is of order $\alpha/2$ so that the transition strength is reduced by of order $(\alpha/2)^4 \approx 10^{-10}$. The transition probability can be of order unity with interaction time of $t \sim 10^{-1}$s.

To maximise the transition strengths a magnetic dipole (M1) transition would be desirable, but this requires two levels of the *same* angular momentum in the ground state configuration. In some atoms (eg bismuth) and ions, relativistic effects make M1 transitions between configurations possible. An example is the well known bismuth $^4S_{3/2} \rightarrow {}^2D_{3/2}$ $(876nm)$ resonance shown in figure 7.4, which has M1 dipole amplitude from relativistic effects of order $\left\langle {}^2D_{3/2} \| \boldsymbol{\mu} \| {}^4S_{3/2} \right\rangle \sim \mu_B$.

The analysis of the ordinary and PPP transition strength is similar to the E1 system. The Rabi matrix elements can be written in exactly the same way as two amplitudes of scalar/tensor and vector character. It is still possible to assume the same Doppler free geometry with the wavevectors $\boldsymbol{k}_{A,B}$ along the z axis, and $\boldsymbol{\varepsilon}_A$ along the x axis and $\boldsymbol{\varepsilon}_B$ in the x, y plane at an angle θ to $\boldsymbol{\varepsilon}_A$

$$A_{ST} = \langle f \,|\, \mu_y \,|\, e \rangle \langle e \,|\, \mu_y \,|\, i \rangle \cos\theta \tag{7.92}$$

$$iA_V = \langle f \,|\, \mu_x \,|\, e \rangle \langle e \,|\, \mu_y \,|\, i \rangle \sin\theta \tag{7.93}$$

where in the usual phase convention, both A_{ST} and A_V are real. In terms of these amplitudes, the two photon transition strength has exactly the same form as for the allowed transitions, except for an overall reduction in the transition strength.

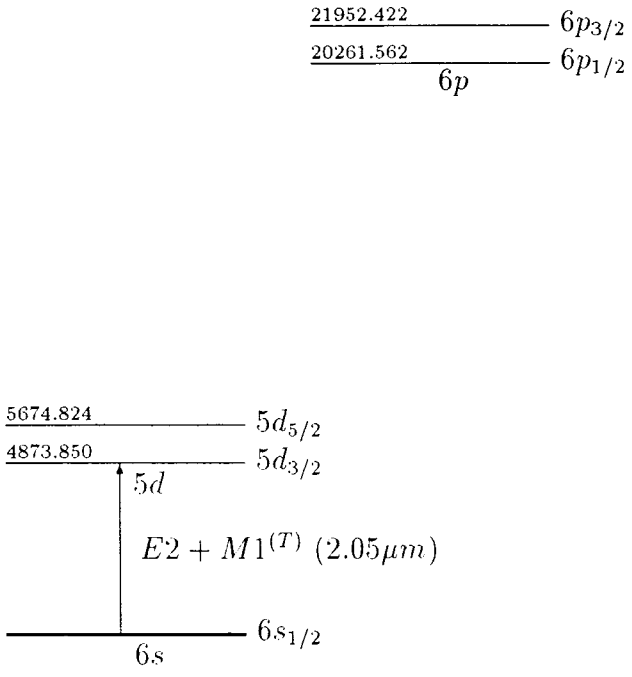


Figure 7.5: Low lying terms of Ba II

An alternative to M1 systems is to use E2 transitions which are weaker, but not limited in the same way. Enhancement is possible if the T impurity allows the stronger M1 transition over an E2 background. An example is the Ba II ion, which is caesium-like with a very low $5d$ configuration as shown in figure 7.5. For the E2 PPP system, the scalar/tensor and vector amplitudes are

$$A_{ST} = \langle f \,|\, Q_{xz} \,|\, e \rangle \langle e \,|\, Q_{xz} \,|\, i \rangle \cos\theta \tag{7.94}$$

$$iA_V = \langle f \,|\, Q_{xz} \,|\, e \rangle \langle e \,|\, Q_{yz} \,|\, i \rangle \sin\theta \tag{7.95}$$

where in the usual phase convention, both A_{ST} and A_V are real. Compared to the two E1 transition strength, the two E2 strength is smaller by a factor of order $(\omega/\omega_{au})^2\alpha^4 \sim 10^{-12}$. However, the transition probability can be increased to of order unity with a sufficiently long interaction time $t \sim 1$s or by increasing the intensity of the driving fields, both of which are not unreasonable in an ion trap where coherence time is very long, and the ion is highly localised, so that the incident light can be highly focussed. If a T-odd interaction mixes the $s_{1/2}$ and $d_{3/2}$ levels, then the channel phase for each channel will be the ratio of the $M1$ transition through the T impurities, to the background E2 rate, so that the T ratio is of order

$$T \sim \frac{\langle M1 \rangle}{\langle E2 \rangle}\delta_T \sim \frac{\omega_{au}}{\omega}\delta_T \sim 10^2\delta_T \tag{7.96}$$

where δ_T is the T impurity and the enhancement factor is 10^2. At the same time, the

decay PPP strength has been suppressed relative to the total signal because of the reduced decay width.

7.9 Summary

The PPP effect is a T-odd phenomenon in coherent two photon transitions, which can arise either from genuine T violation in the atom or through the decay of the intermediate levels. The characteristic signature $\boldsymbol{\sigma}'.\boldsymbol{\varepsilon}_A \times \boldsymbol{\varepsilon}_B \, \boldsymbol{\varepsilon}_A.\boldsymbol{\varepsilon}_B$ can exist for *plane* polarisations. The polarisation of $\boldsymbol{J}$ (ie its projection on $\boldsymbol{\sigma}'$) with the axis defined by $\boldsymbol{\varepsilon}_A \times \boldsymbol{\varepsilon}_B \boldsymbol{\varepsilon}_A.\boldsymbol{\varepsilon}_B$ is forbidden in a T invariant evolution, since the latter is T-even, and results in a different rate for the $m \rightarrow m$ and $-m \rightarrow -m$ transitions. The two photon transition can of course be differentiated from the background by its dependence on the angle θ between $\boldsymbol{\varepsilon}_A$ and $\boldsymbol{\varepsilon}_B$.

In the Doppler free configuration, PPP pumping occurs in $\Delta m = 0$ transitions only, and is independent to first order of misalignment of the pumping axis $\boldsymbol{\varepsilon}_A \times \boldsymbol{\varepsilon}_B$ and the quantisation axis $\boldsymbol{\sigma}'$ of measurement. If the polarisation of the driving fields contain some circular polarisation impurity, then the background transition rate will contain an ordinary optical pumping effect through spontaneous emission, but to first order such impurities have no effect on the two photon transition strength.

The T violation and decay effects are separable both from their different frequency dependence and by comparison of the pumping component with the reversed transition processes. Raman systems between ground state hyperfine components are particularly favourable for the latter technique. Algebraically the decay PPP effect is due to the imaginary part $i\gamma$ in the energy denominator of the intermediate level resonances, which has the effect of adding a phase of order $\gamma/\Delta\omega$ to the effective two photon transition amplitude. The *absence* of an effect would be of significance in elucidating the limitations of the usual treatments of unstable states such as density matrix or dressed states theory which both yield the same prescription.

As a measurement of T violation, the sensitivity is limited: there is no enhancement, and the T violating part must be separated from the much larger decay effect. In the next chapter the PPP effect is calculated in detail for caesium $6s, 6p$ Raman transitions.

We note however that the system so far considered has been involving two *allowed* (E1) transitions. In section §7.8 we generalised the results of this chapter to include forbidden transition systems. The motivation for using forbidden transitions is clear from section §7.4, which showed that the decay effect is of order $\gamma/\Delta\omega$ of the ordinary two photon rate. Forbidden (ie even parity transitions) involve long lived (metastable) levels for which γ can be very small. In practice, a lower limit on the effective linewidth is either the interaction time (eg the transit time of an atomic beam) or the radiation bandwidth. In some systems, the T violating channel can also be enhanced in addition to suppressing the decay effect if the T impurity channel is a more allowed transition.

Chapter 8

The PPP effect in caesium

In this chapter, the PPP effect in a near resonant Raman system in caesium is calculated in detail as a worked example of the PPP theory developed in the last chapter. The nuclear spin of ^{133}Cs is $I = 7/2$, so the $6s_{1/2}$ ground state has hyperfine components $F = 3, 4$, and these are separated by the very precisely known frequency 9192.63177 MHz. It is possible, by modulation of a laser, to maintain a precise two photon resonance while scanning over the intermediate level resonances.

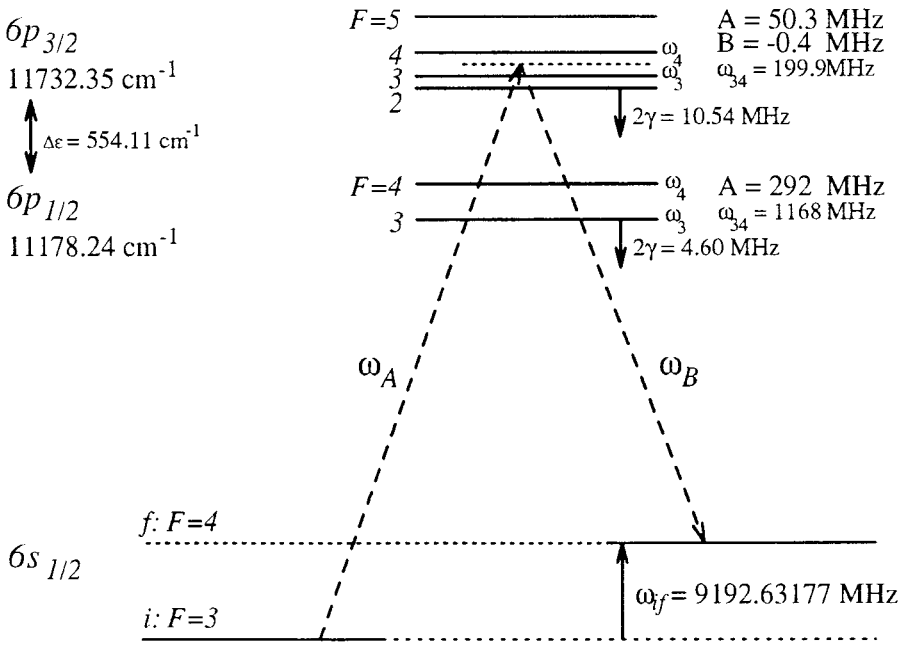


Figure 8.1: Caesium Raman transition

Figure 8.1 shows the ground state and $6p_{1/2}$, $6p_{3/2}$ configurations, with term energies (in cm^{-1}), hyperfine structure coefficients A, B and decay widths (in MHz) for each level (which are equal for all the hyperfine components of each level). The

frequency splitting of adjacent hyperfine levels F and $F' = F - 1$ is given by

$$\omega_{F-1,F} = AF + \frac{3BF(F^2 + 1/2)}{I(2I-1)J(2J-1)} \tag{8.1}$$

where the second term is zero unless $I \geq 1$ and $J \geq 1$. Only the $F = 3, 4$ levels contribute to the two photon transition rate, since the upwards and downwards transitions must both have $\Delta F \leq 1$. There is therefore only one PPP term of magnitude γ/ω_{34}, where ω_{34} is the frequency splitting of the $F = 3$ and $F = 4$ hyperfine levels. The relative magnitude of the PPP effects for $6p_{1/2}$ and $6p_{3/2}$ Raman systems are

$$\frac{\Delta S_\gamma}{S_0} \sim \frac{\gamma}{\omega_{34}} = \begin{cases} \frac{2.30}{1168} = 0.2\% & \ldots \quad 6p_{1/2} \\ \frac{5.27}{199.9} = 2.6\% & \ldots \quad 6p_{3/2} \end{cases} \tag{8.2}$$

using the decay widths and frequency splittings shown in figure 8.1. The PPP effect is larger for the $6p_{3/2}$ level both because the scale of the level splitting to the decay width is larger.

In this chapter, the background and decay PPP contributions to the two photon transition strength, including their frequency and M dependence, are calculated in detail for the $6p_{3/2}$ resonance. In addition, the T violation PPP effect is calculated assuming an atomic TO,PE interaction which mixes the close $6p_{1/2} = 6p_{3/2}$ levels.

8.1 Dipole matrix elements

A complete calculation of the PPP effects in caesium requires only the two dipole matrix elements $6s, 6p_{1/2}$ and $6s, 6p_{3/2}$. The dipole operator has components $d_q^1 = -erC_q^1$ so that its reduced matrix elements which we denote d_j are related to radial integrals of er by

$$d_{j'} \equiv \left\langle 6s_{1/2} \,\|\, \boldsymbol{d} \,\|\, 6p_{j'} \right\rangle = \sqrt{(2j'+1)/3}\, \left\langle 6s_{1/2} \,\|\, er \,\|\, 6p_{j'} \right\rangle \tag{8.3}$$

where for Dirac single particle wavefunctions the radial integral is

$$\left\langle 6s_{1/2} \,\|\, r \,\|\, 6p_{j'} \right\rangle \equiv \int \left(P^*_{6pj'} r P_{6s\frac{1}{2}} + Q^*_{6pj'} r Q_{6s\frac{1}{2}} \right) dr \tag{8.4}$$

The radial integrals for the $6p_{j'=1/2,3/2}$ have been experimentally determined: these are $-5.535(14)ea_0$ and $-5.509(7)ea_0$ respectively [47, 71]. The dipole reduced matrix elements are therefore

$$d_{1/2} = -4.519(11)ea_0 \tag{8.5}$$

$$d_{3/2} = -6.361(8)ea_0 \tag{8.6}$$

Finally, the transition matrix elements between the hyperfine components are all related to the reduced matrix elements between the electronic levels

$$\left\langle 6s_{1/2}\, F \,\|\, \boldsymbol{d} \,\|\, 6p_{j'}\, F' \right\rangle = A_{j'}(F, F') \left\langle 6s_{1/2} \,\|\, \boldsymbol{d} \,\|\, 6p_{j'} \right\rangle \tag{8.7}$$

where the angular factors $A_{j'}(F,F')$ are given by

$$A_{j'}(F,F') = (-1)^{1+F'}\sqrt{(2F+1)(2F'+1)}\begin{Bmatrix} F & 1 & F' \\ j' & \frac{7}{2} & \frac{1}{2} \end{Bmatrix} \tag{8.8}$$

The spontaneous decay rate, ie the Einstein A coefficient for the $6p$ levels is given in terms of their dipole matrix elements $d_{j'}$ by

$$A_{6p_{j'}} = \frac{2\alpha^3\omega_{au}}{3}\left[\frac{\omega}{\omega_{au}}\right]^3 |d_{j'}|^2 \tag{8.9}$$

where the atomic frequency unit $\hbar\omega_{au} = \alpha^2 mc^2$ and the dipole is in units ea_0. In frequency units $\omega_{au} \approx 4.13\times10^{16}\,\mathrm{s}^{-1} = 2\pi \times 6.58\times10^{15}\,\mathrm{Hz}$. The $6p$ levels can only decay to the $6s$ ground state, so the Einstein A coefficient is equal to the total line width $A = 2\gamma$. Taking the values of eqns 8.5 and 8.6 the linewidths of the $6p_{1/2}$ and $6p_{3/2}$ levels are therefore

$$\gamma = \begin{cases} 2\pi \times 2.300(11)\,\mathrm{MHz} & \ldots \quad 6p_{1/2} \\ 2\pi \times 5.268(13)\,\mathrm{MHz} & \ldots \quad 6p_{3/2} \end{cases} \tag{8.10}$$

which are the values shown in figure 8.1.

8.2 The weak field régime

The total transition probability depends on the intensities of the two driving fields I_A and I_B, and the interaction time t. In an atomic beam experiment the interaction time is the transit time for the atoms crossing the interaction region, typically $t \sim 3\,\mu\mathrm{s}$.

The total transition probability to state f contains the two photon term which contains the PPP effect, and the background term from spontaneous decay of the upper level $P_f = P_f^{(2)} + P_f^{bak}$. The population in f from the two photon transitions is

$$P_f^{(2)} = (1.9\times10^3)^2 I_A I_B S_{i\to f} t^2 \tag{8.11}$$

where the units are $I_{A,B}$ in $\mathrm{W/cm^2}$ and the transit time t in $\mu\mathrm{s}$. The two photon strength is the usual form given by eqn 7.15

$$S_{i\to f} = \left|\sum_e \frac{A_{ST}^e + iA_V^e}{\omega_{ie} - \omega - i\gamma_e}\right|^2 \tag{8.12}$$

in which the dipole matrix elements are in atomic units ea_0 and frequencies and decay widths in units $2\pi\times10^6\,\mathrm{s}^{-1}$ (ie MHz values).

With the decay width and interaction time expressed in the same units as above, the spontaneous decay background is proportional to the equilibrium population of the upper level

$$P_f^{bak} = 2\pi \sum_e P'_e \gamma_{e\to f} t \tag{8.13}$$

where

$$P'_e = 3.1\times10^2 I_A \frac{|\boldsymbol{\varepsilon}_A.\boldsymbol{d}_{ei}|^2}{(\omega_{ie}-\omega)^2+\gamma_e^2} \tag{8.14}$$

The partial width $\gamma_{e\to f}$ is the partial decay width from the coherent upper level to the *single* state $f = |4M\rangle$, typically of order $\gamma_{e\to f} \sim \gamma/6$. The total background population in f comes from each upper level with a Lorentzian lineshape. The background is largest when resonant with one of the upper levels, and is of order unity at the 'saturation' intensity $I_{max} \sim 0.5\,\mathrm{mW/cm^2}$ derived in section §7.4.

When detuned between the $F' = 3$ and $F' = 4$ levels, higher intensity fields can be applied to increase the ratio of the two photon to background transitions. Midway between the $F' = 3,4$ resonances the detuning is $\Delta\omega \sim 2\pi \times 100\,\mathrm{MHz}$, at which point the two photon strength is of order $S \sim 10^{-3}$. At the saturation intensity $I = 10\,\mathrm{mW/cm^2}$, the population in the final state is then of order $P_f^{(2)} \sim 1$. At the same time the background transitions are of order $P_f^{bak} \sim \gamma/\Delta\omega \sim 0.05$. The ratio of the two photon signal to the background transitions is therefore of order 20 : 1.

8.3 Ordinary transition strength

We now evaluate the ordinary transition strength S_0 given by eqn 7.48 for the $3M \to 4M$ Raman transition. Since x and y are not spherical tensor components (they are combinations of $d^1_{\pm1}$) it is convenient to use the a and b matrix element form introduced in section §7.1.4, which are defined by

$$A_{ST} = (a+b)\cos\theta \tag{8.15}$$

$$A_V = (a-b)\sin\theta \tag{8.16}$$

and given in terms of x and y matrix elements by eqns 7.19 and 7.20 respectively. Using these for each $6p_{j'}F'$ level has the additional advantage of making the angular dependence explicit. There are only two $6p_j$ hyperfine levels $F' = 3,4$, so the ordinary transition strength S_0 given by eqn 7.48 is the sum of two background Lorentzian terms and one two photon term, each with an associated lineshape function

$$\begin{aligned} S_0 = {} & \left[\left|A^{(3)}_{ST}\right|^2 + \left|A^{(3)}_V\right|^2\right] f_0^{(3)}(\omega) + \left[\left|A^{(4)}_{ST}\right|^2 + \left|A^{(4)}_V\right|^2\right] f_0^{(4)}(\omega) \\ & + 2\left[A^{(3)}_{ST}A^{(4)}_{ST} + A^{(3)}_V A^{(4)}_V\right] f_1^{(3,4)}(\omega) \end{aligned} \tag{8.17}$$

The strength S_0 contains terms proportional to $A^2_{ST} \propto \cos^2\theta = |\boldsymbol{\varepsilon}_A.\boldsymbol{\varepsilon}_B|^2$ and to $A^2_V \propto \sin^2\theta = |\boldsymbol{\varepsilon}_A\times\boldsymbol{\varepsilon}_B|^2$, so that the net angular dependence has a component independent of θ, and a component proportional to $\cos 2\theta$. Putting $x = -\sqrt{1/2}(d^1_1 - d^1_{-1})$, the a and b matrix element expressions for the $3M \to 4M$ transition are

$$a = -\frac{1}{2}\left\langle 6s\,4M \left| d^1_{-1} \right| 6p_{j'}F'M+1\right\rangle \left\langle 6p_{j'}F'M+1 \left| d^1_1 \right| 6s\,3M\right\rangle \tag{8.18}$$

$$b = -\frac{1}{2}\left\langle 6s\,4M \left| d^1_1 \right| 6p_{j'}F'M-1\right\rangle \left\langle 6p_{j'}F'M-1 \left| d^1_{-1} \right| 6s\,3M\right\rangle \tag{8.19}$$

$a+b$	$F'=3$	$F'=4$
$M=-3$	$\sqrt{\frac{7}{16}}$	$-\sqrt{\frac{7}{16}}$
$M=-2$	$\sqrt{\frac{1}{3}}$	$-\sqrt{\frac{1}{3}}$
$M=-1$	$\sqrt{\frac{5}{48}}$	$-\sqrt{\frac{5}{48}}$
$M=0$	0	0
$M=1$	$-\sqrt{\frac{5}{48}}$	$\sqrt{\frac{5}{48}}$
$M=2$	$-\sqrt{\frac{1}{3}}$	$\sqrt{\frac{1}{3}}$
$M=3$	$-\sqrt{\frac{7}{16}}$	$\sqrt{\frac{7}{16}}$

$a-b$	$F'=3$	$F'=4$
$M=-3$	$\sqrt{\frac{7}{16}}$	$\sqrt{\frac{175}{144}}$
$M=-2$	$\sqrt{\frac{3}{4}}$	$\sqrt{\frac{100}{48}}$
$M=-1$	$\sqrt{\frac{15}{16}}$	$\sqrt{\frac{125}{48}}$
$M=0$	1	$\frac{5}{3}$
$M=1$	$\sqrt{\frac{15}{16}}$	$\sqrt{\frac{125}{48}}$
$M=2$	$\sqrt{\frac{3}{4}}$	$\sqrt{\frac{100}{48}}$
$M=3$	$\sqrt{\frac{7}{16}}$	$\sqrt{\frac{175}{144}}$

Table 8.1: Values for $a \pm b$ for $6p_{1/2}$ $F' = 3, 4$ and $M = -3 \ldots 3$ in units $d^2_{1/2}/16$

$a+b$	$F'=3$	$F'=4$
$M=-3$	$-\sqrt{\frac{7}{64}}$	$\sqrt{\frac{7}{64}}$
$M=-2$	$-\sqrt{\frac{1}{12}}$	$\sqrt{\frac{1}{12}}$
$M=-1$	$-\sqrt{\frac{5}{192}}$	$\sqrt{\frac{5}{192}}$
$M=0$	0	0
$M=1$	$\sqrt{\frac{5}{192}}$	$-\sqrt{\frac{5}{192}}$
$M=2$	$\sqrt{\frac{1}{12}}$	$-\sqrt{\frac{1}{12}}$
$M=3$	$\sqrt{\frac{7}{64}}$	$-\sqrt{\frac{7}{64}}$

$a-b$	$F'=3$	$F'=4$
$M=-3$	$-\sqrt{\frac{7}{64}}$	$-\sqrt{\frac{175}{576}}$
$M=-2$	$-\sqrt{\frac{3}{16}}$	$-\sqrt{\frac{100}{192}}$
$M=-1$	$-\sqrt{\frac{15}{64}}$	$-\sqrt{\frac{125}{192}}$
$M=0$	$-\frac{1}{2}$	$-\frac{5}{6}$
$M=1$	$-\sqrt{\frac{15}{64}}$	$-\sqrt{\frac{125}{192}}$
$M=2$	$-\sqrt{\frac{3}{16}}$	$-\sqrt{\frac{100}{192}}$
$M=3$	$-\sqrt{\frac{7}{64}}$	$-\sqrt{\frac{175}{576}}$

Table 8.2: Values for $a \pm b$ for $6p_{3/2}$ $F' = 3, 4$ and $M = -3 \ldots 3$ in units $d^2_{3/2}/16$

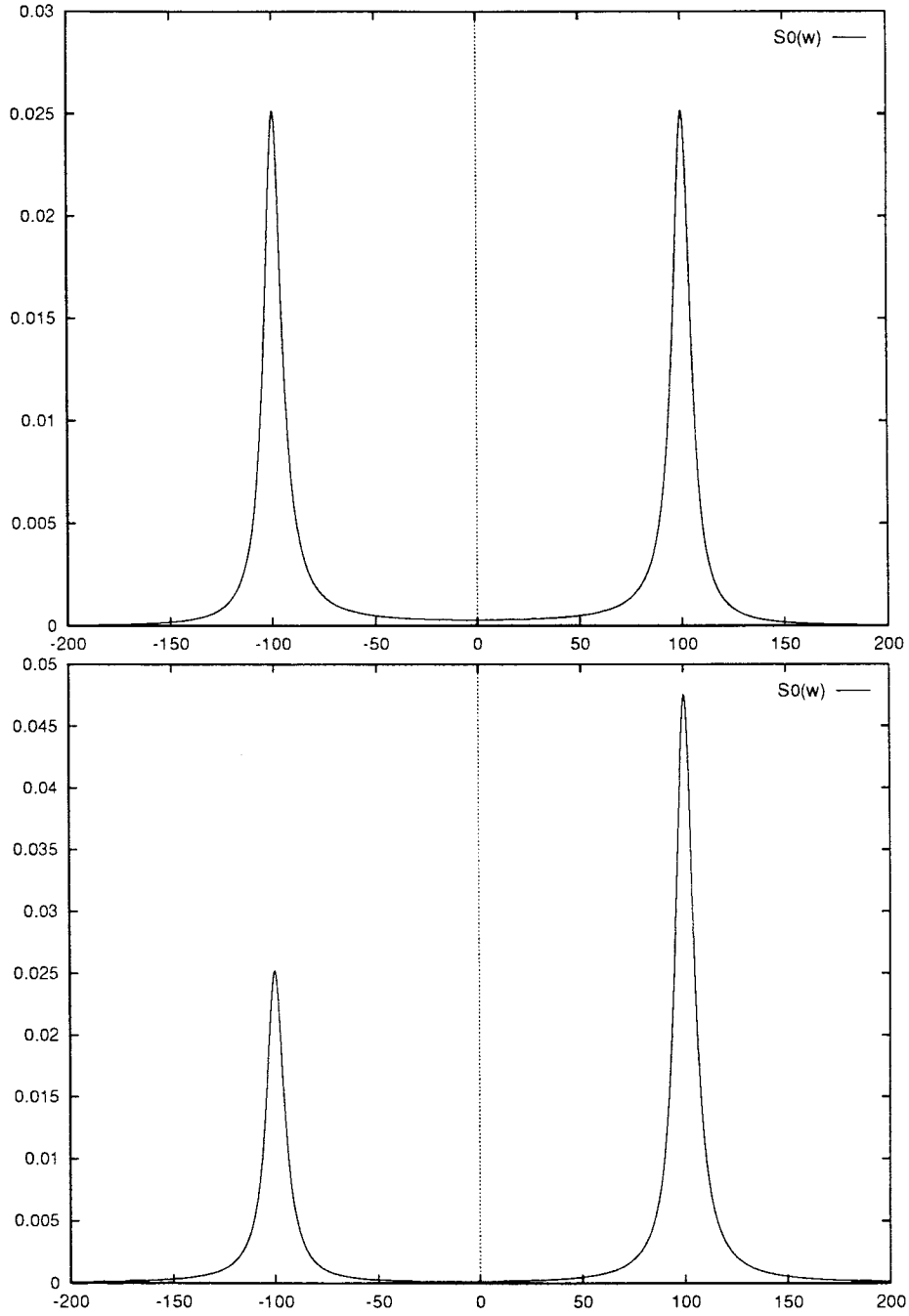


Figure 8.2: Ordinary strength S_0 of $6s\ 33 \rightarrow 43$ transition, frequency in MHz over $6p_{3/2}\ F' = 3, 4$ resonances, *top*: with angle $\theta = 0$, *bottom*: $\theta = \pi/4$

for $F' = 3, 4$, and from rotational symmetry, the $\pm M$ values are related by $b(M) = -a(-M)$.

The scalar/tensor and vector amplitudes are proportional to $a \pm b$ respectively and the angular factors for these are tabulated for the $6p_{j'}$ $F' = 3, 4$ levels in tables 8.1 and 8.2 for each $3M \rightarrow 4M$ Raman transition, $M = -3 \ldots 3$. The tabulated values are in units $d_j^2/16$, and are given by

$$a + b = (-1)^{j'-\frac{1}{2}} \frac{2M(2F'-7)}{3(2j'+1)} \left(1 - \frac{M^2}{16}\right)^{\frac{1}{2}} \frac{d_{j'}^2}{16} \tag{8.20}$$

$$a - b = (-1)^{j'-\frac{1}{2}} \frac{2(2F'-3)}{3(2j'+1)} \left(1 - \frac{M^2}{16}\right)^{\frac{1}{2}} \frac{d_{j'}^2}{16} \tag{8.21}$$

for the $F' = 3, 4$ channels of $j' = \frac{1}{2}, \frac{3}{2}$ configurations. Only the $6p_{3/2}$ channels are of interest here, since the PPP effect is much larger.

At $\theta = 0$ the amplitudes are given by $A_{ST} = a + b$ and $A_V = 0$, However, when $\theta = \pi/4$ the amplitudes become $A_{ST} = (a + b)/\sqrt{2}$ and $A_V = (a - b)/\sqrt{2}$. For instance, the ordinary (non-PPP) rate S_0 for the $M = \pm 3$ transitions in both cases is given by

$$S_0(\theta = 0) = \frac{7 d_{3/2}^4}{16384} \left[f_0^{(3)}(\omega) + f_0^{(4)}(\omega) - 2 f_1^{(3,4)}(\omega) \right] \tag{8.22}$$

$$S_0(\theta = \pi/4) = \frac{7 d_{3/2}^4}{16384} \left[f_0^{(3)}(\omega) + \frac{17}{9} f_0^{(4)}(\omega) + \frac{2}{3} f_1^{(3,4)}(\omega) \right] \tag{8.23}$$

These two strength functions are plotted out in figure 8.2.

8.4 Decay PPP transition strength

The decay term PPP strength ΔS_γ is obtained in a similar way, from eqn 7.49, and has frequency dependence proportional to $f_1(\omega)$ which is different to the dependences of S_0. There is only one contribution from the $F' = 3, 4$ resonances

$$\Delta S_\gamma = 2 \left[A_{ST}^{(3)} A_V^{(4)} - A_V^{(3)} A_{ST}^{(4)} \right] f_2^{(3,4)}(\omega) \tag{8.24}$$

The $a \pm b$ amplitudes for the channels give the following M dependence for the decay PPP strength

$$\Delta S_\gamma = M \left(1 - \frac{M^2}{16}\right) \frac{4}{9} \frac{d_{3/2}^4}{256} f_2^{(3,4)}(\omega) \sin\theta \cos\theta \tag{8.25}$$

which vanishes at $\theta = 0$, and is a maximum for $\theta = \pi/4$. ΔS is odd under reversal of M. The strength is plotted out in figure 8.3 in the same units as the previous plots of the background strength S_0. At the $F' = 3$ line centre, the ordinary two photon transition strength is $S_0 \approx 0.025$ and the decay PPP strength is $\Delta S_\gamma \approx 0.002$, about 10% of the ordinary strength.

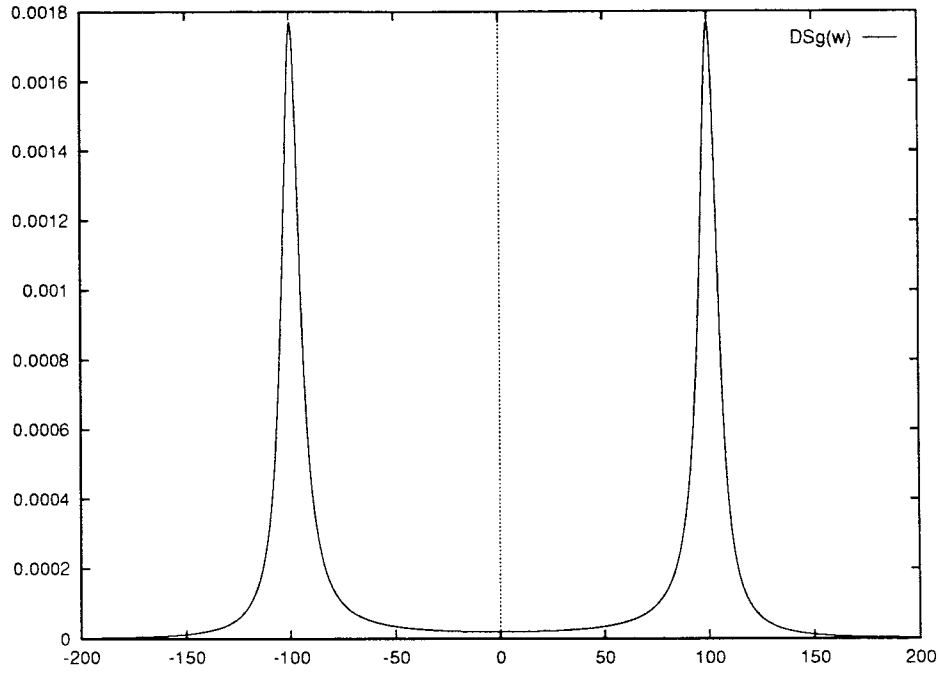


Figure 8.3: Decay PPP strength $|\Delta S_\gamma|$ for $6s\,33 \rightarrow 43$ transition, with angle $\theta = \pi/4$ and frequency in MHz.

8.5 T violating PPP transition strength

The T violating PPP strength ΔS_{TV} is given by eqn 7.54 and has a similar form to the decay strength, but with lineshape function $f_1(\omega)$

$$\Delta S_{TV} = 2\left[A_{ST}^{(3)}A_V^{(4)} - A_V^{(3)}A_{ST}^{(4)}\right]\phi_T f_1^{(3,4)}(\omega) \tag{8.26}$$

where $\phi_T \equiv \phi_T^{(3)} - \phi_T^{(4)}$ is the difference of the $F' = 3, 4$ channel phases. The angular factors and M dependence are the same as for the decay PPP strength, and the ratio of the two PPP strengths gives both the magnitude and sign of the T violating phase. The T violating PPP strength is given by

$$\Delta S_{TV} = M\left(1 - \frac{M^2}{16}\right)\frac{4}{9}\frac{d_{3/2}^4}{256}\phi_T f_1^{(3,4)}(\omega)\sin\theta\cos\theta \tag{8.27}$$

Figure 8.4 is a plot of the T violating PPP strength for T violating phase $\phi_T = 0.1$, relative to the decay PPP strength magnitude.

8.6 Channel phases for 6p TO,PE mixing

The T violation PPP strength is proportional to the phase ϕ_T which is the difference of the $F' = 3, 4$ channel phases. As usual, the channel phases can be directly related to any particular TO,PE state admixtures according to eqn 5.69.

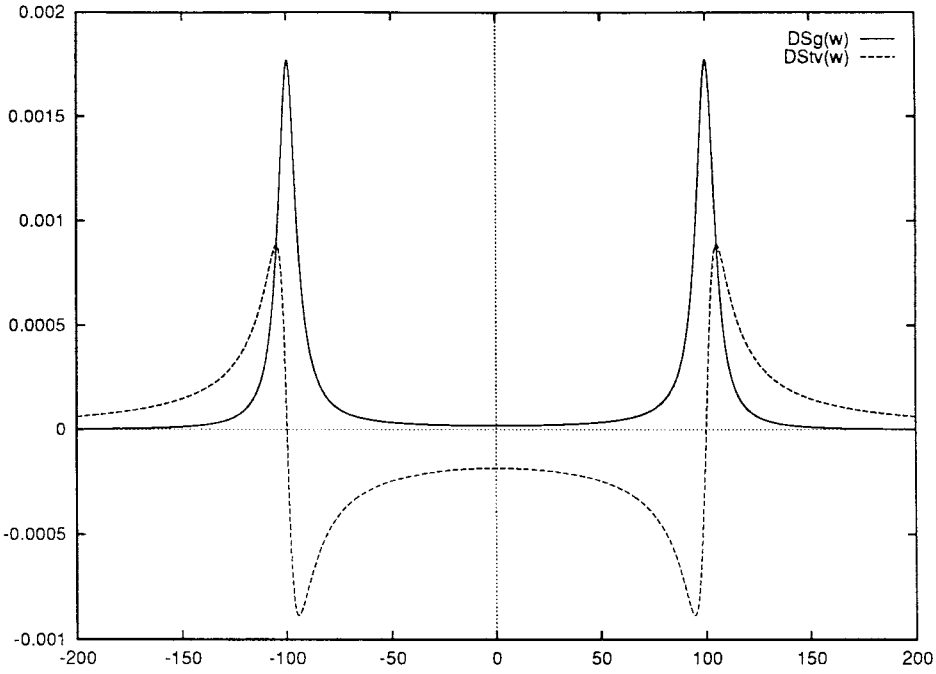


Figure 8.4: T violation PPP strength ΔS_{TV} with $\phi_T = 0.1$, relative to the decay term $|\Delta S_\gamma|$ for $6s\,33 \rightarrow 43$ transition, with angle $\theta = \pi/4$ and frequency units MHz.

We now evaluate the channel phase for mixing of the $6p$ levels, whose closeness (554.11cm^{-1}) enhances their contribution compared to other admixtures. The TO,PE mixing must be hyperfine dependent to distinguish the $F' = 3, 4$ channels, so interactions of ranks $k = 1, 2$ contribute. The channel phases can be expressed in terms of the most 'stretched' relevant admixture of $6p_{1/2}$ into the $6p_{3/2}$ level

$$i\delta_T \equiv \frac{\left\langle 6p_{1/2}\, F'=4 \,|\, H_T \,|\, 6p_{3/2}\, F'=4 \right\rangle}{E_{6p_{3/2}} - E_{6p_{1/2}}} \tag{8.28}$$

For a rank k TO,PE interaction $H_T = \boldsymbol{I}^k.\boldsymbol{T}^k$, the $F' = 3$ mixing parameter is given by

$$\delta_T(F'=3) = (-1)^{k+1}\frac{2k+1}{5}\sqrt{\frac{15}{7}}\,\delta_T \tag{8.29}$$

The channel phases $\phi_T^{(F')}$ for the $3M \rightarrow 4M$ Raman transition can now be directly related to δ_T, which thus characterises the whole problem. We find the following expression for these

$$\phi_T^{(F')} = \left[\frac{\left\langle 6s_{1/2}4 \,\|\, \boldsymbol{d} \,\|\, 6p_{1/2}F' \right\rangle}{\left\langle 6s_{1/2}4 \,\|\, \boldsymbol{d} \,\|\, 6p_{3/2}F' \right\rangle} - \frac{\left\langle 6s_{1/2}3 \,\|\, \boldsymbol{d} \,\|\, 6p_{1/2}F' \right\rangle}{\left\langle 6s_{1/2}3 \,\|\, \boldsymbol{d} \,\|\, 6p_{3/2}F' \right\rangle}\right] \delta_T(F') \tag{8.30}$$

The reduced dipole matrix element ratios in eqn 8.30 can be written in terms of a single ratio of the electronic dipole matrix elements times angular factors from the decoupling of the hyperfine states

$$\phi_T^{(F')} = \frac{\langle 6s_{1/2} \| \boldsymbol{d} \| 6p_{1/2} \rangle}{\langle 6s_{1/2} \| \boldsymbol{d} \| 6p_{3/2} \rangle} \times \begin{cases} (-1)^{k+1}(2k+1)\sqrt{\frac{8}{35}}\,\delta_T & \ldots \quad F'=3 \\ -\sqrt{\frac{8}{35}}\,\delta_T & \ldots \quad F'=4 \end{cases} \tag{8.31}$$

The ratio of reduced matrix elements in the above is

$$\frac{\langle 6s_{1/2} \| \boldsymbol{d} \| 6p_{1/2} \rangle}{\langle 6s_{1/2} \| \boldsymbol{d} \| 6p_{3/2} \rangle} \equiv \frac{d_{1/2}}{d_{3/2}} \approx -0.710 \tag{8.32}$$

so finally, the anomalous T violation phase ϕ_T is given by

$$\phi_T \equiv \phi_T^{(3)} - \phi_T^{(4)} = (-1)^{k+1}\, 0.710 \times 4\sqrt{\frac{8}{35}}\,\delta_T \approx (-1)^{k+1}\, 5\delta_T \tag{8.33}$$

in terms of the admixture δ_T.

8.7 Summary

We have calculated the two photon Raman transition probability in caesium close to resonance with the $6p_{3/2}$ level. The decay PPP strength in this system is expected to be of order 10% of the ordinary two photon strength. There are four different procedures for separating out the terms of interest from measurements:

1. Pumping: Comparison of the $\pm m$ transitions, distinguishes optical pumping terms which are *odd* in m, including the PPP part of the two photon transitions.

2. Polarisation: Only the PPP part of the two photon transitions have the characteristic $\boldsymbol{\varepsilon}_A \times \boldsymbol{\varepsilon}_B\, \boldsymbol{\varepsilon}_A.\boldsymbol{\varepsilon}_B = \sin\theta\cos\theta$ dependence on the polarisation vectors, where θ is their relative angle. The PPP signal changes sign every 90° and can be exctracted by taking linear combinations of measurements such as eqn 7.86.

3. Lineshape: The T violation and decay contributions to the PPP signal each have different frequency dependence over the intermediate level resonances. Their lineshapes are $\Delta S_{TV} \propto f_1(\omega)$ and $\Delta S_\gamma \propto f_2(\omega)$, where $f_{1,2}(\omega)$ are defined by eqns 7.46-7.47. The lineshapes are quite different and their relative sign changes when tuned between the upper level resonances.

4. Reversed processes: Comparison of the $i \rightarrow f$ and reversed $f \rightarrow i$ transitions is a further discriminant between the T violation and decay PPP transitions, which change their relative sign.

We note here that an extension of no. 3 in the above, provides a novel measurement of the linewidth, which can be extracted from the lineshape function of the decay PPP term $f_2(\omega)$. The linewidth measured is the 'damping' term of the off-diagonal components in the density matrix treatment.

Regrettably the sensitivity to T violation is washed out by the large decay PPP effect. The sensitivity to the anomalous phase due to T violation is as discussed in section §7.7: taking $N \sim 10^{10}$ atoms, the signal to noise is sensitivity to $\phi_T > 1/\sqrt{N}$. For TO,PE mixing of the $6p$ levels, the phase ϕ_T is given by eqn 8.33, which gives sensitivity

$$\delta_T > 2 \times 10^{-6} \tag{8.34}$$

where δ_T is the mixing coefficient of the stretched $F' = 4$ states.

Chapter 9

T clocks

When three or more atomic transitions are driven coherently in a closed loop, the evolution of the system depends in detail on the phases of the three transition amplitudes. A variety of uses for the phase-dependent behaviour of the atomic population have been proposed in atomic interferometry and population trapping [19]. In such closed excitation linkages, the net phase of the transition matrix elements depends on the geometry and phases of the three driving fields, as well as the transition process. We call this phase the *loop* phase, which for a linkage of three states $1, 2, 3$ is defined by

$$\phi = arg\ [b_{12}b_{23}b_{31}] \tag{9.1}$$

where b_{ij} are the complex Rabi amplitudes of the $i \rightarrow j$ transition.

In the evolution of a coherently driven loop, the population of the states oscillates at characteristic frequencies. If the loop phase is suitably chosen, then the population in the upper states can have beat frequencies. Since anomalous phases of the transition amplitudes due to T violation contribute directly to the loop phase, quantum population beats can be a measure of the T impurities in the atomic states.

Recently the Michigan group [23] have proposed an experiment to exploit possible T violation contributions to the loop phase in a three level system. They have proposed to use three hyperfine magnetic states of the rubidium $5s_{1/2}$ ground state, linked by radio frequency (rf) magnetic dipole transitions.

In this chapter, another sort of three level system is discussed, with two optical frequency transitions and one rf magnetic dipole transition between two hyperfine states. We find that the frequency detuning of the optical transitions mimics to some degree the effects of an anomalous loop phase, and that these cannot be distinguished from T violation, using only measurements of beat frequencies.

9.1 A simple 3 state system

A convenient starting point for discussing T clocks, is the case where the fields driving the transitions, in a closed linkage of three states, are exactly on resonance. In the

current work we make the assumption that decay effects can be ignored, and it is sufficient in this case to use a Scrödinger equation evolution to describe the atomic state vector $\psi(t)$ in a time independent basis set $|1\rangle, |2\rangle, |3\rangle$. The wavefunction of the atom at time t can be written

$$\psi(t) = \sum_{i=1,2,3} c_i(t) e^{-i\omega_i t} |i\rangle \tag{9.2}$$

where $\hbar\omega_i$ are the energy eigenvalues of the three states, and the coefficients c_i have no oscillatory time dependence. The equation of motion describing the evolution of ψ can be written as a Schrödinger equation in which the Hamiltonian contains the diagonal atomic part H_0 and interactions with the driving fields V^{EM}

$$i\hbar \frac{\partial}{\partial t}\psi(t) = \left(H_0 + V^{EM}\right)\psi(t) \tag{9.3}$$

The interaction matrix V^{EM} contains the matrix elements of each transition. These can be written as effective Rabi rates without specifying the processes to be electric dipole, magnetic dipole or higher order, for each of the three resonant driving fields. In the approximation where one can ignore diagonal terms, the 3×3 matrix form of the interaction term V^{EM} in eqn 9.3 is

$$V^{EM} = \hbar \begin{pmatrix} 0 & b_{12}e^{-i\omega_{12}t} & b_{13}e^{-i\omega_{13}t} \\ b_{21}e^{-i\omega_{21}t} & 0 & b_{23}e^{-i\omega_{23}t} \\ b_{31}e^{-i\omega_{31}t} & b_{32}e^{-i\omega_{32}t} & 0 \end{pmatrix} \tag{9.4}$$

where the field frequencies, exactly on resonance, are $\nu_{ij} = \omega_{ij} = \omega_j - \omega_i$ (downwards transitions, ie stimulated emissions, are driven by the negative frequency component - the same form applies with $\omega_{ji} = -\omega_{ij}$). The complex Rabi matrix elements b_{ij}, defined in the usual way, have no residual time dependence.

9.1.1 Formal solution of the evolution

The Schrödinger equation 9.3 can be recast in terms of the vector $\boldsymbol{c} = (c_1, c_2, c_3)$ applying the unitary operator $T_{ij} = e^{i\omega_i t}\delta_{ij}|i\rangle\langle j|$. The H_0 term is exactly cancelled and the equation for $\boldsymbol{c}$ becomes

$$\frac{\partial \boldsymbol{c}}{\partial t} = -iB\boldsymbol{c} \tag{9.5}$$

where the matrix $B = TV^{EM}T^{-1}/\hbar$ is time independent, and contains the Rabi transition rate amplitudes

$$B = \begin{pmatrix} 0 & b_{12} & b_{13} \\ b_{21} & 0 & b_{23} \\ b_{31} & b_{32} & 0 \end{pmatrix} \tag{9.6}$$

The formal solution to the differential equation 9.5 is $\boldsymbol{c}(t) = e^{-iBt}\boldsymbol{c}_0$, where $\boldsymbol{c}_0$ is the initial state of the atom at time $t = 0$, eg $\boldsymbol{c}_0 = (1, 0, 0)$ if all the population starts in

state $|1\rangle$. This formal solution involving the exponential of a non-diagonal matrix is not very useful. However, the technique for expressing e^{-iBt} in a more useful form is well known, and uses the eigenvectors and eigenvalues of B, defined by the eigenvector equation $B\boldsymbol{e}_j = \lambda_j \boldsymbol{e}_j$. In this way, the formal solution for $\boldsymbol{c}(t)$ can be written as

$$\boldsymbol{c}(t) = E e^{-i\Lambda t} E^\dagger \boldsymbol{c}_0 \tag{9.7}$$

where Λ is a diagonal matrix of the eigenvalues, and E is a unitary matrix of the unit eigenvectors $E = (\boldsymbol{e}_1, \boldsymbol{e}_2, \boldsymbol{e}_3)$. The eigenvalues specify the periodicities of the state amplitudes, therefore there are only two periodicities present in the evolution of the population $p_j = |c_j|^2$, which are the differences of the eigenvalues $\Omega_1 = \lambda_1 - \lambda_2$ and $\Omega_2 = \lambda_2 - \lambda_3$; a third frequency $\Omega_3 = \lambda_3 - \lambda_1$ is related to the other two by $\Omega_1 + \Omega_2 + \Omega_3 = 0$.

9.1.2 Analytical solutions

For the case when all the Rabi rates are equal in magnitude, ie $|b_{12}| = |b_{23}| = |b_{31}| = b$, the solution for the population of the states as a function of time, can be found analytically. In a suitable choice of phases of the states, b_{12} and b_{23} can be made real, and the phase of b_{13} is ϕ, where ϕ is the loop phase, so that

$$B = b \begin{pmatrix} 0 & 1 & e^{-i\phi} \\ 1 & 0 & 1 \\ e^{i\phi} & 1 & 0 \end{pmatrix} \tag{9.8}$$

The eigenvalues required in eqn 9.7 are obtained from solving $|B - \lambda I| = 0$, which yields the cubic

$$\lambda^3 - 3b^2\lambda - 2b^3 \cos\phi = 0 \tag{9.9}$$

which has solutions

$$\lambda_1 = 2b\cos(\phi/3) \tag{9.10}$$
$$\lambda_2 = 2b\cos(\phi/3 - 2\pi/3) \tag{9.11}$$
$$\lambda_3 = 2b\cos(\phi/3 + 2\pi/3) \tag{9.12}$$

and corresponding unit eigenvectors

$$\boldsymbol{e}_1 = (1, e^{i\phi/3}, e^{2i\phi/3})/\sqrt{3} \tag{9.13}$$
$$\boldsymbol{e}_2 = (1, e^{i(\phi/3-2\pi/3)}, e^{2i(\phi/3-2\pi/3)})/\sqrt{3} \tag{9.14}$$
$$\boldsymbol{e}_3 = (1, e^{i(\phi/3+2\pi/3)}, e^{2i(\phi/3+2\pi/3)})/\sqrt{3} \tag{9.15}$$

The formal solution, eqn 9.7, is therefore simple enough to write down analytically in this case. The particular solution with initial state $\boldsymbol{c}_0 = (1, 0, 0)$ is

$$c_1(t) = \frac{1}{3}\left(e^{-i\lambda_1 t} + e^{-i\lambda_2 t} + e^{-i\lambda_3 t}\right) \tag{9.16}$$

$$c_2(t) = \frac{1}{3}\left(e^{i\phi/3}e^{-i\lambda_1 t} + e^{i(\phi/3-2\pi/3)}e^{-i\lambda_2 t} + e^{i(\phi/3+2\pi/3)}e^{-i\lambda_3 t}\right) \quad (9.17)$$

$$c_3(t) = \frac{1}{3}\left(e^{2i\phi/3}e^{-i\lambda_1 t} + e^{2i(\phi/3-2\pi/3)}e^{-i\lambda_2 t} + e^{2i(\phi/3+2\pi/3)}e^{-i\lambda_3 t}\right) \quad (9.18)$$

and the populations $p_j = |c_j|^2$ are

$$p_1(t) = \frac{1}{3} + \frac{2}{9}\left(\cos(\Omega_1 t) + \cos(\Omega_2 t) + \cos(\Omega_3 t)\right) \quad (9.19)$$

$$p_2(t) = \frac{1}{3} + \frac{2}{9}\left(\cos(\Omega_1 t - 2\pi/3) + \cos(\Omega_2 t - 2\pi/3) + \cos(\Omega_3 t - 2\pi/3)\right) \quad (9.20)$$

$$p_3(t) = \frac{1}{3} + \frac{2}{9}\left(\cos(\Omega_1 t + 2\pi/3) + \cos(\Omega_2 t + 2\pi/3) + \cos(\Omega_3 t + 2\pi/3)\right) \quad (9.21)$$

where the frequencies in the evolution of the populations are the *differences* of the eigenvalues $\Omega_1 = \lambda_1 - \lambda_2$, $\Omega_2 = \lambda_2 - \lambda_3$ and $\Omega_3 = \lambda_3 - \lambda_1$.

9.2 Population beats as a measure of T violation

The analytical solutions for the simplest case of equal transition Rabi rates $|b_{12}| = |b_{23}| = |b_{31}| = b$, show that the population in the states during the evolution depend on the loop phase. The T impurities in the atomic states give rise to an additional net phase to the three transitions around the T clock loop, ie a T-odd contribution to the loop phase. The total loop phase ϕ is then

$$\phi = \phi_0 + \phi_T \quad (9.22)$$

where ϕ_0 is the loop phase in the absence of T violation, and ϕ_T is the T violating phase. The ordinary loop phase ϕ_0 is determined by the transition character (electric or magnetic) and by the relative phases of the three driving fields. Two cases of interest are when the driving fields are set so that $\phi_0 = 0$ and $\phi_0 = \pi/2$, assuming ϕ_T to be small:

1. $\phi_0 = 0$: The expressions for the eigenvalues λ can be expanded in this approximation, so $\lambda_1 = 2b$, $\lambda_2 = (-1 + \phi_T/\sqrt{3})\,b$ and $\lambda_3 = (-1 - \phi_T/\sqrt{3})\,b$ to order ϕ_T^2. The periodicities in the evolution of the populations, which are the frequencies Ω, are therefore

$$\Omega_1 = (3 - \phi_T/\sqrt{3})\,b \quad (9.23)$$

$$\Omega_2 = -(3 + \phi_T/\sqrt{3})\,b \quad (9.24)$$

$$\Omega_3 = 2\,\phi_T\,b/\sqrt{3} \quad (9.25)$$

The time dependence of the populations of the states therefore has two components, with angular frequencies $(3 \pm \phi_T)\,b$ which give a rapid oscillation at frequency $3b$ and a beat frequency

$$\Omega_{beat} = \phi_T\,b/\sqrt{3} \quad (9.26)$$

which defines an envelope for the rapidly oscillating populations.

2. $\phi_0 = \pi/2$: Applying the same process as above, the eigenvalues λ for this case are $\lambda_1 = 2\,\phi_T b/3$, $\lambda_2 = (-\sqrt{3} - \phi_T/3)\,b$ and $\lambda_3 = (\sqrt{3} - \phi_T/3)\,b$ to order ϕ_T^2. The Ω frequencies for this case are

$$\Omega_1 = (\sqrt{3} + \phi_T)\,b \tag{9.27}$$
$$\Omega_2 = -2\sqrt{3}\,b \tag{9.28}$$
$$\Omega_3 = (\sqrt{3} - \phi_T)\,b \tag{9.29}$$

There are again two components in the time dependence, with angular frequencies $(\sqrt{3} \pm \phi_T)\,b$ which give a rapid oscillation at frequency $\sqrt{3}\,b$ and the beat frequency

$$\Omega_{beat} = \phi_T\,b \tag{9.30}$$

which defines the envelope for the rapidly oscillating populations.

In both of these cases, there is a beat frequency proportional to the T violating phase ϕ_T. The plots in figures 9.1-9.2 illustrate the beat frequencies in the population of state $|2\rangle$, taking $\phi_T = 0.1$ in the analytical solution, eqn 9.20. The period of the population beats is given by

$$\tau_{beat} = 2\pi/\Omega_{beat} \propto 1/\phi_T\,b \tag{9.31}$$

so that τ_{beat} can be a measure of T violation.

9.2.1 The T ratio for T clocks

In the previous section, it was shown that beat frequencies in the evolution of the populations can be a measure of T violation. If the frequencies, amplitudes and phases of the driving fields can be sufficiently controlled, then the *period* of the population beats is directly related to the T impurities in the atomic states

$$\tau_{beat} = 2\pi/\Omega_{beat} = 2\pi\kappa/\phi_T\,b \tag{9.32}$$

where the constant of proportionality is $\kappa = \sqrt{3}$ for $\phi_0 = 0$ and $\kappa = 1$ for $\phi_0 = \pi/2$. The T violating phase is a property of the atomic states, so that on changing the phase ϕ_0 by π (eg by reversing any one of the driving field vectors), the relative signs of the ordinary and T violating phases are reversed. In an experiment, the ordinary phase is set to $\phi_0 + \phi_1$, where ϕ_1 is a small additional phase between the driving fields. The beat frequencies depend on the difference of the loop phase from ϕ_0 which is now $\phi - \phi_0 = \phi_1 + \phi_T$. The phase ϕ_1 therefore gives beat frequencies just like the T violating phase ϕ_T. If ϕ_1 is chosen to be

$$\phi_1 = 2\pi\kappa/b \tag{9.33}$$

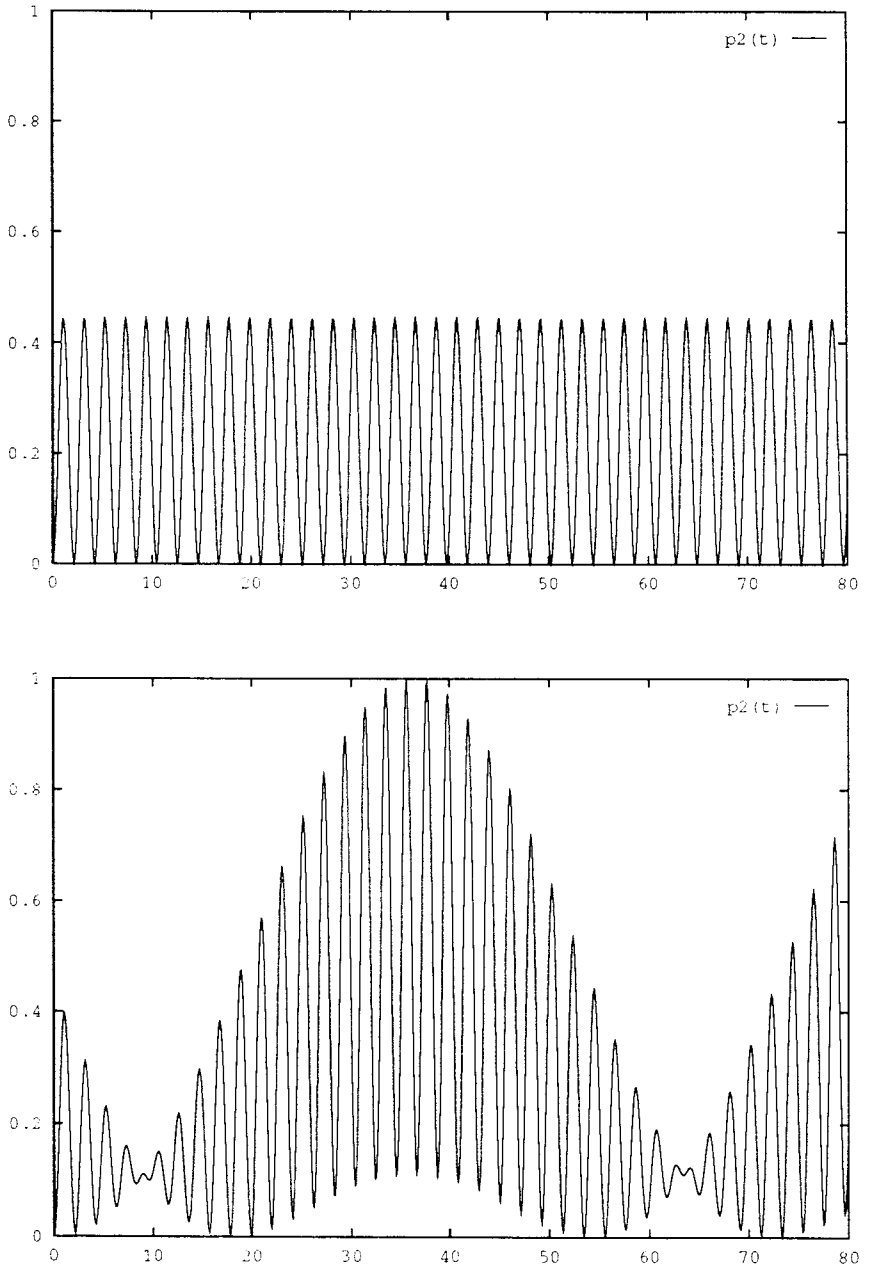


Figure 9.1: Population beats in $p_2(t)$, *top*: the loop phase $\phi_0 = 0$ in the absence of T violation, *bottom*: with additional T-odd phase $\phi_T = 0.1$.

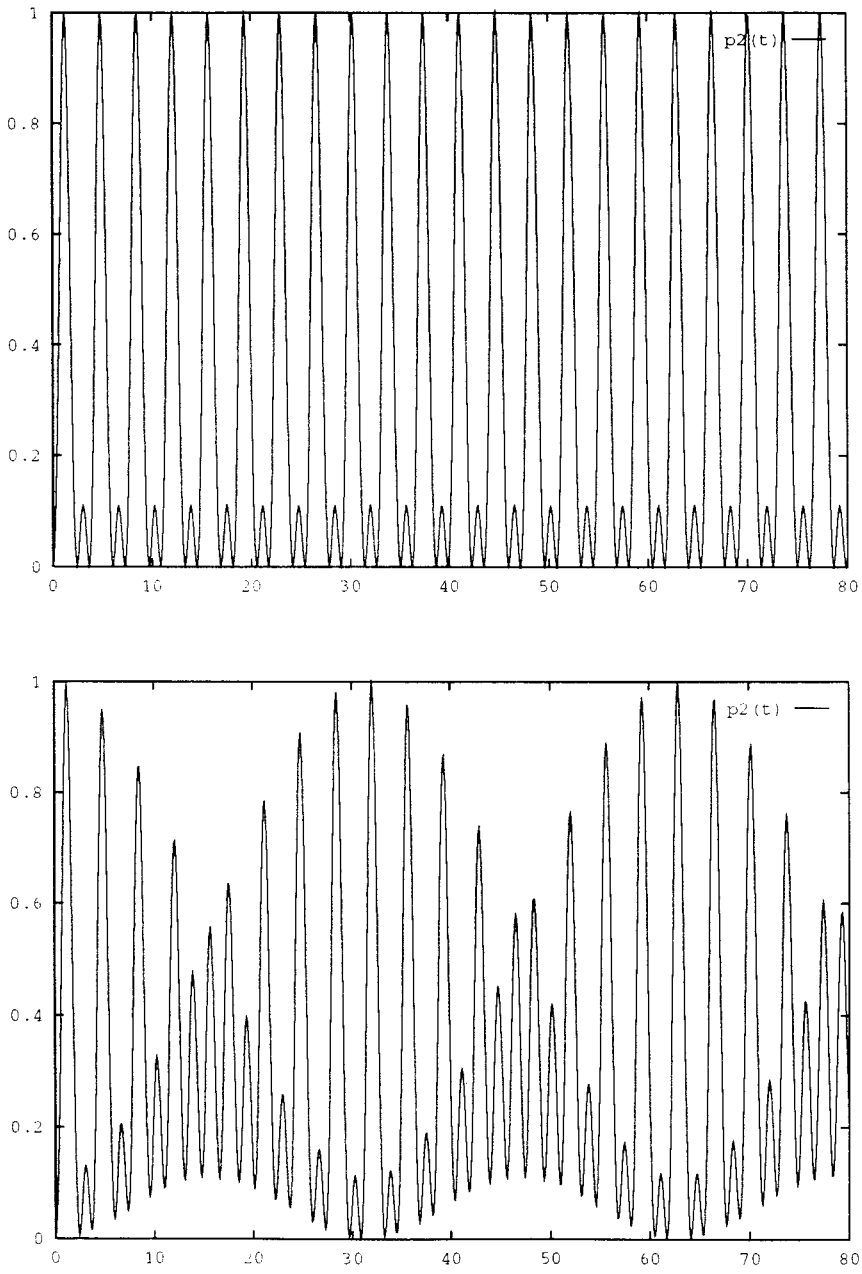


Figure 9.2: Population beats in $p_2(t)$, *top*: the loop phase $\phi_0 = \pi/2$ in the absence of T violation, *bottom*: with additional T-odd phase $\phi_T = 0.1$.

then there is a population beat in the absence of T violation, with beat period $\tau = 1s$.

When there is T violation present, the beat period now depends on $\phi_1 + \phi_T$. The relative signs of ϕ_1 and ϕ_T are reversed on reversing any one of the driving fields, which has the effect of changing the phase of the fields $\phi_0 + \phi_1$ by π. The beat period therefore has two possible values

$$\tau_\pm = \frac{2\pi\kappa}{(\phi_1 \pm \phi_T)\, b} = 1 \pm \frac{\phi_T}{\phi_1} \tag{9.34}$$

As for other T violation schemes, we define a T ratio in terms of the periods $\tau_\pm$ to be proportional to ϕ_T

$$T = \frac{\tau_+ - \tau_-}{\tau_+ + \tau_-} = \frac{\phi_T\, b}{2\pi\kappa} \tag{9.35}$$

The enhancement factor here is essentially the number times the population cycles around the T clock in the observation time, and relies on controlling the frequencies, amplitudes and phases of all three driving fields to sufficient accuracy. For instance, if the Rabi rate is of order $b \sim 100\,\mathrm{MHz}$, then the enhancement factor is 10^8.

9.2.2 Sensitivity

The sensitivity depends on the signal to noise ratio in the measurement of the beats. Averaged over many fast oscillations, the populations of the states are constant, and do not vary with the beat. The amplitude of the fast oscillation (ie the envelope) can be extracted by phase sensitive detection. If a large number N atoms are sampled, then the statistical noise in the beat period τ will be of order $\delta\tau = \tau/\sqrt{N}$. For a positive measurement of ϕ_T, the T ratio should be greater than the fractional statistical noise

$$T > \frac{\delta\tau}{\tau} = \frac{1}{\sqrt{N}} \tag{9.36}$$

which from eqn 9.35 gives sensitivity to

$$\phi_T > \frac{2\pi\kappa}{b\sqrt{N}} \tag{9.37}$$

Thus for $N \sim 10^8$ atoms, which gives statistical noise in the beat period $\delta\tau \sim 10^{-4}$s, and Rabi rate of order $b \sim 100$MHz, then the T clock is sensitive to T odd phase $\phi_T > 10^{-12}$.

This sensitivity is for the 'ideal' T clock, assuming the amplitudes and frequencies of the driving fields are controlled to sufficient accuracy. The following sections discuss the way that differences in the field intensities and offsets from resonance can produce beat frequencies, which mimic T violation.

9.3 Dependence on intensity

In the simple model T clock all the Rabi rate amplitudes were equal. While possible because the intensities of the three driving fields are independent, it is necessary to know how differences between any of the Rabi amplitudes mimic beats in the populations. In particular, whether this effect is linear near the point of interest. We find that such beat frequencies do occur unless the ordinary loop phase is chosen to be $\phi_0 = \pm\pi/2$.

In the formal solution, eqn 9.7, the periodicities in the state amplitudes, and hence in the populations, come only from the eigenvalues. Therefore it is sufficient only to work out the eigenvalues of the problem to extract the periodicities from the population. For the more general case $b_{12} \neq b_{23} \neq b_{31}$, where the b_{ij}'s are complex with phase ϕ_{ij}, the matrix B is

$$B = \begin{pmatrix} 0 & b_{12} & b_{13} \\ b_{21} & 0 & b_{23} \\ b_{31} & b_{32} & 0 \end{pmatrix} \tag{9.38}$$

The eigenvalues of B give the periodicities in the state amplitudes, and are obtained from the determinant equation $|B - \lambda I| = 0$. It is convenient to make the following definitions

$$b^3 e^{i\phi} = b_{12} b_{23} b_{31} \tag{9.39}$$

$$\bar{b}^2 = \frac{1}{3}\left[|b_{12}|^2 + |b_{23}|^2 + |b_{31}|^2\right] \tag{9.40}$$

$$\cos\beta = \left(b/\bar{b}\right)^3 \cos\phi \tag{9.41}$$

The loop phase is defined as $\phi = \phi_{12} + \phi_{23} + \phi_{31}$, and can be written $\phi = \phi_0 + \phi_T$ to distinguish the loop phase in the absence of T violation and due to the T impurities. The identification of β as an *angle* is possible since the ratio $b/\bar{b} \leq 1$ ($b/\bar{b} = 1$ when $|b_{12}| = |b_{23}| = |b_{31}|$). Figure 9.3 shows a plot of the ratio $b/\bar{b}$ against varying any one of the b_{ij} rates. Near the maximum point, the ratio $b/\bar{b}$ can be written in terms of the difference of any one Rabi rate from the average $b_{ij}/\bar{b} = 1 + \delta b/\bar{b}$

$$\frac{b}{\bar{b}} = 1 - \frac{2}{9}\left(\frac{\delta b}{\bar{b}}\right)^2 \tag{9.42}$$

which is quadratic in the amplitude difference δb.

The natural frequency unit of the oscillations is $\bar{b}$, which is the root mean square of the transition Rabi rates. The eigenvalues are given by the following cubic equation

$$\lambda^3 - 3\bar{b}^2\lambda - 2\bar{b}^3\cos\beta = 0 \tag{9.43}$$

the eigenvalues are therefore analogous to the previous case with the angle β taking the place of ϕ. The previous results carry through, but with changes in β responsible

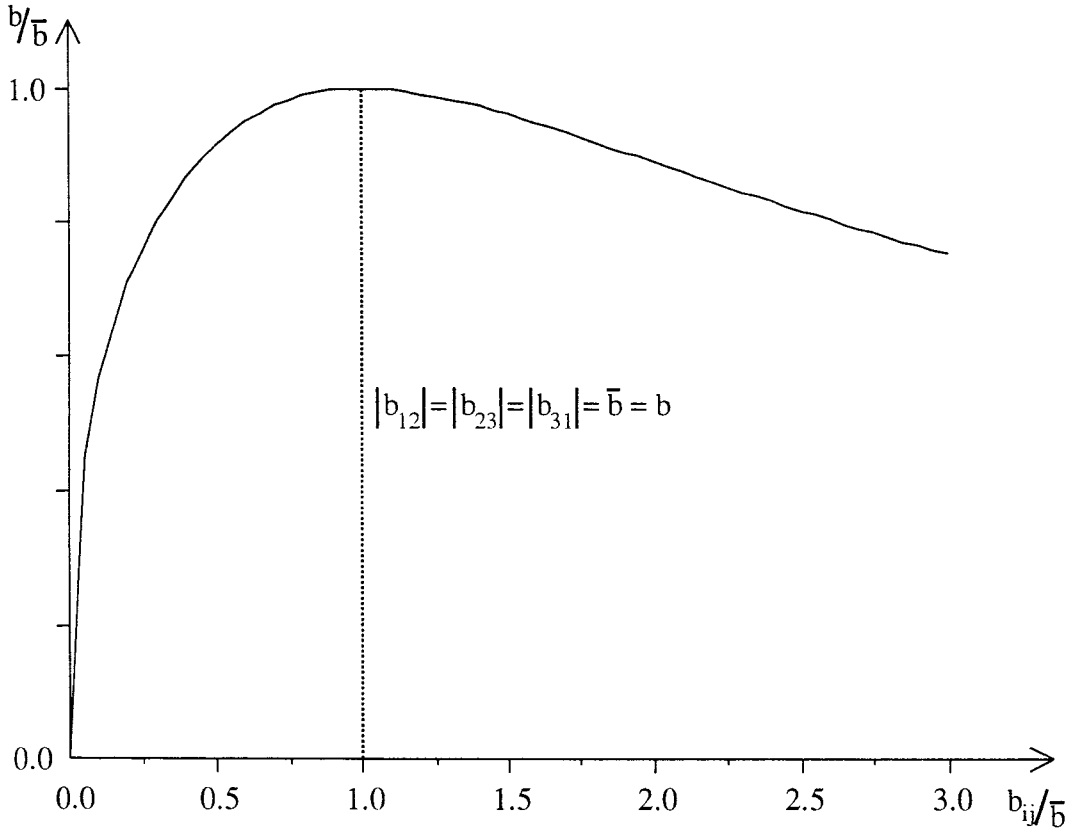


Figure 9.3: Ratio $b/\bar{b}$ against any one of b_{ij}

for the beat frequencies. It is readily seen from eqn 9.41, that if $\phi_0 = 0$ then β has a *linear* dependence on $\delta b/\bar{b}$ amplitude variations. On the other hand, if $\phi_0 = \pm\pi/2$, then β and hence the population beats become quadratic in $\delta b/\bar{b}$ and linear in ϕ_T. Close to the $b/\bar{b} = 1$ point, the beat period given by eqn 9.32 is therefore

$$\tau_{beat} = 2\pi/\phi_T \bar{b} \tag{9.44}$$

as long as $\phi_0 = \pm\pi/2$, and is *quadratic* in the field amplitudes.

9.4 Off resonant T clocks

In previous sections it has been shown that the period of population beats in the evolution of T clocks, can be a measure of T violation. To measure the T violating phase ϕ_T, we have shown that the loop phase in the absence of T violation ϕ_0 should be close to $\pm\pi/2$. With this phase relationship between the driving fields, the beat period becomes independent to first order of differences in the driving field intensities.

We now consider the dependence of the evolution on detuning of the three driving fields. The driving field frequencies ν_{12}, ν_{23} and ν_{31} of the three respective transitions, with $\nu_{ji} = -\nu_{ij}$, can still satisfy the triple resonance condition $\nu_{12} + \nu_{23} + \nu_{31} = 0$, if one of the frequencies is generated coherently from the other two. When the triple resonance is not met, the evolution of the populations becomes complex for times t for which $(\nu_{12} + \nu_{23} + \nu_{31})t > 1$. The behaviour of driven systems not satisfying the triple resonance condition is beyond the scope of this thesis. In practice, the frequencies of the three driving fields can be coherently generated from suitable combinations of two reference frequencies. The triple resonance condition is then very precisely met. We therefore consider here the T clock evolution assuming $(\nu_{12} + \nu_{23} + \nu_{31})t \ll 1$ for arbitrarily long time t.

It is again sufficient to use a Scrödinger equation evolution to describe the atomic state vector $\psi(t)$ in the time independent basis $|1, 2, 3\rangle$

$$\psi(t) = \sum_{i=1,2,3} c_i(t) e^{-i\omega_i t} |i\rangle \tag{9.45}$$

and the interaction of the driving fields with the atom is now given by the matrix

$$V^{EM} = \hbar \begin{pmatrix} 0 & b_{12}e^{-i\nu_{12}t} & b_{13}e^{-i\nu_{13}t} \\ b_{21}e^{-i\nu_{21}t} & 0 & b_{23}e^{-i\nu_{23}t} \\ b_{31}e^{-i\nu_{31}t} & b_{32}e^{-i\nu_{32}t} & 0 \end{pmatrix} \tag{9.46}$$

It is more convenient to express the driving field frequencies in terms of their difference from the atomic resonance ω_{ij}, ie the detuning $\Delta_{ij} = \nu_{ij} - \omega_{ij}$. On triple resonance, these detunings can be written $\Delta_{ij} = \Delta_j - \Delta_i$ where $\Delta_{1,2,3}$, are suitably chosen to sum to zero. The Schrödinger equation 9.3 can be recast in terms of the vector $\boldsymbol{c} = (c_1, c_2, c_3)$ applying the unitary operator $T_{ij} = e^{i(\omega_i + \Delta_i)t}\delta_{ij} |i\rangle \langle j|$. The H_0 term is no

longer exactly cancelled, and the remaining diagonal terms are just the offsets Δ_i. The evolution equation for the vector $\boldsymbol{c}$ is finally reduced to the time independent form

$$\frac{\partial \boldsymbol{c}}{\partial t} = -i(B - \Delta)\boldsymbol{c} \tag{9.47}$$

where B is the matrix of Rabi amplitudes given by eqn 9.38 and Δ is the diagonal matrix of the offsets $\Delta_{1,2,3}$.

Equation 9.47 is of the same soluble form as the previous analysis, but with additional diagonal terms from the offsets. The formal solution is therefore $\boldsymbol{c}(t) = e^{-i(B-\Delta)t}\boldsymbol{c}_0$, where $\boldsymbol{c}_0$ is the initial state of the atom. The exponential of the non-diagonal matrix is expressed in terms of the eigenvalues and eigenvectors, but as before, only the eigenvalues determine the periodicities in the evolution of $\boldsymbol{c}(t)$.

The eigenvalues $\lambda_{1,2,3}$ are solutions of the determinant equation $|B - \Delta - \lambda I| = 0$. It is convenient to introduce some more definitions involving the detunings: a mean square frequency detuning $\bar{\Delta}$, and a frequency f composed of both detunings and Rabi amplitudes

$$\bar{\Delta}^2 = \frac{1}{3}\left[|\Delta_{12}|^2 + |\Delta_{23}|^2 + |\Delta_{31}|^2\right] \tag{9.48}$$

$$f^3 = \Delta_1 |b_{23}|^2 + \Delta_2 |b_{31}|^2 + \Delta_3 |b_{12}|^2 - \Delta_1\Delta_2\Delta_3 \tag{9.49}$$

Also, since only the differences of the offsets $\Delta_j - \Delta_i$ are physical, a zero sum condition $\Delta_1 + \Delta_2 + \Delta_3 = 0$ can be imposed without loss of generality. It can then be shown that $\Delta_1\Delta_2 + \Delta_2\Delta_3 + \Delta_3\Delta_1 = -\frac{1}{2}\bar{\Delta}^2$. Using these definitions the cubic equation for the eigenvalues can be simplified to an identical form as in the previous analysis

$$\lambda^3 - 3b_0^2\lambda - 2b_0^3\cos\varepsilon = 0 \tag{9.50}$$

where the eigenvalues depend on just two parameters, which are a natural frequency b_0 for the fast oscillations

$$b_0^2 = \bar{b}^2 + \frac{1}{6}\bar{\Delta}^2 \tag{9.51}$$

and an angle ε which determines the beat frequency

$$\cos\varepsilon = (b/b_0)^3\left[\cos\phi + \frac{1}{6}(f/b)^3\right] \tag{9.52}$$

As in section §9.3 the angle ε takes the place of the loop phase ϕ in determining the beat periods. The ordinary parts of the loop phase ϕ_0 must be set to $\pm\pi/2$ to make the dependence on the field amplitudes quadratic. If the detunings are all zero, then the angle $\varepsilon = \phi$, so that in the absence of T violation with the frequency detunings small, ε will be close to ϕ_0. Writing $\varepsilon = \phi_0 + \varepsilon'$ for the two choices $\phi_0 = \pm\pi/2$ gives

$$\varepsilon' = (b/b_0)^3\left[\phi_T \mp \frac{1}{6}(f/b)^3\right] \tag{9.53}$$

and the corresponding beat period of the populations is

$$\tau_{beat} = 2\pi/\varepsilon' b_0 \tag{9.54}$$

From the form of eqn 9.53, it is apparent that the ratio f/b mimics a T violating phase by producing population beats in the absence of T violation. The quantity f, which mimics T violation, is defined by eqn 9.49 and depends on both the Rabi amplitudes and frequency offsets. In terms of the detunings Δ_{ij}, f is given by

$$f^3 = \frac{1}{3}\left[(|b_{12}|^2 + \frac{1}{9}\Delta_{12}^2)(\Delta_{23} - \Delta_{31}) + \textit{cyclic permutation}\right] \tag{9.55}$$

Close to $b/\bar{b} = 1$, the dependence on the Rabi rates cancel, but the detuning terms still remain.

The T violation mimicking quantity f/b ratios the frequency detunings and Rabi rates of the three channels. The available frequency stabilization depends on the frequency range involved, so that two types of three state T clocks are very different in this respect:

1. Rf T clocks: If all three states are close enough to be driven by radio frequency transitions then the field frequencies can be controlled to much less than the Rabi rates $\bar{\Delta} \ll \bar{b}$. In this approximation, the T violation mimicking term is $(f/b)^3 \approx \bar{\Delta}/3\bar{b} \ll 1$.

2. Optical T clocks: Our treatment is restricted to the narrow linewidth limit, ie $\gamma \ll \bar{b}$ or $\bar{\Delta}$. The decay width is therefore a lower limit for frequency precision in our analysis.

A first conclusion is that given the situation for optical frequency stabilization, there seems little hope of constructing a T clock using optical frequency transitions. Apart from the problem of determining the phase of the fields at the site of the atom, the mimicking of population beats by the detunings is much larger than the change in the beat periods due to T violation on reversal of any of the fields. There is also the unresolved question of how spontaneous decays of excited states can affect the population beats. We therefore focus our discussion in the next section on requirements and properties of radio frequency T clocks.

9.5 Radio frequency T clocks

If the states involved in a T clock are close enough, then all three driving fields can be generated by radio frequency sources. This range of frequencies is limited to levels separated by of order the typical hyperfine structure scale. Hyperfine configurations have levels separated typically by a few GHz. Commercially available oscillators in the MHz range have stability of at least 1 part in 10^{12}, leading to mHz precision

for GHz frequencies. With such precision, the typical detunings can therefore much less than the Rabi oscillations.

In a hyperfine configuration $(jI)F$ of an atomic level there may be three or more hyperfine levels as long as if $j \geq 1$ and $I \geq 1$. In this case, there can be a three M1 linkage between states of the same hyperfine multiplet. However, the T violation that can be observed must be associated with the interaction of the atom and *external* fields. The reason is that the phases of the states within a single hyperfine manifold can be chosen to make all magnetic dipole matrix elements real, even in the presence of arbitrary internal T-odd mixings.

Radio frequency T clocks can still be constructed avoiding this limitation. These fall into three categories

- External: A T clock scheme has been recently proposed by the Michigan group [23] within the rubidium ground state hyperfine configuration in an applied magnetic field. However, the T clock linkage within a single hyperfine manifold can only be sensitive to *external* T violating interactions.

- Rf E1's: There are a number of instances of nearly degenerate *opposite* parity levels. These are not pushed apart by the atomic Hamiltonian which is P-even, and can be linked by rf E1 transitions. A remarkable near degeneracy in dysprosium (odd isotopes ^{161,163}Dy with nuclear spin $I = 5/2$) has recently been studied [20]. The two levels $4f^{10}5d6s$ $J = 10$ and $4f^{9}5d^{2}6s$ $J = 10$, at energy $19797.96\,\mathrm{cm}^{-1}$, have overlapping hyperfine configurations with a large number of possible rf E1 transitions. The linkage is therefore of two rf E1's and an rf M1. Importantly, all the levels are metastable so that our analysis, which ignores decay effects, is valid for a T clock within these levels.

- Rf M1's: In some atoms, eg rare earth atoms, there are atomic levels of the same parity which are by coincidence separated by only a hyperfine structure splitting. Levels of the same J are repelled by fine structure splittings, but there can be close $\Delta J = 1$ pairs in which there can be T clocks using three rf M1 transitions.

The Michigan experiment aims to achieve coherence time 0.1 s using laser cooling techniques in a neutral atom trap. Being within the ground state hyperfine configuration, there are no radiative decays, and the initial state is selected as part of the cooling process. An additional handle on systematics comes from measuring the two isotopes ^{85,87}Rb. They anticipate that precision on the T-odd phase at the 10^{-4} level should be readily attainable [23]. If the Rabi rates are of order $10^{8}\,\mathrm{s}^{-1}$, then in 0.1 s a maximum sensitivity to the T impurities would then be of order $\delta_T \sim 10^{-11}$.

9.6 Summary

The sensitivity of T clocks depends on precisely controlling the frequencies, amplitudes, and phases of three driving fields. The enhancement is essentially the number of times the atom is coherently cycled around the linkage in a reference beat period, for example of order 10^8 in a second.

In the 'ideal' T clock, all the transition rates are set equal and the population beat period then depends only on the loop phase $\phi \equiv arg[b_{12}b_{23}b_{31}]$. When the transitions are not driven equally, then there can be population beats in the absence of T violation. These are proportional to the difference of the transition strengths which depend on the field amplitudes. The dependence on the field amplitudes is made quadratic, as shown in section §9.3, if all three transition rates are nearly equal and the loop phase ϕ is close to $\pm\pi/2$.

More serious problems arise as a consequence of frequency detunings, as shown in section §9.4, which can directly produce population beats, thus mimicking T violation. There therefore seems little hope for T clocks involving optical transitions which don't have the frequency stability of radio frequency sources. An unresolved question is the effect of decays on the quantum population beats; whether these mimic T violation and how, if this is the case, the T violation can be distinguished. On the other hand, currently proposed radio frequency T clocks are be restricted to T violating interactions with external fields. Rf T clocks could also exploit nearly degenerate levels of the same or opposite parity, although the question of decays again becomes important unless both levels are metastable.

Coherently driven systems with more than three transitions can be treated analogously to the three level systems, but where the three level system has only one non-arbitrary phase (the loop phase), more complicate linkages have more degrees of freedom, and can exhibit a variety of population trapping phenomena [19]. For instance, a four level linkage can act as a balanced detector analogous to a Wheatstone bridge, sensitive to the various phases present in the system.

In the radio frequency three level T clocks we have discussed in this chapter, quantum beats in the populations of the states can be sensitive to T violating admixtures of order 10^{-11}.

Chapter 10

Conclusion

In this thesis we have discussed the observable consequences of time reversal violating but parity invariant interactions in atomic systems. Parity invariant T violation is associated, through the CPT theorem, with the unsolved problem of CP asymmetry in kaon decay. To date there is no established theory of CP or T violation, so our focus has therefore been on the sensitivity of atomic measurements to possible T impurities in the atomic states.

Atomic state	T impurity	Limit on δ_T	Rank
Caesium, $6s_{1/2}$	$7s_{1/2}$	$< 100\times10^{-6}$	$k=0,1$
	$5d_{3/2}$	$< 20\times10^{-6}$	$k=1,2$
Thallium, $6p_{1/2}$	$7p_{1/2}$	$< 6\times10^{-6}$	$k=0,1$
	$6p_{3/2}$	$< 2\times10^{-6}$	$k=0,1$
Mercury, $6s^2\,{}^1S_0$	$6s7s\,{}^3S_1$	$< 1.4\times10^{-9}$	$k=1$
	$6s5d\,{}^3D_1$	$< 2.8\times10^{-9}$	$k=1$

Table 10.1: Indirect limits on atomic T-odd P-even impurities

At present, little is known about the T purity of atomic states. Some limits can be deduced from the very precise measurements of atomic electric dipole moments. These are presented in table 10.1 and expressed as admixture coefficients δ_T into the ground state, where we have distinguished the limits by the tensor rank k of the T-odd P-even interaction with their nuclear spin.

The fact that the atomic states are parity eigenstates means that a convenient phase convention can be used which determines the phase of matrix elements purely

Scheme	Signature	Type	TO,PE mixing	Sensitivity
Correlations	$\boldsymbol{E}.\boldsymbol{k}$	Cs beam	$6s_{1/2}, 7s_{1/2}$	$1\times10^{-6}\ldots k=0$ $5\times10^{-11}\ldots k=1,2$
		Tl gas	$6p_{1/2}, 6p_{3/2}$	$7\times10^{-10}\ldots k=1$
		Cs gas	$6s_{1/2}, 7s_{1/2}$	$2.5\times10^{-8}\ldots k=0$ $1.4\times10^{-12}\ldots k=1,2$
Raman PPP	$\boldsymbol{J}.\boldsymbol{\varepsilon}\times\boldsymbol{\varepsilon}'\,\boldsymbol{\varepsilon}.\boldsymbol{\varepsilon}'$	Cs trap	$6p_{1/2}, 6p_{3/2}$	$2\times10^{-6}\ldots k=1,2$
T clocks	$\boldsymbol{b}_1.\boldsymbol{b}_2\times\boldsymbol{b}_3$	Rb trap	$5s_{1/2}$ (3 rf's)	$\sim 10^{-11}\ldots$ external

Table 10.2: Summary of scheme sensitivities to T impurities δ_T

in terms of the symmetries of the operator and not the wavefunctions. In this phase convention, all of the usual T-even P-even interaction terms are real, while the T-odd P-even admixtures are imaginary.

Since observables are real, an extra phase i is required for a T-odd P-even effect to be observable in first order. It may come from three sources: the relative phase between multipoles of a radiation field, the 'geometrical' phase between x and y matrix elements of tensor operators for angular momentum states, and finally a phase can be externally applied between three or more coherent fields.

We have discussed three classes of experiment which can be sensitive to atomic T violation. These are different from both an experimental and theoretical point of view:

- Correlations: T violation can lead to correlations in the transition strength proportional a TO,PE combination of external fields. In single photon schemes, T violation can lead to $\boldsymbol{E}.\boldsymbol{k}$ correlations in the excitation rate of atoms in an atomic beam, or in the refractive index in a gas cell.

- Plane polarised pumping: in coherent two photon Raman transitions, T violation can lead to optical pumping along a spatial direction $\boldsymbol{\varepsilon}\times\boldsymbol{\varepsilon}'$ defined by the plane polarisations $\boldsymbol{\varepsilon}, \boldsymbol{\varepsilon}'$ of two driving lasers. Damping of the upper levels by spontaneous decay gives rise to a similar effect, which mimics the T violation to some extent. Regrettably this decay PPP effect masks the T violation, but in itself it is an interesting effect, and a novel way to measure the linewidth of the upper levels.

- T clock quantum beats: in a coherently driven linkage of three or more transitions, T violation can give rise to quantum beats in the populations of the

states. The frequencies, amplitudes, phases and polarisations must all be precisely controlled in these experiments. By suitably choosing these values, the quantum beats can be a sensitive measure of T violation. Although the only proposed T clock, using rubidium, is only sensitive to external TO,PE interactions, there exist near degenerate levels which can have sensitivity to internal TO,PE mixing.

We have analysed each of these schemes for their sensitivity to relevant TO,PE mixing, and our results are presented in table 10.2. The different T impurities are distinguished either by their interaction rank k, or else as TO,PE interactions with external fields.

We conclude by reiterating our aim of stimulating more detailed experimental study of this subject. T violation is directly connected with the unsolved problem of the kaon CP asymmetry in particle physics. To date there is no confirmed theory of CP or T violation, and we therefore consider studies of atomic T violation a valuable and distinct contribution to fundamental physics.

Appendix A

Angular momentum and tensor coupling

The properties of the rotation group and angular momentum operator are discussed in great detail in standard texts [18,28]. Because of the importance of angular momentum in time reversal theory, a careful review is necessary.

A.1 Angular momentum eigenstates

The angular momentum operator $\boldsymbol{j}$ can be defined as the generator of infinitesimal rotations, from which follow the usual commutation relations

$$[j_x, j_y] = i\, j_z \quad \textit{and cyclic permutations} \tag{A.1}$$

The P and T symmetry of $\boldsymbol{j}$ are

$$P : \boldsymbol{j} \rightarrow \boldsymbol{j} \tag{A.2}$$
$$T : \boldsymbol{j} \rightarrow -\boldsymbol{j} \tag{A.3}$$

It can be shown that state vectors $|j,m\rangle$ are an irreducible representation of the rotation group, with $2j+1$ values $m = -j \ldots j$ in integer steps. These states are eigenvectors of j_z and $\boldsymbol{j}^2$

$$j_z\, |j,m\rangle = m\, |j,m\rangle \tag{A.4}$$
$$\boldsymbol{j}^2\, |j,m\rangle = j(j+1)\, |j,m\rangle \tag{A.5}$$

The phases of the states $|j,m\rangle$ and $|j,m'\rangle$ are arbitrary, but normally the ladder operators $j_\pm = j_x \pm i j_y$ are chosen to have real matrix elements thus fixing the phase of all the m states in a $|j,m\rangle$ level [22]

$$\langle j,m\,|\,j_z\,|\,j,m\rangle = m \tag{A.6}$$
$$\langle j,m\pm 1\,|\,j_\pm\,|\,j,m\rangle = ((j\pm m+1)(j\mp m))^{\frac{1}{2}} \tag{A.7}$$

Recursive use of the ladder operators for coupled angular momentum wavefunctions $|(j_1 j_2)JM\rangle$ yields their expansion in terms of the uncoupled product basis

$$|(j_1 j_2)JM\rangle = \sum_{m_1,m_2} |j_1 m_1, j_2 m_2\rangle \langle j_1 m_1, j_2 m_2 | JM\rangle \tag{A.8}$$

where the coefficients $\langle j_1 m_1, j_2 m_2 | JM\rangle$ are the Clebsch-Gordan coefficients which are all real in the usual phase convention. The following are some symmetries of the Clebsch-Gordan coefficients

$$\langle j_2 m_2, j_1 m_1 | JM\rangle = (-1)^{j_1+j_2-J} \langle j_1 m_1, j_2 m_2 | JM\rangle \tag{A.9}$$

$$\langle j_1 - m_1, j_2 - m_2 | J - M\rangle = (-1)^{j_1+j_2-J} \langle j_1 m_1, j_2 m_2 | JM\rangle \tag{A.10}$$

$$\langle J - M, j_2 m_2 | j_1 - m_1\rangle = (-1)^{j_2+m_2} \left[\frac{2j_1+1}{2J+1}\right]^{\frac{1}{2}} \langle j_1 m_1, j_2 m_2 | JM\rangle \tag{A.11}$$

It is often convenient to express the angular momentum coupling coefficients in terms of the more symmetrical Wigner 3j symbol (for the relationships between the V-C and 3j symbols defined by different authors, see eg Edmonds [28])

$$\langle j_1 m_1, j_2 m_2 | j_3 m_3\rangle = (-1)^{j_1-j_2+m_3}(2j_3+1)^{\frac{1}{2}} \begin{pmatrix} j_1 & j_2 & j_3 \\ m_1 & m_2 & -m_3 \end{pmatrix} \tag{A.12}$$

where the frequently used 'box' notation is shorthand for $[J] \equiv 2J+1$. Permutation of the columns in the $3j$ symbol give a phase

$$\begin{pmatrix} j_2 & j_1 & j_3 \\ m_2 & m_1 & m_3 \end{pmatrix} = (-1)^{j_1+j_2+j_3} \begin{pmatrix} j_1 & j_2 & j_3 \\ m_1 & m_2 & m_3 \end{pmatrix} \tag{A.13}$$

so that the $3j$ symbols are invariant to even permutations of the columns. Similarly reversing the m's gives

$$\begin{pmatrix} j_1 & j_2 & j_3 \\ -m_1 & -m_2 & -m_3 \end{pmatrix} = (-1)^{j_1+j_2+j_3} \begin{pmatrix} j_1 & j_2 & j_3 \\ m_1 & m_2 & m_3 \end{pmatrix} \tag{A.14}$$

Some particular $3j$ symbol expressions are

$$\begin{pmatrix} j & 0 & j \\ -m & 0 & m \end{pmatrix} = (-1)^{j-m}\sqrt{2j+1} \tag{A.15}$$

$$\begin{pmatrix} j & 1 & j \\ -m & 0 & m \end{pmatrix} = (-1)^{j-m} m \sqrt{j(j+1)(2j+1)} \quad (j \neq 0) \tag{A.16}$$

$$\begin{pmatrix} j & k & j \\ -j & 0 & j \end{pmatrix} = (2j+k+1)^{-\frac{1}{2}} \left[\frac{(2j)!(2j)!}{(2j+k)!(2j-k)!}\right]^{\frac{1}{2}} \tag{A.17}$$

The following sum rules come from the orthogonality of the Clebsch-Gordan coefficients

$$\sum_{m_1,m_2} [j_3] \begin{pmatrix} j_1 & j_2 & j_3 \\ m_1 & m_2 & m_3 \end{pmatrix} \begin{pmatrix} j_1 & j_2 & j_3' \\ m_1 & m_2 & m_3' \end{pmatrix} = \delta_{j_3,j_3'}\delta_{m_3,m_3'} \tag{A.18}$$

$$\sum_{j_3,m_3} [j_3] \begin{pmatrix} j_1 & j_2 & j_3 \\ m_1 & m_2 & m_3 \end{pmatrix} \begin{pmatrix} j_1 & j_2 & j_3 \\ m_1' & m_2' & m_3 \end{pmatrix} = \delta_{m_1,m_1'}\delta_{m_2,m_2'} \tag{A.19}$$

A.2 Spherical tensors and tensor coupling

The q component of a spherical tensor Q^k is defined by its rotational properties relative to a defined z axis

$$\left[j_z, Q_q^k\right] = q\,Q_q^k \tag{A.20}$$

$$\left[j_\pm, Q_q^k\right] = ((k \pm q + 1)(k \mp q))^{\frac{1}{2}}\, Q_{q\pm1}^k \tag{A.21}$$

also

$$\left[\boldsymbol{j}^2, Q_q^k\right] = k(k+1)\,Q_q^k \tag{A.22}$$

If A^{k_a} and B^{k_b} are tensors of rank k_a and k_b, then the components Q of the *coupled* tensor of rank K are

$$\begin{aligned} \left(A^{k_a}B^{k_b}\right)_Q^K &= \sum_{q_a,q_b} A_{q_a}^{k_a} B_{q_b}^{k_b} \langle\, k_a q_a\, k_b q_b \mid K Q \,\rangle \\ &= \sum_{q_a,q_b} (-1)^{k_a-k_b+Q} [K]^{\frac{1}{2}}\, A_{q_a}^{k_a} B_{q_b}^{k_b} \begin{pmatrix} k_a & k_b & K \\ q_a & q_b & -Q \end{pmatrix} \end{aligned} \tag{A.23}$$

If all the components of A and B commute, then

$$\left(A^{k_a}B^{k_b}\right)_Q^K = (-1)^{K-k_a-k_b}\left(B^{k_b}A^{k_a}\right)_Q^K \tag{A.24}$$

When $K = 0$ and $k_a = k_b = k$ the coupled tensor is proportional to the scalar product

$$\left(A^k B^k\right)_0^0 = (-1)^k\,[k]^{-\frac{1}{2}}\, A^k.B^k \tag{A.25}$$

where conventionally

$$A^k.B^k = \sum_q (-1)^q A_q^k B_{-q}^k \tag{A.26}$$

When one of the tensors is in fact a scalar $A^0 = A$ then

$$\left(A^0 B^k\right)_q^k = A B_q^k \tag{A.27}$$

The complex conjugate of a tensor component T_q^k is related to the $-q^{th}$ component of the complex conjugate tensor T^*

$$T_q^{k*} = (-1)^q T^{*k}_{-q} \tag{A.28}$$

the complex conjugate of a tensor coupling is

$$\left(A^{k_a} B^{k_b}\right)^{K*}_{Q} = (-1)^Q \left(B^{*k_b} A^{*k_a}\right)^{K}_{-Q} \tag{A.29}$$

The spherical tensor components of a cartesian vector are obtained by projection onto the unit vector basis $\boldsymbol{e}_q^1$ of the spherical coordinate system

$$\begin{aligned} \boldsymbol{e}_0 &= \boldsymbol{e}_z \\ \boldsymbol{e}_{\pm 1} &= \mp \frac{1}{\sqrt{2}} (\boldsymbol{e}_x \pm i \boldsymbol{e}_y) \end{aligned} \tag{A.30}$$

and in terms of cartesian vector components $A_{x,y,z}$, the spherical tensor components are given by

$$A_0^1 = A_z \tag{A.31}$$

$$A_{\pm 1}^1 = \mp \frac{1}{\sqrt{2}} (A_x \pm i A_y) \tag{A.32}$$

In terms of scalars and cartesian vectors, the coupling of rank 0 (scalar) and 1 (vector) spherical tensors is as follows

$$\left(\phi^0 \psi^0\right)^0_0 = \phi\, \psi \tag{A.33}$$

$$\left(\phi^0 A^1\right)^1_q = \phi\, A^1_q \tag{A.34}$$

$$\left(A^1 B^1\right)^0_0 = -\frac{1}{\sqrt{3}} \boldsymbol{A}.\boldsymbol{B} \tag{A.35}$$

$$\left(A^1 B^1\right)^1_q = \frac{i}{\sqrt{2}} (\boldsymbol{A} \times \boldsymbol{B})_q \tag{A.36}$$

also the following is an identity for recoupling vectors

$$\boldsymbol{A}.\boldsymbol{B}\ \boldsymbol{C}.\boldsymbol{D} = \sum_J (-1)^J\ (AC)^J\ .\ (BD)^J \tag{A.37}$$

The compositions of the rank 0, 1 and 2 products of two cartesian vectors $\boldsymbol{A}$ and $\boldsymbol{B}$ in terms of the cartesian components are

$$(\boldsymbol{A}\boldsymbol{B})^0_0 = -\frac{1}{\sqrt{3}} (A_x B_x + A_y B_y + A_z B_z) \tag{A.38}$$

$$(\boldsymbol{A}\boldsymbol{B})^1_0 = \frac{i}{\sqrt{2}} (A_x B_y - A_y B_x) \tag{A.39}$$

$$(\boldsymbol{AB})^1_{\pm 1} = \mp\frac{1}{\sqrt{2}}\left((A_zB_x - A_xB_z) \pm i(A_zB_y - A_yB_z)\right) \quad \text{(A.40)}$$

$$(\boldsymbol{AB})^2_0 = \frac{1}{\sqrt{6}}\left(2A_zB_z - A_xB_x - A_yB_y\right) \quad \text{(A.41)}$$

$$(\boldsymbol{AB})^2_{\pm 1} = \mp\frac{1}{2}\left((A_zB_x + A_xB_z) \pm i(A_zB_y + A_yB_z)\right) \quad \text{(A.42)}$$

$$(\boldsymbol{AB})^2_{\pm 2} = \frac{1}{2}\left((A_xB_x - A_yB_y) \pm i(A_xB_y + A_yB_x)\right) \quad \text{(A.43)}$$

The Wigner 6j symbol is defined as a recoupling coefficient between states of three angular momenta

$$\langle((j_1j_2)j_{12},j_3)J|(j_1,(j_2j_3)j_{23})J\rangle \equiv (-1)^{j_1+j_2+j_3+J}\,[j_{12},j_{23}]^{\frac{1}{2}} \begin{Bmatrix} j_1 & j_2 & j_{12} \\ j_3 & J & j_{23} \end{Bmatrix} \quad \text{(A.44)}$$

In terms of the 3j symbols, the 6j is the fully contracted product of four 3j symbols, involving six angular momenta

$$\begin{Bmatrix} j_1 & j_2 & j_3 \\ j_4 & j_5 & j_6 \end{Bmatrix} = \sum_{all\ m's} \begin{pmatrix} j_1 & j_2 & j_3 \\ m_1 & m_2 & m_3 \end{pmatrix} \begin{pmatrix} j_1 & j_5 & j_6 \\ m_1' & m_5 & m_6' \end{pmatrix} \times \begin{pmatrix} j_4 & j_2 & j_6 \\ m_4' & m_2' & m_6 \end{pmatrix} \begin{pmatrix} j_4 & j_5 & j_3 \\ m_4 & m_5' & m_3' \end{pmatrix} \quad \text{(A.45)}$$

The 6j symmetries is invariant to any permutations of columns, and to interchange of the upper and lower arguments of any two columns. When one of the angular momenta is zero, then

$$\begin{Bmatrix} j_1 & j_2 & j_3 \\ j_2' & j_1' & 0 \end{Bmatrix} = \delta_{j_1,j_1'}\delta_{j_2,j_2'}(-1)^{j_1+j_2+j_3}\,[j_1,j_2]^{-\frac{1}{2}} \quad \text{(A.46)}$$

The following is a sum rule for 6j symbols

$$\sum_j [j] \begin{Bmatrix} j_1 & j_2 & j_3 \\ j_4 & j_5 & j \end{Bmatrix} \begin{Bmatrix} j_1 & j_2 & j_3' \\ j_4 & j_5 & j \end{Bmatrix} = \delta_{j_3,j_3'}\,[j_3]^{-1} \quad \text{(A.47)}$$

The Wigner 9j symbol is defined as a recoupling coefficient between states of four angular momenta

$$\langle((j_1j_2)j_{12},(j_3j_4)j_{34})J|((j_1j_3)j_{13},(j_2j_4)j_{24})J\rangle \equiv [j_{12},j_{34},j_{13},j_{24}]^{\frac{1}{2}} \begin{Bmatrix} j_1 & j_2 & j_{12} \\ j_3 & j_4 & j_{34} \\ j_{13} & j_{24} & J \end{Bmatrix} \quad \text{(A.48)}$$

In terms of the 3j symbols, the 9j is the fully contracted product of six 3j symbols, involving nine angular momenta.

The recoupling coefficients of spherical tensor products can be written in terms of 6j and 9j symbols

$$\left(\left(A^{k_a}B^{k_b}\right)^{k_{ab}}C^{k_c}\right)^K_Q =$$

$$\sum_{k_{bc}}(-1)^{K+k_a+k_b+k_c}\left[k_{ab},k_{bc}\right]^{\frac{1}{2}}\begin{Bmatrix}k_c & k_b & k_{bc}\\ k_a & K & k_{ab}\end{Bmatrix}\left(A^{k_a}\left(B^{k_b}C^{k_c}\right)^{k_{bc}}\right)^K_Q \tag{A.49}$$

$$\left(A^{k_a}\left(B^{k_b}C^{k_c}\right)^{k_{bc}}\right)^K_Q =$$

$$\sum_{k_{ab}}(-1)^{K+k_a+k_b+k_c}\left[k_{ab},k_{bc}\right]^{\frac{1}{2}}\begin{Bmatrix}k_c & k_b & k_{bc}\\ k_a & K & k_{ab}\end{Bmatrix}\left(\left(A^{k_a}B^{k_b}\right)^{k_{ab}}C^{k_c}\right)^K_Q \tag{A.50}$$

$$\left(\left(A^{k_a}B^{k_b}\right)^{k_{ab}}\left(C^{k_c}D^{k_d}\right)^{k_{cd}}\right)^K_Q =$$

$$\sum_{k_{ac},k_{bd}}\left[k_{ab},k_{bc},k_{ac},k_{bd}\right]^{\frac{1}{2}}\begin{Bmatrix}k_a & k_c & k_{ac}\\ k_b & k_d & k_{bd}\\ k_{ab} & k_{cd} & K\end{Bmatrix}\left(\left(A^{k_a}C^{k_c}\right)^{k_{ac}}\left(B^{k_b}D^{k_d}\right)^{k_{bd}}\right)^K_Q \tag{A.51}$$

A.3 Properties of matrix elements

A consequence of angular momentum symmetry is that matrix elements of angular momentum states can be expressed in terms of a reduced matrix element which does not depend on the magnetic quantum numbers. The reduced matrix element is defined by the Wigner-Eckart theorem

$$\left\langle j',m'\left|Q^k_q\right|j,m\right\rangle = (-1)^{j'-m'}\begin{pmatrix}j' & k & j\\ -m' & q & m\end{pmatrix}\left\langle j'\left\|Q^k\right\|j\right\rangle \tag{A.52}$$

Summing over m,m' gives

$$\sum_{m,m'}\left|\left\langle j',m'\left|Q^k_q\right|j,m\right\rangle\right|^2 = \frac{1}{2k+1}\left|\left\langle j'\left\|Q^k\right\|j\right\rangle\right|^2 \tag{A.53}$$

and if Q^k is a Hermitian tensor then

$$\left\langle j'\left\|Q^k\right\|j\right\rangle^* = (-1)^{j'-j}\left\langle j\left\|Q^k\right\|j\right\rangle \tag{A.54}$$

The following are recoupling identities involving coupled wavefunctions and operators of different vector spaces, T operating only in space 1 and U only in space 2

$$\left\langle(\gamma_1'j_1',\gamma_2'j_2')J'\left\|\left(T^{k_1}U^{k_2}\right)^K\right\|(\gamma_1j_1,\gamma_2j_2)J\right\rangle = \left[J,K,J'\right]^{\frac{1}{2}}$$

$$\times\begin{Bmatrix}j_1' & j_1 & k_1\\ j_2' & j_2 & k_2\\ J' & J & K\end{Bmatrix}\left\langle\gamma_1'j_1'\left\|T^{k_1}\right\|\gamma_1j_1\right\rangle\left\langle\gamma_2'j_2'\left\|U^{k_2}\right\|\gamma_2j_2\right\rangle \tag{A.55}$$

$$\left\langle (\gamma_1' j_1', \gamma_2' j_2') J' \left\| T^k \right\| (\gamma_1 j_1, \gamma_2 j_2) J \right\rangle = \delta_{\gamma_2', \gamma_2} \delta_{j_2', j_2} (-1)^{j_1' + j_2 + J + k} [J, J']^{\frac{1}{2}}$$
$$\times \begin{Bmatrix} J' & k & J \\ j_1 & j_2 & j_1' \end{Bmatrix} \left\langle \gamma_1' j_1' \left\| T^k \right\| \gamma_1 j_1 \right\rangle \tag{A.56}$$

$$\left\langle (\gamma_1' j_1', \gamma_2' j_2') J' \left\| U^k \right\| (\gamma_1 j_1, \gamma_2 j_2) J \right\rangle = \delta_{\gamma_1', \gamma_1} \delta_{j_1', j_1} (-1)^{j_1 + j_2 + J' + k} [J, J']^{\frac{1}{2}}$$
$$\times \begin{Bmatrix} J' & k & J \\ j_2 & j_1 & j_2' \end{Bmatrix} \left\langle \gamma_2' j_2' \left\| U^k \right\| \gamma_2 j_2 \right\rangle \tag{A.57}$$

$$\left\langle (\gamma_1' j_1', \gamma_2' j_2') J' M' \left\| T^k . U^k \right\| (\gamma_1 j_1, \gamma_2 j_2) J M \right\rangle = \delta_{J', J} \delta_{M', M} (-1)^{j_1 + j_2' + J}$$
$$\times \begin{Bmatrix} j_1 & j_1' & k \\ j_2' & j_2 & J \end{Bmatrix} \left\langle \gamma_1' j_1' \left\| T^k \right\| \gamma_1 j_1 \right\rangle \left\langle \gamma_2' j_2' \left\| U^k \right\| \gamma_2 j_2 \right\rangle \tag{A.58}$$

Some common reduced matrix elements are

$$\langle \gamma' j' \| 1 \| \gamma j \rangle = \delta_{\gamma', \gamma} \delta_{j', j} [j]^{\frac{1}{2}} \tag{A.59}$$

$$\langle \gamma' j' \| \boldsymbol{j} \| \gamma j \rangle = \delta_{\gamma', \gamma} \delta_{j', j} (j(j+1)(2j+1))^{\frac{1}{2}} \tag{A.60}$$

$$\left\langle \gamma' j' \left\| (\boldsymbol{j}\boldsymbol{j})^2 \right\| \gamma j \right\rangle = \delta_{\gamma', \gamma} \delta_{j', j} \frac{1}{4} \left(\tfrac{2}{3} (2j-1)(2j)(2j+1)(2j+2)(2j+3) \right)^{\frac{1}{2}} \tag{A.61}$$

$$\left\langle l' \left\| C^k \right\| l \right\rangle = (-1)^{l'} [l, l']^{\frac{1}{2}} \begin{pmatrix} l' & k & l \\ 0 & 0 & 0 \end{pmatrix} \tag{A.62}$$

$$\langle l' \| \boldsymbol{\nabla} \| l \rangle = (-1)^{l'} [l]^{\frac{1}{2}} \begin{pmatrix} l' & 1 & l \\ 0 & 0 & 0 \end{pmatrix} \left\langle l' \left\| \frac{d}{dr} + \frac{a}{r} \right\| l \right\rangle \tag{A.63}$$

where in eqn A.63 the constant a takes the value $-l'$ if $l = l' + 1$ and $l' + 1$ if $l = l' - 1$. Also for spin $\frac{1}{2}$ orbitals

$$\left\langle l' j' \left\| C^k \right\| l j \right\rangle = (-1)^{j' + \frac{1}{2}} [j, j']^{\frac{1}{2}} \begin{pmatrix} j' & k & j \\ \frac{1}{2} & 0 & -\frac{1}{2} \end{pmatrix} \pi(l, k, l') \tag{A.64}$$

where $\pi(l, k, l')$ is 1 for $l + k + l' = even$, and 0 otherwise.

Appendix B

Spherical harmonics

B.1 Scalar field expansions

Scalar fields may be expanded as a sum of terms with the rotational symmetry of spherical tensors, and these terms each consist of a suitably defined radial function times a spherical harmonic function. The properties of the spherical harmonics are related to the orbital angular momentum operator $\boldsymbol{L} = \boldsymbol{r} \times \boldsymbol{p}$. In polar coordinates the z component L_z and the ladder operators $L_\pm = L_x \pm iL_y$ have the explicit forms

$$L_z = -i\frac{\partial}{\partial\phi} \tag{B.1}$$

$$L_\pm = \pm e^{\pm i\phi}\left(\frac{\partial}{\partial\phi} \pm i\cot\theta\frac{\partial}{\partial\phi}\right) \tag{B.2}$$

and

$$\boldsymbol{L}^2 = -\left[\frac{1}{\sin\theta}\frac{\partial}{\partial\theta}\left(\sin\theta\frac{\partial}{\partial\theta}\right) + \frac{1}{\sin^2\theta}\frac{\partial^2}{\partial\phi^2}\right] \tag{B.3}$$

The spherical harmonics C^l_m have the rotational properties of spherical tensors and are eigenfunctions of L^2 and L_z

$$L_z C^l_m = m\, C^l_m \tag{B.4}$$

$$\boldsymbol{L}^2 C^l_m = l(l+1)\, C^l_m \tag{B.5}$$

They satisfy the orthogonality relation

$$\int C^{l'}_{m'}(\theta,\phi)^* C^l_m(\theta,\phi)\, d\Omega = \frac{4\pi}{2l+1}\delta_{l',l}\delta_{m',m} \tag{B.6}$$

where $d\Omega = \sin\theta\, d\theta d\phi$. Some explicit forms of the C^l_m spherical harmonics are

$$C^l_0(\theta,\phi) = P_l(\cos\theta) \tag{B.7}$$

$$C^l_m(0,\phi) = \delta_{m,0} \tag{B.8}$$

$$C^l_m(\theta,\phi)^* = (-1)^l C^l_{-m}(\theta,\phi) \tag{B.9}$$

where the functions $P_l(\cos\theta)$ are Legendre polynomials [2]. The normalised spherical harmonics Y_m^l are related to the C_m^l harmonics by

$$Y_m^l = \left(\frac{2l+1}{4\pi}\right)^{\frac{1}{2}} C_m^l \tag{B.10}$$

and satisfy the orthogonality relation

$$\int Y_{m'}^{l'}(\Omega)^* Y_m^l(\Omega)\, d\Omega = \delta_{l',l}\delta_{m',m} \tag{B.11}$$

The spherical harmonics form a complete set for expanding the angular dependence of an arbitrary scalar field.

The following are some additional properties

$$\left(C^{l_1}C^{l_2}\right)_m^l = (-1)^l [l]^{\frac{1}{2}} \begin{pmatrix} l_1 & l & l_2 \\ 0 & 0 & 0 \end{pmatrix} C_m^l \tag{B.12}$$

$$\left(C^{l-1}C^1\right)_m^l = \left(\frac{l}{2l-1}\right)^{\frac{1}{2}} C_m^l \tag{B.13}$$

$$\boldsymbol{A}.\boldsymbol{\nabla}\, r^l C_m^l = (l(2l-1))^{\frac{1}{2}} \left(\boldsymbol{A} r^{l-1} C^{l-1}\right)_m^l \tag{B.14}$$

$$\boldsymbol{A}.\boldsymbol{\nabla}\, \frac{1}{r^{l+1}} C_m^l = ((l+1)(2l+3))^{\frac{1}{2}} \left(\boldsymbol{A} \frac{1}{r^{l+2}} C^{l+1}\right)_m^l \tag{B.15}$$

$$\boldsymbol{r}.\boldsymbol{\nabla}\, f(r)\, C_m^l = \frac{df(r)}{dr} C_m^l \tag{B.16}$$

$$\boldsymbol{\nabla} \times \boldsymbol{L}\, r^l C_m^l = i\,(l+1)\boldsymbol{\nabla} r^l C_m^l \tag{B.17}$$

$$\boldsymbol{\nabla}^2 r^\lambda C_m^l = -\frac{(\lambda-l)(\lambda+l+1)}{2l+1} r^{\lambda-2} C_m^l \tag{B.18}$$

$$\left(\boldsymbol{\nabla} r^l C^l\right)_m^{l-1} = -(l(2l+1))^{\frac{1}{2}} r^{l-1} C_m^{l-1} \tag{B.19}$$

$$\left(\boldsymbol{\nabla} \frac{1}{r^{l+1}} C^l\right)_m^{l+1} = -((l+1)(2l+1))^{\frac{1}{2}} \frac{1}{r^{l+2}} C_m^{l+1} \tag{B.20}$$

and also the integral relation

$$\int C_{m_1}^{l_1}(\Omega) C_{m_2}^{l_2}(\Omega) C_{m_3}^{l_3}(\Omega)\, d\Omega = 4\pi \begin{pmatrix} l_1 & l_2 & l_3 \\ 0 & 0 & 0 \end{pmatrix} \begin{pmatrix} l_1 & l_2 & l_3 \\ m_1 & m_2 & m_3 \end{pmatrix} \tag{B.21}$$

B.2 Vector field expansions

Vector fields may also be expanded as a sum of terms of definite rotational symmetry in an analogous manner to scalar fields. The expansion basis functions are the vector spherical harmonics $\boldsymbol{C}^{(l,1)L}{}_M(\Omega)$, which are components of the spherical harmonic components C_m^l coupled with the spherical basis unit vectors to total rank L

$$\boldsymbol{C}^{(l,1)L}{}_M(\Omega) = \left(C(\Omega)^l \boldsymbol{e}^1\right)_M^L \tag{B.22}$$

The set of $(2L+1)$ fields $\boldsymbol{C}^{(l,1)\,L}_{\quad M}(\Omega)$ satisfy the orthogonality relation

$$\int \boldsymbol{C}^{(l',1)\,L'}_{\quad M'}(\Omega)^{*}\,\boldsymbol{C}^{(l,1)\,L}_{\quad M}(\Omega)\,d\Omega = \frac{4\pi}{2l+1}\delta_{l',l}\delta_{L',L}\delta_{M',M} \tag{B.23}$$

and form a complete set for expanding the angular dependence of an arbitrary vector field. The normalised vector spherical harmonics $\boldsymbol{Y}^{(l,1)\,L}_{\quad M}$ are defined in the same way in terms of the normalised scalar spherical harmonics. In the special case $L = l$ then

$$\boldsymbol{C}^{(L,1)\,L}_{\quad M} = (L(L+1))^{-\frac{1}{2}}\boldsymbol{L}\,C^{L}_{M} \tag{B.24}$$

Appendix C

Spherical delta functions

The spherical delta functions used in the current work are those of Brink and Satchler [18]. The lm spherical delta function $\delta^l_m(\boldsymbol{r})$ is defined to project the coefficient of $r^l\,C^l_m$ at the origin of an integrand,

$$\int r^{l'}\,C^{l'}_{m'}(\Omega)\,\delta^l_m(\boldsymbol{r})^*\,d\tau = \delta_{l',l}\,\delta_{m',m} \tag{C.1}$$

which gives unity for $l' = l$ and $m' = m$ and zero otherwise. In an expansion of suitably regular functions $\delta^l_m(\boldsymbol{r})$ therefore projects out then the coefficient of $r^l\,C^l_m$ at the origin, so that

$$\begin{aligned} f(\boldsymbol{r}) &= \sum_{l,m} f_{lm}\,r^l\,C^l_m(\Omega) \\ f_{lm} &= \int \delta^l_m(\boldsymbol{r})^*\,f(\boldsymbol{r})\,d\tau \end{aligned} \tag{C.2}$$

The spherical delta functions have the following property as source terms in the Poisson equation

$$\boldsymbol{\nabla}^2\left[\frac{1}{r^{l+1}}C^l_m(\Omega)\right] = -4\pi\,\delta^l_m(\boldsymbol{r}) \tag{C.3}$$

where C^l_m/r^{l+1} are rank l multipole fields.

The lowest order $\delta^l(\boldsymbol{r})$ can be written in terms of the ordinary three dimensional delta function $\delta(\boldsymbol{r})$

$$\delta^0(\boldsymbol{r}) = \delta(\boldsymbol{r}) \tag{C.4}$$

$$\delta^1(\boldsymbol{r}) = -\left[\boldsymbol{\nabla}, \delta(\boldsymbol{r})\right] \tag{C.5}$$

The following commutation relation follows from eqn C.3

$$\Big(\Big[\boldsymbol{\nabla}, \delta^l(\boldsymbol{r})\Big]\Big)^{l+1} = -((l+1)(2l+1))^{\frac{1}{2}}\,\delta^{l+1}(\boldsymbol{r}) \tag{C.6}$$

from which successive integration by parts yields the integral relation

$$\int \delta(\boldsymbol{r})\left((\boldsymbol{\nabla}\ldots\boldsymbol{\nabla})^{k-1}\boldsymbol{A}\right)^k_q\,d\tau = ((k-1)!(2k-3)!!)^{\frac{1}{2}}\int\left(\delta^{k-1}(\boldsymbol{r})\,\boldsymbol{A}\right)^k_q\,d\tau \tag{C.7}$$

Appendix D

Dirac matrices and wavefunctions

The Dirac equation for a single particle in a central potential $V(r)$

$$i\hbar\frac{\partial\psi}{\partial t} = \left(c\boldsymbol{\alpha}.\boldsymbol{p} + (\beta - 1)mc^2 + V(r)\right)\psi \tag{D.1}$$

where $\boldsymbol{p} = -i\hbar\boldsymbol{\nabla}$. The matrices $\boldsymbol{\alpha}$ and β are defined in terms of the 2x2 unit matrix I and the Pauli matrices $\boldsymbol{\sigma}$

$$\boldsymbol{\alpha} = \begin{pmatrix} 0 & \boldsymbol{\sigma} \\ \boldsymbol{\sigma} & 0 \end{pmatrix}, \quad \beta = \begin{pmatrix} I & 0 \\ 0 & -I \end{pmatrix} \tag{D.2}$$

The Pauli matrices $\boldsymbol{\sigma}$ are

$$\sigma_x = \begin{pmatrix} 0 & 1 \\ 1 & 0 \end{pmatrix}, \quad \sigma_y = \begin{pmatrix} 0 & -i \\ i & 0 \end{pmatrix}, \quad \sigma_z = \begin{pmatrix} 1 & 0 \\ 0 & -1 \end{pmatrix} \tag{D.3}$$

and have the following properties

$$\sigma_x\sigma_y = i\sigma_z \text{ and cyclic permutations} \tag{D.4}$$

$$[\sigma_i, \sigma_j]_+ = 2\delta_{i,j} \tag{D.5}$$

$$\boldsymbol{\sigma}.\boldsymbol{A}\,\boldsymbol{\sigma}.\boldsymbol{B} = \boldsymbol{A}.\boldsymbol{B} + i\,\boldsymbol{\sigma}.(\boldsymbol{A}\times\boldsymbol{B}) \tag{D.6}$$

The Dirac matrices γ^μ are defined as a covariant four-vector

$$\gamma^\mu = (\gamma^0, \boldsymbol{\gamma}), \quad \gamma^0 = \beta, \quad \boldsymbol{\gamma} = \beta\boldsymbol{\alpha} \tag{D.7}$$

and have the anticommutation rule

$$[\gamma^\mu, \gamma^\nu]_+ = 2g^{\mu\nu} \tag{D.8}$$

where $g^{\mu\nu}$ is the metric tensor. The matrix γ^5 is defined by

$$\gamma^5 = i\gamma^0\gamma^1\gamma^2\gamma^3 \tag{D.9}$$

In this representation

$$\gamma^0 = \begin{pmatrix} I & 0 \\ 0 & -I \end{pmatrix}, \quad \boldsymbol{\gamma} = \begin{pmatrix} 0 & \boldsymbol{\sigma} \\ -\boldsymbol{\sigma} & 0 \end{pmatrix} \tag{D.10}$$

and

$$\gamma^5 = \begin{pmatrix} 0 & I \\ I & 0 \end{pmatrix} \tag{D.11}$$

The solutions $\psi(\boldsymbol{r})$ for stationary states of ls coupled quantum numbers $n(ls)jm$ are of the form

$$\psi_{n,\kappa,m}(\boldsymbol{r},\boldsymbol{\sigma}) = \frac{1}{r}\begin{bmatrix} P_{n,\kappa}(r)\chi_{\kappa,m}(\Omega,\boldsymbol{\sigma}) \\ iQ_{n,\kappa}(r)\chi_{-\kappa,m}(\Omega,\boldsymbol{\sigma}) \end{bmatrix} \tag{D.12}$$

where $P(r)$ and $Q(r)$ are real radial functions. For $s = \frac{1}{2}$ the quantum number κ is unique for each $(l\frac{1}{2})j$ level

$$\kappa = l(l+1) - j(j+1) - \frac{1}{4} = \begin{cases} -(j+\frac{1}{2}) = -(l+1) & \text{for } j = l+\frac{1}{2} \\ (j+\frac{1}{2}) = l & \text{for } j = l-\frac{1}{2} \end{cases} \tag{D.13}$$

The functions $\chi_{\kappa,m}(\Omega,\sigma)$ are spin-space coupled wavefunctions of spherical harmonics $Y^l_m(\Omega)$ and two-spinors $\xi(\sigma)$

$$\chi_{\kappa,m}(\Omega,\boldsymbol{\sigma}) = \left(Y^{\,l}(\Omega)\xi^{\frac{1}{2}}(\boldsymbol{\sigma})\right)^j_m \tag{D.14}$$

They are normalised

$$\int \chi^\dagger_{\kappa',m'}\chi_{\kappa,m}\,d\Omega = \delta_{\kappa',\kappa}\delta_{m',m} \tag{D.15}$$

The following are also properties of the $\chi_{\kappa,m}$ functions

$$\begin{aligned} (\boldsymbol{l}.\boldsymbol{\sigma}+1)\,\chi_{\kappa,m} &= -\kappa\,\chi_{\kappa,m} \\ \hat{\boldsymbol{r}}.\boldsymbol{\sigma}\,\chi_{\kappa,m} &= \chi_{-\kappa,m} \end{aligned} \tag{D.16}$$

Appendix E

Parity violating weak interactions

E.1 Electroweak theory

In the theory of Weinberg and Salam [73], the weak and electromagnetic force are part of the same interaction whose symmetry is spontaneously broken at energies of order the boson mass or below. The interaction is mediated by an isospin triplet of fields $(W^{(1)\mu}, W^{(2)\mu}, W^{(3)\mu})$ and a hypercharge field singlet B^μ [62], where the isospin operator is $\hat{\boldsymbol{I}} = (\hat{I}^{(1)}, \hat{I}^{(2)}, \hat{I}^{(3)})$ and the hypercharge operator is $\hat{Y} = \hat{Q} - \hat{I}^{(3)}$ ($\hat{Q}$ is the ordinary charge operator). The particle current operators are defined by

$$\begin{aligned} \boldsymbol{J}^\mu &= \bar{\psi}\gamma^\mu \hat{\boldsymbol{I}}\psi \\ J^{(Y)\mu} &= \bar{\psi}\gamma^\mu \hat{Y}\psi \end{aligned} \tag{E.1}$$

The interaction between particle current and the boson field is given by the Lagrangian in terms of two coupling constants g and g'

$$\mathcal{L} = g\boldsymbol{J}_\mu.\boldsymbol{W}^\mu + g' J^{(Y)}_\mu B^\mu \tag{E.2}$$

The symmetry of the interaction is broken because the fields $\boldsymbol{W}$ and B are not the appropriate fields at low energy, which are the *mass* eigenstate fields. The mass eigenstate fields are linear combinations of $\boldsymbol{W}$ and B and can be are identified with the electromagnetic field A^μ, the charged weak current fields $W^{(\pm)\mu}$ and the weak neutral current field Z^μ

$$\begin{aligned} W^{(\pm)\mu} &= \mp\tfrac{1}{\sqrt{2}}\left(W^{(1)\mu} \pm W^{(2)\mu}\right) \\ Z^\mu &= \cos\theta_W W^{(3)\mu} + \sin\theta_W B^\mu \\ A^\mu &= -\cos\theta_W W^{(3)\mu} + \cos\theta_W B^\mu \end{aligned} \tag{E.3}$$

The Weinberg mixing angle θ_W is given by $\tan\theta_W = g'/g$ and has the experimental value $\sin^2\theta_W \approx 0.230$. The Lagrangian interaction in eqn E.2 is given by

$$\begin{aligned} \mathcal{L} = \; & \tfrac{g}{\sqrt{2}}\left(J^{(-)}_\mu W^{(+)\mu} + J^{(+)}_\mu W^{(-)\mu}\right) \\ & + \tfrac{g}{\cos\theta_W}\left(J^{(3)}_\mu - \sin^2\theta_W J^{(em)}_\mu\right) Z^\mu + g\sin\theta_W J^{(em)}_\mu A^\mu \end{aligned} \tag{E.4}$$

The first term corresponds to the W^+ and W^- charged current interactions, the second term to the Z^0 weak neutral current interaction, and the last term to the ordinary electromagnetic interaction. The electromagnetic interaction has coupling constant e, which must be equal to $g \sin\theta_W$ in eqn E.4, so that $g = e/\sin\theta_W$ where e is the electronic charge. In an atomic system, the charged currents do not contribute to the lowest order interactions, and the parity violating part is contained in the neutral current interaction

$$\mathcal{L}^{(NC)} = \frac{g}{\cos\theta_W} J_\mu^{(NC)} Z^\mu \tag{E.5}$$

where $J_\mu^{(NC)} = \bar{\psi}\gamma^\mu(\hat{I}^{(3)} - \sin^2\theta_W \hat{Q})\psi$ is the particle current interacting with the neutral current field Z^μ. The eigenvalues of $\hat{I}^{(3)}$ and $\hat{Q}$ in the standard model are different for the left and right handed projections of the particle. Therefore the left and right handed projections of the particle couple differently to the neutral current field, and parity is violated.

It is usual to write the particle wavefunction $\psi = \psi_L + \psi_R$ where the left and right hand projections are given by the projection operators $P_{L,R} = \frac{1}{2}(1 \pm \gamma_5)$. The projections are diagonal in isospin and charge, with eigenvalues τ_3 and q. The eigenvalues of the left and right handed projections of some standard model particles are given in table E.1.

The coupling constants of the left and right handed projections are not the same, and can be written in terms of their quantum numbers $g_{L,R} = \tau_3 + q\sin^2\theta_W$. The particle current is a sum of vector and axial vector parts

$$\boldsymbol{J}^{(NC)\mu} = \frac{1}{2}\bar{\psi}\gamma^\mu(c_V + \gamma_5 c_A)\psi \tag{E.6}$$

where the vector coupling $c_V = g_L + g_R$ and the axial vector coupling $c_A = g_L - g_R$ are given for some standard model particles in table E.2.

The fermion-fermion neutral current interaction is the product of the current interactions

$$H_{(NC)} = \mathcal{L}^1\mathcal{L}^2 = \frac{g^2}{\cos^2\theta_W} J_\mu^{(NC)}(1) Z^\mu Z^\nu J_\nu^{(NC)}(2) \tag{E.7}$$

where the product of the boson fields is proportional to the Z^0 propagator [4]. In the limit of low momentum transfer $q^2 \to 0$ the interaction is pointlike

$$Z^\mu Z^\nu = \frac{g^{\mu\nu}}{M_Z^2}\delta(x_2 - x_1) \tag{E.8}$$

It can also be shown that the mass of the $W^\pm$ and Z^0 particles are related by the Weinberg angle $M_W = M_Z \rho \cos\theta_W$ [8], where the factor ρ depends on the Higgs mechanism. Experiments to date find $\rho = 1$ consistent with the Salam-Weinberg model. It is usual to write the interaction in terms of the Fermi constant G_F of β decay theory

$$G_F = \frac{\sqrt{2}g^2}{8M_W^2} \tag{E.9}$$

Particle	τ	τ_3	$y = q - \tau_3$
$(\nu_e\,,\,e^-)_L$	$\frac{1}{2}$	$\left(+\frac{1}{2}\,,\,-\frac{1}{2}\right)$	$-\frac{1}{2}$
e_R^-	0	0	-1
$(\bar{\nu}_e\,,\,e^+)_R$	$\frac{1}{2}$	$\left(-\frac{1}{2}\,,\,+\frac{1}{2}\right)$	$\frac{1}{2}$
e_L^+	0	0	$+1$
$(u\,,\,d)_L$	$\frac{1}{2}$	$\left(+\frac{1}{2}\,,\,-\frac{1}{2}\right)$	$\frac{1}{6}$
u_R	0	0	$\frac{2}{3}$
d_R	0	0	$-\frac{1}{3}$
$\left(\bar{u}\,,\,\bar{d}\right)_R$	$\frac{1}{2}$	$\left(-\frac{1}{2}\,,\,+\frac{1}{2}\right)$	$\frac{1}{6}$
$\bar{u}_L$	0	0	$-\frac{2}{3}$
$\bar{d}_L$	0	0	$\frac{1}{3}$

Table E.1: Particle properties in the standard model

Particle	g_L	g_R	$c_V = g_L + g_R$	$c_A = g_L - g_R$
e^-	$-\frac{1}{2} + \sin^2\theta_W$	$\sin^2\theta_W$	$-\frac{1}{2} + 2\sin^2\theta_W$	$-\frac{1}{2}$
e^+	$-\sin^2\theta_W$	$\frac{1}{2} - \sin^2\theta_W$	$+\frac{1}{2} - 2\sin^2\theta_W$	$-\frac{1}{2}$
ν_e	$\frac{1}{2}$	0	$+\frac{1}{2}$	$+\frac{1}{2}$
$\bar{\nu}_e$	0	$-\frac{1}{2}$	$-\frac{1}{2}$	$+\frac{1}{2}$
u	$\frac{1}{2} - \frac{2}{3}\sin^2\theta_W$	$-\frac{2}{3}\sin^2\theta_W$	$\frac{1}{2} - \frac{4}{3}\sin^2\theta_W$	$+\frac{1}{2}$
$\bar{u}$	$\frac{2}{3}\sin^2\theta_W$	$-\frac{1}{2} - \frac{2}{3}\sin^2\theta_W$	$-\frac{1}{2} + \frac{4}{3}\sin^2\theta_W$	$+\frac{1}{2}$
d	$-\frac{1}{2} + \frac{1}{3}\sin^2\theta_W$	$\frac{1}{3}\sin^2\theta_W$	$-\frac{1}{2} + \frac{2}{3}\sin^2\theta_W$	$-\frac{1}{2}$
$\bar{d}$	$-\frac{1}{3}\sin^2\theta_W$	$\frac{1}{2} - \frac{1}{3}\sin^2\theta_W$	$+\frac{1}{2} - \frac{2}{3}\sin^2\theta_W$	$-\frac{1}{2}$

Table E.2: Electroweak couplings of some particles

so that finally the interaction is

$$H_{(NC)} = \sqrt{2}G_F \left[\bar{\psi}\gamma_\mu(c_V + \gamma_5 c_A)\psi\right]_1 \left[\bar{\psi}\gamma_\nu(c_V + \gamma_5 c_A)\psi\right]_2 g^{\mu\nu}\delta(x_2 - x_1) \qquad \text{(E.10)}$$

which is in the form of a *Vector + Axial-Vector* coupling to each particle. The vector part is proportional to $\gamma^\mu = (\gamma_0, \boldsymbol{\gamma})$ which has parity transformation $P : \gamma^\mu = (\gamma_0, -\boldsymbol{\gamma})$. The axial vector part is proportional to $\gamma^\mu\gamma_5$, where γ_5 is a pseudoscalar with parity transformation $P : \gamma_5 = -\gamma_5$.

E.2 Atomic parity non-conservation

The principle parity violating interaction present in an atom arises from the electron-quark interaction. This PNC interaction must be of the form *vector*$\times$*axial-vector*: either $V_e \times A_q$ or $A_e \times V_q$. The space and time parts of the interaction in eqn E.10 can be separated. To lowest order, the nuclear state is a parity eigenstate, so only P-even terms in the nuclear matrix element need be retained

$$H_{PNC} = \sqrt{2}G_F \left[\left(\bar{\psi}c_A\beta\gamma_5\psi\right)_e \left(\bar{\psi}c_V\beta\psi\right)_q - \left(\bar{\psi}c_V\beta\boldsymbol{\alpha}\psi\right)_e \cdot \left(\bar{\psi}c_A\beta\boldsymbol{\alpha}\gamma_5\psi\right)_q\right] \qquad \text{(E.11)}$$

The particle field operators ψ and $\bar{\psi}$ here can be related to wavefunctions $\psi(\boldsymbol{r})$ of ordinary quantum mechanics, by the replacements $\psi \to \psi(\boldsymbol{r})$ and $\bar{\psi} \to \psi(\boldsymbol{r})^\dagger\beta$. In a matrix element between electron states ψ_i and ψ_f, the nuclear wavefunction Ψ is the same for both initial and final states. The quark parts of H_{PNC} are single particle operators, so the nuclear part is a sum over the expectations of individual quarks q or equivalently over the Z protons (uud) and N neutrons (udd) whose wavefunctions are appropriately antisymmetrised products of quark flavour and spin states [62]. The first term in eqn E.11 then becomes a sum over the c_V coefficients of the $2Z + N$ up quarks ($c_V(u) = \frac{1}{2} - \frac{4}{3}\sin^2\theta_W$) and the $Z+2N$ down quarks ($c_V(d) = -\frac{1}{2} + \frac{2}{3}\sin^2\theta_W$), where the experimentally determined Weinberg angle is $\sin^2\theta_W \approx 0.230$

$$\left(\bar{\psi}c_V\beta\psi\right)_q \to \langle\Psi \mid c_V \mid \Psi\rangle = \frac{1}{2}Q_W\rho_N(\boldsymbol{r}) \qquad \text{(E.12)}$$

where the nuclear density $\rho_N(\boldsymbol{r})$ is normalised to unity, and the *weak charge* is $Q_W = -N + (1 - 4\sin^2\theta_W)Z$. The second term is more problematic since it depends on the spin structure of the nucleus, however the operator $\boldsymbol{\alpha}\gamma_5 = \boldsymbol{\sigma}$ is an axial vector so by analogy with the weak charge, we define a weak magnetic moment $\boldsymbol{\mu}_W$. The nuclear part of the matrix element is then

$$\left(\bar{\psi}c_A\beta\boldsymbol{\alpha}\gamma_5\psi\right)_q \to \langle\Psi \mid c_A\boldsymbol{\sigma} \mid \Psi\rangle = \frac{1}{2}\boldsymbol{\mu}_W\rho_N(\boldsymbol{r}) \qquad \text{(E.13)}$$

These results lead to the usual form of the atomic PNC Hamiltonian in two terms, the spin independent (SI) term depending on the weak charge Q_W and the spin dependent

term depending on the weak magnetic moment $\boldsymbol{\mu}_W$ of the nucleus

$$H_{PNC} = \frac{G_F}{2\sqrt{2}}[Q_W \gamma_5 \rho_N(\boldsymbol{r}) + \boldsymbol{\mu}_W . \boldsymbol{\alpha} \rho_N(\boldsymbol{r})] \tag{E.14}$$

The PNC interaction with the electrons cause opposite parity electron states to be mixed so that the parity quantum number is no longer a conserved quantity. The electronic states mixed are the $s_{1/2}$ and $p_{1/2}$ levels which have opposite parity and penetrate the nucleus. The spin dependent interaction can also connect $p_{3/2}$ levels, being of rank 1, but this interaction is zero in the non-relativistic limit and can usually be neglected [14].

Other contributions to atomic PNC arise from electron-electron and nucleon-nucleon effects. The electron-electron interaction can arise from Z^0 exchange but is not enhanced as much as the electron-nucleon interaction, and is further suppressed by a factor $1 - 4\sin^2\theta_W$. The nucleon-nucleon interaction can also give rise to a P-odd nuclear anapole moment, whose ordinary electromagnetic interaction with the atomic electrons contributes to the spin dependent PNC effect.

The spin independent part of the PNC interaction in eqn E.14 is the dominant contribution in heavy atoms, since its matrix elements scale as Z^3 for large Z. The PNC matrix element between alkali atom states $ns_{1/2}$ and $n'p_{1/2}$ was worked out by Bouchiat and Bouchiat [17], and for heavy atoms is given by

$$\left\langle ns_{1/2} \left| H_{PNC} \right| n'p_{1/2} \right\rangle = \frac{i\hbar G_F}{2\sqrt{2}} \frac{Z^2 Q_W K_R(Z,A)}{2\pi m_e c a_0^4 n^{*3/2} n'^{*3/2}} \tag{E.15}$$

where Z and A are the atomic number and mass, Q_W is the weak charge of the nucleus, n^* and n'^* are the effective quantum numbers of the states and a_0 is the Bohr radius. The effective quantum numbersoi of the levels are obtained from quantum defect theory ($n^* = n - \delta_l$) by fitting the energy terms to hydrogenic energies of the form $\varepsilon_{nl} \propto 1/n^{*2}$. Finally, $K_R(Z,A)$ is a relativistic correction factor given by

$$K_R(Z,A) = \left[\frac{\Gamma(3)}{\Gamma(2\gamma+1)} \left(\frac{2ZR_N}{a_0} \right)^{\gamma-1} \right]^2 \tag{E.16}$$

for heavy atoms, the nuclear radius is taken to be $R_N = 1.2A^{1/3} fm$ and the Dirac exponent $\gamma = \sqrt{1 - Z^2\alpha^2}$ of Rose [64]. The correction factor is close to unity for light elements, but significant for elements like caesium, mercury and lead. Values for some isotopes of these nuclei are $K_R(^{133}Cs) = 2.8$, $K_R(^{201}Hg) = 8.0$ and $K_R(^{208}Pb) = 9.0$.

Bibliography

[1] Abdullah, K., Carlberg, C., et al. New experimental limit on the electron electric dipole moment. *Phys. Rev. Lett.*, 65:2347, 1990.

[2] Abramowitz, M., and Stegun, I. *Handbook of Mathematical Functions.* NBS, 1964.

[3] Adeva, B., et al. (L3 collaboration). A determination of electroweak parameters from Z^0 decays into charged leptons. *Phys. Lett. B*, 250:183, 1990.

[4] Aitcheson, I. J. R. *Relativistic Quantum Mechanics.* Macmillan Press, 1972.

[5] Akravi, M. Z., et al. (OPAL collaboration). Measurement of the cross sections of the reactions $e^+e^- \rightarrow \gamma\gamma$ and $e^+e^- \rightarrow \gamma\gamma\gamma$ at LEP. *Phys. Lett. B*, 257:531, 1991.

[6] Apenko, S. M., and Lozovik, Y. E. Parity non-conservation and anapoles. *J. Phys. B*, 15:L57, 1982.

[7] Ashkin, J., and Kabir, P. K. Graphical representation of CP non-conservation parameters in K^0 decay. *Phys. Rev. D*, 1:868, 1970.

[8] Bailin, D. *Weak Interactions.* Sussex University press, 1977.

[9] Baird, P. E. G. Private communication.

[10] Bastrukov, S. I., Misicu, S., and Sushkov, A. V. Dipole torus mode in nuclear fluid dynamics, 1992.

[11] Bethe, H. A. *Intermediate Quantum Mechanics.* Benjamin, 1964.

[12] Bjorkholm, J. E., and Liao, P. F. Line shape and strength of two photon absorption in an atomic vapour with a resonant or nearly resonant intermediate state. *Phys. Rev. A*, 14:751, 1976.

[13] Blundell, S. A., Hartley, A. C., et al. Calculations of the parity non-conserving $6s \rightarrow 7s$ transition in caesium. *Theor. Chim. Acta*, 80:257, 1991.

[14] Boston, E. R. *Theory of Parity Non-Conservation in Atoms.* D.Phil Thesis, Oxford University, 1990.

[15] Boston, E. R., and Sandars, P. G. H. The anapole moments of hydrogenic atoms. *J. Phys. B*, 23:2663, 1990.

[16] Bouchiat, M. A. Atomic Parity Violation, a low energy test of the electroweak standard model. In *Atomic Physics XII*, page 399. AIP, 1991.

[17] Bouchiat, M. A., and Bouchiat, C. C. Weak neutral currents in atomic physics. *Phys. Lett.*, 48B:111, 1974.

[18] Brink, D. M., and Satchler, G. R. *Angular Momentum.* Oxford University Press, 1962.

[19] Buckle, S. J., Barnett, S. M., Knight, P. L., et al. Atomic interferometers: Phase-dependence in multilevel atomic transitions. *Optica Acta*, 33:1129, 1986.

[20] Budker, D., DeMille, D., and Commins, E. D. Experimental investigation of nearly degenerate excited states of opposite parity in atomic dysprosium. *Submitted to Phys. Rev. A*, 1993.

[21] Christenson, J. H., Cronin, J. W., et al. Evidence for the 2π decay of the K^0 meson. *Phys. Rev. Lett.*, 13:138, 1964.

[22] Condon, E., and Shortley, G. *Theory of Atomic Spectra.* Cambridge University press, 1963.

[23] Conti, R. S. Search for T-odd P-even interactions with a three level, directional clock. In *Time Reversal - the Art Rich Memorial Symposium.* AIP, 1993.

[24] Conti, R. S., and Khriplovich, I. B. New limits on T-odd P-even interactions. *Phys. Rev. Lett.*, 68:3262, 1992.

[25] Conti, R. S., Hatamian, S., et al. Search for C violating, P conserving interactions and observation of 2^3S_1 to 2^1P_1 transitions in positronium. *Phys. Lett. A*, 177:43, 1993.

[26] Corson, D., and Lorrain, P. *Introduction to Electromagnetic Fields and Waves.* Freeman, 1962.

[27] Coveney, P., and Highfield, R. *The Arrow of Time.* Flamingo, 1991.

[28] Edmonds, A. R. *Angular Momentum in Quantum Mechanics.* Princeton University press, 1957.

[29] Edwards, M. H. Zero angular momentum turns. *Am. J. Phys.*, 54:846, 1985.

[30] Emmons, T. P., Reeves, J. M., and Fortson, E. N. Parity non-conserving optical rotation in atomic lead. *Am. J. Phys.*, 54:846, 1985.

[31] Flambaum, V. V., and Khriplovich, I. B. P-odd nucleus forces - a source of parity violation in atoms. *Sov. Phys. JETP*, 52:835, 1980.

[32] Flambaum, V. V., Khriplovich, I. B., and Sushkov, O. P. Nuclear anapole moments. *Phys. Lett. B*, 146:367, 1984.

[33] Fortson, N. Recent experimental T tests. In *Time Reversal - the Art Rich Memorial Symposium.* AIP, 1993.

[34] Gasiorowicz, S. *Quantum Physics.* Wiley, 1974.

[35] Gilbert, S. L., Watts, R. N., and Wieman, C. E. Measurement of the $6s \rightarrow 7s$ M1 transition in caesium with the use of crossed electric and magnetic fields. *Phys. Rev. A*, 29:137, 1984.

[36] Goldstein, H. *Classical Mechanics.* Addison-Wesley, 1950.

[37] Golub, R., and Pendlebury, J. M. The electric dipole moment of the neutron. *Contemp. Phys.*, 13:519, 1972.

[38] Halzen, F., and Martin, A. D. *Quarks and Leptons.* Wiley, 1984.

[39] Hartley, A. C. Private communication.

[40] Hinds, E. Private communication.

[41] Holstein, B. R. Time reversal tests with nuclei. In *Time Reversal - the Art Rich Memorial Symposium.* AIP, 1993.

[42] Jackson, J. D. *Classical Electrodynamics.* Wiley, 1962.

[43] Jacobs, J. P., Lamoreux, S. K., et al. To be published, 1992.

[44] Khatsymovsky, V. M., and Khriplovich, I. B. CP-odd interaction of light quarks and the neutron electric dipole moment. *Phys. Lett. B*, 296:219, 1992.

[45] Khriplovich, I. B. Private communication.

[46] Khriplovich, I. B. New upper limits of the T invariance violation in β decay. *Pis'ma ZhETF*, 52:1065, 1990.

[47] Khriplovich, I. B. *Parity Non-Conservation in Atomic Phenomena.* Gordon and Breach, 1990.

[48] Khriplovich, I. B. What do we in fact know about T-odd but P-even interactions? *Nucl. Phys. B*, 352:385, 1991.

[49] Khriplovich, I. B. T-odd P-even photon-fermion interactions. International conference on weak and electromagnetic interactions in nuclei (WEIN 92), Dubna, 1992.

[50] Khriplovich, I. B., and Pospelov, M. E. Anapole moment of a chiral molecule. *Z. Phys. D*, 17:81, 1990.

[51] Kozlov, M. G., and Porsev, S. G. The possibility to study the break of time reversal invariance in atoms. *Phys. Lett. A*, 142:233, 1989.

[52] Lee, T. D., and Yang, C. N. Question of parity conservation in weak interactions. *Phys. Rev.*, 104:254, 1956.

[53] Lloyd, S. P. 2^{L-1}-electric 2^L-magnetic interference terms in γ-γ-angular correlations. *Phys. Rev.*, 81:161, 1951.

[54] Loudon, R. *The Quantum Theory of Light.* Clarendon Press, Oxford, 1983.

[55] MacPherson, D., Zetie, K. P., et al. Precise measurement of parity nonconserving optical rotation at 876 nm in atomic bismuth. *Phys. Rev. Lett.*, 67:2784, 1991.

[56] Marey, M. Photographs of a tumbling cat. *Nature*, 51:80, 1894.

[57] Messiah, A. *Quantum Mechanics.* North-Holland, 1962.

[58] Misicu, S. Classical radiation of the toroidal dipole moment. *Rom. J. Phys.*, 37:855, 1992.

[59] Murthy, S. A., Krause, D., et al. New limits on the electron electric dipole moment from caesium. *Phys. Rev. Lett.*, 63:965, 1989.

[60] Noecker, M. S., Masterson, B. P., and Weiman, C. E. Precision measurement of parity nonconservation in atomic caesium: a low energy test of the electrweak theory. *Phys. Rev. Lett*, 61:310, 1988.

[61] Painlevé, P. Sur le théorème des aires et les systèmes conservatifs. *Comptes Rendus*, 139:1170, 1904.

[62] Perkins, D. H. *Introduction to High Energy Physics.* Addison-Wesley, 1987.

[63] Peskin, M. E., and Takeuchi, T. New constraints on a strongly interacting Higgs sector. *Phys. Rev. Lett.*, 65:964, 1990.

[64] Rose, M. E. *Relativistic Electron Theory.* Wiley, 1961.

[65] Sachs, R. G. *The Physics of Time Reversal.* Chicago, 1987.

[66] Sakurai, J. J. *Invariance Principles and Elementary Particles.* Princeton, 1964.

[67] Sandars, P. G. H. The electric dipole moment of an atom. *J. Phys. B*, 1:499, 1968.

[68] Sandars, P. G. H. Parity and time reversal in atoms and molecules. *Physica Scripta*, 36:904, 1987.

[69] Sandars, P. G. H. Parity and time reversal invariance in atoms. In *Physics of Highly Ionised Atoms*, page 1. Plenum, 1988.

[70] Sandars, P. G. H. Atomic T violation: a biased history. In *Time Reversal - the Art Rich Memorial Symposium.* AIP, 1993.

[71] Shabanova, L. N., Monakov, Yu. N., et al. Oscillator strengths of lines in the principal series of caesium. *Opt. i Spektr.*, 47:1, 1979.

[72] Stacey, D. N. Parity non-conservation in atoms. In *Atomic Physics 13*, 1992.

[73] Weinberg, S. A model of leptons. *Phys. Rev. Lett.*, 19:1264, 1967.

[74] Wolfenden, T., Baird, P., and Sandars, P. G. H. Observation of parity violating optical rotation in atomic thallium. *Europhys. Lett.*, 15:731, 1991.

[75] Woodgate, G. K. *Elementary Atomic Structure.* Clarendon press, Oxford, 1980.

[76] Wu, S. L., Ambler, E., et al. Experimental test of parity conservation in beta decay. *Phys. Rev.*, 105:1413, 1957.

[77] Zel'dovich, Ya. B. Electromagnetic interaction with parity violation. *Sov. Phys. JETP*, 33:1531, 1957.